School of Pharmacy

University of Nottingham

MODIFIED CELL PENETRATING PEPTIDES FOR EFFICIENT POLYMER NANO/MICROPARTICLE DELIVERY FOR BONE DIFFERENTIATION APPLICATIONS

Aveen Jalal, MSc

Thesis submitted to the University of Nottingham

for the degree of Doctor of Philosophy

Jan 2020

Acknowledgment

I would like to thank my primary supervisor Assistant Prof. James Dixon for his support and guidance particularly his open-door policy and availability in the Lab throughout the project. Your enthusiasm for high impact work has pushed me to conduct good quality research and made me develop from a student to an independent researcher.

I would also like to thank my second supervisor Prof. Kevin Shakesheff, for his availability and help during difficult times trying to make scene of results especially at the beginning of the project. You have always been motivating and inspiring.

I cannot thank my husband Rawaz Tawfeeq enough for believing in me and fully fund my PhD! Thanks for your great effort and hard work to put our family in the best possible position for a great future.

A very special thanks to my colleagues (Sahrish, Lia, Hosam, Inchi, Jopeth and Franchesco) in the Lab for all the laughs and personal help I got, you have always been the hidden support.

Last but by no means least, a very exceptional thanks to my mum. Your sacrifices have made me stand where I am here today.

Abstract

Nano/microparticle based gene therapy, the next generation of therapeutics could potentially cure inherited and acquired diseases through delivering nucleic acid intracellularly which otherwise are difficult to treat. Developing non-viral gene therapy vectors that both protect and deliver nucleic acid cargoes efficiently will be vital if gene augmentation and editing strategies are to be effectively combined with advanced regenerative medicine approaches. Currently, these methodologies utilise high concentrations of recombinant growth factors, which result in toxicity and off-target effects. Herein, the use of modified cell penetrating peptides (CPPs), termed Glycosaminoglycan (GAG) binding Enhanced Transduction (GET) with plasmid DNA (pDNA) encapsulated poly (lactic-co-glycolic acid) PLGA nano/microparticles (pDNA encapsulated PLGA NP/MPs) is demonstrated. In order to encapsulate the pDNA in PLGA NP/MPs, it was first condensed with several condensing agents such as high and low molecular weight cationic polypeptides and alcohol. Low molecular weight Poly L-Lysine (PLL) produced the smallest and most homogenous population of pDNA nanoparticles (pDNA NPs) in the range of 10-50 nm. These pDNA NPs were then encapsulated in PLGA MPs by double emulsion methods; yielding encapsulation efficiencies (EE) of ~ 30 %. pDNA encapsulated PLGA MPs were in the range of 0.35 μm in diameter with a negative surface charge. PLGA MPs complexed with GET peptides show enhanced intracellular delivery (up to seven folds) and transfection efficiencies (up to five orders of

magnitude). Moreover, the pDNA cargo has enhanced protection from nucleases (i.e. DNase I) promoting their translatability.

The biomedical applications of these MPs were tested in bone regeneration. For that, pBMP2 encapsulated PLGA-GET MPs were shown to efficiently deliver pBMP2 which can promote bone regeneration in human mesenchymal stem cells (hMSCs) *in vitro.* The bone lineage differentiations were confirmed by Alizarin red calcium staining and detection of bone lineage specific genes by Quantitative Reverse Transcription-Polymerase Chain Reaction (QRT-PCR).

By combining FDA-approved PLGA polymer nano/microtechnology with the GET delivery system, therapeutic non-viral vectors could have a significant impact on cellular therapy and regenerative medicine applications.

Table of Contents

List of Figures

List of Tables

Abbreviations

AFM Atomic Force Microscopy

ALP Alkaline Phosphatase

BGLAP Bone Gamma-Carboxyglutamate Protein

BMP2 Bone Morphogenic Protein 2

bp base pair

BSA Bovine Serum Albumin

cAMP Adenosine 3'5' Cyclic Monophosphate

CFU-F colony-forming unit-fibroblast

CME Clathrin-mediated endocytosis

CMV Cytomegalovirus

CPPs Cell Penetrating Peptides

CREB cAMP Response Element-Binding Protein

CvME Caveolae-mediated endocytosis

DCM Dichloromethane

DEPC Diethylpyrocarbonate

Dex Dexamethasone

DLS Dynamic Light Scattering

DMEM Dulbecco's Modified Eagle Medium

DNA Deoxyribonucleic acid

dsDNA double stranded DNA

EDTA Ethylenediaminetetraacetic acid

EE Encapsulation Efficiency

EGF Epidermal Growth Factor

ESC Embryonic Stem Cells

EtBr Ethidium bromide

FCS Foetal Calf Serum

FDA Food and Drug Administration

FGF Fibroblast Growth Factor

FITC Fluorescein IsoThioCyanate

GAG Glycosaminoglycan

GET Glycosaminoglycan-binding Enhanced Transduction

GF growth factor

GM Growth Media

HBD Heparan sulphate Binding Domain

HBSS Hanks' Balanced Salt solution

hESCs human Embryonic Stem Cells

HM High Molecular weight

hiPSCs human induced Pluripotent Stem Cells

hMSC human Mesenchymal Stem Cells

IFNγ Interferon gamma

IGF Insulin-like Growth Factor

IHMSCs Immortalised Human Mesenchymal Stem Cells

LM Low Molecular weight

mESCs Mouse Embryonic Stem Cells

µm micrometre

MPs Microparticles

mRNA messenger RNA

MSC Mesenchymal Stem Cells

MYOD myoblast determination protein

Mw molecular weight

nm nanometre

NPs Nanoparticles

OI Osteoinductive

OP Osteopermissive

PAA Poly L-aspartic acid

P-Arg Poly arginine

PBS Phosphate Buffered Saline

pBMP2 Bone Morphogenic Protein 2 encoded plasmid

PCL Poly caprolactone

PDGF Platelet Derived Growth Factor

PDI Poly Despersity Index

PDL Diffuse Double Layer

pDNA plasmid DNA

PEG Polyethylene glycol

PEG2 Prostaglandin E2

PEI Poly ethylenimine

PFA Paraformaldehyde

pGluc Gaussia Luciferase encoded plasmid

PLGA Poly (Lactic-co-Glycolic Acid)

PLL Poly L-lysine

PTH parathyroid hormone

PVA Polyvinyl alcohol

QRT-PCR Quantitative Reverse Transcription-Polymerase Chain Reaction

RFP Red Fluorescent Protein

RI Refractive Index

RNA Ribonucleic acid

rpm rotations per minute

SFM Serum Free Media

siRNA small interfering RNA

SOP Standard Operating Procedure

SPP1 Secreted Phosphoprotein 1

TAE buffer Tris-acetate-EDTA buffer

TE buffer Tris-EDTA buffer

TEM Transmission Electron Microscopy

TGF Transforming Growth Factor

TGFβ Transforming Growth Factor beta

TNFα Tumour necrosis factor alpha

VEGF Vascular Endothelial Growth Factor

W/O/W Water/Oil/Water

Chapter 1.

Introduction

1.1 Nano/Micro technologies in gene delivery

Nanotechnology, as a reteach area, has emerged in scientific fields in the 1950s (Feynman, 1960, Sharma *et al*., 2016a, Krukemeyer *et al*., 2015). In medicine and pharmaceutical fields, nanotechnology describes the development of engineered nanoscale materials that interact with cells and tissues with a high degree of specificity (Silva, 2004). This degree of specificity allows advancement in designing drug/gene delivery devices to reduce toxicity and/or improve the efficiency of conventional therapies (Martis *et al.*, 2012, Nikalje, 2015, Silva, 2004). Nanoparticles (NPs) exist as the same small size as cellular compartments. This unique size feature of NPs allows their interaction with cellular components as small as 5 nanometre (nm) sized protein molecules which are comparable to the smallest manmade NP (Gehr, 2018). Nanoparticles, as defined by the European commission, are particles where 50 % or more of the population is in the size range of 1-100 nm by number size distribution (EU, 2011, Bleeker *et al*., 2013). On the other hand, particles of more than 100 nm but sub-micron range (Microparticles (MPs)) have been utilised as carriers and protectants of NPs for intracellular gene delivery (Blanco *et al*., 2015, Lima *et al*., 2016). Technologies such as packaging NPs in MPs are of increasing importance in the field of gene delivery to offer improved efficacy, environmental protection, feasibility of functionalisation for targeted delivery (Nie *et al*., 2008, Tang *et al*., 2012, Dordelmann *et al*., 2014). Gene delivery comprises the process of introducing an exogenous gene into mammalian cells utilising

colloidal NP/MPs (Niven *et al*., 1997, Tabatt *et al*., 2004, Hu *et al*., 2009). Solid colloidal NP/MPs, defined as systems that contain particles in size range of 1-1000 nm and generally referred to as nano/microspheres or nano/microcapsules are the most studies class of NP/MPs in biomedical fields (Guterres *et al*., 2007, Colson and Grinstaff, 2012, Hu *et al*., 2009). Mostly these NP/MPs are prepared from preformed polymers and some are synthesised during polymerisation process (Mora-Huertas *et al*., 2010). These colloidal NP/MPs have displayed ability in loading/encapsulating drug/biological molecules and releasing their payload in a controlled manner (Cruz *et al*., 2006, Leite *et al*., 2007). Many biological and non-biological organic and inorganic materials have been used to develop nano/microstructured carriers to deliver nucleic acids (DNA and RNA) that encode a therapeutic gene or silence the gene of interest in the case of siRNA delivery (Miele *et al*., 2012, Wu *et al*., 2018).

1.1.1 Types of nano/microparticle vectors for nucleic acid delivery

Gene therapy for the delivery of DNA and RNA to correct a defective gene or to express a therapeutic protein is the emphasis in the development of future medicine (Brown *et al*., 2001). Direct delivery of naked nucleic acids efficiently to targeted cells is challenging for many reasons. The major obstacle is their large size and negative surface charge which prevents them from penetrating the cytoplasmic membrane. In addition, nucleic acids lose their efficacy and function by the time they reach the targeted site due to

extra and intracellular nuclease degradation (Wong *et al*., 2017). Physical methods such as microinjection, gene gun, electroporation and sonoporation were amongst the first techniques applied to transfer nucleic acid directly into the nucleus or cytoplasm (Yoshida *et al*., 1997, Harrison *et al*., 1998, Manome *et al*., 2000, Lechardeur *et al*., 2005). While these methods have the advantage of nucleic acid bypassing the endo/lysosome compartment (Zhang, 2013), they are not cell specific, and are associated with low cell viability and augmenting the risk of developing cellular senescence (Mellott *et al*., 2013, Nayerossadat *et al*., 2012). Moreover, expensive equipment and highly skilled personnel are required to conduct basic laboratory research when using these approaches (Sato *et al*., 2016, Meacham *et al*., 2014). Packaging the genetic molecules in a vector is another method of gene delivery. In contrast to physical methods, this method has the advantage of reducing labour, and offers variety in biomaterials and designs, which allows for the possibility of enhancing efficacy and reducing toxicity, as well as being more straightforward in terms of developing basic research tools or pharmaceutical products (Ramamoorth and Narvekar, 2015). Viral vectors are highly efficient transfection tools due do their evolutionary infectious properties and long-term gene expression capabilities (Kay *et al*., 2001, Bouard *et al*., 2009). Viral vectors and recombinant viruses, such as retroviruses (Yanez-Munoz *et al*., 2006), adeno-associated viruses (Barnard *et al*., 2014) and lentiviruses (Griesenbach and Alton, 2012) constitute the majority of gene therapy clinical trials. However, they are associated with many serious problems

such as genomic integration (Zheng *et al*., 2000) and immunogenicity against viral capsids and oncogenicity (Brown *et al*., 2001). Moreover, they are limited in terms of the amount of DNA they incorporate and are not suitable for large-scale production (Luten *et al*., 2008). Furthermore, high production cost of these treatments has also limited their use (Ramamoorth and Narvekar, 2015, Goswami *et al*., 2019). Therefore, many research groups are investigating various non-biological, nano/micro-sized structures ranging in size from 5-1000 nm to deliver one or more macromolecular nucleic acid. An ideal synthetic gene delivery vector should fulfil the following requirements: It should lack the immunogenicity associated with viral vectors, protect the incorporated nucleic acid from degradation by nucleases, reproducible and easily scalable for pharmaceutical-grade output and quality control (Leong *et al*., 1998). To date, numerous non-biological vectors have been engineered, most of which are bio-inert and lack or reduce the immunogenicity issues associated with viral vectors. In addition, one could tailor the encapsulation efficiency and release profile of the therapeutic agent by adjusting the physico-chemical properties of these nano/micro-carriers (Goodman *et al*., 2008).

Different types of non-biological organic and inorganic materials have been used as nano/micro-carriers of nucleic acids (Yousefi *et al*., 2013, Niidome *et al*., 2004). Although they are different in terms of raw materials, size and design, they all share the same aim of protecting the nucleic acid and delivering it to the target site. Two main mechanisms are observed in nucleic acid delivery with non-viral vectors. Numerous vectors depend on

electrostatic interaction between the positively charged vector and the negatively charged nucleic acid to condense and partially encapsulate the nucleic acid within the condensing vector, or to adsorb it on their surfaces. Due to their easy condensation step and relatively higher rate of cellular internalisation, natural and synthetic cationic polymers are the most frequently used vectors (von Gersdorff *et al*., 2006, Christie *et al*., 2010). The resultant NP/MPs of cationic polymer nucleic acid condensation are known as polyplexes (Keles *et al*., 2016, Pun and Hoffman, 2013, Lachelt and Wagner, 2015). Another class of cationic vectors is liposomes. These vectors work according to the same principles of electrostatic interaction between the cationic lipid and the nucleic acid to form lipoplexes (Simoes *et al*., 1999, Xu *et al*., 1999, Tros de Ilarduya *et al*., 2010). Lipofectamine family agents (Life Technologies) are by far the most well-known commercial liposome-based gene carriers. Furthermore, inorganic materials such as gold, silver and silica NP/MPs and carbon nanotubes have been investigated as attractive gene delivery vectors due to their ease of production, controlled size and high transfection efficiency. Similar to the other vectors, these NP/MPs bind to nucleic acid electrostatically. In this regard, each of these nano/micro-carriers could bind to numerous nucleic acids at the same time, which increases their loading and transfection efficiency. However, these NP/MPs are colloidally unstable and many researchers have focused on addressing the problem of aggregation of these NP/MPs (Niidome *et al*., 2004, Dizaj *et al*., 2014).

Another mechanism of encapsulating nucleic acids is to embed them into a polymer matrix during the fabrication of the NP/MPs. Biodegradable polymers have been used to formulate NP/MPs in which encapsulated nucleic acid is located within the polymer matrix. Among these polymers, PLGA is the most abundantly used polymer because it is approved by Food and Drug Administration agency (FDA). The method of DNA encapsulation depends on the nature of the organic solvent used in the encapsulation process. The polymer hardens into NP/MPs as the solvent diffuses into the water compartment or evaporates in nanoprecipitation (Bilati *et al*., 2005a) and double emulsion (Abbas *et al*., 2008, Cohen-Sela *et al*., 2009, Cun *et al*., 2011), respectively. In the following sections, the advantages and limitations of each of the electrostatic (cationic polymers) and non-condensing (hard polymer) NP/MP vectors are clarified.

1.1.2 The limitations of cationic vectors for nucleic acid delivery

Various cationic polymers have been used for nucleic acid delivery. The most used cationic polymer is linear or branched Poly ethylenimine (PEI) (Fella *et al*., 2008, Wolff and Rozema, 2008). Owing to their high positive charge, these polymers can bind and condense the negatively charged nucleic acid to form nano/micro-sized polyplexes. These electrostatic forces allow high encapsulation efficiencies. In addition, the overall positively charged NP/MPs are attracted to the negatively charged cell membrane proteoglycans and glycoproteins which yields efficient *in vitro* transfection (Boussif *et al*., 1995). Their extensive positive charge, however, causes

cytotoxicity due increase in caspase-3 activity which causes loss of mitochondrial membrane potential and cell apoptosis (Moghimi *et al*., 2005). In addition, these polymers are non-bio-erodible which increases the risk of their accumulation in the body. Reducing their positive charge seems to be a straightforward method to reduce their toxicity. Many researchers have modified the original high molecular weight PEI to lower molecular ones. However, according to (Schulze *et al*., 2003, Ward *et al*., 2001) lower molecular weight and less positively charged PEI showed less DNA condensation ability, as well as less efficient transfection. In addition, the problem of the lack of biodegradation of these polymers causes serious risks, particularly upon repeated administration. Other cationic but natural polymers such as Chitosan and Gelatin have the same mechanism of binding to DNA through electrostatic interaction to generate NP/MPs. Nonetheless, they have the advantage of biodegradation which eliminates one aspect of toxicity associated with PEI (Dai *et al*., 2006, Lavertu *et al*., 2006, Kushibiki *et al*., 2005, Dang and Leong, 2006). Another example of gene carrier which use the same principle of cationic polymers for condensing nucleic acid is cationic lipids. In 1987, Felgner and colleagues were the first to introduce cationic lipids as gene delivery vectors. Likewise, cationic lipids electrostatically interact with negatively charged nucleic acids to form lipoplexes. Sharing the same principle of action with cationic polymers would mean having the same problem of cytotoxicity due to their excessive positive surface charges. Nevertheless, lipoplexes exhibit a lower rate of cytotoxicity than the polyplexes due to their biocompatibility. However, they

are associated with more immunogenicity problems (Ramamoorth and Narvekar, 2015). Moreover, Vectors encapsulating nucleic acids based on electrostatic interactions do not fully protect the encapsulated cargo from enzymatic degradation, therefore, results in low transfection efficiencies (Fihurka *et al*., 2018, Grigsby and Leong, 2010). Furthermore, these vectors are associated with poor stability and not suitable for long term storage limiting the possibility of commercialisation of these non-viral vectors (Romoren *et al*., 2004, Adolph *et al*., 2014).

1.1.3 PLGA NP/MPs for nucleic acid delivery

The selection of an appropriate gene-delivery vector that is safe, efficient, allows for long-term storage and scalability for pharmaceutical production is essential in the development of future gene delivery products for basic research, disease modelling, gene therapy and regenerative medicine applications. As a biocompatible and biodegradable FDA-approved polymer for drug delivery, PLGA fulfils the basic requirements of safety as its degradants are eliminated completely from the body through the Krebs cycle in which its lactate and glycolate monomers degrades to glycine, serine, and pyruvate or directly excreted through the kidneys (glycolate) or the lungs as CO2 (lactate) (Makadia and Siegel, 2011, Danhier *et al*., 2012, Mir *et al*., 2017). Moreover, unlike the other excessively positively charged non-viral vectors, due to the presence of uncapped carboxyl group, and depending on the surfactant used during the fabrication process, PLGA NP/MPs are highly negatively charged (Xu *et al*., 2009, Roointan A 2018).

This feature is also important for the chemical conjugation of variable moieties for targeted delivery, labelling (Vasconcelos *et al*., 2015, Streck *et al*., 2019), or for tailored coating with cationic agents to enhance their transfection efficiency (Moon *et al*., 2012, Gomes Dos Reis *et al*., 2019).

Furthermore, the encapsulation of nucleic acid in the hard PLGA matrix fully protects the nucleic acid from the surrounding digestive effect of nucleases (He *et al*., 2004, Intra and Salem, 2010, Zhao *et al*., 2013). The degradation of nucleic acid during intracellular delivery due to nucleases has been linked to a decrease in the efficiency of transfection (Grigsby and Leong, 2010, Fihurka *et al*., 2018). Other important aspects are the ease of preparation and the long-term stability of cryoprotected PLGA NP/MPs, which are critical for the commercialisation of gene delivery products (Romoren *et al*., 2004, Adolph *et al*., 2014).

PLGA has a long and successful history in drug delivery. PLGA NP/MPs are versatile vectors for the encapsulation of many small molecules, fluorescent dyes and pharmaceutical compounds. Countless studies have demonstrated the relatively easy and successful process of encapsulation of these molecules in PLGA NP/MPs (Betancourt *et al*., 2007, Pramod *et al*., 2012, Liu *et al*., 2019). High encapsulation efficiency of these molecules can be achieved simply by adjusting factors such as the polymer lactic/glycolic acid ratio, the polymer concentration, the organic solvent, the type and concentration of surfactants and the speed of sonication or homogenisation (Yeo and Park, 2004, Keum *et al*., 2011). However, despite the promise that

PLGA NP/MPs-based drug delivery holds for the field of gene therapy, the process of encapsulation of nucleic acids such as plasmid DNA (pDNA) is difficult due to all the differences in the physico-chemical nature of the pDNA and the PLGA polymer (Walter *et al*., 2001, Cun *et al*., 2011). Firstly, the size of a single supercoiled pDNA of approximately 4k base pairs (bp) using AFM is > 300 nm (Witz and Stasiak, 2010, Lyubchenko and Shlyakhtenko, 2016). Secondly, the charge of water soluble pDNA molecules is highly negative, which produces forces that repulse negatively charged PLGA during encapsulation (Ravi Kumar *et al*., 2004, Ramezani *et al*., 2017). Lastly, the hydrophilic characteristics of pDNA do not allow for their combination with hydrophobic PLGA in the same solvent (Iwahara *et al*., 2015, Swider *et al*., 2018). Moreover, this feature causes the pDNA to escape to the aqueous phase in solvent (organic)/non-solvent (aqueous) systems (Freitas *et al*., 2005, Cun *et al*., 2011). Therefore, many researchers have overcome the problem of the low encapsulation efficiency of pDNA in PLGA NP/MPs by condensing the pDNA, thus reducing the size, altering the charge and hydrophilicity characteristics of pDNA (Gebrekidan *et al*., 2000, Mok and Park, 2008).

Fulfilling these requirements, pDNA encapsulated PLGA NP/MPs have broad applicability in gene therapy and regenerative medicine. In this regard, they have been used to direct the differentiation of adult (Kim *et al*., 2011) and pluripotent stem cells (Levi *et al*., 2012). The gene that encodes for the growth or transcription factor involved in directing the differentiation of these stem cell to a specific lineage is encapsulated in the PLGA NP/MPs and

delivered intracellularly. In addition, delivering an exogenous nucleic acid to activate or silence the gene of interest has the potential to cure many diseases such as cancer, genetic disorders and viral infections that existing pharmaceutical treatments have failed to cure, or have unbearable side effects (Naldini, 2015, Grabowska *et al*., 2019). Therefore, in the present study, PLGA polymer has been chosen to encapsulate pDNA as it is an excellent raw material for developing a safe and effective gene delivery vector.

1.2 pDNA condensation

pDNA condensation is a necessary step in order to enhance its encapsulation in PLGA NP/MPs (Abbas *et al*., 2008, Lee *et al*., 2015, Lu *et al*., 2020). Understanding the factors affecting DNA condensation could lead to the efficient encapsulation of the DNA molecule in polymer NP/MPs.

1.2.1 Mechanisms of DNA condensation

DNA condensation is described as the state of a collapsed DNA molecule of a finite size (in the nano/micro-range). This phenomenon occurs as a result of neutralisation of charges in the DNA polymer backbone or its less interaction/hydration state with the solvent (water) molecules or a combination of both processes. Consequently, the size of the DNA molecule decreases dramatically from a highly extended wormlike chain into a compact NP/MP (Bloomfield, 1991, Heinonen *et al*., 1996, Bloomfield, 1997). The first mechanism requires a minimum polycation valence of three

to neutralise the valence three, negative phosphate group in every nucleotide (Estévez-Torres and Baigl, 2011, Arscott *et al*., 1990). The second mechanism of DNA compaction is through reducing its interaction with the water molecules to reduce its hydration. This could occur as a result of altering the properties of water by the addition of alcohol (Arscott *et al*., 1990) or a neutral polymer such as Polyethylene glycol (PEG) (Mok and Park, 2008). Consequently, this process reduces the water molecule availability necessary for DNA dissolution. Another mechanism is to use a combination of both polycation and agents that reduce DNA water molecule interaction. In this case, lower valence of two or even one and smaller alcohol/water volume ratios is needed to achieve the same degree of condensation.

1.2.2 Factors affecting DNA particle size

The size of the DNA particle is related to the nature of the condensation process, namely intramolecular or intermolecular condensation. In the intramolecular mode, the condensation of one molecule of DNA occurs in a NP, while intermolecular condensation refers to multi-molecular DNA condensation in a larger NPs or MPs. Both processes could occur based on the concentration of the DNA and the condensing agent in the solvent, the chemical nature of the condensing agent and environmental conditions (such as the presence of salt) (Nayvelt *et al*., 2007, Bloomfield, 1991). For example, it has been reported that high concentrations of DNA are mainly associated with the aggregation and production of MPs due to intermolecular condensation processes. At this point, the DNA MPs are

called aggregates. On the other hand, a low concentration of DNA allows for the condensation of a smaller number of DNA molecules in a particle, thus producing DNA NPs (Mann *et al*., 2007, Mann *et al*., 2008a).

The shape, molecular size and chemical structure of the condensing agents are the most frequently studied factors that affect DNA particle size. The best example is the various arrangements of Poly L-lysine (PLL) molecules in their linear, branched, hyper-branched and dendriplex forms. These arrangements of PLL molecules affect the chemical structure and molecular weight and, consequently, the mechanism of DNA condensation (Mannisto *et al.*, 2002, Kadlecova *et al.*, 2013). The PLL form with lower number of residues produces DNA NPs. Moreover, increasing the number of residues in any single form of PLL above, for example linear PLL, will affect its resultant DNA particle size and mostly produce DNA MPs due to the change in its molecular weight (Mann *et al*., 2008a).

Another factor, affecting DNA particle size is the composition of the media. A high salt concentration in the media affects the stability of DNA particles as a result of compression and neutralisation in the diffuse double layer (DDL). In turn, the neutralisation of charges eliminates repulsive forces, which then decreases colloidal stability and causes the aggregation of the condensed DNA. (Bostrom *et al*., 2001, Edwards and Williams, 2004).

Furthermore, the concentration of the condensing agents can control the size and shape of the condensed DNA particles to some extent. (Mann *et al*., 2008a) used AFM to clarify the effect of charge ratio (+ amine in PLL/-

phosphate in DNA) on pDNA condensation. They reported that pDNA condensation occurred even at charge ratios of 0.1 and 0.25. However, the pDNA particles formed at these charge ratios were rod-like in shape, and they were slightly shorter in length and thicker in width than was a tight, supercoiled pDNA molecule which was concluded by the authors as inefficient condensation. Increasing the charge ratio to greater than one resulted in the alteration of the mechanism of condensation by decreasing the length and increasing the thickness of the particles to produce NPs that were more spherical. The same experiment was conducted using poly arginine (P-Arg) at molar ratios of 0.1, 0.2, 0.5 and 1 (P-Arg/DNA). The fluorescent microscopic observations revealed a gradual reduction in the length of linear Bacteriophage T4 DNA molecules upon condensation with increasing molar concentrations of P-Arg (Minagawa *et al*., 1991). Furthermore, (Brgles *et al*., 2012) tested charge ratios 1, 25 and 50, and found that the DNA particle size formed with cationic lipids decreased from 400 to 200 and 100 nm, respectively.

The size of the DNA particles are independent of the size of DNA molecules. It has been reported that DNA molecules from 400 to 40,000 bp lead to the same DNA NP size. However, the number of DNA molecules/particle increases with reducing the size of the DNA molecule without affecting the overall size of the DNA particle. These observations were recorded when other parameters, such as size, shape and the concentration of the condensing agent were kept constant (Arscott *et al*., 1990, Bloomfield, 1991, Kreiss *et al*., 1999).

1.3 Preparation of pDNA encapsulated PLGA NP/MPs

Many techniques have been employed to prepare NP/MPs using biodegradable PLGA polymer. The double emulsion and nanoprecipitation techniques are cited most frequently in the literature. Other techniques such as salting out, dialysis and supercritical fluid technology have also been used occasionally (Dinarvand *et al*., 2011, Casettari *et al*., 2011, Rezvantalab *et al*., 2018). The primary function of the prepared particles is to protect the encapsulated drug molecule within the polymer matrix from enzymatic degradation, light and oxidation (Kakran and Antipina, 2014, Iqbal *et al*., 2015).

1.3.1 Double emulsion

In double emulsion, the pDNA is dissolved in water (W) and dispersed in an organic solvent containing the PLGA polymer (O) by sonication or homogenisation. The resulting W/O emulsion is then added to a continuous aqueous phase containing a hydrophilic stabiliser to form a W/O/W emulsion with the aid of another sonication step (McCall and Sirianni, 2013). NPs are formed in the interphase of the aqueous/organic compartment in line with the organic phase evaporation to encapsulate the pDNA molecules during PLGA NP/MP formation (Arshad *et al*., 2015, Cohen-Sela *et al*., 2009a). The use of stabilisers in the first and second emulsions is necessary to maintain the physico-chemical state of the dispersion and to prevent the separation of the two immiscible phases (that is, water and the organic solvent) (Liu *et al*., 2005, Yang *et al*., 2001). Polyvinyl alcohol (PVA) is widely

used as a hydrophilic stabiliser in double emulsion due to its biocompatibility and biodegradability (Tsujiyama *et al*., 2011).

1.3.2 Nanoprecipitation

Nanoprecipitation, which is also called solvent displacement or interfacial deposition, was first developed and patented by Fessi and colleagues in 1989. The principles of NP/MP formation rely on the interfacial deposition of the polymer between the miscible solvent (organic) and the non-solvent (aqueous) phases governed by the Marangoni law (Fessi *et al*., 1989a, Hornig *et al*., 2009). Marangoni effect takes place as a result of gradient in surface tension at the interface of the two phases due the difference in PLGA concentration between the two phases (Sternling and Scriven, 1959, Schubert *et al*., 2011). Unlike double emulsion, the pDNA is solubilised in the organic phase through condensation with alcohol or other condensing agents followed by freeze drying to remove the water compartment. The freeze-dried pDNA NPs are then incorporated with the PLGA in the organic phase. When mixing the two phases, the organic phase diffuses quickly into the aqueous phase, which results in a mildly turbulent effect that leaves the polymer behind to solidify in the water (Luque-Alcaraz *et al*., 2016).

The processes of double emulsion and nanoprecipitation have both been employed for the encapsulation of hydrophilic drug molecules. However, double emulsion is considered to be more suitable for the encapsulation of hydrophilic molecules, (Crotts and Park, 1998, Sinha and Trehan, 2003)

specifically pDNA in PLGA NP/MPs, than is nanoprecipitation (Cohen *et al*., 2000, Oster and Kissel, 2005).

Nanoprecipitation is more applicable to the encapsulation of hydrophobic drug molecules due to the possibility of combining the drug to be encapsulated and the polymer in the same organic phase, instant NP/MP formation and the minimal escape of the hydrophobic molecule to the outer, non-solvent aqueous phase. However, this combination is not applicable in the case of hydrophilic molecules resulting in their low encapsulation efficiencies (Xu, 2016). Modified nanoprecipitation techniques have been developed to encapsulate water-soluble drugs, either by changing the pH of the non-solvent phase to decrease the solubility and consequent leakage of the drug to the non-solvent phase (Govender *et al*., 1999), or the inclusion of the water soluble drug in the aqueous phase instead of in the organic phase (Morales-Cruz *et al*., 2012). However, these modifications have not been sufficiently successful to be considered as standard methods for the encapsulation of pDNA in PLGA NP/MPs due the effect of these modifications on other parameters in the encapsulation process and the non-reproducibility of these method by other research groups *(*Niu *et al.,* 2009*,* Morales-*Cruz et al*., 2012).

1.4 Cellular barriers to non-viral gene delivery

Despite the proposed advantages they bring to the field of gene- and cell-based therapy in terms of safety, reproducibility and industrial-scale production over the viral vectors, non-viral gene delivery vectors (including

PLGA NP/MPs and cationic vectors) lack the intrinsic invading characteristics of viral vectors; hence, they decrease the efficiency of cellular transfection substantially (Hardee *et al*., 2017). In order to achieve efficient gene delivery outcomes, the vector carrying the exogenous genetic material has to enter the target cell and deliver therapeutically useful levels of the carried gene. This is not a simple task, since the vectors encounter numerous extracellular and intracellular barriers. Firstly, the vector has to overcome extracellular nucleases (Section 1.4.1) and immune responses (Section 1.4.2). Next, it has to pass through the cell membrane (Section 1.4.3) and/or escape the endosome (Section 1.4.4) to reach the nucleus where the transcription occurs (Lechardeur and Lukacs, 2002, Perez-Martinez *et al*., 2011, Jones *et al*., 2013). Therefore, the intracellular delivery of these non-viral vectors is mainly enhanced with delivery and transfection agents such as cationic cell penetrating peptides (CPPs), cationic polymers and cationic lipids. Nonetheless, the efficiency of these vectors is still not adequate to produce therapeutic effects. Large, toxic doses of these agents are required to produce an optimal effect in this instance, which would compromise the overall transfection outcome (Hardee *et al*., 2017, Carvalho *et al*., 2017, Hacobian and Hercher, 2018).

1.4.1 Extracellular nucleases

Regardless of the method of administration (for example, intravenously, intramuscularly, inhalation or local implantation), the non-viral gene delivery vectors will unavoidably interact with the extracellular environment

before reaching the target cell. The intravenous delivery of naked pDNA has resulted in the degradation of the pDNA within 20 minutes after administration due to extracellular DNases (Houk *et al*., 1999, Houk *et al.*, 2001). The same degradation effect of extracellular DNases was observed when naked pDNA was administered intramuscularly (Mumper *et al*., 1996). The degradation effect of DNases reduces the amount of pDNA available for desired levels of transfection. DNases degrade single or double stranded DNA through the hydrolysis of the phosphodiester backbone in the presence of divalent metal ions (Varela-Ramirez *et al*., 2017). Therefore, DNA stabilisation is a prerequisite for successful gene delivery. Non-condensing polymers, such as neutral or negatively charged Gelatin (Kommareddy and Amiji, 2005, Magadala and Amiji, 2008, Kriegel and Amiji, 2011), Poly caprolactone (PCL) (Palama *et al*., 2015, Bhavsar and Amiji, 2008) and the most widely studied PLGA, (Jones *et al*., 1997, Mundargi *et al*., 2008, Okada and Toguchi, 1995, Abbas *et al*., 2008) can encapsulate the nucleic acid physically in the polymer matrix for maximum nuclease protection.

1.4.2 Immune responses

While viral vectors are well-known for initiating immune responses, some non-viral vectors are also associated with the release of pro-Inflammatory cytokines, namely the tumour necrosis factor alpha (TNFα) and interferon gamma (IFNγ). One of the typical non-viral vectors to induce these inflammatory responses is cationic lipids (Dow *et al*., 1999, Ferencik *et al*., 1990). Moreover, PEI has also been reported to activate immune responses

related to the T-helper cells (Th1 and Th2) (Regnstrom *et al*., 2003). Furthermore, avoiding these immune responses through the standard technique of PEGylation of these vectors has been shown to induce an anti-PEG IgM immune response on repeated administration (Dams *et al*., 2000, Wang *et al*., 2007).

1.4.3 The plasma membrane

Passing the first two barriers in the journey of the intracellular delivery of non-viral vectors, obtaining useful amounts of the vector through the cell membrane is still the hurdle to efficient transfection. Non-viral vectors predominantly pass through the cytoplasmic membrane via nonspecific electrostatic interaction with negatively charged Heparan Sulphate (HS) proteoglycans (Ramamoorth and Narvekar, 2015, Wu *et al*., 2018). Many endocytotic pathways have been studied in the process of cellular internalisation, including phagocytosis, clathrin-mediated endocytosis (CME), macropinocytosis and caveolae-mediated endocytosis (CvME). These processes could occur individually or in combination based on the nature and size of the vector (Hillaireau and Couvreur, 2009, KOU *et al*., 2013). While phagocytosis is mainly associated with phagocytic cells, macrophages, monocytes, neutrophils and dendritic cells (Aderem and Underhill, 1999), the other three pathways are seen in almost all types of cells including phagocytic cells (Xiang *et al*., 2012). CME is the most characterised receptor-dependent type of endocytosis. In this pathway, cellular membrane pits of about 100–150 nm form at the cellular membrane, followed by deep

invagination and fission of the pits. The endocytosed vesicular pits integrate with late endosome and lysosome for degradation if their contents had not escaped the early endosomes (Pearse, 1976, Takei and Haucke, 2001). Macropinocytosis is a distinctive pathway that collects large amounts of fluid-phase content. It occurs via the formation of membrane protrusions called macropinosomes, which collapse and fuse with the plasma membrane instead of zipping up the particle in phagocytosis. Macropinosomes are heterogeneous in size and mainly uptake particles that are larger than 200 nm in size (Hewlett *et al*., 1994, Swanson and Watts, 1995). CvME begins with the formation of a caveola, which is a flask-shaped structure in the cytoplasmic membrane. This type of endocytosis is mainly specific to endothelial cells. Similar to CME, caveolae are receptor-mediated deep invagination pits with diameters ranging from 50–100 nm (Nichols, 2003, Wang *et al*., 2009). It has been demonstrated that PLGA NP/MPs utilise macropinocytosis for cellular internalisation (Sahin *et al*., 2017, Cartiera *et al*., 2009). While The mechanism of intracellular delivery of polyplexes and lipoplexes is examined to be caveolae-mediated endocytic (CvME) pathway (Elouahabi and Ruysschaert, 2005, Selby *et al*., 2017). Figure 1-1 illustrates various intracellular pathways of NP/MPs.

Surface charge of the NP/MPs is another important factor that dictates the process of their internalisation through the plasma membrane. Positively charged NP/MPs easily attach to the plasma membrane through their electrostatic interaction with the negatively charged proteoglycans and glycoproteins in the plasma membrane which in turn facilitates their cellular

internalisation. On the other hand, neutrally charged or negatively charged NP/MPs' rate of cellular internalisation are known to be lower than that of positively charged NP/MPs due to less their interaction or repulsion with the cell membrane, respectively (Villanueva *et al*., 2009, Mailander and Landfester, 2009).

Other highly invasive non-endocytic pathways have also been investigated, and are mainly associated with physical methods of gene transfer such as microinjection or cell membrane pore formation (Xiang *et al*., 2012, Gascón *et al*., 2013).

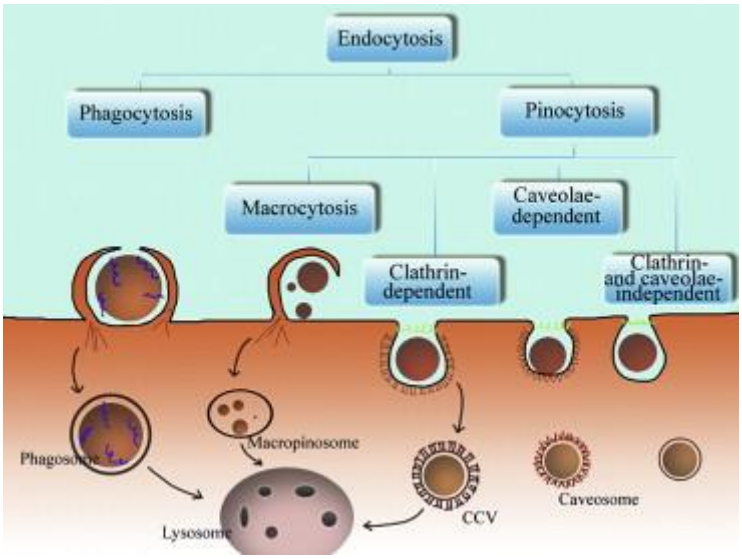

Figure 1-1 Cellular internalisation pathways of NP/MPs. Phagocytosis occurs mainly in professional cells such as macrophages, and other immune cells. CME is a widely shared receptor dependent pathway of nanoparticle internalization characterised by the formation of 100–150 nm pits at the cellular level. CvME occurs in typical flask-shaped invaginations of the membrane of around 50–100 nm. Macropinocytosis is engulfing larger NP/MPs with a poor selectivity. Image is from (Kou *et al*., 2013).

1.4.4 Endosomal escape

Endocytosis is the primary method of the cellular internalisation of non-viral gene vectors. Endosomes are another major barrier to efficient gene delivery, and form directly after the internalisation of the vector. They are highly dynamic recycling intracellular structures that start with the formation of the early endosome, in which the pH drops from neutral to a pH of 6. The next stage in the vector trafficking process is late endosome, which is characterised by the acidic pH of 5 as a result of the membrane proton-pump effect. Late endosomes are then fused with lysosomes, which acidify rapidly to around pH 4.5 along with the presence of other degradative enzymes. The non-viral gene delivery vector usually degrades in these harsh acidic and proteolytic conditions (Mellman *et al*., 1986, Pack *et al*., 2005, Khalil *et al*., 2006). Therefore, non-viral gene delivery vectors have adopted mechanistic approaches that are likely to increase the endosomal escape of the vector. Such mechanisms include membrane fusion and the proton-sponge effect (Thomas and Klibanov, 2003, Durymanov and Reineke, 2018). It has been reported that some liposomes, such as DOPE, can transition from a bilayer to a hexagonal structure that can fuse to the endosomal membrane and result in the endosomal escape of the vector (Koltover *et al*., 1998, Noguchi *et al*., 1998). Moreover, PEI has high buffering capacity due to the protonation of their amine groups in the acidic environment of endosomes and the subsequent influx of chloride ions and the osmotic rupture of the

endosome, thereby releasing the vector (Figure 1-2) (Akinc *et al*., 2005, Kichler *et al*., 2001, Grant *et al*., 2018).

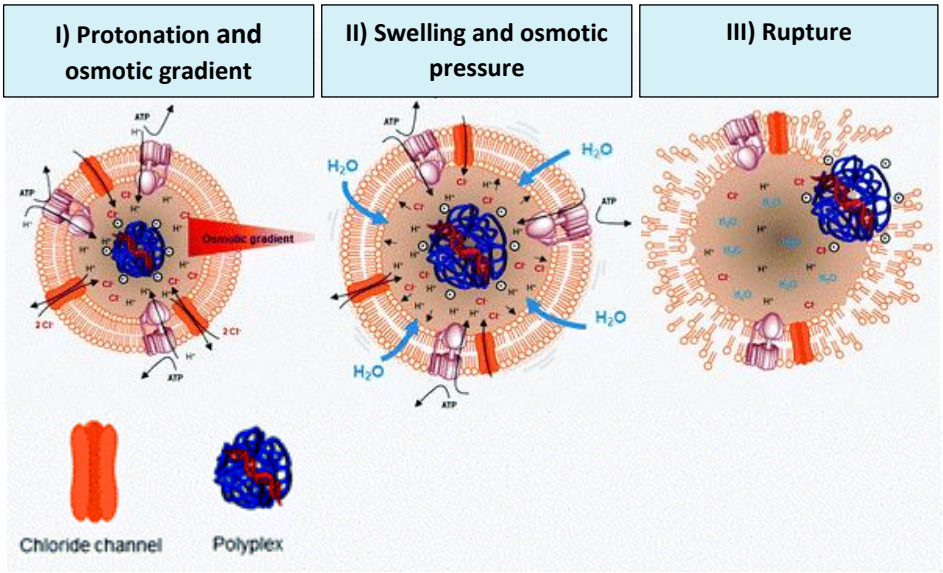

Figure 1-2 schematic illustration of the proton-sponge effect of polyplexes (PEI). The polyplex protonates in the acidic late endosome due to its buffering capacity (I) Osmotic imbalance is caused by the influx of chloride ions. (II) Entrance of water, as result of this osmotic imbalance, causes swelling of the endosome (III) Release of the polyplex due to endosomal rupture. Image is modified from Grant *et al*., 2018.

1.4.5 Intracellular trafficking

After endosomal escape of the carrier vector, the nucleic acid must then traffic to the nucleus for gene expression to occur. The cytosolic microenvironment represents another barrier for efficient gene delivery. Firstly, the cytoplasm contains nucleases that degrade unprotected DNA (Davis, 2002, Gottfried and Dean, 2012). Studies have demonstrated that non-complexed pDNA is degraded in the cytosol within 50 to 90 minutes (Lechardeur *et al*., 1999). Unpackaging of the DNA from the delivery vector may occur upon endosomal escape or any time thereafter. Opening the

packed DNA too soon is problematic due the degradation of the nucleic acid by intracellular nucleases (Luo and Saltzman, 2000, Forrest and Pack, 2002). For example, cationic lipids mediate endosomal escape partly through lipid exchange at the membrane level. This process facilitates the endosomal escape and the release of the nucleic acid from lipoplexes in to the cytoplasm at the same time (Koynova *et al*., 2007, Wittrup *et al*., 2015). This feature of lipoplexes poses a problem for the stability of the released DNA due to cytoplasmic enzymatic degradation. On the other hand, polyplexes are more stable and allow the release of the DNA complex form the endosome in a NP/MP form (Forrest and Pack, 2002, Ni *et al*., 2019). The DNA then may be released in the cytoplasm upon interaction and charge exchange of the cationic polymer with anionic cellular components (Huth *et* al., 2006, Schaffer *et al*., 2000). This feature of the cationic polymers allows improved stability of the DNA in the cytoplasm. Secondly, the released DNA from lipoplexes or polyplexes faces another barrier in the cytoplasmic crowded environment. This environment forms diffusional barriers to the DNA to reach the nucleus. Therefore, it difficult for the DNA to diffuse towards the nucleus if it was released from the packaging vector at a distant site from the nucleus (Clamme *et al*., 2003, Bai *et al*., 2017). This poses an additional problem for some of the early released DNA from lipoplexes (Zabner *et al*., 1995). On the other hand, studies have shown that released DNA from polyplexes uses the microtubule cellular machinery to traffic to the nucleus. This occurs through its indirect binding to these microtubules via transcription factors (Mesika *et al*., 2005, Badding *et al*., 2012).

Moreover, other methods such as nuclear localization signal peptides (NLS) (Misra and Sahoo, 2010, Greb-Markiewicz *et al*., 2018), Fibroblast growth factors (FGF) (Fisher *et al*., 2000, Davis, 2002) enhance the delivery of polyplex mediated gene delivery vectors to the nucleus.

1.4.6 Nuclear import

Nuclear membranes form the last barrier to the vector trafficking process inside the cells after their internalisation. Research has shown that 1-37 % of the DNA present in the cytoplasm after their release from the endosomes is localised in the nucleus (Cohen *et al*., 2009, Glover *et al*., 2010). Nuclear internalisation of DNA mainly occurs via cellular division, which means that the transfection of non-dividing primary cells is even more difficult. Studies have shown that 30-100 times more plasmid DNA was required when microinjected into the cytoplasm of non-dividing cells to produce the same levels of transfection as in dividing cells using the same procedure (Dean *et al*., 1999, Ludtke *et al*., 2002).

1.5 Glycosaminoglycan binding Enhanced Transduction (GET) peptides

Strategies to improve the delivery and transfection levels of non-viral vectors are still ongoing. However, the intracellular levels of their genetic payload are still not enough to produce therapeutic effects, Moreover, it is important to consider the prerequisite of balance between safety and efficacy in research concerning the enhancement of transfection (Katz *et al*., 2013, Jones *et al*., 2013). Numerous NP/MP designs that allows superior

transfection activities have been developed. However, their cytotoxic effects have hampered their widespread application (Kim and Eberwine, 2010, Caffery *et al*., 2019). CPPs are known to enhance the delivery of cargoes to the cytoplasmic and nuclear compartment of targeted cells. Moreover, they are associated with minimal toxicity in comparison to other cationic gene delivery tools (Derakhshankhah and Jafari, 2018, Chugh *et al*., 2010, Habault and Poyet, 2019). However, inefficient delivery has hindered their use in biomedical applications (Richard *et al*., 2003). Glycosaminoglycan binding Enhanced Transduction; GET peptides (Dixon *et al*., 2016, Eltaher *et al*., 2016, Thiagarajan *et al*., 2017, Spiliotopoulos *et al*., 2019, Osman *et al*., 2018, Raftery *et al*., 2019, Abu-Awwad *et al*., 2017) are delivery peptides that enhance the transduction and endosomal escape of cargoes for efficient gene transfection. They contain Heparin Sulphate (HS) binding domain (HBD) that specifically bind to cell surface glycosaminoglycans (GAGs) which concentrate the cargo on cell membranes, combined with CPP and endosomal escaping peptide elements to mediate uptake and escape, respectively. Our group have previously published the enhanced delivery characteristics and the versatile use of GET peptides termed PR (P218R), PLR (P21LK158R) and FLR (FGF2BLK158R). These sequences can be used as synthesized L-amino acid peptides or recombinant protein fusions to deliver recombinant or native proteins, pDNA, mRNA, siRNA, and magnetic NPs (Dixon *et al*., 2016). Importantly, their utility in regenerative medicine has been shown by delivering transcription factors such as RUNX2 and MYOD for osteogenesis and zonal myogenesis in a three-dimensional gradient

(Thiagarajan *et al*., 2017, Eltaher *et al*., 2016) respectively. Moreover, GET peptides have been used to enhance the delivery and transfection of nucleic acids for lung gene therapy and gene activated scaffold bone regeneration *in vivo*, (Raftery *et al*., 2019, Osman *et al*., 2018). The later delivering growth factor (GF) genes to enhance the repair of a critical size calvarial bone defect in rats (Raftery *et al*., 2019). The first generation of these GET peptides, PR and PLR comprises of P21 HBD. P21 is a short peptide (KRKKKGKGLGKKRDPCLRKYK) which has been isolated from epidermal growth factor (EGF) that specifically binds to HS molecules on the cell surface (Sakuma *et al*., 1997, Dixon *et al*., 2016). The later generation of GET; FLR, contains FGF2B. FGF2B is a short 16-residue peptide (TYRSRKYTSWYVALKR) that has been isolated from fibroblast growth factor 2 (FGF2) (Chua *et al*., 2004, Lee *et al*., 2007, Osman *et al*., 2018). Owing to their high negative charges (Jung *et al*., 2016), HS on the cell membrane interact non-specifically through electrostatic interaction with the positively charged GET peptides and specifically thorough P21 and FGF2B to enhance the cellular association of cargoes.

1.6 Applications of non-viral gene delivery in bone regeneration

Bone autografts and allograft transplantation are the gold standard treatments for major bone loss. However, major drawbacks of these treatments include donor-site morbidity, the limited availability of autographs, the risk of disease transmission and immune rejections of allographs (Yang *et al*., 2018a, Wu *et al*., 2018). Bone tissue regeneration

through the delivery of recombinant GFs is a well-established method. However, the instability of the protein and its degradation soon after its introduction to the site of injury (James *et al*., 2016, Shields *et al*., 2006) means that there is a need for supra-physiological concentrations to maintain its action within the therapeutic level. This means that dosages in orders of milligrams of these GFs are required. These high levels of GFs are associated with serious side effects such as ectopic bone formation, osteolysis, immune responses and neurotoxicity (Lewandrowski *et al*., 2007, Tannoury and An, 2014). Moreover, the use of recombinant proteins increases the overall cost of the treatment due to the high costs involved in utilising the eukaryotic cells that are needed for the correct folding and glycosylation of the produced protein and/or repeated administration (Evans, 2012, Balmayor and van Griensven, 2015).

Originally assigned for the correction of genetic defects, applications of gene therapy are expanding to other areas, including tissue regeneration. In this case, gene therapy is meant to accelerate or replicate a biological process that has occurred naturally in the body. This process is achieved via the delivery of genetic material encoded for cytokines, GFs and morphogens (Krebsbach *et al*., 2000, Partridge and Oreffo, 2004, Franceschi *et al*., 2004). The best example is bone regeneration via the delivery of plasmid encoded for Bone Morphogenic Protein 2 (BMP2) and platelet-derived GF (PDGF) (Yue *et al*., 2015, Chen *et al*., 2015b) in extensive bone loss following non-union fractures, bone resections, osteosarcomas or bone infections (Krebsbach *et al*., 2000, Partridge and Oreffo, 2004).

Triggering MSCs to produce elevated but not supra-physiological levels of GF, either from their own genome or via delivered ectopic transgenes, is a smart approach that does not rely on recombinant proteins. This can be achieved through the upregulation of the bone differentiation gene regulatory network by transcription factors (Thiagarajan *et al*., 2017) or by direct gene delivery to express new GF encoded pDNA copies. In this case, the lower level of produced protein from transfected cells is more physiologically relevant than current approaches resulting in minimal or no off-target effects when applied *in vivo* (Raftery *et al*., 2019, Lieberman *et al*., 1998).

The gene delivery approach can be applied *in vivo* or *ex vivo,* where the gene therapy product is injected into the site of injury, or autologous MSCs are manipulated by the gene therapy product *ex vivo* and returned to the body. Many researchers have applied a single GF encoded gene (Pola *et al*., 2004, Tierney *et al*., 2012), while others have encoded multiple GFs at a time (Peng *et al*., 2002). The combination of GFs has proven to be advantageous in enhancing bone differentiation. Moreover, the incorporation of therapeutic gene encapsulated NP/MPs within tissue engineering solutions could provide a bridge between macro-sized tissue engineering constructs and biological constituents at the molecular level. These features are required to improve the properties of the tissue engineering constructs, such as by providing greater control of the release of bioactive molecules from the NP/MP incorporated in the tissue engineering construct rather than the release of the bioactive molecule from the large-scale construct (Perez *et*

al., 2013, Cheng *et al*., 2015, Park *et al*., 2012). Furthermore, limitations such as the rapid clearing or the short circulation and half-life of GFs and cytokines released on the large-scale scaffold could be addressed with the nano-scale release of these incorporated gene encapsulated NP/MPs (Fathi-Achachelouei *et al*., 2019, Shi *et al*., 2010, Hasan *et al*., 2018).

1.6.1 Cell therapy in bone regeneration

Many cells have been nominated as precursors for bone differentiation *in vitro*. Amongst them, embryonic stem cells (ESCs) and mesenchymal stem cells (MSCs) are the stem cell types that are used most often. ESCs are totipotent and can differentiate to any cell lineage including bone. On the other hand, MSCs are multipotent and can only differentiate to several lineages, which are typically bone, cartilage and fat, tendons and, occasionally, neurons and muscle tissues (Caplan, 1991, Buttery *et al*., 2001, Pittenger *et al*., 1999, Chaudhury, 2012, Linard *et al*., 2018, Urrutia *et al*., 2019). The advantages of the use of MSCs over ESCs for bone differentiation are reduced chances of tumour formation when using MSCs due to their lower plasticity, and no association with ethical issues. Moreover, they are intrinsically immunomodulatory cells that not only lack immune responses but also balance immune reactions by modulating the effect of T cells and B cells (Herberts *et al*., 2011, Noronha *et al*., 2019, Girdlestone, 2016).

The classical characterisation of MSCs *in vitro* is their ability to differentiate to at least the three mesodermal lineages of bone, cartilage and adipocytes in cell culture dishes (Dominici *et al*., 2006, Pittenger *et al*., 1999). MSCs are

abundant in the body, primarily in bone marrow, muscle and adipose tissue. However, their potential for bone differentiation could vary, with MSCs derived from bone marrow being identified as the most reproducible source for bone differentiation *in vitro* (Xu *et al*., 2017).

In vivo bone regeneration in experimental animals requires several components for improved bone differentiation results. MSCs are the most frequently applied precursor cell lineage for advanced bone tissue regeneration strategies. Studies that use biomaterials in conjunction with exogenous MSCs or those that rely on endogenous populations have shown significantly enhanced bone formation in critical-size defects when GFs (Kolambkar *et al*., 2011, Baylink *et al*., 1993, Osman *et al*., 2018) and gene encoded GF are ectopically employed. Therefore, the combination of gene and cell therapy in bone regeneration is more effective than is applying each separately (Amini *et al*., 2012, Guldberg *et al*., 2007).

1.6.2 Bone differentiation during development/injury

Bone is a highly specialised connective tissue that is composed of living cellular and structural compartments (Dimitriou *et al*., 2011). The process of bone regeneration during development, maintenance/continuous remodelling, and minor bone losses is similar and comprises highly regulated series of bone formation and resorption as a result of cellular and extracellular signalling pathways (Einhorn, 1998, Cho *et al*., 2002). Unlike other injured tissues, the newly regenerated bone is an exact replica of the original or the unaffected surrounding bone without the formation of scar

tissue (Dimitriou *et al*., 2011). Three types of cells are involved in bone formation and maintenance process *in vivo*, namely osteoblasts, osteocytes and osteoclasts. These cells work in harmony to maintain bone volume and structure (Rodan, 1992, Piette *et al*., 1985). The two mechanisms whereby bone starts to develop are intramembranous or endochondral ossification depending on whether the type of bone is long or flat. Intramembranous bone regeneration starts with MSC recruitment to form bone marrow, mitosis and differentiation into osteoblasts (Kofron and Laurencin, 2006). With regard to endochondral ossification, hypertrophic chondrocytes start to provide the environment for bone development by forming calcified areas in the cartilage and drawing MSCs to differentiate into osteoblasts. These osteoblasts secrete a protein known as collagen 1, which forms the structure of the extracellular matrix. The differentiation of MSCs to osteoblasts is associated with the upregulation of osteogenic genes that include alkaline phosphatase (*ALP*), runt related transcription factor 2 (*RUNX2*), bone gamma-carboxyglutamate protein (*BGLAP*, also called osteocalcin), and secreted phosphoprotein (*SPP1*, also called osteopontin) during the course of differentiation (Hishikawa *et al*., 2004, Mundlos *et al*., 1997, Masuda-Robens *et al*., 2003, Lian *et al*., 1989).

1.6.3 Bone differentiation *in vitro*

MSCs are non-immunogenic and immunosuppressive by modulating the action of T cells, B cells and dendritic cells (Di Nicola *et al*., 2002, Bartholomew *et al*., 2002). Therefore, investigating the therapeutic

potential of these cells through testing their *in vitro* differentiation capacities is pivotal. MSCs are fibroblastic, spindle-shaped, colony forming cells (colony-forming unit-fibroblast; CFU-F) in culture dishes (Friedenstein *et al*., 1987, Owen, 1988). Osteogenic differentiation in culture dishes is a two-phase process. In the first phase, the MSCs differentiate into mature osteoblasts, while the second phase is the deposition of a mineralised matrix by these mature osteoblasts. Osteoblasts are cuboidal, post-proliferative, ALP positive cells that are recognised by their ability to excrete bone matrix proteins such as collagen 1 (Aubin, 1998).

In vitro bone differentiation involves feeding a confluent monolayer of MSCs with media supplemented with dexamethasone (Dex), beta-glycerophosphate and ascorbic acid for several weeks (Vater *et al*., 2011). Dex (glucocorticoid) has been described as an essential supplement in bone differentiation (McCulloch and Tenenbaum, 1986). (Leboy *et al*., 1991) concluded that Dex treated cultures as well as mineral deposition, they were characterised by elevated levels of *ALP* and osteopontin mRNA compared to cultures that had not been treated with Dex. The exact mechanism whereby Dex induces differentiation is unknown, however, some insights indicate that Dex activates RUNX2-dependent gene transcription via the improved expression of the b-catenin-like molecule TAZ and integrin α5 (Hong *et al*., 2009b, Hamidouche *et al*., 2009, Langenbach and Handschel, 2013). The effective concentration of Dex varies in different studies. 10 nM resembles the physiological concentration of glucocorticoid and is the ideal concentration for bone differentiation in some studies (Walsh *et al*., 2001,

Hong *et al*., 2009a), while others have reported that 100 nM is required for bone differentiation *in vitro* (Mostafa *et al*., 2012, Ghali *et al*., 2015, Jaiswal *et al*., 1997). Various parameters such as culture conditions, the source of the MSC, and the donor's age and species could affect the osteogenic potentials of these MSCs in culture dishes (Ding *et al*., 2013, Choudhery *et al*., 2014, Yuan *et al*., 2019, Zhou *et al*., 2013).

The presence of beta-glycerophosphate is essential for the release of inorganic phosphate ions (Pi) for mineral deposition. The need for the addition of ester phosphates such as beta-glycerophosphate in *in vitro* conditions originated from the fact that bone cells hydrolyse phosphoric esters in the blood to release inorganic phosphate ions specifically through the use of monophosphoric esterase, later named alkaline phosphatase enzyme (Robison and Soames, 1924, Chang *et al*., 2000, Robison, 1923, Siller and Whyte, 2018).

Ascorbic acid acts as a cofactor in the hydroxylation of the proline and lysine needed for the synthesis of collagen 1; this is the main type of collagen in ECM, plays a role in the elevation of *ALP* levels (Vater *et al*., 2011, Langenbach and Handschel, 2013). The more stable form of ascorbic acid (L-ascorbic acid 2-phosphate sesquimagnesium salt) is used in the culture conditions of 7.4, 37°C, a humidified atmosphere and 5% CO_2 (Takamizawa *et al*., 2004, Hata and Senoo, 1989).

1.6.4 BMP2 in bone differentiation

Several GFs have been identified as essential in bone formation *in vivo* and *in vitro.* These GFs are platelet-derived growth factor (PDGF), fibroblast growth factor (FGF), insulin-like growth factor (IGF), vascular endothelial growth factor (VEGF), and transforming growth factors (TGFs) that control the process of bone formation in a temporal special manner (Kofron and Laurencin, 2006). BMPs are members of the TGF beta (TGFβ) superfamily, and are the most frequently studied due to their potent and direct relationship with bone differentiation. The first study concerning bone induction properties of BMPs was their ability to induce ossification in decalcified bone matrixes when implanted intramuscularly (Urist, 1965). Later, with the advancement in recombinant DNA technology, it was recognised that BMP2, as well as BMP4 and BMP7, has potent osteoinductive (OI) properties when delivered in combination with biomaterials in bony defects (Johnson *et al*., 1992, Inoda *et al*., 2004, Smith *et al*., 2014). As it is FDA approved, (Valentin-Opran *et al*., 2002, Friedlaender, 2004), BMP2 has attracted a great deal of research focus in bone regeneration by means of gene delivery.

Molecular mechanisms whereby BMP2 influences bone formation include the Wnt/βcatenin pathway during postnatal development (Silverio *et al*., 2012). The same mechanism has been detected during ALP activation as a result of BMP2 induction of C3H10T1/2 and C2C12 (Bain *et al*., 2003, Rawadi *et al*., 2003), MC3T3-E1 (Zhang *et al*., 2013, Fu *et al*., 2017) mouse cell lines

and MSCs (Harris *et al*., 2003, Zhao *et al*., 2002) into osteoblasts *in vitro* BMP2 itself is regulated via other bone factors and signalling pathways, including TGF-β, hedgehog/Gli, PTH/CREB, oestrogen receptors and PGE2 (Arikawa *et al*., 2004, Zhang *et al*., 2011).

1.7 Aims and Objectives

The aim of this work is to enhance the intracellular delivery and transfection of PLGA NP/MPs with GET peptides. Moreover, to examine the biomedical applications of enhanced PLGA NP/MPs transfection in bone differentiation to potentially develop safe and effective non-viral methods for gene delivery.

The novelty of this study is the enhanced delivery and transfection of PLGA NP/MPs with GET peptides. As far as is known, this is the first study of its kind in which the nucleic acid protection characteristics of PLGA NP/MPs have been combined with the enhanced intracellular delivery and transfection characteristics of GET, and in which their application in stem cell differentiation has been tested.

The key steps and aims of the current project are as follows:

1. The fabrication of PLGA NP/MPs and testing the effect of formulation parameters on the size, morphology and structure of these NP/MPs to obtain PLGA NP/MPs that are suitable for intracellular delivery and gene transfection.

2. The encapsulation of pDNA in the PLGA NP/MPs and the enhancement of the encapsulation process via the condensation of pDNA with low molecular weight cationic peptides to form small, positively charged pDNA NPs suitable for PLGA encapsulation.

3. The characterisation of the pDNA encapsulated PLGA NP/MPs and the development of experimental comparisons to control the process of encapsulation and to determine the potential pDNA NPs surface binding to PLGA NP/MPs by comparison to blank PLGA MPs and other experimental controls.

4. To study the complexation of PLGA NP/MPs with GET peptides in terms of the physico-chemical characteristics of the resultant PLGA-GET NP/MPs and their effect on intracellular delivery and transfection.

5. The comparison of GET peptides with their non-modified CPP forms in terms of intracellular delivery and the transfection of complexed PLGA NP/MPs.

6. To determine the effect of cell culture conditions on the PLGA-GET NP/MPs and subsequent physico-chemical characteristics and transfection.

7. To assess the colloidal stability, advantages and limitations of the PLGA-GET NP/MPs.

8. The application of the enhanced intracellular delivery and transfection characteristics of PLGA-GET NP/MPs in bone differentiation.

Chapter 2.

Materials and Methods

2.1 Optimisation of PLGA NP/MP fabrication

2.1.1 Preparation of PLGA NP/MPs by nanoprecipitation method

Nano/microparticles (NP/MPs) were prepared by modified nanoprecipitation technique (Morales-Cruz *et al*., 2012, Bilati *et al*., 2005a, Yadav and Sawant, 2010, Fessi *et al*., 1989b). PLGA polymer (with terminal carboxyl group, PLGA, 50:50, Mw 52000 Da from Rosemer Evonic) was used for all types of NP/MP preparation. 50 mg or 20 mg of PLGA polymer was dissolved in 1 ml of Dimethylformamide (DMF, molecular biology grade, Sigma, UK) or Dimethyl Sulfoxide (DMSO, 99.8+ % anhydrous, Alfa Aesar) to prepare 5 % and 2 % (w/v) polymer concentration, respectively. DMF and DMSO solvents were chosen due to their miscibility with water and low concentrations of 5% and 2% of PLGA were applied to produce uniform relatively small PLGA particles. For preparation of blank NP/MPs, PLGA alone was dissolved in the organic solvent. The clear solution was added dropwise by a micro syringe pump using 21G needle at a rate of 0.5 ml/min to magnetically stirring 20 ml of 0.5 % Pluronic F127 (Sigma, UK) aqueous solution at 600 rpm. The formed NP/MPs were collected by centrifugation at 20,000 x g at 4 ˚C for 1 hr. To remove the residual DMSO, the NP/MP pellet was re-suspended/washed in the same volume of Pluronic solution and filtered through a 0.45 µm nitrocellulose filter (MF-Millipore, Merk) followed by centrifugation at the same rate. The PLGA NP/MPs were re-suspended in Trehalose solution (1:1.5) by weight (from 1.6 % (w/v) stock solution) (Sigma, UK), respectively. These NP/MPs were frozen quickly in -80 ˚C then freeze

dried for 24 hours and stored at -20 ˚C for physico-chemical characterisation and delivery to cells.

2.1.2 Preparation of PLGA MPs by double emulsion W/O/W solvent evaporation method

PLGA MPs were also prepared by double emulsion method (Dördelmann *et al*., 2014). Three different concentrations of PLGA and two different concentrations of stabiliser were tested. 10 or 4 mg of PLGA 5050 was dissolved in 750 µl of Dichloromethane (DCM, analytical grade, Thermo Fisher Scientific) (oil phase) to prepare 1.3 % and 0.5 % of PLGA, respectively. 250 µl of water was added to the oil phase to prepare blank MP (W/O). 40 µl aqueous solution of 0.5 % (w/v) Bovine Serum Albumin (BSA Sigma, UK) was added to the oil phase as the inner phase surfactant. The W/O emulsion was sonicated for 20 sec. at 70 % amplitude and 70 % on, 30 % off time cycle on ice. The sonicated W/O emulsion was added to 3 ml of 1 % or 3 % (w/v) Polyvinyl alcohol (PVA, 86-89% hydrolysed, medium Mw, Alfa Aesar) solution to form W/O/W emulsion and sonicated again at the same rate and time. The whole system was agitated for 1 hour to allow for the evaporation of DCM. PLGA MPs were collected by centrifugation at 20,000 x g at 4 ˚C for 20 min and washed twice with deionised water to remove the residual PVA. The MPs were lyophilised as previously (Section 2.1.1) for physico-chemical characterisation. To measure the percentage yield of PLGA MPs using this method, the MPs were freeze dried without the addition of Trehalose and the percentage yield was calculated as below:

$$PLGA\ NP/MP\ yeild\ \% = \frac{amount\ of\ PLGA\ NP/MP\ recovered}{amount\ of\ initial\ PLGA\ used} * 100$$

2.2 Preparation of fluorescent dye encapsulated PLGA MPs

To prepare fluorescent dye encapsulated PLGA MPs, 1 mg of hydrophilic or hydrophobic fluorescent dyes: Atto 590 (Sigma, UK), and Nile Red (Thermo Fisher Scientific) were encapsulated in PLGA MPs, respectively. As well as these MPs, covalently conjugated FITC labelled PLGA MPs (a kind gift from Cameron Alexander, Boots Science Building, University of Nottingham) were used in a ratio of 30/70 labelled/unlabelled PLGA for the transduction studies below (Section 2.13).

2.3 Preparation of Plasmid DNA (pDNA)

5764 base pair (bp) Gluc luciferase expression vector reporter plasmid DNA (pDNA) expressing *gaussia* luciferase (*Gluc*) from New England Biolabs (pGluc) was used for luciferase assays. For Bone differentiation assays, 3486 bp *BMP2* expressing pDNA (pBMP2) was a kind gift from Royal College of Surgeons in Ireland (RCSI) and that used in Raftery *et al*., 2019. Both plasmids are driven by cytomegalovirus (CMV) enhanced promoter. The plasmids were transformed in DH5α competent Escherichia coli (*E.coli)* cells and purified by Maxi-prep kit (Qiagen, UK) according to the manufacturer's protocol. The plasmids were re-suspended in nuclease free not (DEPC) treated water (Qiagen) and store at -20 ˚C.

2.4 DNA fluorescent labelling

pGluc was labelled with MFP488 proprietary pH stable green dye (Label IT® Nucleic Acid Labelling Kit, Mirus Bio LLC, Cambridge, UK) according to manufacturer's instruction. Using 1:1 (v:w) ratio of Label IT® Reagent to nucleic acid results in a labelling density of 1 label per every 20-60 bases of nucleic acid.

2.5 Preparation of pDNA NP/MPs

Condensing agents; isopropanol (molecular grade; Thermo Fisher Scientific), low 1000-5000 Da and high molecular weight (Mw) 30,000-70,000 Da Poly L-Lysine hydrobromide (PLL) (Sigma, UK) were used in the optimisation of pDNA NP/MPs preparations for encapsulation in PLGA MPs. A 5764 bp pGluc luciferase expression vector or 3486 bp pBMP2 vector was complexed with PLL in a charge ratio of 1, 3, 6, 9, and 12 (+ amine groups in PLL/- phosphate groups in pDNA). The NP/MPs were formed by dropwise addition of pDNA solution to PLL solution using a P200 pipette tip while vortexing. Only low Mw PLL condensed pDNA NPs (named pDNA-PLL NPs hereafter) at charge ratio of 12 were used in the encapsulation studies. At this charge ratio, the working concentration of pDNA and PLL was 40 μg/ml and 200 μg/ml in nuclease free water respectively (Wolfert and Seymour, 1996). PLL powder was reconstituted and the solution was used within three months from the preparation date according to the manufacturer's instructions.

For the encapsulation studies, 100 µg of pGluc or pBMP2 was complexed with 500 µg of PLL by adding every 10 µg of pDNA to 50 µg of PLL. This mixture of pDNA-PLL NPs in a volume of 5 ml was then concentrated to a total volume of 250 µl using Amicon® Ultra Centrifugal Filters units (Thermo Fisher Scientific). This volume was then used in the encapsulated in PLGA NPs.

pBMP2-FLR NPs; control in bone differentiation studies were prepared by complexing 3486 bp pBMP2 vector with FLR in charge ratio of six (+/-) in serum reduced media; Opti-MEM (Gibco, UK) following a previous protocol (Dixon *et al*., 2016, Osman *et al*., 2018). 0.5 µg of pBMP2 was added to 0.5 µl of FLR peptide (from 1mM stock solution) in a final volume of 50 µL. The mixtures were left to electrostatically interact for 15 min at room temperature.

1 µg pGluc complexed with 1 µl PLR peptide (from 1mM stock solution) in was used as a positive control in transfection studies (Dixon *et al*., 2016). These pGluc-PLR NPs were transfected in NIH3T3 cells (seeded at 100k per 1.9 cm^2 in a 24-well plate). pDNA and GET peptides solutions were always stored on ice during pDNA NP preparation. To determine the enhanced effect of PR in transfection, 1 µg of MFP488 labelled pGluc was complexed with 1 µl of 1 mM PR or PLR in a total volume of 50 µl. pDNA NP/MPs refers to the condensation of pDNA with any of the condensing agents (isopropanol, PLL, PR, PLR and FLR). pDNA-PLL NPs refers to either pGluc-PLL

or pBMP2-PLL. NPs refers to particles ≤ 100 nm by number size distribution. MPs refers to particles >100 nm by number size distribution.

2.5.1 PicoGreen binding assay

A range of consecrations of naked pDNA and pDNA-PLL NPs were complexed with PicoGreen fluorescent dye; Quant-iT PicoGreen dsDNA (double stranded DNA) Assay Kit (Thermo Fisher Scientific). The fluorescence intensity of the dye complexed with naked pDNA and pDNA-PLL NPs was measured at excitation and emission wavelengths of 480 and 520 nm using a plate reader (TECAN Infinite PRO). To allow comparison between replicates, the gain was set manually at 98 % for all pDNA quantification assays.

2.5.2 Dissociation of pDNA-PLL NPs

pDNA-PLL NPs were dissociated by the addition of polyanion; poly L-aspartic acid sodium salt (PAA) of Mw of 4100 Da (Alamanda Polymers). 1X (5 µg) and 10X (50 µg) concentration of PLL were tested. The amount of released pDNA from pDNA-PLL NPs after 1 hour PAA treatment was measured and compared to 1 µg naked pDNA control using Quant-iT PicoGreen dsDNA Assay Kit as previously (Section 2.5.1). PLL and PAA solutions were used as negative controls.

2.6 Preparation of pGluc and pBMP2 encapsulated PLGA NP/MPs

Nanoprecipitation and Double emulsion (W1/O/W2) were applied to encapsulate pGluc-PLL and pBMP2-PLL NPs (W1) into PLGA NP/MPs. For nanoprecipitation, parameters described in Section 2.1.1 was employed. To encapsulate naked pDNA by nanoprecipitation, the naked DNA was dissolved in pH reduced (pH 4.5) aqueous phase. To encapsulated pDNA-PLL NPs in nanoprecipitation, pDNA-PLL NPs were included in the aqueous phase. For double emulsion, only one optimized experimental setup was chosen for DNA encapsulation. 10 mg of PLGA polymer was dissolved in DCM at a concentration of 1.3 % (w/v) and used as the oil phase (O). 40 µL an aqueous solution of 0.5 % BSA (w/v) was applied as the inner phase surfactant. The aqueous phase (W1; pDNA-PLL NPs +BSA solution) was sonicated in the oil phase for 20 sec. at 70 % amplitude and 70 % on, 30 % off time cycle on ice. The first emulsion was immediately poured into 3 % (w/v) PVA aqueous solution (W2) and sonicated again at the same rate. The mixture was rotated at 600 rpm for 1 hour to allow DCM evaporation and PLGA MP formation. The PLGA MPs were collected by centrifugation at 20,000 x g at 4 ˚C for 20 min and washed twice with deionised water to remove excess PVA and unbound pDNA. The PLGA MPs were re-suspended in Trehalose solution (1:1.5) by weight (from 1.6 % (w/v) stock solution) respectively then freeze dried and stored at -20 C˚ for further use. 100 µg of naked pDNA in 250 µl nuclease free water instead of pDNA-PLL NPs was also encapsulated in PLGA MPs using double emulsion method described above.

These DNA encapsulated PLGA MPs were used in the transfection studies in Section 2.13.

2.7 Characterisation of pDNA NP/MP and PLGA NP/MPs

2.7.1 Size measurements

pDNA and PLGA NP/MPs hydrodynamic size were measured by Dynamic Light Scattering (DLS) at 173° detection angle using Malvern Zetasizer Nano Zs instrument. Briefly, lyophilised PLGA NP/MPs was re-suspended at a concentration of 10 µg/ml with deionised water and bath sonicated before each measurement. The 1 ml aliquots were then transferred to 4 ml disposable Cuvettes and passed through the laser light. The size was measured according to the Mie theory where the intensity of light produced by particles is proportional to particle diameter.

pDNA NP/MPs were characterised using DLS at pDNA concentration of 1 µg/50µl in 40 µl cuvette disposable cells. The measurements are presented as mean value ± standard deviation (mean ± SD).

PDI values were also recorded to detect heterogeneity in the NP/MP population. Refractive Index (RI) of 0.1 and 1.332 was manually imputed in the Standard Operating Procedure (SOP) for each of PLGA and pDNA, respectively. The viscosity of water was automatically set up in both SOPs. A total of three readings were taken per replicate. Measurements were recorded at 25 ˚C. The size distribution by intensity was converted to number distribution when the size of NP/MPs from the Zetasizer and

microscopic imaging (TEM) were compared. The conversion was carried out for samples passed the quality report criteria only.

2.7.2 Zeta potential measurements

Surface charge of pDNA NP/MPs, PLGA NP/MPs, PLGA-GET MPs was measured using Malvern Zetasizer Nano Zs. A minimum of 800 µL of each of the NP/MPs solution at the same concentrations above (Section 2.7.1) were analysed in disposable capillary cells. The cells were rinsed with 70 % ethanol to prevent bubble formation prior to the sample loading. Measurements were recorded at 25 ˚C. An average of three measurements per replicate was recorded.

2.7.3 Morphology

To demonstrate the morphology of pDNA NP/MPs and PLGA NP/MPs, one drop of each sample in solution was placed on a Holey Carbon Film on 300 Mesh Copper grid and allowed to dry. The samples were imaged using FEI Tecnai BioTwin-12 TEM. These TEM images were also used to measure the size of these NP/MPs and compare the size results from the Zetasizer and TEM. The arbitrary distance measurement tool was used to measure the diameter of individual NP/MPs during imaging.

2.8 Measurement of the encapsulation efficiency (EE%)

To measure the EE % of pDNA-PLL NPs in PLGA NP/MPs, 5.5 mg of pDNA encapsulated PLGA NP/MPs were dissolved in 1 ml DCM. 1ml of 1X TE buffer (Tris-EDTA, Thermo Fisher Scientific) aqueous solution was added to the

dissolved PLGA NP/MPs to extract the encapsulated pDNA. The immiscible mixture of DCM/aqueous layer was separated by brief centrifugation. The aqueous layer was then transferred to a fresh Eppendorf. The EE % was measured by the direct method in which the amount of pDNA detected from the solubilised PLGA NP/MPs was subtracted from the total amount of pDNA used as equation below and this EE % was taken into account when characterising pDNA encapsulated PLGA NP/MPs. pDNA-PLL NPs and naked pDNA was used to construct a standard curve to measure the EE % of each of pDNA-PLL NPs (Ribeiro *et al*., 2005) or naked pDNA, respectively. Freshly prepared standard curves were used in every measurement. The amount of pDNA was calculated using Quant-iT PicoGreen dsDNA Assay Kit as previously (Section 2.5.1).

$$Encapsualtion\ Efficiency\ \% = \frac{amount\ of\ pDNA\ detected}{Total\ pDNA\ content} * 100$$

2.9 In vitro release study

To measure the release of pDNA-PLL from the PLGA MPs, 5.5 mg of lyophilised pDNA encapsulated PLGA MPs were incubated in 1 ml of Phosphate-Buffered Saline (PBS) at 37 ˚C for 40 days. To detect the released pDNA, the PLGA MPs in 1 ml PBS were centrifuged and the 1 ml supernatant was collected during every measurement. The first supernatant was collected after the first 24 hour followed by collection at three day intervals. The amount of released pDNA was measured using Quant-iT PicoGreen detection assay as previously using pDNA-PLL standard curve.

2.10 Bacterial transformation studies

To determine the effect of sonication on supercoiling and integrity of pDNA during formulation, equivalent of 1 ng pDNA from sonicated and non-sonicated naked pDNA, pDNA-PLL NPs (controls) and pDNA-PLL extracted from PLGA MPs samples was transformed into competent DH5α *E-coli* and the number of bacterial colonies were compared.

2.11 DNase protection Assay

To confirm the pDNA protection ability of PLGA MPs, 0.5 µg of naked or encapsulated pDNA was incubated with increasing concentrations of DNase I at 37 ˚C for 15 min. DNase I was prepared by diluting DNase I stock solution of 2.72 U/µl to 0.025 U/µl, 0.0025 U/µl and 0.00025 U/µl in DNase buffer according to the manufacturer's instruction (RNase-Free DNase kit, Qiagen). The buffer was 2.5 mM magnesium chloride and 1 mM Calcium chloride in PBS. The digestion reaction was stopped by adding EDTA at 0.5 M final concentration. Naked pDNA and pDNA encapsulated PLGA MPs were run on 1 % (w/v) agarose gel against 1-5 kb pDNA ladder in 1X TAE (Tris-acetate-EDTA) buffer with Ethidium bromide (EtBr). The gel was run at 85 volts for 25 min and imaged on Luminescence Image Analyser (LAS-4000).

2.12 Preparation of PLGA-GET MPs

Lyophilized PLGA MPs was re-suspended in PBS at a concentration of 0.2 mg/50µl and complexed with the GET peptides (transfection media). The mixture was left to electrostatically interact for 15 min at room temperature.

To confirm the formation of PLGA-GET MPs by Zeta potential measurements, this volume was diluted to 10 µg/ml and measured by the zeta sizer (described in Section 2.7.1).

2.13 Transduction and transfection studies

NIH3T3 were transfected with pDNA encapsulated PLGA MPs. IHMSCs were used to deliver pBMP2-FLR (control) and pBMP2 encapsulated PLGA MPs for bone differentiation assays. The IHMSCs were maintained in expansion media; Dulbecco's modified Eagle medium (DMEM) supplemented with 20 % (v/v) FCS, 2 mM L-glutamine, 100 units/ml penicillin, 100 mg/ml streptomycin and 1 % Antibiotic/Antimycotic. The cells were passaged at 80 % confluency and used at passages below passage 20. For intracellular delivery, transfection and differentiation studies, NIH3T3 and IHMSCs were seeded at a density of 100k and 35k in 24-well plate culture dishes, respectively. The cells were then incubated overnight to allow attachment. For transduction and transfection studies with PLGA-GET MPs, the old media was removed, and cells were washed with PBS. 200 µl of GM or SFM media was added followed 50 µl transfection media (Section 2.12). Cells were incubated at 37 ˚C and 5 % CO2.

2.14 Fluorescent microscopy imaging

After overnight transduction studies and before imaging, the old media was removed, and the cells were washed extensively with PBS to remove any surface attached NP/MPs. The controls and transduced samples were

imaged using fluorescent microscope (Leica DM IRB) and the green light for Atto 590 and Nile Red encapsulated PLGA MPs and blue light for MFP488 labelled pDNA and FITC labelled PLGA MPs before being processed for flow cytometry.

2.15 Flow cytometry analysis

For flow cytometry, cells were trypsinized with trypsin/EDTA (0.25 % (w/v) trypsin/ 2 mM EDTA) and fixed with 4 % (w/v) paraformaldehyde (PFA). PLGA-GET MPs cellular internalization was quantified using a Beckman Astrios Cell Sorter and 590 nm laser for Atto 590 and Nile Red encapsulated PLGA MPs and 488 nm laser for MFP488 labelled pDNA and FITC labelled PLGA MPs (20,000 cells, gated on untreated cells by forward/side scatter). Mean fluorescence intensity was used for statistical analysis. Scatter plot and histogram graphs were produced using Weasel flow cytometry analysis software. Untreated cells were used as negative controls.

2.16 Metabolic activity assays

Metabolic activity of NIH3T3 and IHMSCs were detected after transfection with BMP-2-FLR, DNA encapsulated PLGA-GET MPs using Prestoblue assay. 200 µl of 10 % (v/v) of the reagent in HBSS (Hanks' Balanced Salt solution, Thermo Fisher Scientific) was added to 24-well plate. Prior to the addition of the reagent, the old media was removed, and the cells were washed with PBS trice. The reagent was left for 20-25 min. or until the colour of the untreated control samples changed to light purple.

2.17 Bone differentiation assays

The osteogenic assays were first optimised and adapted for FLR transfection. To do so, pBMP2-FLR NPs were made by mixing pBMP2 with FLR at a ratio charge (+/-) of six and a peptide final concentration of 2 µM in serum reduced media (OPTI-MEM) (Gibco, UK) as described previously (Raftery *et al*., 2019). IHMSCs were seeded, incubated overnight and transfected with 0.5 µg pBMP2-FLR NPs. DMEM/F12 Ham 1:1 (Life technologies, UK) supplemented with 10 % (v/v) FCS, 2 mM L-glutamine, 100 units/ml penicillin, and 100 mg/ml streptomycin, 50 µg/ml L-ascorbic acid 2-phosphate sesquimagnesium salt hydrate (Sigma, UK) and 10 mM b-glycerophosphate disodium salt pentahydrate (Acros Organics, UK) was used as basal media (BM). Osteopermissive (OP) and Osteoinductive (OI) media contained low (10 nM) and high (100 nM) Dexamethasone (Dex) in BM, respectively. These media combinations were used to test the effectiveness of pBMP2 delivery to induce bone differentiation. The cells were transfected and maintained in OP media (Thiagarajan *et al*., 2017). The media was changed twice a week until the end of osteogenesis study at week four. For bone differentiation with pBMP2 encapsulated PLGA MPs, 0.2 mg of PLGA MPs equivalent to 1 µg of encapsulated pBMP2 content was complexed with FLR at a final concentration of 4 µM of FLR. In both cases of pBMP2-FLR and pBMP2-encapsulated PLGA-FLR MPs, the cells were induced with a single transfection.

2.18 Alizarin Red staining

At week three, cells were checked microscopically for extracellular matrix and bone nodule formation. At week four, the osteogenic cultures were stained for calcium deposit using 2 % (w/v) Alizarin Red solution (Alfa Aesar). To do so, the cultures were washed trice with PBS and fixed with 4 % PFA (paraformaldehyde) followed by the removal of PFA and washing with deionised water three times. For stained calcium quantification, the stained cultures were washed three times with deionised water and Alizarin Red was extracted by the addition of 200 µl 10 % (v/v) acetic acid (Sigma, UK) for 30 minutes while shaking. The eluted stain was transferred to Eppendorf tubes and heated at 85°C for 10 minutes, cooled and neutralised with 10 % ammonium hydroxide (Sigma, UK). The absorbance was read at 405 nm on a plate reader (Gregory *et al*., 2004). Fold increase in absorbance was compared to controls maintained in Expansion media, OP or OI 10nm Dex (Gregory *et al*., 2004).

2.19 Gene Expression Analysis

Quantitative Reverse Transcription-Polymerase Chain Reaction (QRT-PCR) was used to detect the level of osteogenic genes upregulated. Total RNA was extracted from differentiated IHMSCs using RNeasy kit (Qiagen, UK). On column DNase I treatment was applied using RNase-free DNase kit (Qiagen). 0.4 µg total RNA was reverse transcribed in 20 µl reaction using SuperScript III Reverse Transcriptase (Life technologies) according to the manufacturer's protocol. QRT-PCR reaction was performed using Taqman assay. Osteogenic

genes (*ALP–Hs01029144_m1; RUNX2–Hs00231692_m; BGLAP–Hs01587814_g1; SPP1–Hs00959010_m1*) were detected against *B-actin* (*ACTB-Hs99999903-m1)* reference gene. Relative expression level was calculated using ΔΔCт method. Biological replicates number of five with three technical replicates was performed for each treatment. Reaction primers and probes were from Applied Biosystems, Life technologies, UK.

2.20 Statistical Analysis

Statistical analysis and graphs were generated using GraphPad Prism software package. Unpaired t-test and One-way Anova were used to determine significant variances between two treatments or more respectively. Two-way Anova was used for grouped data. One-way and two-way Anova were followed by Tukey test to determine significance between means in multiple comparisons. The data represented as mean ± SD. Variances between means were considered statistically significant with P values: 0.0332 (*), 0.0021 (**), 0.0002 (***) and < 0.0001 (****). Experimental number minimum of three was used in every experiment.

Chapter 3.

Encapsulation of pDNA in PLGA MPs

3.1 Introduction

The use of PLGA for the encapsulation of high and low molecular weight (Mw) molecules is a well-known practice in the field of pharmaceutical sciences. Many PLGA based FDA approved pharmaceutical products such as Vivitrol®, Lupron® and Sandostatin LAR® are currently in clinical use (Lu *et al*., 2009, Makadia and Siegel, 2011). PLGA has the benefits of being bio-inert and biocompatible for improved safety. Moreover, inclusive for nucleic acid, protection against nucleases is an added advantage of PLGA. Furthermore, control over the physical properties of PLGA NP/MPs for long-term storage makes them attractive candidates for the development of nucleic acid delivery vectors (Zhao *et al*., 2013, Adolph *et al*., 2014).

In this chapter, PLGA polymer was employed for the encapsulation of plasmid DNA (pDNA). Unlike low Mw drug molecules, pDNA is a biological hydrophilic negatively charged macromolecule. These characteristics limit its successful encapsulation in PLGA MPs. In this study, several PLGA NP/MP formulation parameters and methodologies were exploited for maximum pDNA encapsulation in PLGA MPs. Moreover, the different properties of condensing agents in producing more water insoluble, smaller sized and neutral or positively charged pDNA NPs were investigated. pDNA NPs that are more compatible with PLGA properties were produced for maximum encapsulation efficiency (EE). Definition of the physico-chemical properties

of pDNA NPs prior to their encapsulation in PLGA MPs is an important aspect in controlling the process of encapsulation and ensuring high EE%.

3.2 Optimisation of PLGA NP/MP fabrication

Prior to the encapsulation of pDNA in PLGA MPs, the fabrication process of blank PLGA NP/MPs was optimised to achieve optimum size, structure and morphology that are suitable for pDNA encapsulation and are within the range of intracellular delivery limits (Albanese *et al*., 2012, Blanco *et al*., 2015). To do this, the literature was examined for formulation parameters such as methods of preparation, the concentration of PLGA, and stabilisers and types of organic solvents that are known to affect the size of PLGA NP/MPs (Adebileje *et al*., 2017, Huang and Zhang, 2018).

3.2.1 Preparation of PLGA NP/MPs by modified nanoprecipitation method

Different formulation parameters were tested to optimise the size of blank NP/MPs. For modified nanoprecipitation (Bilati et al., 2005a, Morales-Cruz et al., 2012, Yadav and Sawant, 2010, Fessi et al., 1989b), two organic solvents were chosen based on their miscibility with water (non-solvent) and dielectric constant values. 50 or 20 mg of PLGA was dissolved in 1 ml of DMF or DMSO to prepare 5 % and 2 % (w/v) polymer concentrations, respectively. The PLGA NP/MPs were formed instantly, as the clear non-solvent solution turned cloudy upon the addition of the solvent containing the PLGA. The hydrodynamic size, shape, and surface charge of the PLGA NP/MPs prepared via modified nanoprecipitation were determined by Zetasizer Nano Zs and

TEM. Table 1 summarises the particle size and Zeta potential of blank PLGA NP/MPs prepared using the modified nanoprecipitation and double emulsion method. Moreover, Appendix 1 shows size and zeta potential measurements of multiple batches of PLGA NP/MPs. PLGA NPs prepared using the modified nanoprecipitation method at a low (2 %) concentration of PLGA were in the range of 100 nm and monodispersed with a PDI value of 0.14 ± 0.06 (mean ± SD). However, a higher PDI of 0.4 ± 0.22 and more polydispersed MPs sized 509 ± 417 nm (mean ± SD) were recorded when higher concentrations (5 %) of PLGA were used. Overall, by decreasing the PLGA concentration from 5 % to 2 % and changing the organic solvent from DMF to DMSO, a uniform and significantly smaller population of NPs was achieved ($p < 0.0001$) (Table 1, representative batch in Figure 3-1 and more replicates in Appendix 1 Section 8.1.1.1.2 and 8.1.1.2.2). The mass percentage (yield) after the NP/MPs were centrifuged, washed twice and freeze dried was 25 % of the original polymer mass used in the formulation. The morphology of these NP/MPs, as indicated by TEM imaging (Figure 3-2 and Appendix 1 Section 8.1.1.1.1 and 8.1.1.2.1), was spherical and smooth on the surface. Furthermore, the Zeta potential of the same NP/MPs recorded using Zetasizer was around -40 mV due to the negatively charged carboxylic end group in the PLGA composition (Table 1, Figure 3-3 and Appendix 1 Section 8.1.1.2.3).

A

		Size (d.nm):	% Intensity:	St Dev (d.nm):
Z-Average (d.nm): 399.5	Peak 1:	115.7	100.0	15.75
PdI: 0.442	Peak 2:	0.000	0.0	0.000
Intercept: 1.03	Peak 3:	0.000	0.0	0.000

Result quality : Refer to quality report

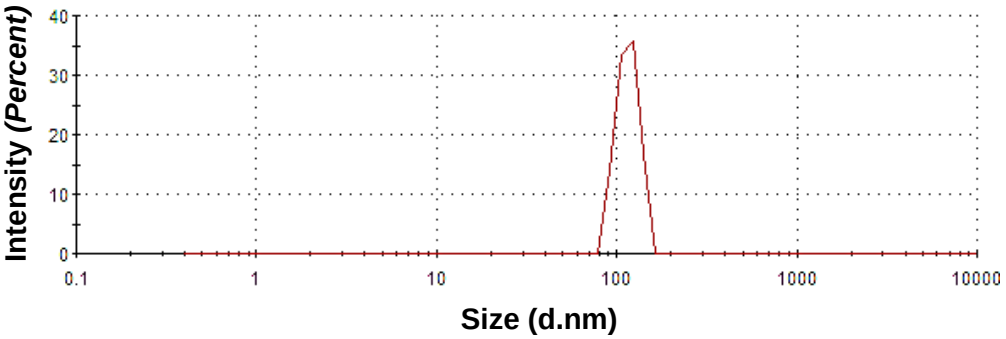

B

		Size (d.nm):	% Intensity:	St Dev (d.nm):
Z-Average (d.nm): 78.02	Peak 1:	87.45	100.0	30.24
PdI: 0.103	Peak 2:	0.000	0.0	0.000
Intercept: 0.921	Peak 3:	0.000	0.0	0.000

Result quality : Good

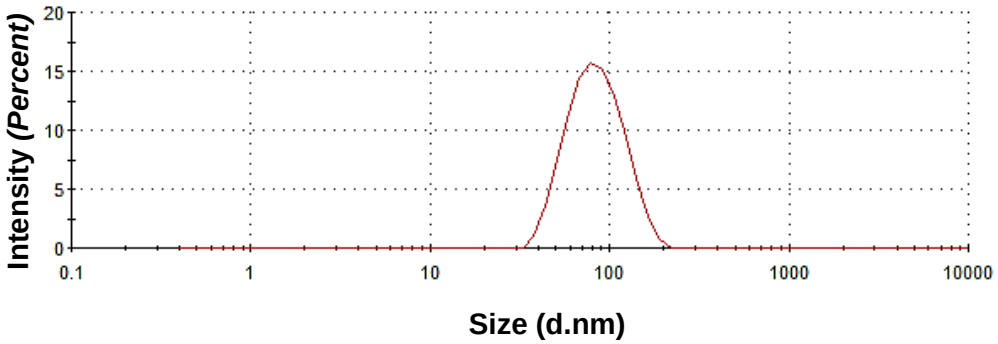

Figure 3-1 Size of PLGA NP/MPs prepared with modified nanoprecipitation. Representative Zetasizer reports indicate the intensity distribution of PLGA NP/MP size and PDI. (A) A sample result of a heterogeneous population of PLGA MPs prepared with 5 % (w/v) PLGA which did not pass the quality report criteria and shows a mean size of 0.399 µm with PDI value of 0.4. (B) A sample result of a homogenous population of PLGA NPs which passed the quality report criteria prepared with 2 % (w/v) PLGA and shows a mean size of 78.02 nm with PDI value of 0.1.

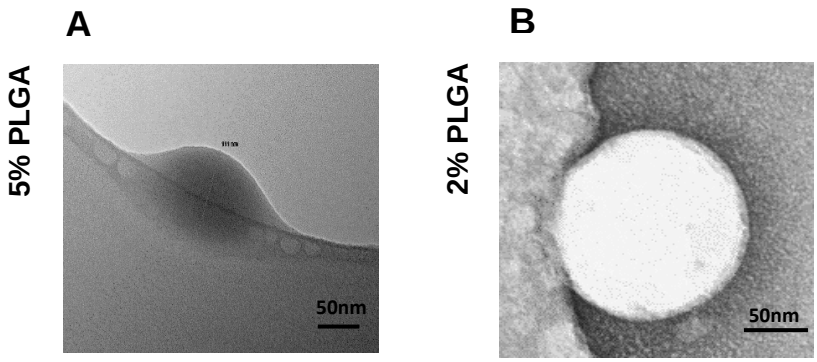

Figure 3-2 Size and morphology of PLGA NP/MPs prepared by modified nanoprecipitation. TEM images of PLGA NP/MPs prepared with 5 % (A) and 2 % of PLGA (B) show size and spherical smooth surfaced PLGA NP/MPs. Smaller PLGA NPs were produced at lower concentration of PLGA (B).

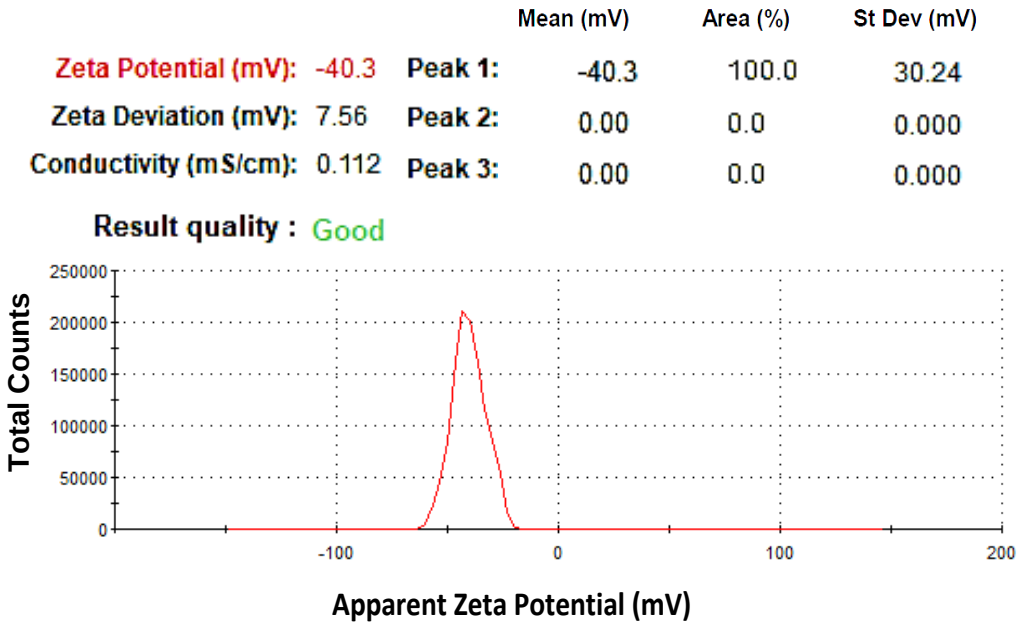

Figure 3-3 Zeta potential measurements of PLGA NP/MPs prepared by modified nanoprecipitation. Zetasizer report shows homogenous population of highly negatively charged PLGA NP/MPs prepared with 5 or 2 % (w/v) PLGA and low concentration of Pluronic F127 non-ionic surfactant (0.5 % w/v). The report has passed the quality criteria. Mean Zeta potential value of -40.3 mV, with zeta deviation of 7.56 mV and conductivity of 0.112 (mS/cm) exhibits good quality and colloidally stable PLGA NP/MPs.

3.2.2 Preparation of PLGA MPs by double emulsion W/O/W solvent evaporation method

To achieve the target particle size and suitable pDNA encapsulation efficiency, the double emulsion method was also applied. When using 1.3 % (w/v) PLGA and 1 % (w/v) stabiliser (PVA) in the second emulsion, the mean hydrodynamic size of the resultant MPs was 2.5 µm with a mean PDI value of 0.8 (Table 1, Figure 3-4A and Appendix 1 Section 8.1.2.1.2). These results were also confirmed by TEM images (Figure 3-5A and Appendix 1 Section 8.1.2.1.1). To achieve smaller MPs, the concentration of the PLGA was reduced to 0.5 % using the same type and concentration of stabiliser. As a result, the size of the PLGA MPs was decreased to 0.815 ± 0.259 µm (mean ± SD) (Table 1, Figure 3-4B and Appendix 1 Section 8.1.2.2.2). However, the MPs produced were irregularly shaped with a thin surface and a compromised structure, as shown in Figure 3-5B and Section 8.1.2.2.1. To achieve structurally intact and relatively small PLGA MPs, the percentage of PVA was increased to 3 %, keeping the original PLGA concentration of 1.3 %. Moreover, an inner stabiliser of 0.5 % bovine serum albumin (BSA) was applied in the first emulsion. The resultant PLGA MPs were 0.35 ± 0.0487 µm in diameter with a lower PDI of 0.17 ± 0.02 (mean ± SD) and were negatively charged with a mean Zeta potential of -22.74 ± 3.22 (Table 1 and Appendix 1 Section 8.1.2.3.3.1). This population of PLGA MPs was considered suitable for pDNA encapsulation in terms of size, structure and reproducibility. PLGA MPs prepared with a low concentration of PVA were recorded as being highly negatively charged (Figure 3-6 and Appendix 1 Section 8.1.2.2.3).

Table 1: physico-chemical characteristics of PLGA NP/MPs prepared by double emulsion and modified nanoprecipitation methods.

Method	NP/MPs	NP/MPs diameter (nm) (mean ± SD)	PDI ± SD	Zeta Potential (mV) (mean ± SD)
Double Emulsion	1.3% P LGA [a]	2256 ± 2019	0.89 ± 0.21	- 41.3 ± 5.3
Double Emulsion	0.5% PLGA [a]	815 ± 259	0.32 ± 0.24	-41 ± 5.2
Double Emulsion	1.3% PLGA [b]	350 ± 48.75	0.17 ± 0.02	-22.74 ± 3.22
Nanoprecipitation	5% PLGA [c]	509 ± 417	0.45 ± 0.22	-42 ± 5.6
Nanoprecipitation	2% PLGA [d]	107.5 ± 13	0.14 ± 0.06	-42.06 ± 0.1

a : Solvent: DCM, stabiliser: PVA (1 %), b: Solvent: DCM, stabiliser: PVA (3 %), c: Solvent: DMF, stabiliser: Pluronic F 127 (0.5 %), d: Solvent: DMSO, stabiliser: Pluronic F 127 (0.5 %).

A

		Size (d.nm):	% Intensity:	St Dev (d.nm):
Z-Average (d.nm): 2027	Peak 1:	351.6	100.0	20.66
PdI: 1.000	Peak 2:	0.000	0.0	0.000
Intercept: 1.04	Peak 3:	0.000	0.0	0.000

Result quality Refer to quality report

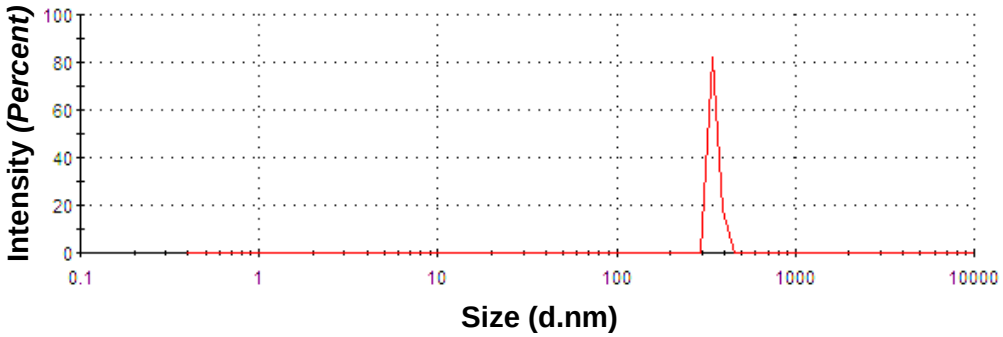

B

		Size (d.nm):	% Intensity:	St Dev (d.nm):
Z-Average (d.nm): 987.7	Peak 1:	1050	100.0	156.4
PdI: 0.101	Peak 2:	0.000	0.0	0.000
Intercept: 0.934	Peak 3:	0.000	0.0	0.000

Result quality Refer to quality report

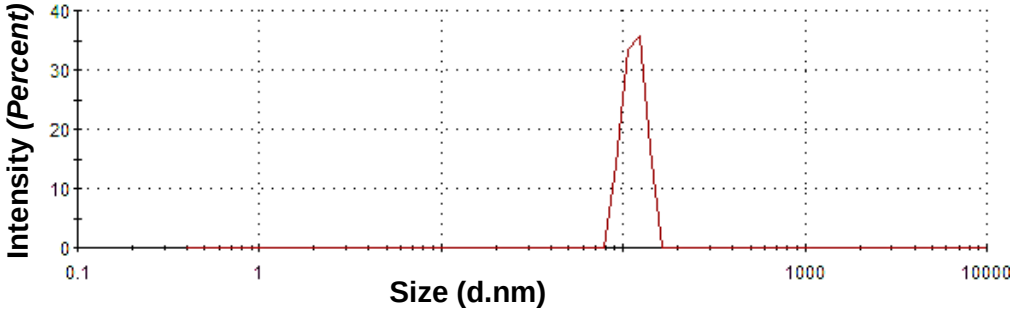

Figure 3-4 Size of PLGA MPs prepared by double emulsion solvent evaporation method. Representative Zetasizer reports indicate the intensity distribution of PLGA MP size and PDI. (A) A sample result of a population of PLGA MPs prepared with 1.3 % PLGA and 1 % PVA (w/v) shows a mean size of 2.027 µm with PDI value of 1. (B) A sample result of a population of PLGA MPs prepared with 0.5 % (w/v) PLGA shows a mean size of 0.987 µm with PDI value of 0.1. Both MP populations were heterogeneous and did not pass the quality report criteria.

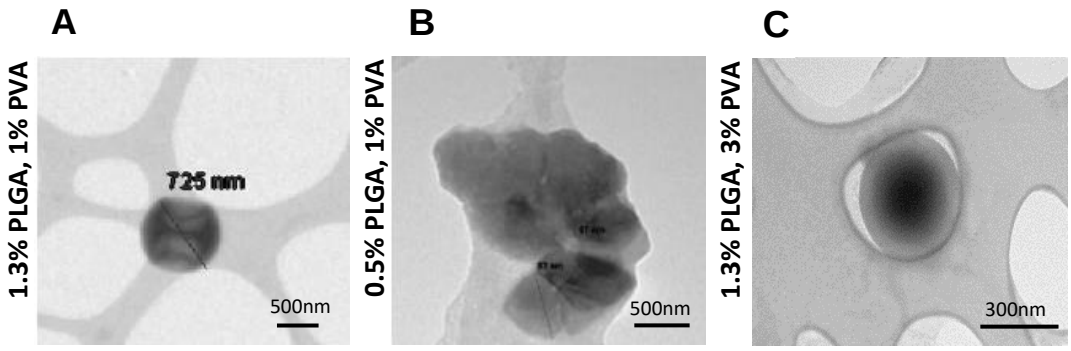

Figure 3-5 Size and morphology of PLGA MPs prepared by double emulsion. (A) TEM image of PLGA MPs prepared at 1.3 % and 1 % PVA. (B) Irregular shaped structurally compromised PLGA MPs at low PLGA concentration of 0.5 %. (C) PLGA MPs prepared with 1.3 % PLGA and 3 % PVA shows relatively small and structurally intact PLGA MPs. A and C show spherical smooth surfaced PLGA MPs at high concentration of PLGA. TEM micrograph of PLGA MPs confirms the size measurements by Zetasizer.

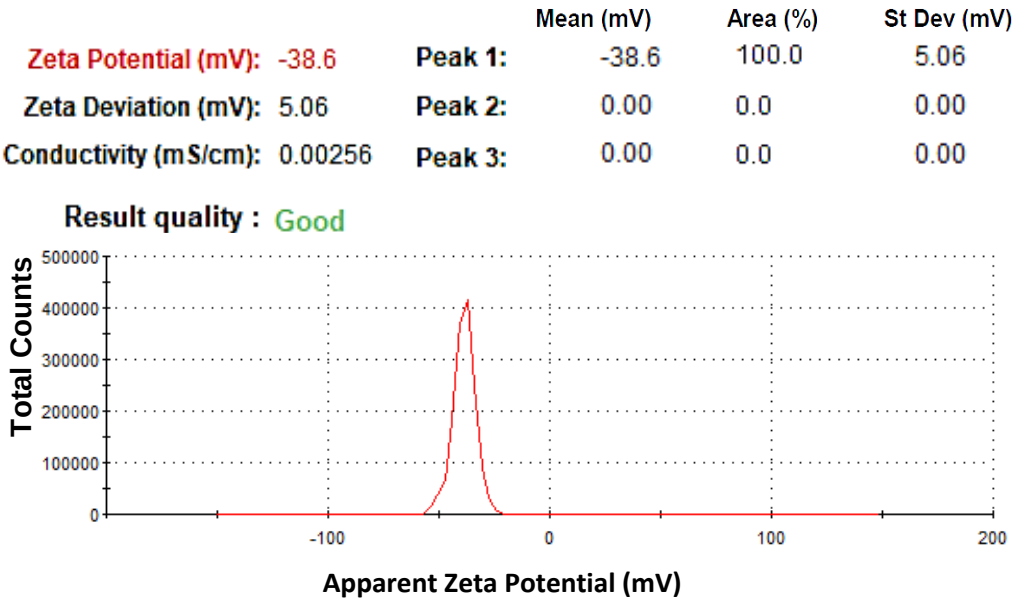

Figure 3-6 Zeta potential measurements of PLGA MPs prepared by double emulsion solvent evaporation method. A representative Zetasizer report shows homogenous population of highly negatively charged PLGA MPs at 1.3 or 0.5 % (w/v) PLGA and low concentration of PVA non-ionic surfactant (1 % w/v). The report has passed the quality criteria. Mean Zeta potential value of -38.6 mV, with zeta deviation of 5.06 mV and conductivity of 0.00256 (mS/cm) exhibit good quality and colloidally stable PLGA MPs.

3.3 pDNA condensation and optimisation of the pDNA NP/MPs formation

In order for macromolecular, negatively charged hydrophilic pDNA to be encapsulated into relatively small hydrophobic PLGA MPs, it is necessary for the pDNA to be condensed into a smaller size in proportion to the PLGA MPs, more water insoluble and positively charged form. pDNA condensation could be achieved by applying he principle of electrostatic interaction between negatively charged phosphate backbone in the pDNA and positively charged amine group in a polycation, or decreasing the interaction of pDNA with water molecules to produce NPs (Bloomfield, 1991, Heinonen *et al*., 1996, Bloomfield, 1997). Herein, several condensing agents were chosen. The selection criteria for the pDNA NPs to be encapsulated in PLGA MPs were based on the size, charge and reproducibility of the resulting pDNA NPs. It was hypothesised that smaller pDNA NPs would allow for the efficient encapsulation of pDNA in PLGA MPs. Moreover, positively charged pDNA NPs would not only decrease the repulsive forces between pDNA and PLGA but would cause the pDNA to accumulate in the vicinity of PLGA, thus enhancing the encapsulation process.

In order to produce small, neutral or preferably positively charged pDNA NPs, many condensing agents were compared such as isopropanol, high (30,000-70,000 Da) and low (1000-5000 Da) Mw Poly L-Lysine (PLL). Dilute pDNA with a 1 µg/50µl working solution was used for all the pDNA condensation experiments described in this chapter.

3.4 Characterisation of pDNA NP/MPs

Confirmation of pDNA NP/MPs formation and defining their physico-chemical characteristics such as size, charge and morphology is important for determining their interaction with the PLGA during encapsulation. Determining these characteristics could be as critical in achieving high EE % as is determining other parameters in the encapsulation process such as methods of PLGA MP preparation, PLGA and surfactant concentration, solvent type and the ratio of the solvent to the non-solvent.

The following section describes the physico-chemical characteristics of pDNA NP/MPs formed using different condensing agents. The pDNA NPs characterised as having the smallest size, a positive charge and reproducibility were taken forward with the encapsulation process in PLGA MPs. The formation of these NPs was further confirmed using PicoGreen binding assay and dissociation with a polyanion.

3.4.1 pDNA NP/MPs size and morphology

The hydrodynamic size of the pDNA NP/MPs was measured using Dynamic Light Scattering (DLS). Moreover, TEM imaging was also used to confirm the size and shape of these NP/MPs. The sizes and shapes of the NP/MPs were found to be largely dependent on the nature of the condensing agents.

3.4.2 Zetasizer measurements

Decreasing the repulsive forces between like-charged pDNA and PLGA is an essential factor in enhancing the encapsulation of pDNA in PLGA MPs (Nafee

et al., 2007). Malvern Zetasizer Nano Zs was used to measure the Zeta potential of the produced pDNA NP/MPs after their condensation with various condensing agents.

3.5 Condensing agents

3.5.1.1 Alcohol

The use of isopropanol (alcohol) is one of the most straightforward and cheapest methods of condensing pDNA. It is also used in the precipitation of pDNA during its extraction and purification from *E-coli* cultures. In this study, pDNA was condensed using isopropanol at a volume ratio of 80 % (v/v) (isopropanol/pDNA) in a dilute (20 µg/ml) pDNA solution. The mean diameter of the particles was found to be in the sub-micron range of 0.258 ± 0.149 µm and highly heterogeneous with a large PDI value of 0.54 ± 0.24 (mean ± SD) as measured by Zetasizer. It is noteworthy that most of the samples did not pass the quality report criteria and not were reproducible due to the mixed population of NP/MPs (Figure 3-7 and Appendix 1 Section 8.1.3.2). The TEM images confirmed this, as they showed rod-shaped pDNA MPs that were ~ 0. 5 µm in length and ~ 0.25 µm in width, and spherical NPs of less than 100 nm (Figure 3-8 and Appendix 1 Section 8.1.3.1). It was concluded that this population of pDNA NP/MPs was not suitable for encapsulation in PLGA MPs Therefore, no further characterisation, such as surface charge, was carried out.

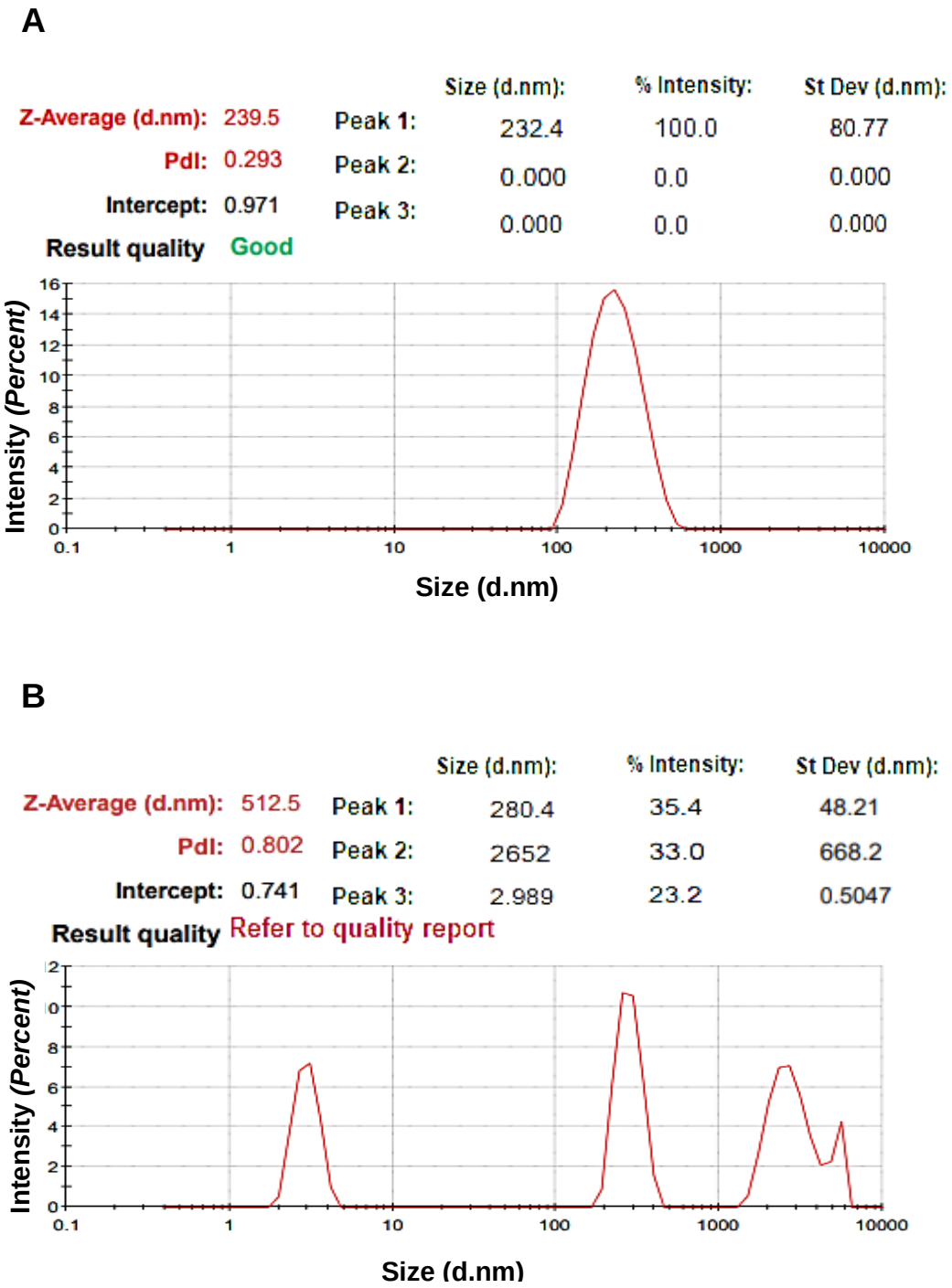

Figure 3-7 Size of pDNA MPs condensed with isopropanol. Representative Zetasizer reports indicate the intensity distribution of pDNA MP size and PDI. (A) A sample result of pDNA MP population passed the quality report criteria shows a mean size of 0.239 µm and PDI value of 0.2. (B) A sample result of heterogeneous population of pDNA MPs which did not pass the quality report criteria shows a mean size of 0.512 µm and a large PDI value of 0.8.

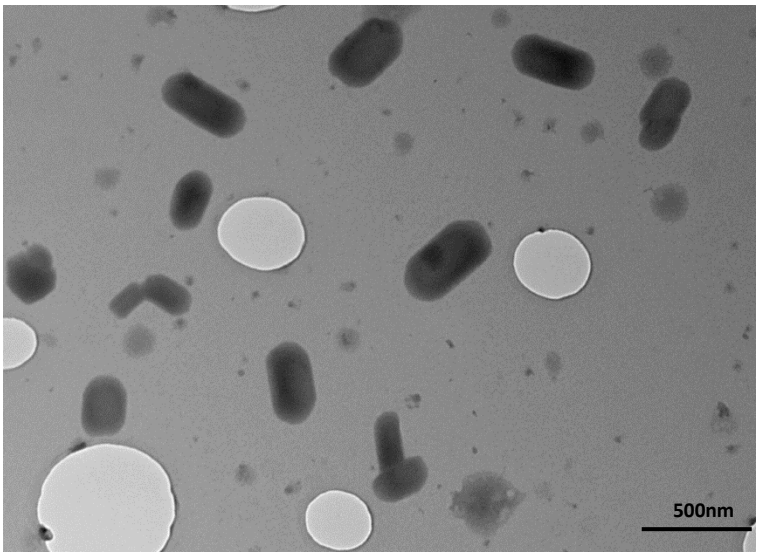

Figure 3-8 size and morphology of pDNA NP/MPs by TEM. TEM image indicates a heterogeneous population and different shapes and sizes of pDNA MPs after condensation with isopropanol at 80 % (v/v) (isopropanol/pDNA) and 20 μg/ml pDNA concentration.

3.5.1.2 High Mw PLL

PLL is one of the most frequently used cationic polymers to condense pDNA efficiently into small NPs (Laemmli, 1975, Wolfert *et al*., 1996, Wagner *et al*., 1998). In this regard, high and low Mw PLL in five different charge ratios (+ amine groups in PLL/- phosphate groups in pDNA) (Appendix 2) were tested to condense pDNA and to achieve the desired small pDNA NP size. The pDNA NP size and PDI values changed when changing the charge ratio. Increasing the charge ratios to 9 and 12 was associated with an increase in pDNA NP size condensed using high Mw PLL. Moreover, the PDI value was large in all the charge ratios tested (1, 3, 6, 9 and 12), indicating mixed populations of

pDNA NP/MPs. The PDI increased to 0.59 in charge ratio 12, with a further increase in MP size indicating a higher degree of aggregation (Figure 3-9 and Section 8.1.4.5.1). Because these pDNA NP populations were highly heterogeneous, they were not considered suitable for PLGA encapsulation and no further characterisation was performed.

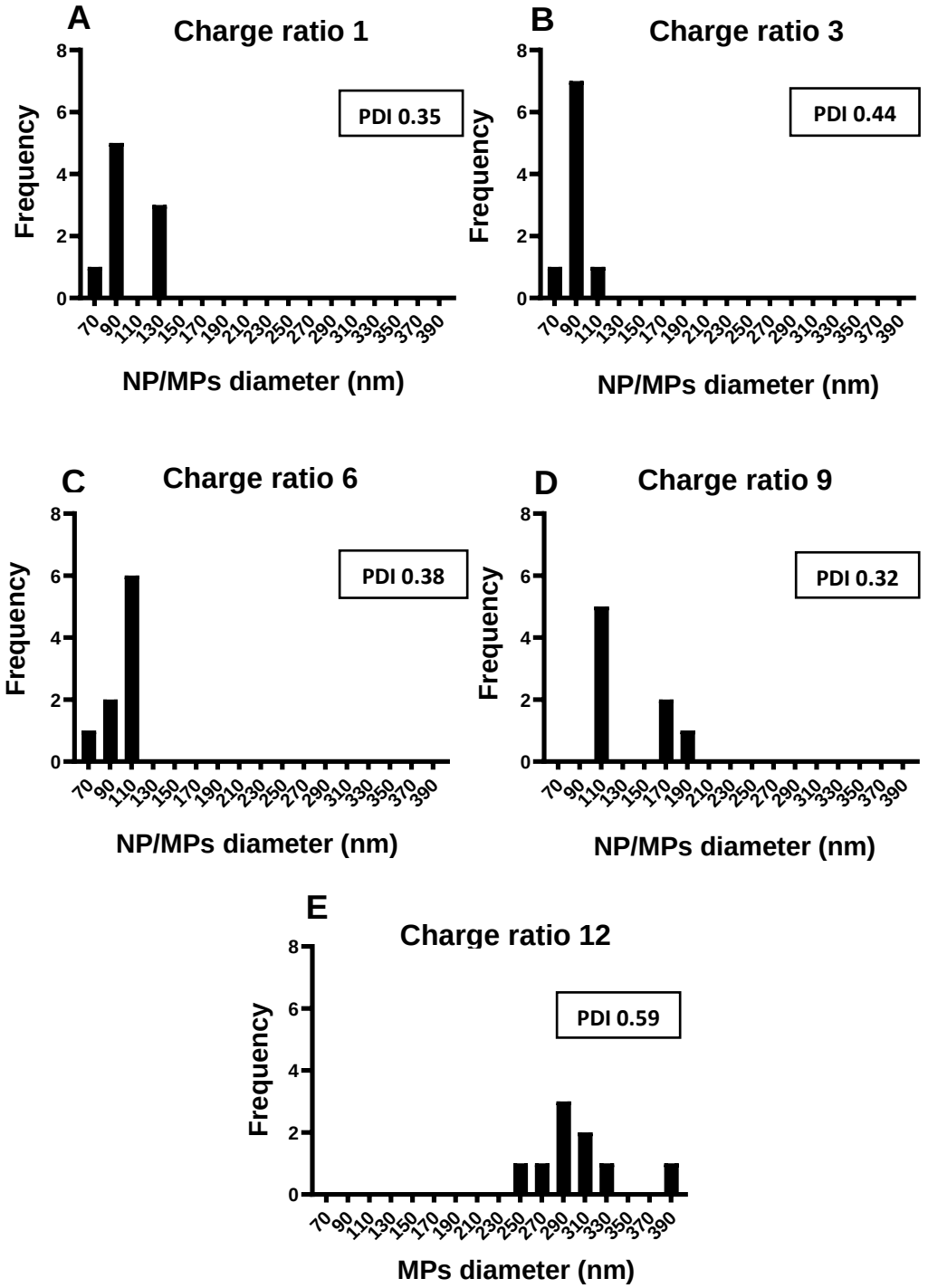

Figure 3-9 condnensation of pDNA with high Mw PLL . A constant 1 µg of pDNA was added to either 0.4, 1.25, 2.5, 3.75 or 5 µg of PLL in a total volume of 50 µl of nucelase free water to condense the pDNA at charge ratios (+/-) 1 (A), 3 (B), 6 (C), 9 (D), 12 (E), respectively. The resultant pDNA NP/MPs were hetrogenous in almost all the charge ratios tested inidicated by relatitvely large PDI values. The mean size of the pDNA NP/MPs was further increased with increasing the charge ratios to 9 and 12 associated with further increase in the PDI values.

3.5.1.3 Low Mw PLL

The charge ratios above were replicated using low Mw PLL. The Zetasizer results indicated a clear relationship between the charge ratio and the size of pDNA-PLL NP/MPs. The pDNA-PLL NP/MP size decreased when the (+/-) charge ratio was increased. Increasing the charge ratio from 1 to 12 resulted in a dramatic reduction in pDNA-PLL NP/MP size from 1656 to 49.7 nm. Moreover, apart from pDNA condensation at charge ratio 1 for which the corresponding PDI value was 0.31 ± 0.05, the PDI values of the resultant pDNA NPs were 0.1 ± 0.05, 0.107 ± 0.09, 0.11 ± 0.09 and 0.1 ± 0.03 (mean ± SD) at charge ratios 3, 6, 9 and 12, respectively (Figure 3-10 and Section 8.1.5). These results indicate a homogenous population and efficient pDNA condensation with low Mw PLL at charge ratios above 1.

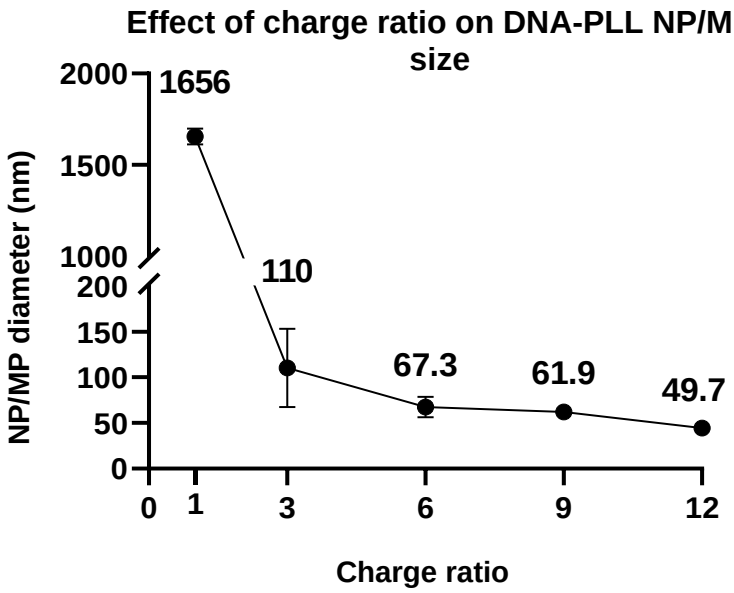

Figure 3-10 pDNA condensation with low Mw PLL. Homogeneous population of pDNA NP/MPs with small PDI in all charge ratios above 1 were produced with low Mw PLL. A constant 1 µg of pDNA was added to either 0.4, 1.25, 2.5, 3.75 or 5 µg of PLL in a total volume of 50 µl of nucelase free water to condense the pDNA at charge ratios (+/-) 1, 3, 6, 9, 12, respectively. The pDNA-PLL NP mean size was reduced with increasing the charge ratio form 1 to 12 with the smallest pDNA NPs reported at charge ratio 12.

3.5.2 pDNA NPs for encapsulation in PLGA MPs

pDNA-PLL NPs at the charge ratio of 12 (Appendix 2) were the smallest pDNA NPs and most reproducible measured by Zetasizer. The size distribution of these NPs revealed a normal distribution curve of NPs ranging from ~30-60 nm with a mean diameter of 49.7 ± 7.5 and a PDI value of 0.1 ± 0.03 (mean ± SD) (Figure 3-11A and Appendix 1 Section 8.1.5.5.2). Moreover, these pDNA NPs were positively charged with a mean Zeta potential of 25 mV (Figure 3-12 and Section 8.1.5.5.3) (Wolfert and Seymour, 1996). Therefore, these population of pDNA NPs were considered the most suitable for encapsulation in PLGA MPs. The TEM size measurements of these NPs

showed spherical NPs and size of around 10 nm or less (Figure 3-11B and Section 8.1.5.5.1).

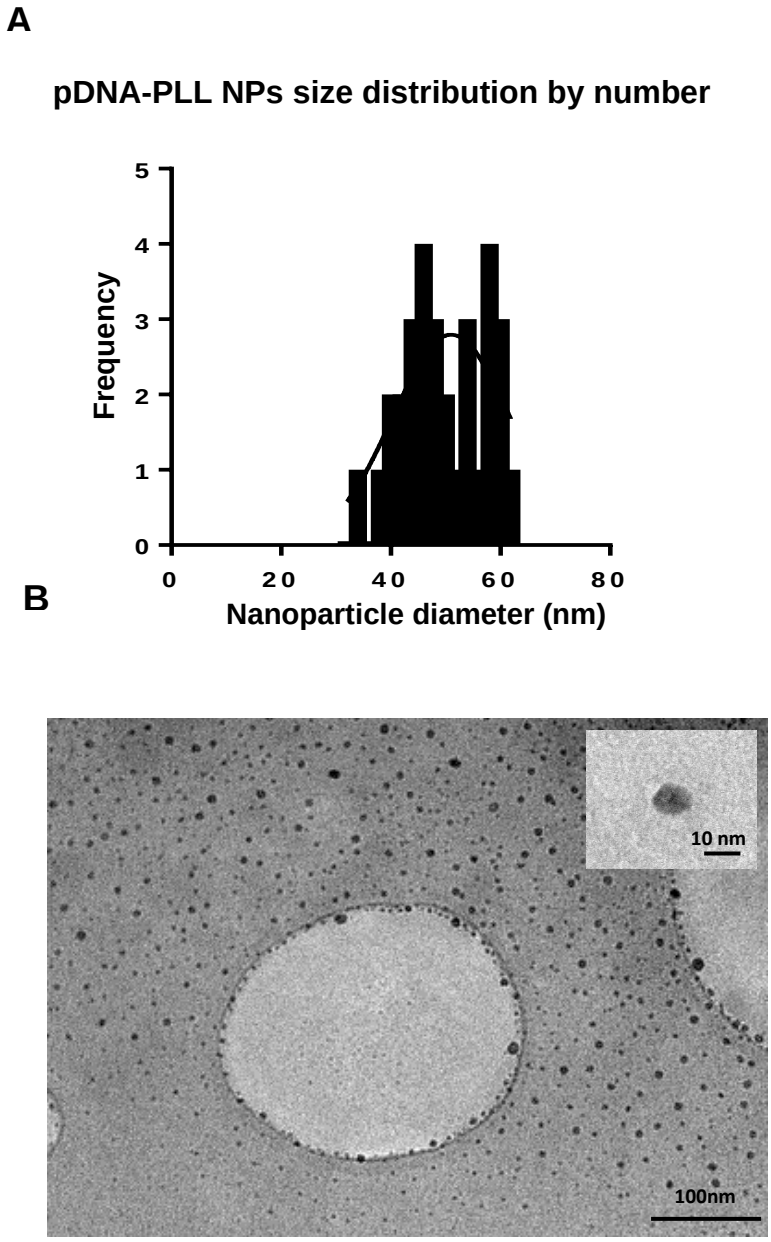

Figure 3-11 Size and morphology of pDNA-PLL NPs at charge ratio of 12. (A) Size distribution of the pDNA-PLL NPs measured with Zetasizer Nano Zs shows relatively small and homogenous NPs with a mean diameter of 49.7 nm. (B) TEM images demonstrates size and morphology of the same NPs. The NPs were prepared and analysed in nuclease free water; the same condition used for encapsulation in the double emulsion process.

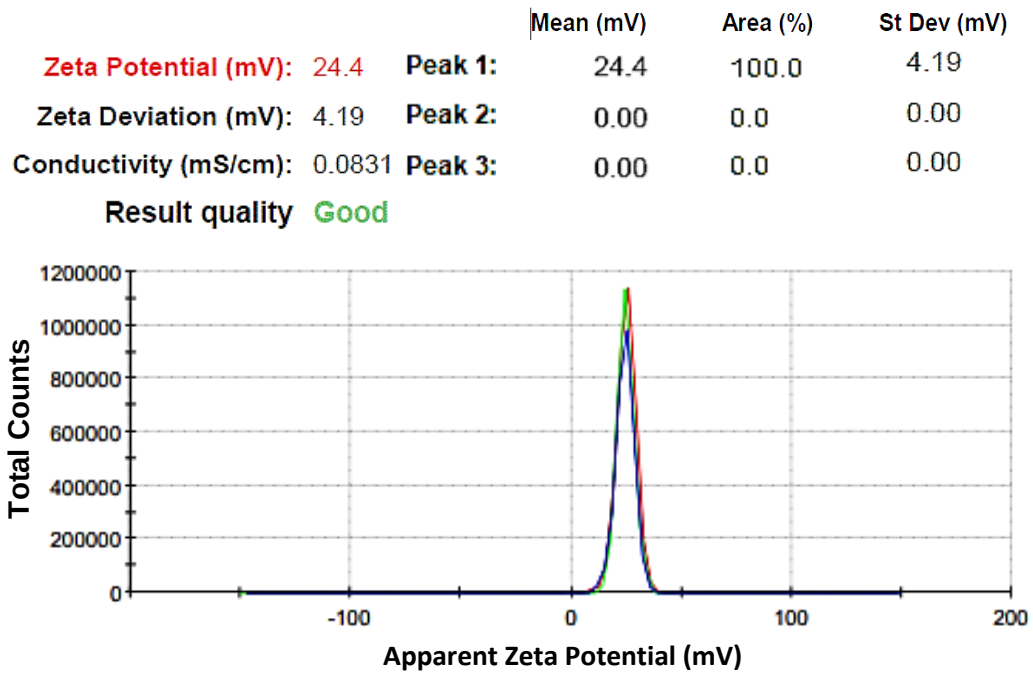

Figure 3-12. **Zeta potential measurements of pDNA-PLL NPs prepared at charge ratio of 12.** Zetasizer report shows homogenous population of highly positively charged pDNA-PLL NPs. The report has passed the quality criteria. Mean Zeta potential value of 24.4 mV, with zeta deviation of 4.19 mV and conductivity of 0.0831 (mS/cm) exhibit good quality and colloidally stable pDNA-PLL NPs.

3.5.3 PicoGreen binding assay

PicoGreen double stranded DNA (dsDNA) binding fluorescent dye has been used for the quantification of DNA and characterisation of DNA-protein bindings in many biophysical studies (Singer *et al*., 1997). Free PicoGreen in solution does not fluoresce. However, when bound to DNA, the intensity of the dye's fluorescence increases due to electrostatic and non-electrostatic between the dye molecules and the DNA (Dragan *et al*., 2010). The aim of this experiment was to provide additional confirmation of the formation of pDNA-PLL NPs using PicoGreen binding assay (Telford *et al*., 1991). For this experiment, the absorbance of different concentrations of naked and DNA-

PLL NPs was compared after their complexation with PicoGreen. In this assay, pDNA was first condensed with PLL and was then bound to PicoGreen. Figures 3-13 and 3-14 show the significantly lower absorbance of the dye (P=0.0021) when pDNA is condensed with PLL in pDNA-PLL NPs in comparison to naked pDNA, indicating the inaccessibility of the condensed pDNA for binding with PicoGreen.

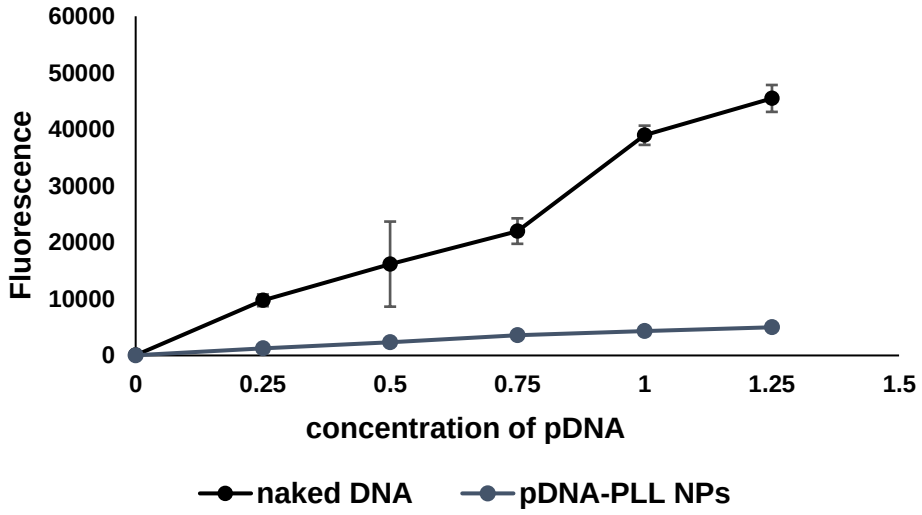

Figure 3-13 PicoGreen binding to naked pDNA in comparison with pDNA-PLL NPs. Naked pDNA complexation with PicoGreen enhances the fluorescence signal of the dye at all concentrations. Significant lower fluorescence signal of PicoGreen when complexed with pDNA-PLL NPs demonstrates the inhibitory effect of PLL on pDNA-PicoGreen binding. The excitation of the dye is dependent on pDNA concentration in both naked pDNA and pDNA-PLL NPs.

3.5.4 Dissociation of pDNA-PLL NPs with negatively charged polyamine

pDNA-PLL NPs produced lower fluorescent signals compared to naked pDNA in the PicoGreen binding assay. To confirm that the low fluorescent signal was due to the inability of PicoGreen to access the condensed pDNA, the pDNA-PLL NPs (1 µg) were dissociated using a polyanion peptide of the same molecular size as PLL; Poly L-aspartic acid (PAA), then assessed whether the released pDNA would bind to PicoGreen after the disassociation of pDNA-PLL NPs. The fluorescent intensity of pDNA-PLL NPs was comparable to that of the naked pDNA control (1 µg) after the addition of PAA at 1X concentration of PLL (Figure 3-14).

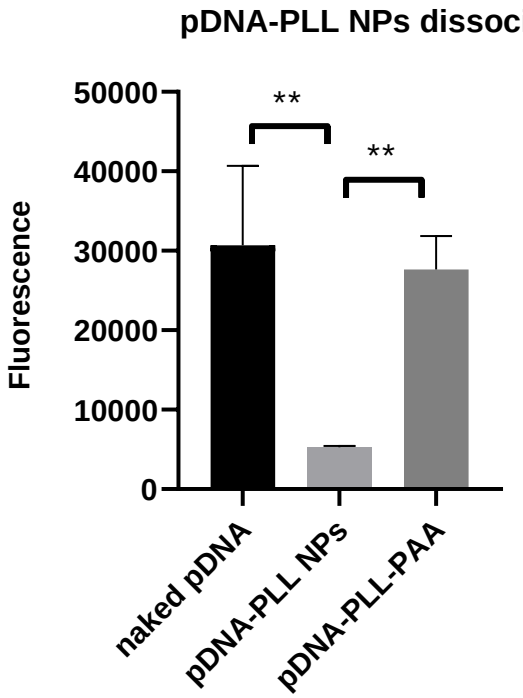

Figure 3-14 pDNA-PLL NP dissociation with PAA. Comparison of the absorbance of PicoGreen complexed with 1 µg naked, condensed pDNA or after the addition of PAA. PAA dissociation the pDNA-PLL NPs at 1X concentration of PLL was confirmed by an increase in the fluorescent signal of PicoGreen which was comparable to the naked pDNA control. The asterisk over the lines indicate significance between groups. One-way Anova statistical analysis was used to generate the graph followed by Tukey test to determine significant difference between each mean in multiple comparison. The data represented as mean ± SD. P value =0.0021.

3.6 Double emulsion for encapsulation of pDNA-PLL NPs in PLGA MPs

Double emulsion is the most frequently cited method for the encapsulation of biological and non-biological molecules in PLGA particles in both the nano and micro size ranges (Abbas *et al*., 2008, Cohen-Sela *et al*., 2009, Cun *et al*., 2011). In this study, double emulsion was used for the encapsulation of a hydrophilic biological molecule, namely pDNA. PLL was used to enhance the process of encapsulation by means of reducing the size and altering the charge of pDNA (Gebrekidan *et al*., 2000, Ribeiro *et al*., 2005). Both pGluc- and pBMP2-PLL NPs were encapsulated in PLGA MPs immediately after their preparation using the double emulsion method illustrated in Figure 3-15. This process yielded a minimum of 5.5 mg (55% of total PLGA) of PLGA MPs, and an EE %) of ~ 30% of the initial amount of pDNA used. This resulted in 1.09 µg of pDNA encapsulation per 0.2 mg of PLGA MPs. This was used as a standard dose in the transfection studies. Published pGluc-PLR NPs were used as a positive control (Dixon *et al*., 2016). Blank PLGA MPs were prepared by substituting the pDNA-PLL with water only and were used as a negative control in the transfection studies. pDNA-PLL NPs that had passed

through the same double emulsion method but without the PLGA were used as a control in the transfection studies (as detailed in Chapter 4 Section 4.13.1). Hydrophilic dye Atto 590 and hydrophobic dye Nile Red encapsulated PLGA MPs yielded EE % of 30 % and 50 %, respectively. The EE % of the hydrophobic Nile Red was higher than was that of the hydrophilic Atto 590. This was expected because of the hydrophobic nature of Nile Red (Iwahara *et al*., 2015, Swider *et al*., 2018).

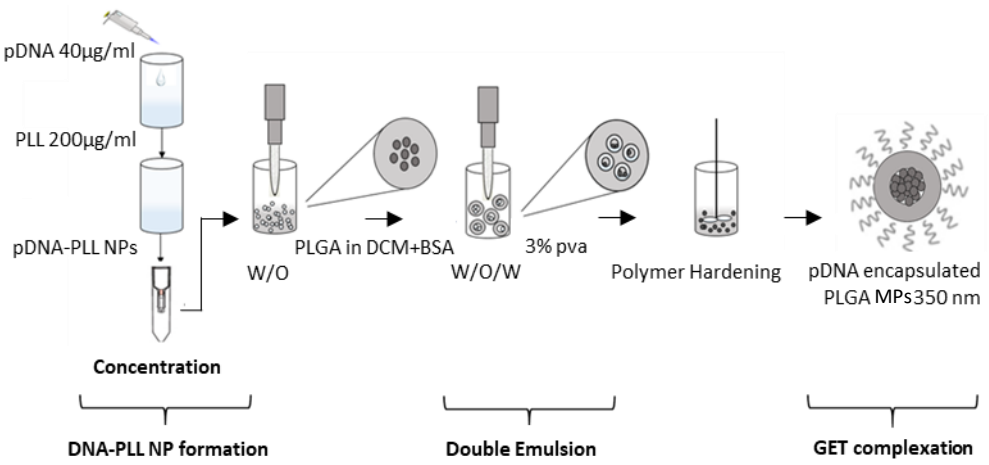

Figure 3-15 A simplified illustration of the process of encapsulation of pDNA in PLGA MPs. Double emulsion was employed for the encapsulation of pDNA-PLL NPs. 1.3 % of PLGA was used. pDNA-PLL NPs (pGLuc or pBMP2 (chapter 5)) were and used in the preparation of the first emulsion immediately after concentration. The first emulsion was added to 3 % (w/v) PVA solution to form the second emulsion. The resulting PLGA MPs were then complexed with GET peptides electrostatically (detailed in chapter 4).

3.7 Characterisation of pDNA encapsulated PLGA MPs

3.7.1 Size and morphology

pDNA encapsulated PLGA MPs were in the same range as blank MPs with a mean diameter of 0.339 ± 0.032 µm in diameter, as shown by the Zetasizer and TEM graphs (Figures 3-16, Appendix 1 Section 8.1.2.3.2 and 3-5C, respectively). The encapsulation of pDNA-PLL NPs did not affect the size of the PLGA MPs. The populations of the blank and encapsulated MPs were found to be homogenous with an average PDI of 0.18 ± 0.02 (mean ± SD).

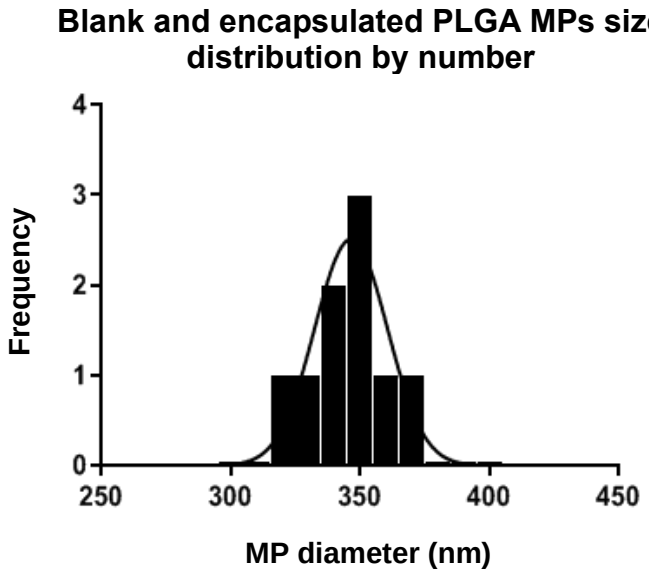

Figure 3-16 size of pDNA encapsulated PLGA MPs. Size distribution by number measured with Zetasizer Nano Zs shows relatively small and homogenous MPs with a mean diameter of 350 nm.

3.7.2 Zeta potential measurements

Zeta potential measurements can be used to detect the surface attachment of positively charged moieties to PLGA MPs (Arakha *et al*., 2015, Carvalho *et al*., 2018). In the current studies, the surfaces of both blank and pDNA encapsulated PLGA MPs were negatively charged. The encapsulation of positively charged pDNA-PLL did not affect the Zeta potential of pDNA encapsulated PLGA MPs and was comparable to that of blank PLGA MPs. The Zeta potential recorded for each of the blank and encapsulated PLGA MPs was -22.39 ± 2.68 mV and -23.06 ± 1.66 mV (mean± SD), respectively (Figure 3-17 and Appendix 1 Section 8.1.2.3.3). These results indicated that the pDNA-PLL NPs were encapsulated in the matrix of PLGA MPs and not electrostatically adsorbed on the surface of the PLGA MPs.

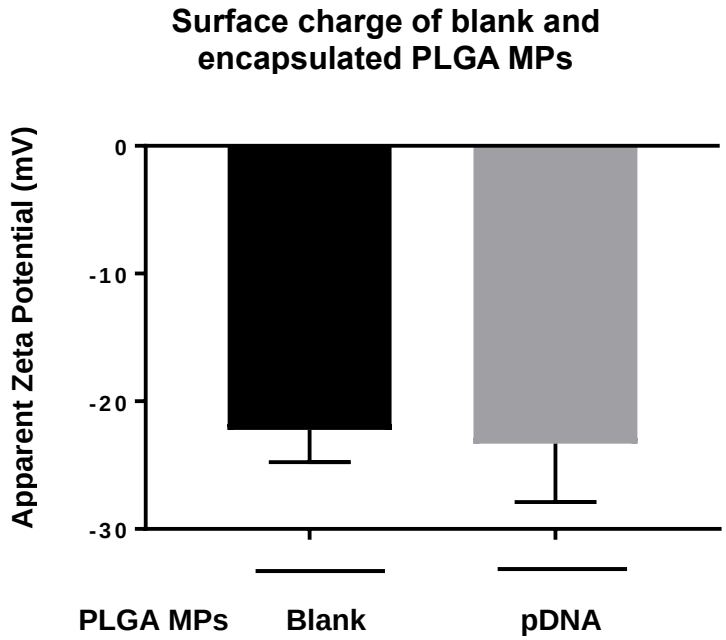

Figure 3-17 Comparison of Zeta potential of blank and pDNA encapsulated PLGA MPs. Surface charge measured by Zetasizer indicates negatively charge pDNA-encapsulated PLGA MPs that is comparable to blank MPs. Data is presented as (mean± SD).

3.7.3 Measurement of EE %

Both naked pDNA and pDNA-PLL NPs were encapsulated in PLGA NP/MPs via modified nanoprecipitation (2 % and 5 % PLGA) and double emulsion method (1.3 % PLGA, 3 % PVA). The EE % of the naked pDNA using both methods was only 2-3 % of the total pDNA used. Moreover, the EE % of the pDNA-PLL NPs using the modified nanoprecipitation method was also very low of about 3 % of the initial pDNA amount. However, the EE % of the pDNA-PLL improved significantly when using the double emulsion method to 30 % of the total pDNA measured by the direct method from dissolved PLGA MPs. The EE % of the naked pDNA and the pDNA-PLL NPs was determined using standard curves prepared from naked pDNA and pDNA-PLL NPs, respectively. Figure 3-18 shows a sample of the standard curves and the R^2 values used in both the EE % measurements and the release studies. The released pDNA-PLL in the first 24 hours (see the release studies below in Section 3.7.4) was also used to confirm the EE %.

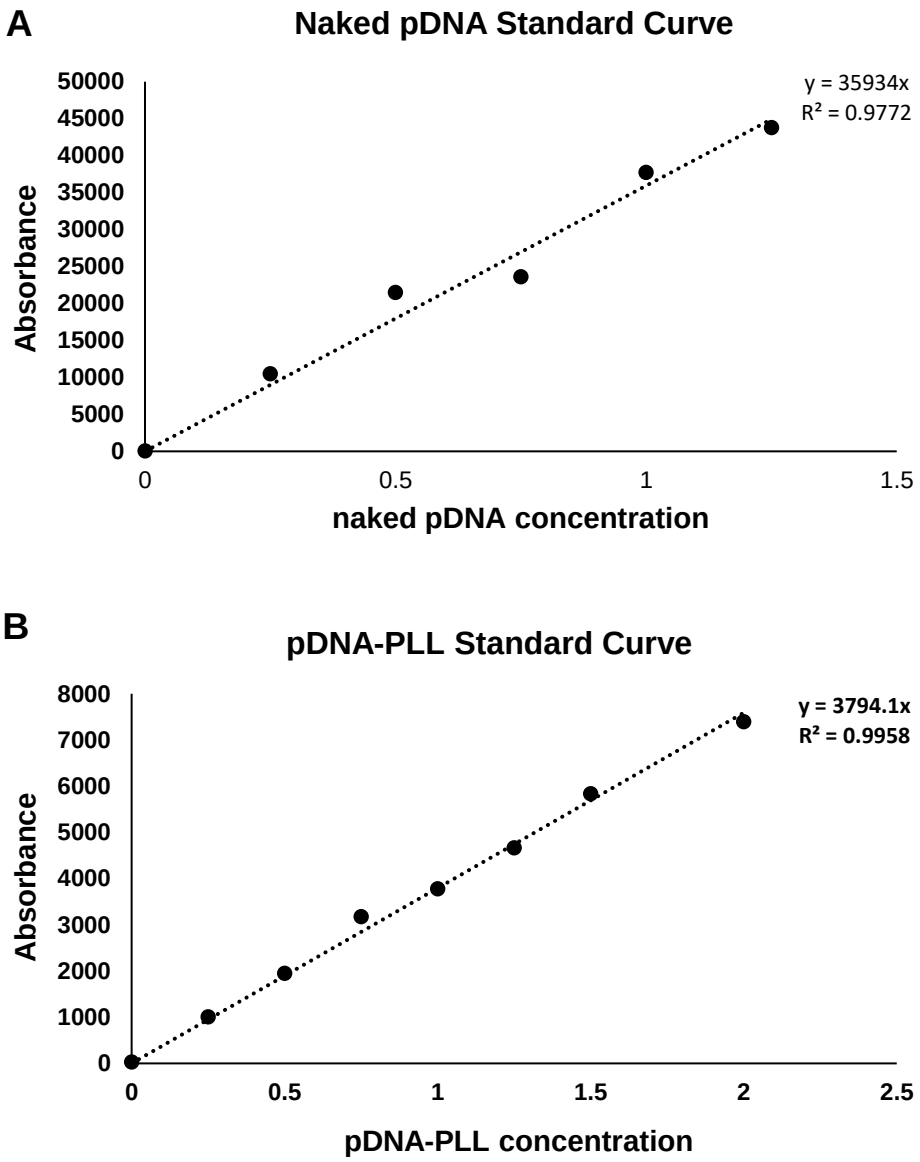

Figure 3-18 Representative standard curves prepared for both EE % measurements and release studies. Different concentrations of naked pDNA (A) and pDNA-PLL NPs (B) ranging from 0 - 2 µg of pDNA in a total volume of 50 µl nuclease free water was quantified using PicoGreen dsDNA quantification dye and used to generate the standard curves. Increase in the pDNA concentration results in an increase in the fluorescence intensity of PicoGreen in a linear manner represented by R^2 of nearly 1.

3.7.4 Release of pDNA from PLGA MPs

The release profile of pDNA-PLL NPs from PLGA MPs followed the typical

release behaviour of PLGA nano and micro particles (Wang *et al*., 2002, Luan and Bodmeier, 2006, Gasmi *et al*., 2016). The pDNA encapsulated PLGA MPs were incubated for a period of 40 days. The release studies showed a cumulative release of 61.9 % of the total pDNA used during the encapsulation process. About 50 % of the encapsulated pDNA, which is equal to 34 % of the total pDNA used, was burst released during the first 24 hours after incubation. This phase was followed by a release of 17 % of the total pDNA in the continuous phase for a period of 29 days. A slight increase in the release rate was found in the last six days of the study during the final and bulk erosion phases, which was equal to 6 % of the total pDNA (Figure 3-19).

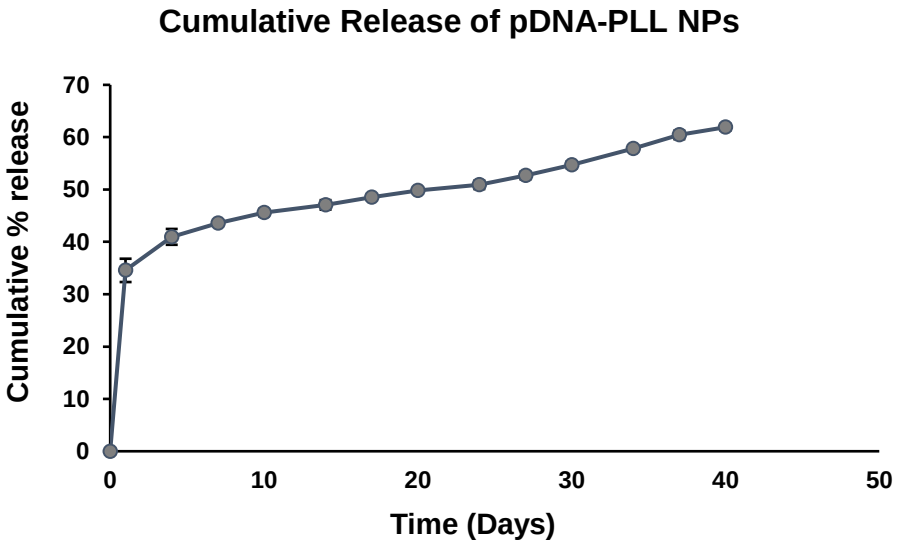

Figure 3-19 Release of pDNA-PLL from PLGA MPs: release study was carried out over the period of 40 days. Cumulative release value of 61.9% of the total pDNA was recorded. The pDNA-PLL encapsulated PLGA NPs followed a typical tri-phasic release behaviour comprised of burst release phase (1 day), followed by continuous phase (29 days) and bulk erosion phase (6 days).

3.7.5 Effect of sonication on pDNA

Double emulsion comprises the process of sonication, which could shear the pDNA and cause fragmentation (Sambrook and Russell, 2006a, Sharma *et al*., 2016b). Moreover, the organic solvent used in the double emulsion process could affect the integrity of pDNA. In this study, the effect of sonication and organic solvent (DCM) on the integrity of the encapsulated pDNA was determined. The number of bacterial colonies of sonicated (that is, passed through the process of double emulsion without the PLGA) and non-sonicated naked pDNA and pDNA-PLL NPs (controls) were comparable to the extracted pDNA-PLL from PLGA MPs (Figure 3-20). Therefore, it was concluded that the amplitude and the time of sonication used in this study did not affect the integrity of the encapsulated pDNA during the encapsulation process.

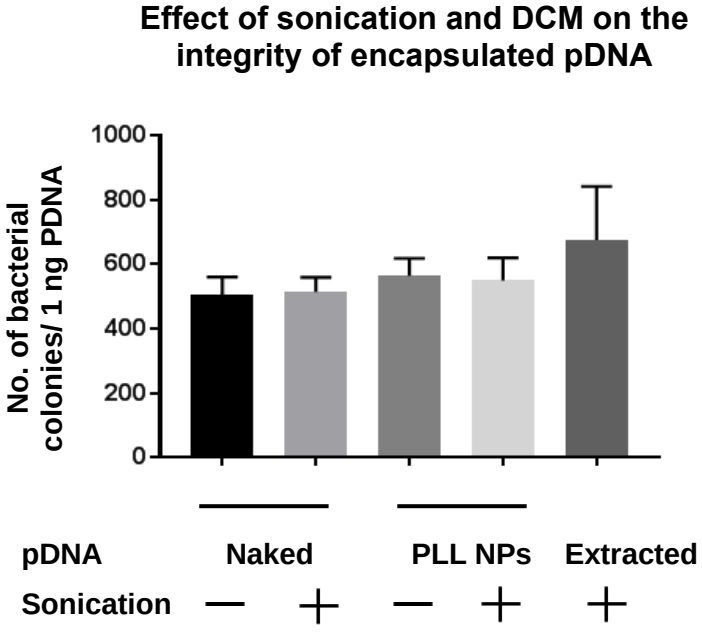

Figure 3-20 Effect of sonication and DCM solvent on the integrity of encapsulated pDNA. The number of bacterial colonies of trasformed DH5α E-coli with extrcted pDNA-PLL NPs from PLGA MPs was comparable to the sonicated and no-sonicated naked pDNA and pDNA-PLL NPs (conrols) indicating that soncation rate and time and the sovent did not affcet in the supercoiled form of naked pDNA and the encapsulated pDNA-PLL NPs.

3.7.6 DNase I protection Characteristics of PLGA MPs

The most important characteristic of PLGA MPs in gene delivery is the protection of the encapsulated pDNA from environmental DNases. Three different doses of DNase I, 0.025 U/µl, 0.0025 U/µl and 0.00025 U/µl were tested to treat naked and encapsulated pDNA according to the manufacture's protocol at the physiological temperature of 37 ˚C for 15 minutes (Figure 3-21). With exception to the lowest dose of DNase I, the higher doses of DNase treated naked pDNA were almost completely degraded, as shown by gel electrophoresis (top panel, lanes 4 and 5). On the other hand, the encapsulated pDNA in PLGA MPs resisted degradation even at the highest dose of DNase I.

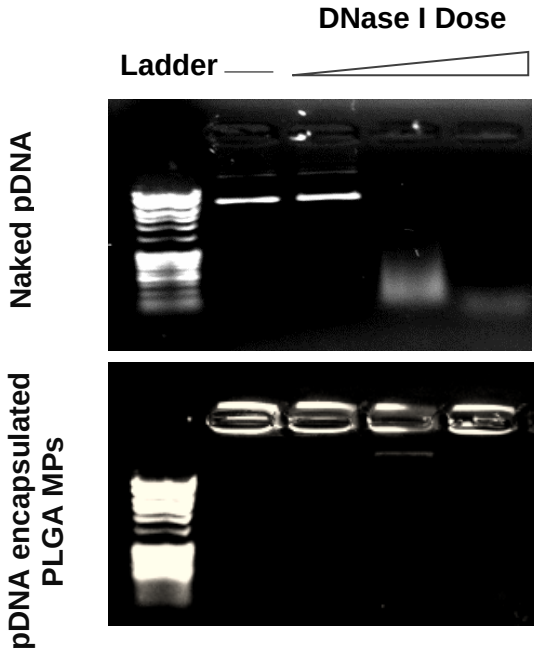

Figure 3-21 DNase protection characteristics of pDNA-PLL encapsulated PLGA MPs. 0.5 µg naked pDNA (top) and pDNA-PLL encapsulated PLGA MPs (bottom) were treated with increasing doses of DNase I (0.025 U/µl, 0.0025 U/µl and 0.00025 U/µ) for 15 min at 37˚C and run of 1 % (w/v) agarose gel. The gel electrophoresis analysis demonstrates the integrity of the encapsulated pDNA-PLL during the enzymatic treatment even with heights dose of DNase I in comparison to degraded naked pDNA (lane 4 and 5, top panel).

3.8 Discussion

Non-viral gene delivery vectors are known for their low efficiency in comparison to viral vectors. Examples of this are cationic polymers, which act as both condensing and gene delivery agents. However, for enhanced gene delivery characteristics, high doses, or highly positive chemically modified versions of them, are applied. (Kadlecova *et al*., 2012, Hall *et al*., 2017). This high positive charge is related directly to cellular toxicities (Moghimi *et al*., 2005). Moreover, cationic agents only partially protect the nucleic acid from enzymatic degradation (Roy *et al*., 2003, Hu *et al*., 2016, Osman *et al*., 2018). On the other hand, hard bio-inert polymers, such as PLGA, represent a significant step forward in non-viral gene delivery because of the advantages of a proven track record in drug and protein delivery, maximum DNase enzymatic protection and low toxicity (Chen *et al*., 2016, Jin *et al*., 2014, Han *et al*., 2000). Therefore, in this study, PLGA was employed as a nano-carrier for the encapsulation and delivery of pDNA (pGluc and pBMP2).

3.8.1 Characterisation of pDNA NPs

Determining the physico-chemical characteristics of pDNA NPs in terms of size, shape and Zeta potential prior to their encapsulation in PLGA MPs is important in order to speculate on their interaction with PLGA and could affect their encapsulation efficiency significantly. During the search for literature concerning pDNA NP encapsulation in Polymer MPs, no studies were found that have experimented with how pDNA NP size could affect

their encapsulation efficiency in a polymer MP such as PLGA. Therefore, in the present work, smaller pDNA NPs' size were logically related to higher EE % in PLGA MPs. Large pDNA NPs might not fit into the relatively small PLGA MPs, but a smaller size of pDNA NPs could increase the chance of their entrapment in PLGA MPs and, consequently, provide more copies of the pDNA to be encapsulated. Moreover, it was hypothesised that positively charged pDNA NPs might increase their attraction to the negatively charged PLGA in the micro droplets of the double emulsion, thus decreasing their chance of escaping to the outer aqueous phase. Therefore, all types of pDNA NP/MPs produced in the present studies were characterised. Several condensing agents that would potentially produce small-sized pDNA NPs were chosen. The smallest, reproducible, more homogenous and positively charged population of pDNA NPs were selected for the encapsulation studies.

The condensation of pDNA can occur in the presence of alcohol at a volume fraction close to 40 % (isopropanol/DNA), and a higher degree of condensation is observed by increasing the alcohol concentration. Therefore, in this study, an 80 % volume fraction, a protocol well known for pDNA condensation during purification and extraction from transformed *E-coli* (Sambrook and Russell, 2006b) was used. These results indicated the presence of a heterogeneous population of pDNA MPs upon condensation of pDNA with isopropanol in both DLS and TEM measurements. The TEM images showed a large proportion of tightly condensed, spherical pDNA NPs of less than 100 nm in diameter. However, rod-shaped pDNA MPs of larger

dimensions were also seen, perhaps due to the partial condensation of some of the pDNA molecules (Appendix 1 Section 8.1.3). The same combination of shapes of pDNA NP/MPs were seen in a study by (Marchetti *et al*., 2007) which indicated the simultaneous presence of partially collapsed coil and compacted globules (other terms for rods and spheres, respectively) upon condensation of a linear DNA molecule with Ethanol. Furthermore, (Bloomfield, 1996) indicates the possibility of the transition of extended DNA molecules into toroids, rods or spheres according to the proportion of alcohol in the solvent.

Due to their direct relationship with the *in vivo* condensation of DNA molecules in chromosomes, lysine residues in histones have attracted greater attention in DNA condensation studies *in vitro* in an attempt to understand and replicate DNA packaging and for *in vivo* gene transfer (Smith and Denu, 2009, Shi and Whetstine, 2007). In this regard, in the current study, high and low Mw PLL was investigated. The influence of the Mw of PLL on the size of the resulting pDNA NP/MPs was assessed. Due to the higher positive charge in a polypeptide chain, high Mw PLL is able to condense pDNA efficiently even at lower charge ratios in comparison to lower Mw PLL. When tested, high Mw PLL condensed pDNA at charge ratio 1 in comparison to charge ratio 3 with low Mw PLL (Mady *et al*., 2011, Mann *et al*., 2011, Alhakamy and Berkland, 2013). However, they tend to condense pDNA at a multi-molecular level, which resulted in a heterogeneous mixture of large and small pDNA particles. This was indicated by the relatively large PDI values (Appendix 1 Section 8.1.4). Low Mw PLL, on the other hand,

produced a homogenous population of pDNA NPs in a range of 49.7 nm at charge ratio 12, as indicated by Zetasizer. Moreover, increasing the charge ratio of high Mw PLL caused further aggregation of pDNA MPs as indicated by a larger pDNA MPs size in charge ratios 9 and 12 with a further increase in PDI, particularly in charge ratio 12. However, an increase in the charge ratio of low Mw PLL resulted in higher degrees of pDNA condensation, as indicated by the gradual reduction in the pDNA-PLL NPs size from charge ratio 1 to 12 (Appendix 1 Section 8.1.5). The DLS mean size of these NPs was converted from intensity to number distribution to allow for the comparison of the sizes obtained by DLS and TEM microscopy imaging. However, this conversion was not carried out for high Mw condensed pDNA due to some of the results not passing the quality report criteria determined by the Zetasizer.

Further confirmation of low Mw condensed pDNA-PLL NPs size by TEM revealed discrepancies in the pDNA-PLL NP size measurements between DLS and TEM. The pDNA-PLL NPs imaged on the TEM showed a much smaller NP size than did the measurements using the Zetasizer, which were in the range of 10 nm. It is likely that the drying step necessary for TEM imaging caused the shrinkage of the pDNA-PLL NPs, thus showing smaller sizes on the TEM. Supporting these data with the literature, similar results were found when the same size plasmid, Mw of PLL, the concentration of both, the salt content and the mixing procedure were used by (Wolfert and Seymour, 1996) and this resulted in pDNA-PLL NPs of 20 nm using atomic microscopy imaging. Moreover, replicating the same parameters motioned above apart from the

pDNA size of 6900 bp (the size difference from the current pDNA construct of 5764 bp would not influence the pDNA NPs size (Arscott *et al*., 1990, Bloomfield, 1991, Kreiss *et al*., 1999)) produced 15-30 nm pDNA NPs by (Liu *et al*., 2001) using TEM measurements. These techniques require the samples to be dried before analysis. Therefore, the Zetasizer measurements are most likely to represent the actual size of the pDNA NPs.

Further methodologies, such as pDNA PicoGreen binding assay (Figure 3-13) and fluorescent enhancement of the dye upon dissociation of these NPs with a counter ion (Figure 3-14), confirmed the condensation process of the pDNA by low Mw PLL. These pDNA-PLL NPs were further characterised in terms of surface charge, which indicated positively charged NPs. Therefore, due to efficient pDNA condensation, the production of a small, homogenous population of positively charged pDNA NPs, low Mw PLL at a charge ratio of 12 was chosen to prepare pDNA encapsulated PLGA MPs.

It is worth noting that pDNA NP/MPs condensed with isopropanol and high Mw PLL were not used for the encapsulation studies due to large and heterogeneous population of these NP/MPs, and the likelihood of low encapsulation efficiency outcomes.

3.8.2 Optimisation of PLGA MP fabrication and the process of pDNA encapsulation

Prior to the encapsulation of pDNA in PLGA MPs, the aim was to optimise the production of blank PLGA MPs and to test their ability to encapsulate hydrophilic and hydrophobic drug models by the encapsulation of Atto 590

and Nile Red fluorescent dyes, respectively. Additionally, to produce PLGA MPs of < 0.5 µm that were suitable for intracellular delivery (Cho *et al*., 2013, Shang *et al*., 2014).

The technique most favoured by researchers for the preparation of nucleic acid encapsulated polymer NP/MPs is the mild method of nanoprecipitation due to the lack of the sonication/homogenisation step included in double emulsion method. In nanoprecipitation, hard polymer NP/MPs are formed spontaneously upon the addition of the miscible organic solvent (solvent) containing the dissolved polymer to an aqueous solution (non-solvent) (Fessi *et al*., 1989b). Formulation parameters such as polymer concentration, and the solvent and non-solvent types have profound effects on the physico-chemical properties of the resultant PLGA NP/MPs. Firstly, nanoprecipitation was employed for the preparation of blank PLGA NP/MPs. Two different concentrations of PLGA and two solvents of different dielectric constants, DMF and DMSO, were tested. Changes in the polymer concentration and the solvent dielectric constants affected the size of the resultant PLGA particles dramatically. A reduction in the polymer concentration resulted in a reduction of the MPs' mean size to produce NPs of around 100 nm and improved their PDI values. These results are in line with those in other research (Xie and Smith, 2010, Feczkó *et al*., 2011). Moreover, change in the dielectric constant of the solvents contributed to these results. Choosing the right solvent and non-solvent depends on the differences in their dielectric constants. If the difference in the dielectric constants is large, the nanoprecipitation is more likely to fail due to less

diffusion of the solvent in the non-solvent and delay in the NP/MP production, which causes aggregation of the polymer and results in large particles being produced (Bilati *et al*., 2005a, Bukhari *et al*., 2014). The difference in dielectric constants between the solvent DMSO and the non-solvent water in the current studies was less than was that between DMF and water, at 34 and 44, respectively. The smaller difference in dielectric constants yielded smaller NPs (Figure 3-1, 3-2 and Appendix 1 Section 8.1.1.2). Therefore, combination of factors such as reduced PLGA concentrations and solvents of dielectric constants closer to that of water produced significantly smaller particles.

Although the use of stabilisers is not crucial in nanoprecipitation according to the broad literature (Bilati *et al*., 2005b), it was clearly important in preventing these NP/MPs from aggregating upon centrifugation. In the current studies, the NP/MPs pellet could not be re-suspended without the presence of the poloxamer Pluronic F127 as a stabiliser.

As far as the encapsulation of pDNA is concerned, nanoprecipitation generally yields low encapsulation efficiencies (Peltonen *et al*., 2004, Martinez Rivas *et al*., 2017, Xu *et al*., 2019). Nanoprecipitation is designed solely to encapsulate hydrophobic molecules. When applied to water soluble molecules such as proteins and nucleic acids, the modification of nanoprecipitation such as the insolubilisation of the pDNA (pDNA condensation) and/or the inclusion of the pDNA/pDNA NPs in the aqueous phase instead of the solvent have been necessary (Yadav and Sawant, 2010,

Morales-Cruz *et al*., 2012, Chidambaram and Krishnasamy, 2014). In the current study, the encapsulation of naked pDNA and pDNA-PLL NPs in PLGA MPs using the modified nanoprecipitation method resulted in only a small percentage (2-3 %) of the initial amount of pDNA being encapsulated when the naked pDNA and pDNA-PLL NPs were included in the aqueous phase. This was possibly due to changes in the positive charge of PLL when in contact with DMSO or DMF due to changes in the pH when these solvents were added in nanoprecipitation. Evidently, PLL only becomes positively charged and shows pDNA condensation abilities at pH 7. When in contact with these solvents, it is possible that the PLL had lost its positive charge (Mikhonin *et al*., 2005, Mirtic and Grdadolnik, 2013) and released the condensed pDNA, hence the low encapsulation efficiency. Moreover, in contrast to the micro-sized droplets in double emulsion, the presence of pDNA-PLL NPs in the large volume aqueous phase in nanoprecipitation made it difficult for the pDNA-PLL to be encapsulated during PLGA NP/MP hardening.

Next, the double emulsion solvent evaporation method was used for the fabrication and encapsulation of naked pDNA and pDNA-PLL NPs in PLGA MPs. As with nanoprecipitation, two different PLGA and stabiliser concentrations, factors that are well known to affect PLGA MP size during preparation, were used. The population of particles produced by using 1.3 % (w/v) PLGA and 1% (w/v) PVA was in a micro size range and was highly polydisperse. To achieve a smaller PLGA particle size, the concentration of PLGA was decreased from 1.3 % to 0.5 % (w/v) while keeping other

formulation parameters such as stabiliser concentration constant. The resulting PLGA MP size was reduced. While the PLGA MPs size of the new batch was still relatively high for intracellular delivery purposes, the structure of the newly formed MPs was compromised as a result of the reduced PLGA concentration, as shown in the TEM images. Moreover, the PDI values had not improved. On the other hand, with the increase of the PVA concentration from 1 % to 3 % (w/v) and the application of 0.5 % (w/v) of BSA as an inner surfactant, a significant reduction in PLGA MP size was observed even when higher concentrations of PLGA (1.3 %) were used. Furthermore, not only did the size of the PLGA MPs decrease, the PDI values also improved dramatically. This could have been due to the increased emulsion stabilisation effect of PVA. It is known that higher concentrations of PVA result in the production of smaller PLGA MPs due to the accumulation of the surfactant molecules on the surface of the oil droplets to prevent their coalescence and the destabilisation of the emulsion (Capan *et al*., 1999a, Abbas *et al*., 2008). Therefore, these optimised parameters were employed for the preparations of PLGA MPs during pDNA-PLL NPs encapsulation.

PLGA MPs are highly negatively charged due to the presence of carboxylic acid end groups (Vandervoort and Ludwig, 2002). In the current study, the surface charge of PLGA MPs was highly negatively charged at around -40 mV when a low concentration of non-ionic Pluronic F123 (0.5 %) and of PVA (1 %) (w/v) was used in nanoprecipitation and double emulsion, respectively. However, when a higher concentration (3 %) of PVA was used, the intensity of the negative charge on the surface PLGA MPs was reduced, as indicated

by Zeta potential measurements. At this point, the Zeta potential of these MPs was only -22.7 mV. This could have occurred as a result of the incorporation of PVA molecules in PLGA MPs, particularly at the surface during PLGA MP formation. PVA is a non-ionic surfactant (Damas *et al*., 2008, Negm *et al*., 2015) that could mask the negative carboxyl groups in PLGA and, consequently, reduce the overall Zeta potential, particularly at high concentrations.

The encapsulation of naked pDNA in PLGA MPs is difficult due to differences in the physico-chemical properties of both. pDNA is a large molecule in the order of hundreds of nanometres, which would Pose a problem for its encapsulation in sub-micron sized PLGA particles. Moreover, its negative charge produces repulsive forces with negatively charged PLGA. Furthermore, the hydrophilic nature of pDNA restricts its combination with PLGA in one solvent and promotes its escape to the aqueous phase during the encapsulation process, hence low encapsulation efficiency (Walter *et al*., 2001, Cun *et al*., 2011) pDNA condensation is the technique that is applied most frequently to enhance its encapsulation in PLGA MPs. This method minimises its size and neutralises its charge, which is necessary in order to facilitate the encapsulation process (Gebrekidan *et al*., 2000, Mok and Park, 2008).

3.8.3 The importance of robust experimental control parameters

For the encapsulation of the nucleic acid, it is important that the process is controlled using robust experimental comparisons, which have been lacking

in some previous studies that used PLGA encapsulation (Zhao *et al*., 2013, Tahara *et al*., 2008, Tahara *et al*., 2010, Patil and Panyam, 2009, Capan *et al*., 1999b). There are several techniques to enhance the encapsulation of macromolecules such as nucleic acids in PLGA MPs (Steinbach *et al*., 2016, Danhier *et al*., 2012, Kim *et al*., 2019), one being the use of cationic reagents to condense and minimise the size of the macromolecule, thus attaining higher encapsulation efficiency. However, the process was controlled poorly in the previous studies, and these did not follow the dynamics of encapsulation and did not specifically address whether the condensed nucleic acid was encapsulated in the core or was bound to the surface of the PLGA MP. It is highly likely that the small-sized, positively charged pDNA NPs (cationic polymer condensed nucleic acids) bind to the surface of negatively charged PLGA MPs through electrostatic interactions. The surface binding produces a slightly positive or neutral PLGA MPs as a result of charge neutralisation, an effect identified by measuring the surface charge in comparison to that of blank MPs. In the present work, this possibility was accounted for, moreover, other parameters as detailed in Chapter 4 Section 4.13.1 were applied. Both controls proved successfully that no surface attachment or sedimentation of pDNA-PLL NPs occurred during the process of PLGA MP preparation, and the resultant EE % was entirely due to encapsulated pDNA in the core of PLGA MPs. It is believed that this work is one of the first studies to consider such controls for encapsulation.

3.8.4 Encapsulation efficiencies and release studies

The encapsulation efficiency of pDNA-PLL NPs was calculated using the so-called direct method in which the amount of released pDNA is measured from dissolved PLGA MPs rather than by subtracting the amount of the pDNA lost in the supernatant (indirect method) from the total amount of pDNA used initially. The reason for this is that a considerable amount of nucleic acid is lost during the encapsulation process, and calculating the amount of released and lost pDNA does not add up to 100 % of the amount of pDNA used initially; therefore, it produces false positive results in EE % measurements (Cun *et al*., 2011). The release studies were used as another method to calculate the percentage of encapsulated pDNA-PLL. Measuring the EE % by dissolving the PLGA MPs and extracting the encapsulated pDNA-PLL revealed that only 30 µg of the total 100 µg of pDNA-PLL was encapsulated. However, about 61.9 µg of pDNA was released from the PLGA MPs during the 40-day release study, indicating an EE of 61.9 %. Therefore, there might have been some loss in the pDNA-PLL during extraction from the PLGA MPs. Only the amount of pDNA (34 µg) released in the first 24 hours was accounted for and used to confirm the EE % because the amount released on the following days did not contribute to the overnight transfection results. The release of pDNA from PLGA MPs was tri-phasic and consisted of burst release, continuous and bulk erosion phases. The burst release phase characteristic of PLGA MPs is mainly affected by its molecular weight and the ratio of lactic acid to glycolic acid. PLGA 5050 is the most

unstable form of PLGA and degrades faster than do other glycolic/lactic acid ratios of PLGA (Schliecker *et al*., 2003, Park, 1995, Milosevic *et al*., 2018); hence, the burst release phenomenon was extremely visible in the present release study.

3.8.5 The integrity of the encapsulated pDNA

In double emulsion, sonication steps are required to produce the first and second emulsions. As sonication is a routine technique for DNA fragmentation in DNA cloning and sequencing procedures and their downstream applications, there are concerns about pDNA integrity during the fabrication process in the double emulsion method. It is worth considering that, depending on the size of the DNA required for cloning, a minimum of two to 20 minutes of sonication is necessary for DNA fragmentation (Pchelintsev *et al*., 2016, Sambrook and Russell, 2006a). In the present study, the duration of sonication was considerably less than the above studies. Therefore, the current results show no effect of sonication on naked, pDNA-PLL NPs, or on pDNA-PLL NPs extracted from PLGA MPs. The integrity of sonicated DNA in these samples were tested by means of bacterial transformation, which is a more sensitive technique than cellular transfection studies for detecting pDNA nicking as the effect of sonication. Moreover, it has been reported that pDNA condensation with PLL further stabilised the pDNA and protects it from the effect of sonication (Wu *et al*., 2009, Goodman *et al*., 2004, An and Jin, 2012).

3.9 Chapter summary

1. The production of PLGA particles in the sub-micron region (PLGA MPs) with useful characteristics for gene delivery in terms of size, morphology, structure and the ability to encapsulate pDNA is achievable through the modification of formulation parameters such as fabrication methods, the concentration of the polymer, the stabiliser and the type of solvent.

2. The condensation of pDNA to decrease its hydrodynamic size and to alter its negative charge is necessary for its encapsulation in PLGA MPs.

3. pDNA NP/MPs' size and morphology are largely dependent on the nature of the condensing agent and its molecular weight. Moreover, the (+/-) charge ratio also has an effect on the degree of pDNA condensation/aggregation and, ultimately, on the size of the pDNA NP/MPs produced.

4. pDNA-PLL NP formation could be confirmed by measuring the size, morphology, surface charge, DNA binding dyes and DNA NPs dissociation assays.

5. The design of experimental controls such as Zeta potential measurements and other controls, is necessary to ensure the successful process of pDNA encapsulation.

6. The direct measurement of the amount of pDNA extracted from dissolved PLGA MP is more reliable to measure the EE % due to the apparent loss of pDNA during the encapsulation process.

7. Other methods, such as pDNA release studies from PLGA MPs, could also be used to confirm the EE % of pDNA.

8. It is important to consider the effect of formulation parameters such as organic solvents and sonication on the integrity of the encapsulated pDNA.

Chapter 4.

Complexation of GET peptides with PLGA MPs

4.1 Introduction

Enhancing the transfection efficiency of non-viral gene delivery vectors is essential before any applications of these are realised and the full potential of these vectors is harnessed. Many agents, such as cationic polypeptides and cell penetrating peptides have been employed to enhance their applicability; however, their transfection levels still lag far behind viral vectors.

In this chapter, the effect of GET peptides in enhancing the intracellular delivery and transfection of PLGA MPs was demonstrated. Moreover, the effect of enhanced transfection on cell viability was determined. Furthermore, the interaction between PLGA MPs and GET peptide is characterised, and the effect of environmental factors such as serum content in growth media on this interaction, and enhanced transfection properties is demonstrated. Finally, orders of magnitude-enhanced levels of intracellular delivery and the transfection of GET peptides are demonstrated in comparison to their non-modified CPP analogues.

4.2 Interaction of PLGA MPs with GET

It is widely accepted that negatively charged PLGA MPs interact with positively charged CPPs and other cationic poly peptides electrostatically, during which the MP surface charge shifts from negative to positive, or the neutralisation of charges occur (Mishra *et al*., 2011, Sah *et al*., 2013, Abu-Awwad *et al*., 2017). Therefore, to demonstrate the effect of GET peptides on the intracellular delivery (transduction) and transfection of pDNA encapsulated PLGA MPs in this study, due to the counterion properties of both, negatively charged PLGA MPs were complexed with positively charged GET peptides to produce PLGA-GET MPs.

Zeta potential studies were employed to confirm the complexation of PLGA MPs and GET peptides. Upon complexation/coating of blank or pDNA encapsulated PLGA MPs with GET peptides, namely P218R (PR), P21LK158R (PLR) and FGF2BLK158R (FLR), the surface charge of these PLGA MPs changed significantly from negative to neutral or slightly positive (Figure 4-1), indicating successful complexation. Regardless of the (+/-) (NH_3 in GET peptide/COOH in PLGA) ratio, the same molar concentration of 4 µM of each of the GET peptides (for 0.2 mg PLGA MPs) shifted the surface charge to almost the same extent except for PLGA-PLR MPs, which recorded more positively charged MPs in comparison to PLGA-PR. No significant difference in Zeta potential was observed between PLGA-PLR and PLGA-FLR or between PLGA-PR and PLGA-FLR MPs (Figure 4-1). This strategy of PLGA MP coating

with GET peptides was used in the transduction, transfection and differentiation studies.

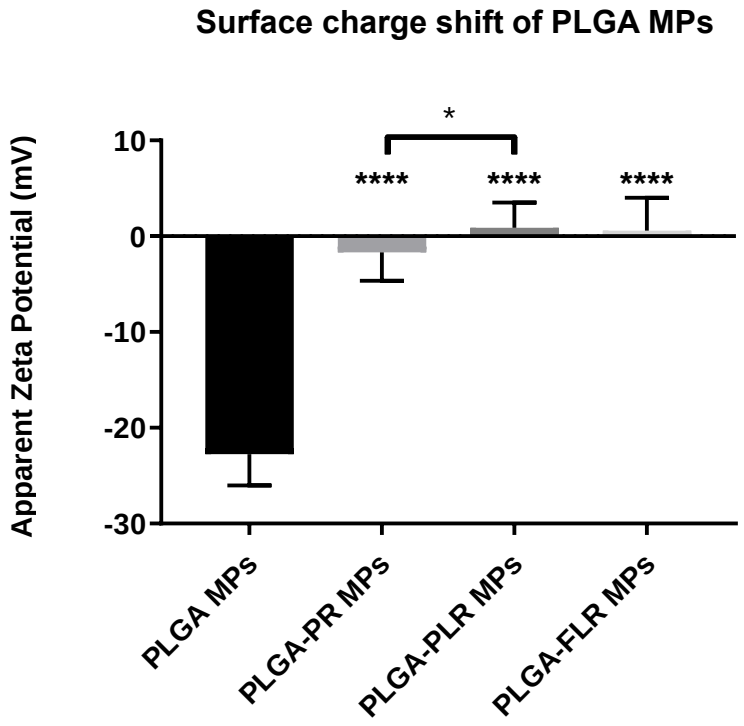

Figure 4-1 Surface charge shift of PLGA MPs coated with GET peptides. PLGA MPs represent blank and pDNA encapsulated PLGA MPs**.** coating of PLGA MPs with PR, PLR or FLR increases their Zeta potential indicating the attachment of these GET peptides on the surface of PLGA MPs. Measurements were carried out 15 min. after complexation. Zeta potential of PLGA MPs changes from ~ -25 mV to almost neutrally charged MPs after complexation except for PLGA-PLR MPs with slight positive charge that was significant to PLGA-PR MPs. The asterisk over the bars indicate significance to control (PLGA MPs), the asterisk over the lines indicate significance between groups. One-way Anova statistical analysis was used to generate the graph followed by Tukey test to determine significant differences between the mean of each treatment. The data presented as mean ± SD. Where significance was **** or *, P value was < 0.0001 or 0.0332 respectively.

4.3 PLGA-GET MPs for enhanced intracellular delivery characteristics

Fluorescence microscopy imaging was used as a qualitative analysis tool to demonstrate the enhanced transduction properties of GET peptides. For the purpose of this study Nile Red (hydrophobic) and Atto 590 (hydrophilic) encapsulated PLGA-GET MPs were delivered to mouse embryonic fibroblast cell line (NIH3T3). Firstly, to demonstrate the enhanced transduction effect of the simplest version of the GET peptides, PLGA MPs were complexed with PR peptide and delivered to cultured cells. The fluorescence microscope images indicated enhanced PLGA transduction when complexed with PR in comparison to PLGA MPs delivered alone. Moreover, the enhanced transduction was more profound in Serum Free Media (SFM) for both Nile Red and Atto 590 encapsulated PLGA MPs (Figure 4-2). To quantify the degree of enhancement in the transduction of PLGA-PR MP treated cells in comparison to non-complexed PLGA MPs, flow cytometry analysis was used to measure the average fluorescence intensity of the two groups of samples. The same imaged samples were considered suitable for flow cytometry analysis due to the photo-bleach resistant properties of the encapsulated fluorescent dyes. In line with the previous microscopic observations, PLGA-PR MP transduced cells recorded higher fluorescence intensity in comparison to control non-complexed PLGA MPs, particularly in SFM.

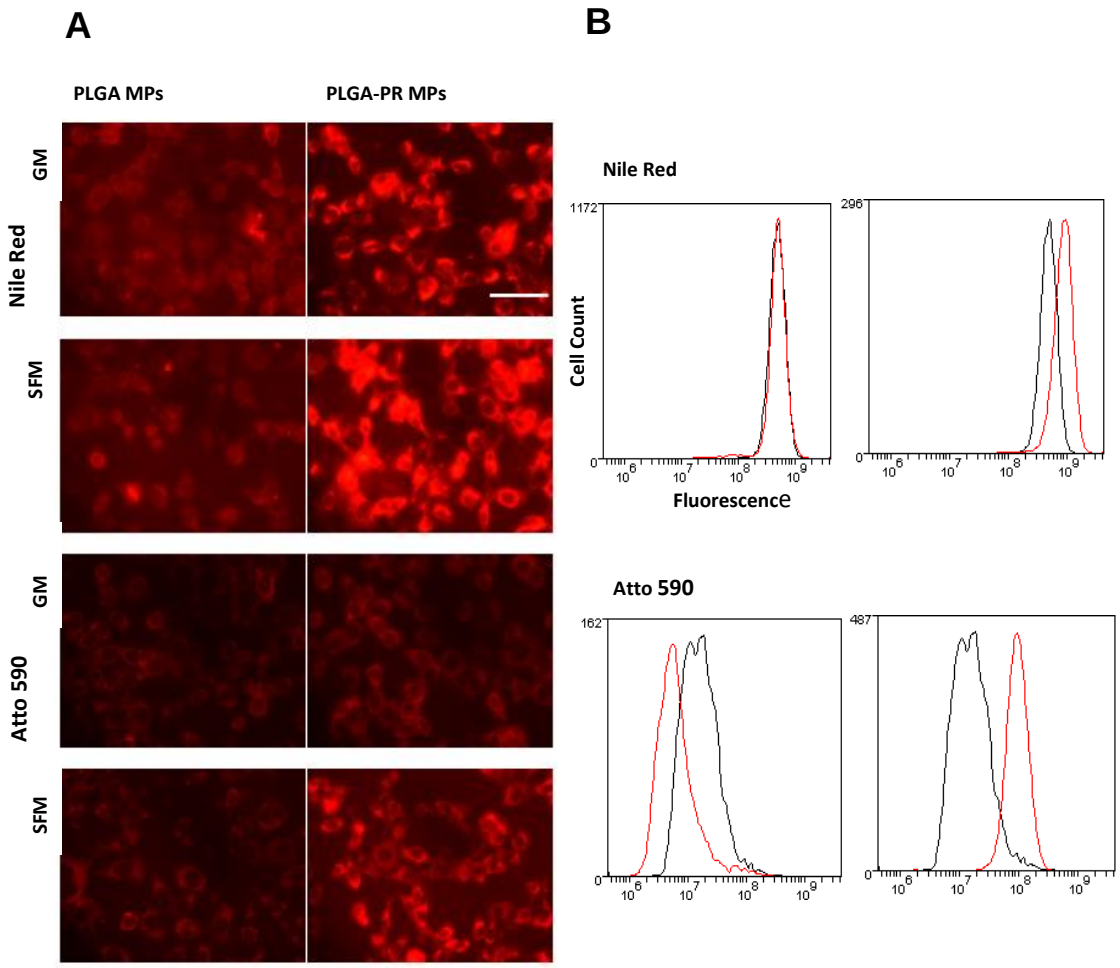

Figure 4-2 Enhanced intracellular delivery of PLGA MPs complexed with PR. (A) Fluorescence microscopy images of NIH3T3 cells after an overnight transduction with Nile red, Atto 590 encapsulated PLGA MPs with and without PR peptide in 10 % FCS containing media (Growth media; GM) or SFM. The peptide significantly enhanced the transduction of PLGA MPs especially in SFM Scale bar 100 µm. (B) Quantitative flow cytometry histogram shows the uptake of the dye encapsulated PLGA MPs by NIH3T3 cells. The black histogram on the right shows delivery in GM, the red histogram shows delivery in SFM. Histograms on the left shows the level of uptake in control PLGA MPs.

4.4 Transfection properties of PR

PR showed significantly enhanced intracellular delivery characteristics compared to non-complexed PLGA MPs in the transduction studies (Section 4.3). However, when employed in the transfection of pDNA encapsulated PLGA MPs, PR complexation resulted in low transfection in NIH3T3 cells *in vitro* in comparison to the positive control (pDNA-PLR MPs) published in Dixon *et al*., 2016, (Figure 4-3). To understand this effect, the transduction and transfection efficiencies of PR were compared to those of other GET peptides (PLR and FLR).

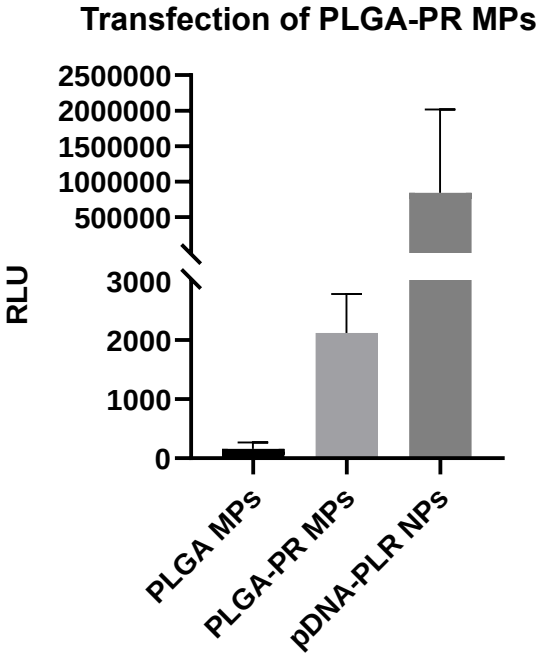

Figure 4-3 Poor transfection characteristic of PR peptide. Overnight transfection of pGluc encapsulated PLGA MPs in NIH3T3 cells resulted in poor transfection which was only slightly higher than the non-complexed PLGA MPs and the background. pDNA-PLR NPs was used as appositive control.

4.5 Comparison of the degree of transduction of GET variants

To employ a suitable GET peptide for transfection and bone differentiation studies (detailed in Chapter 5), a comparison of the degree of enhancement in transduction amongst variants of GET peptides (PR, PLR and FLR) (peptide sequences illustrated in Figure 4-4) was carried out at the same molar concentration using flow cytometry analysis. All three variants of GET peptides enhanced the delivery of PLGA MPs to NIH3T3 cells significantly when compared to non-complexed PLGA MPs. However, a higher degree of MP internalisation was observed when PLGA MPs were complexed with peptides containing LK15 (that is, PLR and FLR) compared to those lacking it (such as PR). This could have been due to the increased overall positive charge in the solution based on molar ratio comparison. Furthermore, substituting the HS binding motif from P21 to FGF2B in PLR had an additional enhanced effect. The highest degree of internalisation (up to seven folds) was recorded with FLR peptide in comparison to non-complexed PLGA MPs. Moreover, the degree of enhancement of FLR was significantly higher than it was when using PR or PLR (Figure 4-5). This result is in line with earlier publications by our group in which FLR peptide recorded higher levels of transduction by almost two orders of magnitude compared to PR in delivering red fluorescent protein (mRFP) in a range of cell types tested (Dixon *et al*., 2016, Osman *et al*., 2018).

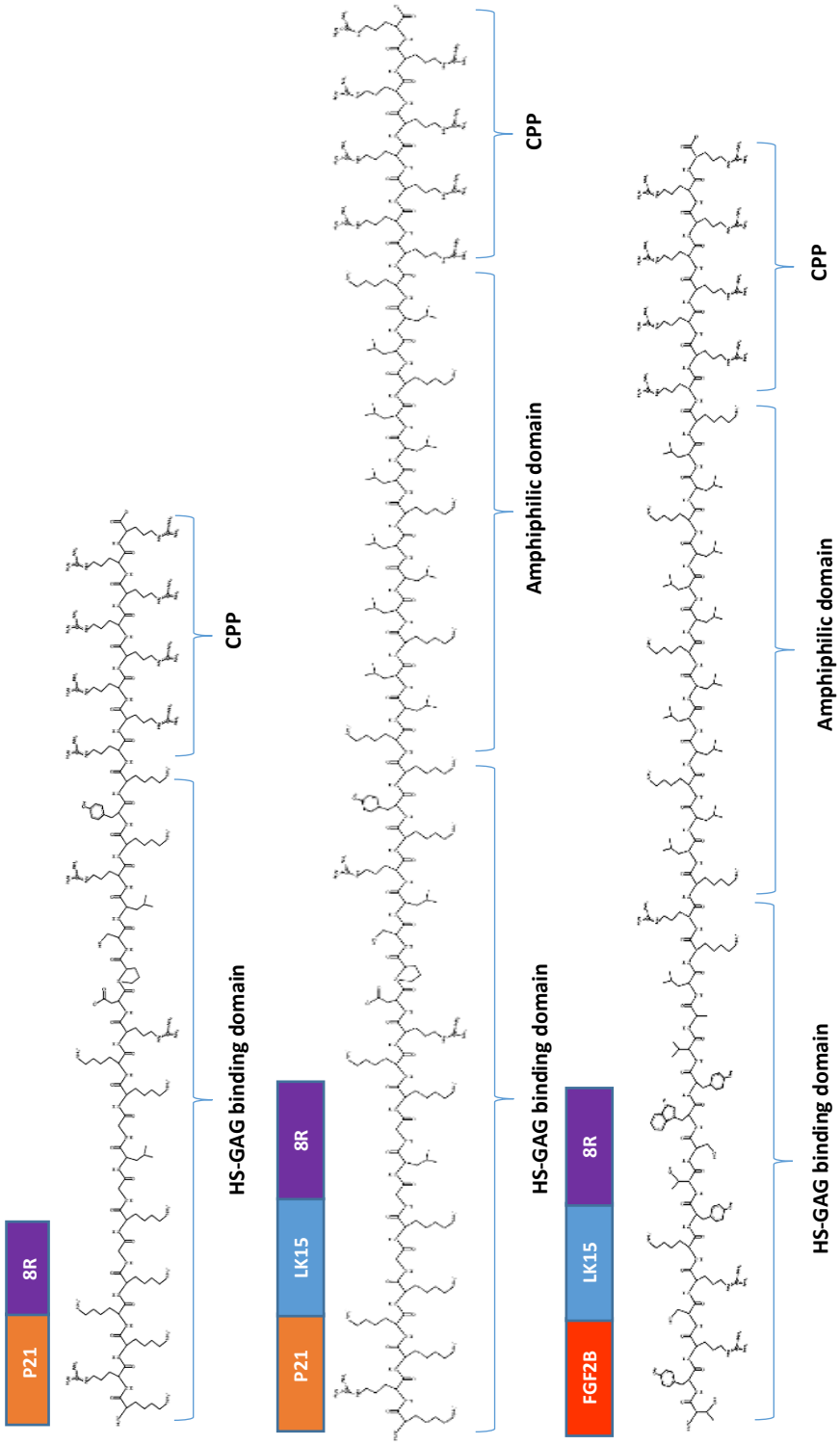

Figure 4-4 Variants of multi-motif GET petpides. PR consist of HBD and a CPP. PLR and FLR have an additional amphiphilic domain for enhacned endosomal escape.

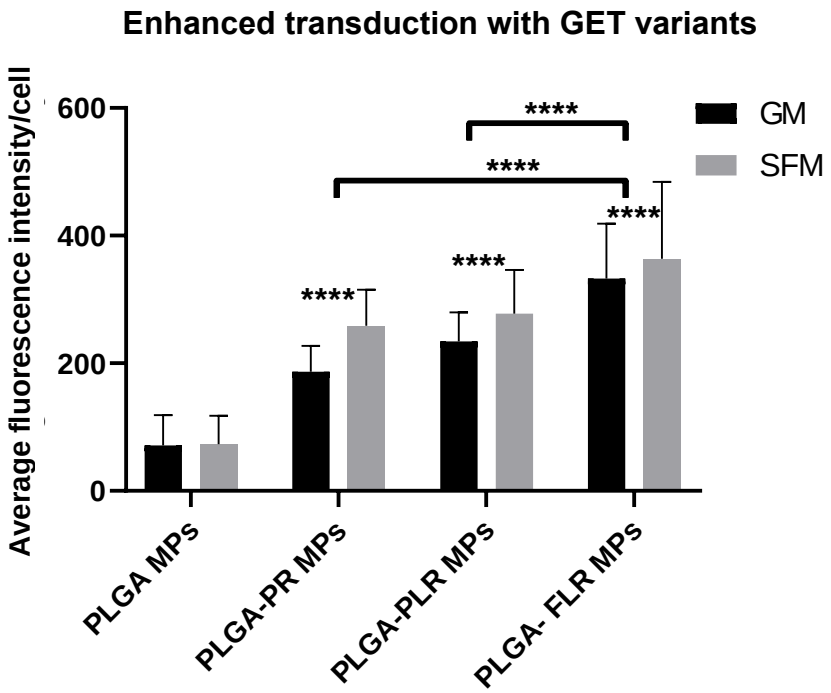

Figure 4-5 Comparison of degree of transduction of GET variants in NIH3T3 cell line. GET peptides; PR, PLR and FLR enhance the intracellular localisation of PLGA MPs significantly in comparison to PLGA MPs delivered alone in overnight transduction using flow cytometry analysis for quantification. FLR complexed PLGA MPs recorded up to seven folds higher degree of intracellular localisation when compared to non-complexed PLGA MPs which was also higher significantly in comparison to PR or PLR complexed PLGA MPs. PLR and PR complexed PLGA MPs recorded up to five and three folds increase in transduction respectively. Levels of enhancement was generally higher in SFM for all the peptides. The asterisk over the bars indicate significance to control (PLGA MPs), the asterisk over the lines indicate significance between peptides. Two-way Anova statistical analysis was used to generate the graph followed by Tukey test to determine significant differences between each mean. The data represented as mean ± SD. P value was < 0.0001.

4.6 Optimizing the GET peptide PLGA MP coating for efficient cell transfection

pGluc encapsulated PLGA MPs were used to assess the level of enhancement in transfection with GET peptides in NIH3T3 cell line. When comparing the transfection efficiency of the three variants of GET peptides, the complexation of PLR or FLR with PLGA MPs increased the level of transfection significantly by four to five orders of magnitude in comparison to non-complexed PLGA MPs. Moreover, the same degree of enhancement of transfection was observed when PLGA-PLR and PLGA-FLR were compared to PLGA-PR MPs. Furthermore, PLGA-FLR was significantly more efficient in transfection than were PLGA-PLR MPs (Figure 4-6). These results were also in line with the transduction studies. Therefore, GET peptides that bear LK15, PLR or FLR were used for these transfection studies. FLR peptide with the highest levels of transduction and transfection was specifically assigned for the bone differentiation studies (detailed in Chapter 5). It is noteworthy that, although there was some degree of internalisation of non-complexed PLGA MPs, this did not result in any levels of transfection

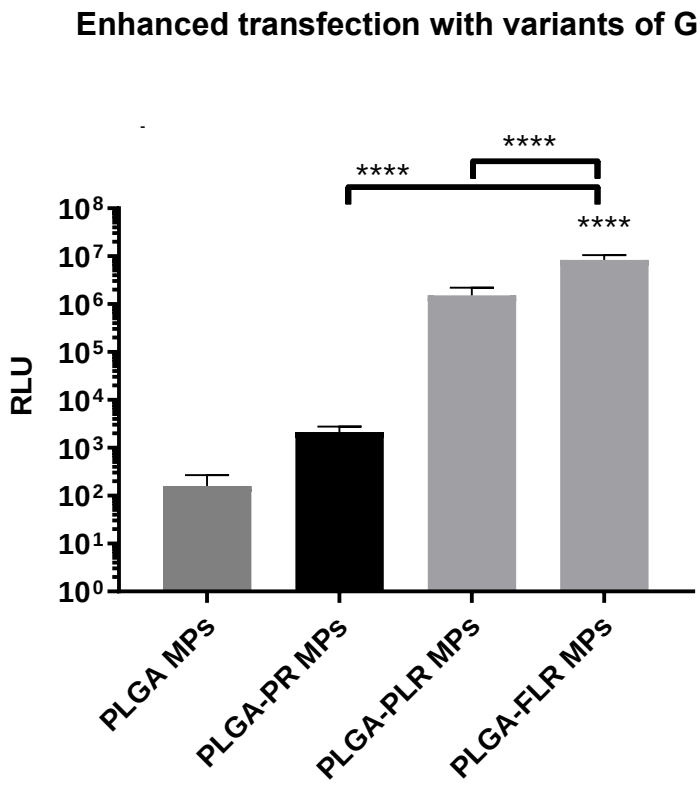

Figure 4-6 Comparison of the degree of transfection of GET variants complexed pDNA encapsulated PLGA MPs in NIH3T3 cell line: GET peptides; PLR and FLR enhance the transfection levels of PLGA MPs significantly in comparison to PLGA MPs delivered alone in an overnight transfection using pGluc. FLR complexed PLGA MPs recorded up to five orders of magnitude higher levels of transfection when compared to non-complexed PLGA MPs which was also higher significantly by almost one order of magnitude compared to PLR complexed PLGA MPs. Transfection of PR complexed PLGA MPs was poor and almost comparable to the control non-complexed PLGA MPs. The NIH3T3 cells were transfected in GM. The asterisk over the bars indicate significance to control (PLGA MPs), the asterisk over the lines indicate significance between groups. One-way Anova statistical analysis was used to generate the graph followed by Tukey test to determine significant differences between each mean. The data represented as mean ± SD. P value was < 0.0001.

4.7 PR produces low level of transfection

PR resulted in low level of transfection despite the enhanced delivery characteristics. This is likely due to PR lacking LK15, the endosomal escape motif of the system. In order to confirm this hypothesis and to understand the effect of LK15 on the transfection of PLGA MPs, the experiments were simplified using fluorescent MFP488 labelled pDNA complexed with PR or PLR to produce pDNA-PR and pDNA-PLR NPs, respectively. These NPs were transfected into NIH3T3 cells.

4.7.1 Physical characteristics

Before the delivery of pDNA-PR and pDNA-PLR NPs to cultured cells, the complexation and formation of NPs were confirmed using Zetasizer measurements. Moreover, to validate the transfection with MFP488 labelled pDNA-PR or pDNA-PLR NP experiments, the size of the resultant pDNA-PR and pDNA-PLR NP was compared; this is an important factor that is known to have a direct relationship with cellular internalisation and transfection levels (Prabha *et al*., 2016, Foroozandeh and Aziz, 2018). The mean diameters of pDNA-PR NPs and pDNA-PLR were 79.8 ± 8.1 and 71.5 ± 7.6 (mean ± SD), respectively. Figure 4-7 demonstrates the size distribution in both populations of NPs. pDNA condensation with PR and PLR produced NPs of the same size range as measured by the Zetasizer, excluding the effect of variance in NP size on cellular internalisation and transfection.

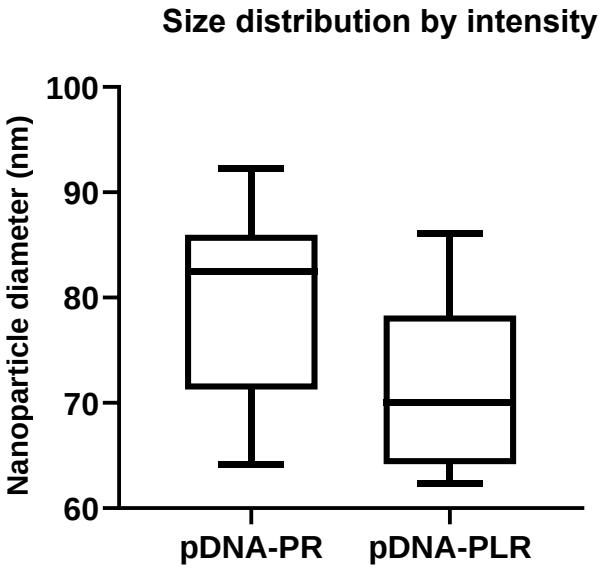

Figure 4-7 size distribution of pDNA-PR and pDNA-PLR NPs measured by Zetasizer. Intensity size distribution indicates the comparable NPs hydrodynamic diameter of both population of the NPs. The mean diameter of pDNA-PR NPs was 79.8 ± 8.1 and that of pDNA-PLR NPs was 71.5 ± 7.6. The data is presented as mean ± SD.

4.7.2 Intracellular delivery

To validate the experiments using MFP488 labelled pDNA-PR or pDNA-PLR NPs for transfection, further, these labelled NPs were delivered to NIH3T3 and the internalisation level of these NPs was observed using the fluorescence microscopy. In addition, the levels of intracellular delivery were compared using the flow cytometer quantification method. Both microscopic imaging and flow cytometry quantification analysis showed the efficient cellular internalisation of pDNA-PR and pDNA-PLR NPs to almost the same extent. Figure 4-8 shows the internalisation and quantification levels of both NPs. it appears in the fluorescence microscopy images that the fluorescent NPs are more diffusely localised in the cytosol in the case of PLR

complexation but mostly accumulated potentially trapped in the endosomes when lacked LK15 in PR.

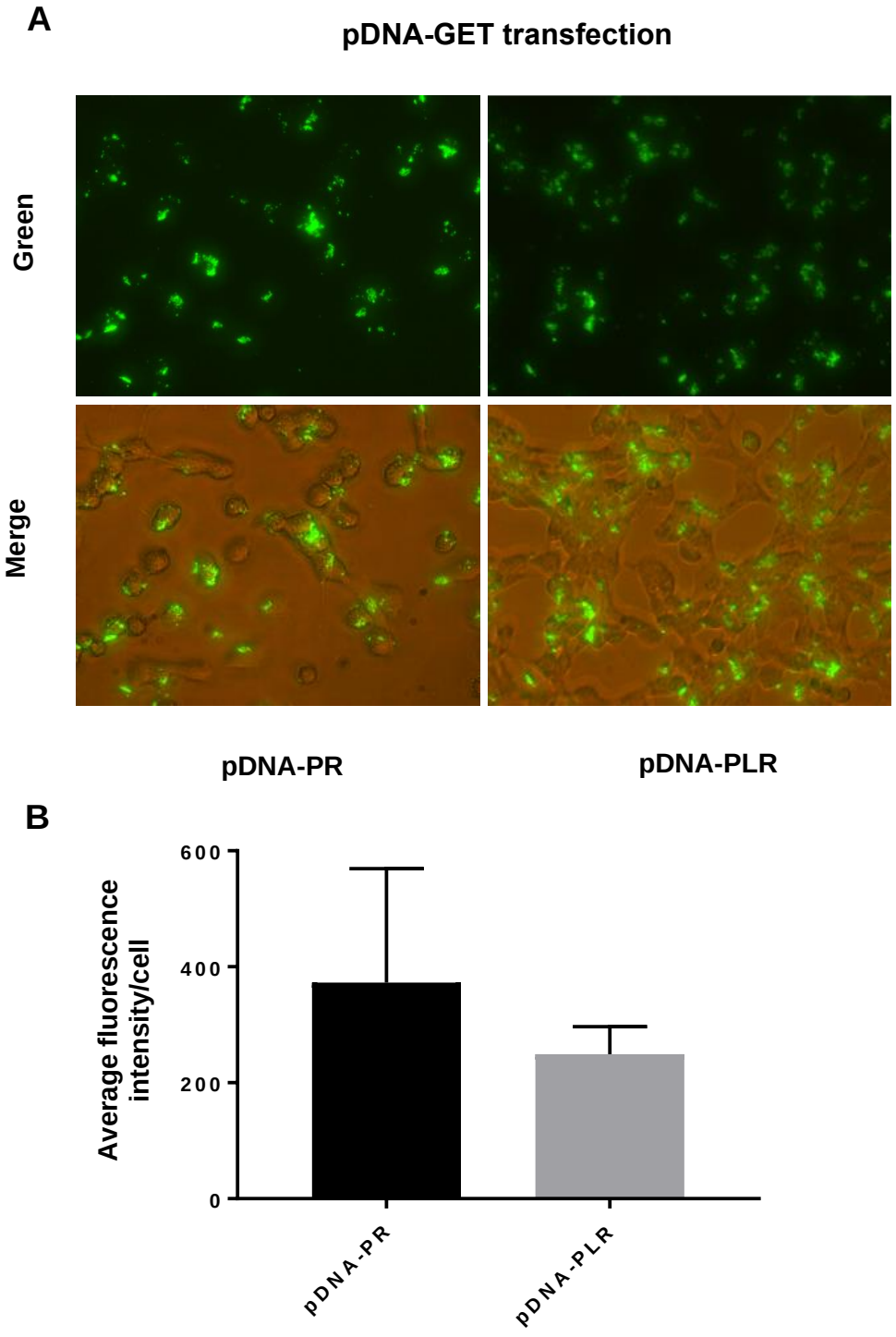

Figure 4-8 Comparison of intracellular delivery and localisation of pDNA-PR and pDNA-PLR NPs. (A) Both NPs show intracellular delivery detected by fluorescent microscopy imaging after overnight transfection of MFP488 labelled pGluc NIH3T3 cells in GM. The pDNA-PR NPs show discrete endosomal fluorescent NP accumulation in contrast to more diffuse pDNA-PLR NPs in the cellular compartments. Scale bar 100 μm. (B) Comparable intracellular levels of the NPs quantified by flow cytometry analysis shows no significant difference between pDNA-PR and pDNA-PLR NP transduction.

4.7.3 Transfection levels of pDNA-PR NPs compared to pDNA-PLR NPs

Next, to demonstrate the effect of the lack of LK15 peptide in PR on transfection, the levels of luciferase expression were compared using the same experimental condition of pDNA fluorescence labelling in the microscopic and flow cytometry analyses. pDNA-PR NPs had minimal transfection in contrast to pDNA-PLR NPs, as demonstrated in Figure 4-9. Consequently, it was concluded that despite the similar levels of internalisation of DNA-PR and DNA-PLR NPs, the presence of LK15 in was necessary for transfection in both non-encapsulated and encapsulated pDNA. Therefore, GET peptides that bear LK15, PLR and FLR were used for transfection and differentiation studies.

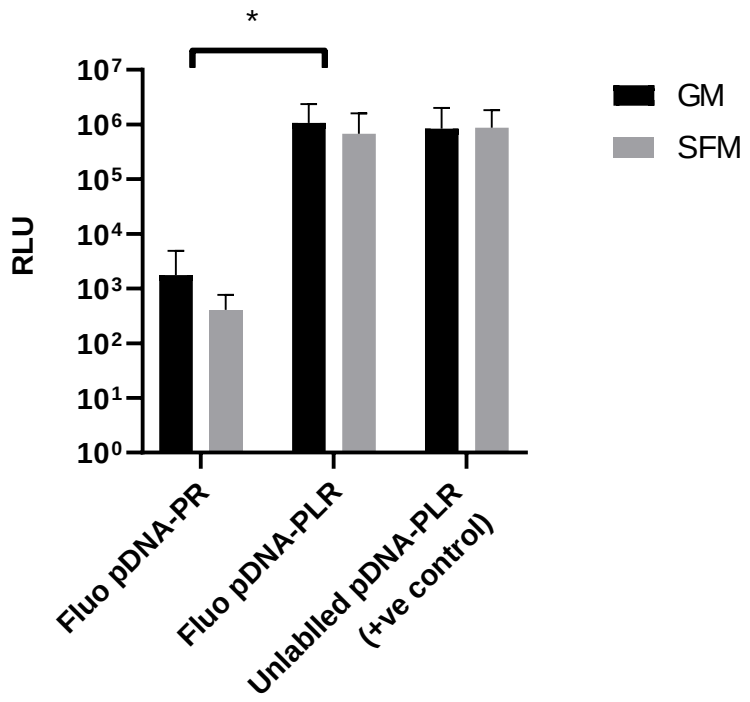

Figure 4-9 Comparison in the transfection levels of pDNA-PR and pDNA-PLR NPs. The graph shows the effect of lack of LK15 peptide in pDNA-PR NPs on their levels of transfection in comparison to pDNA-PLR NPs. pDNA fluorescent labelling does not affect the luciferase signal detected by the luminometer; demonstrated by transfection in unlabelled pDNA-PLR NPs positive control which is comparable to labelled pDNA-PLR NPs.

4.8 Dose optimisation of PLGA-LK15 containing GET MPs

As it was aimed to demonstrate the utility of these PLGA-GET MPs in biomedical applications with a focus on bone differentiation and regenerative medicine (as detailed in Chapter 5), the dose of PLR and FLR peptide coating per weight of PLGA MPs was optimised for transfection

studies in NIH3T3 and IHMSC. The optimised dose was chosen based on levels of internalisation, transfection and cell viability assays.

4.8.1 Optimisation of PLR dose

In order to determine if changes in the dose of PLR were related directly to the intracellular delivery levels, different doses of PLR per constant weight of PLGA MPs was delivered. Doses ranging from 0-40 µM final concentration of the peptide per 0.2 mg of PLGA MPs were delivered to NIH3T3 cells in GM and SFM. It was found that, when increasing the dose of PLR, the transduction level improved until it reached saturation at 4 µM (Figure 4-10). Based on these assays, the dose of 4 µM (per 0.2 mg PLGA) was taken forward in the transfection studies in NIH3T3 cells.

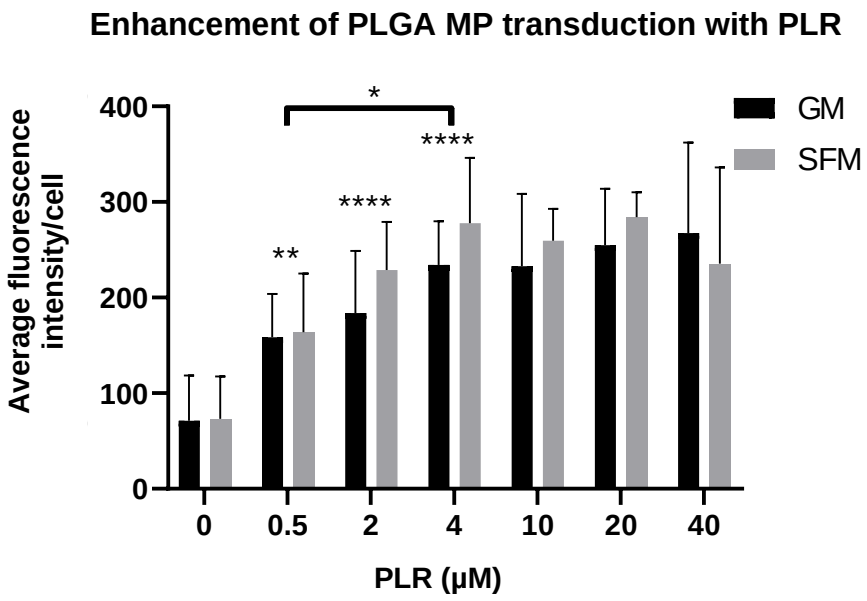

Figure 4-10 Comparison of degree of transduction of different doses of PLR complexed PLGA MPs in NIH3T3 cell line. The enhancement of intracellular delivery quantified with flow cytometry indicates increase in the intracellular levels of PLGA MPs with increasing the dose of PLR until saturation at the dose of 4 µM after overnight transduction of these MPs. The delivery of the MPs was slightly higher in SFM than in GM. The transduction level of PLGA-PLR MPs was three folds higher when compared to PLGA MPs (control). The data is presented as mean ± SD. Where significance was ***,** **or **** P value was 0.0332, 0.0021 or < 0.0001 respectively.

4.8.2 Optimisation of FLR dose

Following the same transduction experiment mentioned earlier using NIH3T3 cells, the dose of FLR was optimised for optimum transfection in IHMSC cells for bone differentiation assays. Similar to dose dependent transduction studies in NIH3T3 cells, a direct relationship between the dose of FLR and the levels of transduction was found in IHMSCs. When increasing the dose of the FLR peptide, the levels of transduction increased until saturation was reached at a 4 µM dose (Figure 4-11).

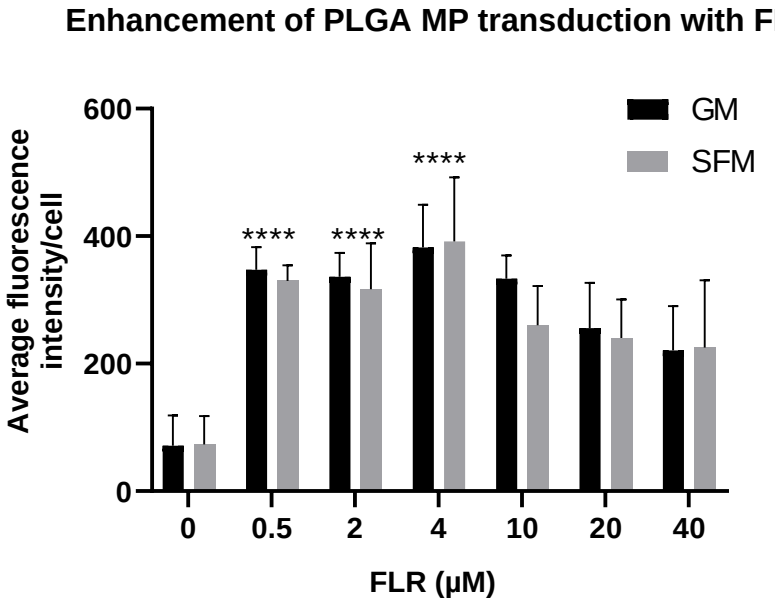

Figure 4-11 Comparison of degree of transduction of different doses of FLR complexed PLGA MPs in IHMSC cell line. The enhancement of intracellular delivery quantified with flow cytometry indicates increase in the intracellular levels with increasing the dose of FLR until saturation at dose of 4 µM after an overnight transduction of these MPs. The transduction levels of PLGA-FLR MPs was seven folds higher when compared to PLGA MPs (control). The data is represented as mean ± SD. P value was < 0.0001.

4.9 Effect of dose-based enhanced transduction on transfection

In order to determine whether dose-dependent enhanced transduction would be reflected in a dose-dependent increase in transfection, NIH3T3 cells were chosen for the transfection of pDNA encapsulated PLGA MPs complexed with increasing doses of PLR. For this experiment, a constant dose of pDNA encapsulated PLGA MPs (1 µg pDNA content per 0.2 mg PLGA MPs) were complexed with PLR in the molar ratios tested in the previous transduction experiments (Section 4.8.1). Figure 4-12A demonstrates dose based enhanced transfection in NIH3T3 cells that were transfected

overnight. The experiment showed enhanced transfection in line with increasing the dose of GET peptide. These experiments conclusively showed the direct effect of enhanced levels of transduction on levels of transfection in response to an increase in the dose of GET peptides. Based on these results, dose of 4 µM of FLR was considered the optimal dose for transfection in IHMSC. Therefore, the transfection efficiency of PLGA-FLR MPs in IHMSC was determined using pGFP. Measuring the transfection efficiency of pGFP encapsulated PLGA-FLR MPs in comparison to pGFP-FLR NPs (positive control) demonstrated approximately 15 % transfection efficiency of the encapsulated GFP at Day 2 post transfection (Figure 4-12B).

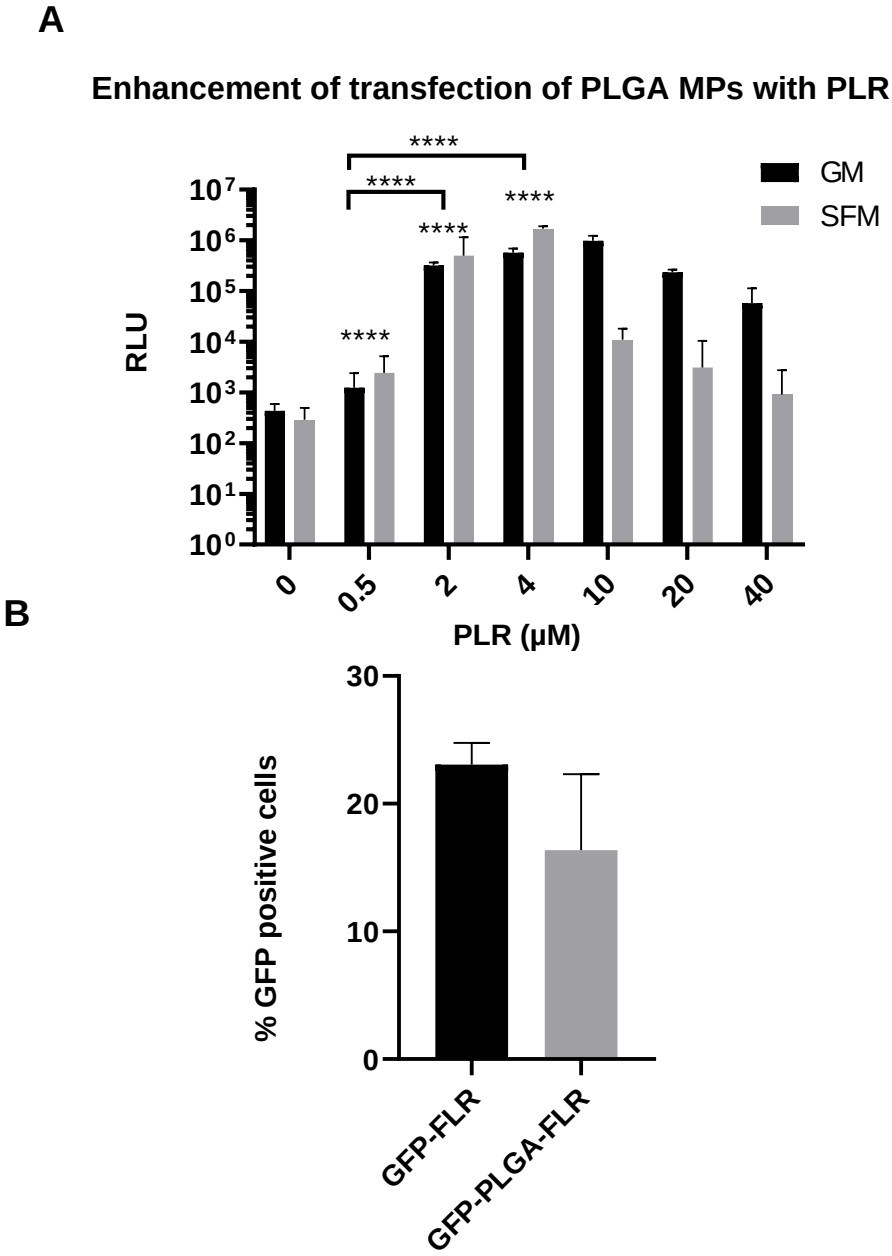

Figure 4-12 Enhanced transfection of PLGA MPs complexed with PLR or FLR. (A) Comparison of degree of transfection of different doses of PLR complexed pGluc encapsulated PLGA MPs in NIH3T3 cell line. The enhancement of transfection levels of PLGA MPs is linear with increase in the dose of PLR. The levels of transfections gradually increase until saturation at 4 µM PLR. The transfection level of the MPs is slightly higher in SFM than in GM at low doses of PLR, however, these levels of transfections reduce in SFM at high doses PLR. The transfection level of PLGA-PLR MPs was higher by almost four orders of magnitude when compared to PLGA MPs (control). (B) % of transfection efficiency of encapsulated pGFP in PLGA MPs complexed with 4 µM FLR in IHMSCs at day two post transfection. The data is presented as mean ± SD. P values were < 0.0001.

4.10 Cell viability studies

Cell viability studies were employed to determine a safe and effective dose of GET peptide for the enhanced transduction and transfection of pDNA encapsulated PLGA MPs. For this experiment, due the direct relationship between enhanced transfection and cellular toxicities (Gao and Huang, 1996, Hofland *et al*., 1996, Betker and Anchordoquy, 2015), FLR peptide was chosen due to it having the highest transduction and transfection characteristics and complexed with pDNA encapsulated PLGA MPs for transfection in IHMSC cells. This cell line is more susceptible than is NIH3T3 and that has higher toxicity with standard transfection reagents such as Lipofectamine 3000 (Tomankova *et al*., 2015, Neumann *et al*., 2013). Moreover, the choice of this experimental set up was also required to optimise the dose of the FLR peptide in IHMSC transfection in bone differentiation assays. For this, the same doses of FLR peptide per weight of PLGA MPs as in the above experiments (Sections 4.8.1 and 4.8.2) were used for the present study. Moreover, the transfection conditions of overnight treatment in both media, GM and SFM, were also replicated in this study. Cell viability assays revealed more than 80 % of viable cells at FLR concentrations as high as 20 μM in GM in comparison to the safest versions of Lipofectamine (Lipofectamine 3000). However, cell viabilities were compromised at concentrations ≥ 4 μM in SFM (Figure 4-13), as seen in other transfection systems (Jeong and Park, 2002). These results demonstrated

the safe and effective dose of ≤ 4 µM GET Peptides for the optimal transfection of pDNA encapsulated PLGA MPs.

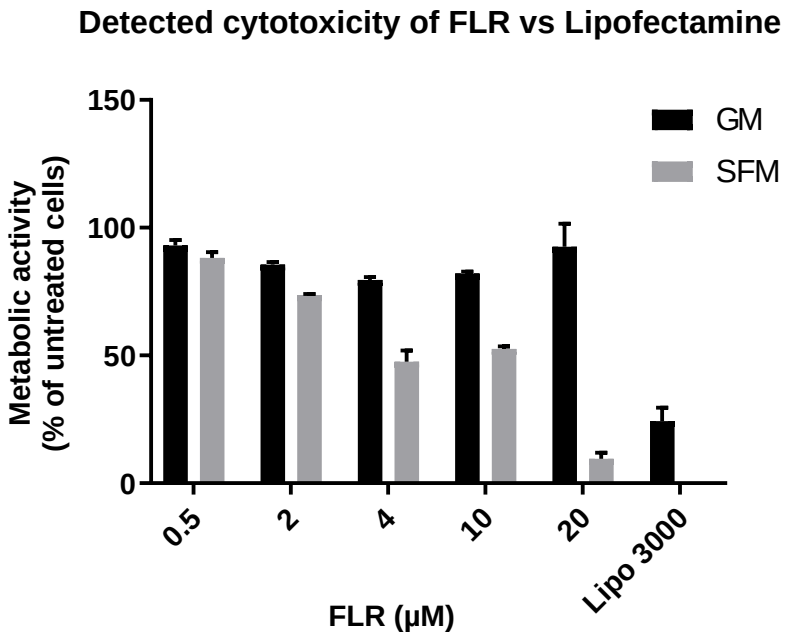

Figure 4-13 Cell metabolic activities in response to increasing doses of FLR peptide 24 hr. after transfection. FLR peptide show high margins of safety especially in GM in comparison to Lipofectamine 3000**.** At least 80 % viable cells treated with as high as 20 µM FLR in GM was recorded. The percentage metabolic activity was calculated in comparison to non-transfected cells which was normalised to 100 %. The data is presented as mean ± SD.

4.11 The effect of serum on PLGA-GET MPs

The stability of the PLGA-GET MPs was studied in the presence of environmental factors that represented both *in vitro* conditions that the MPs encounter during transduction and transfection studies, and *in vivo* applications of non-viral vectors. One of the most important factors is the serum content (foetal calf serum, or FCS) in cell culture media. FCS contain

a negatively charged protein; Albumin, which might compete with the negatively charged PLGA MPs for GET peptide binding. To assess the interaction of FCS with PLGA-GET MPs, PLGA-GET MPs were incubated with increasing concentrations of FCS from 0-10 % resembling the FCS percentage content in cell culture media, in which 0% represents SFM and 10% represents GM. Zeta potential studies were employed to characterise this interaction by measuring the surface charge of PLGA MPs after incubation with SFM or serum containing media for 15 minutes. Upon incubation, the Zeta potential of PLGA-GET MPs reduced gradually when increasing the FCS% content, reaching approximately -10 mV in GM (Figure 4-14).

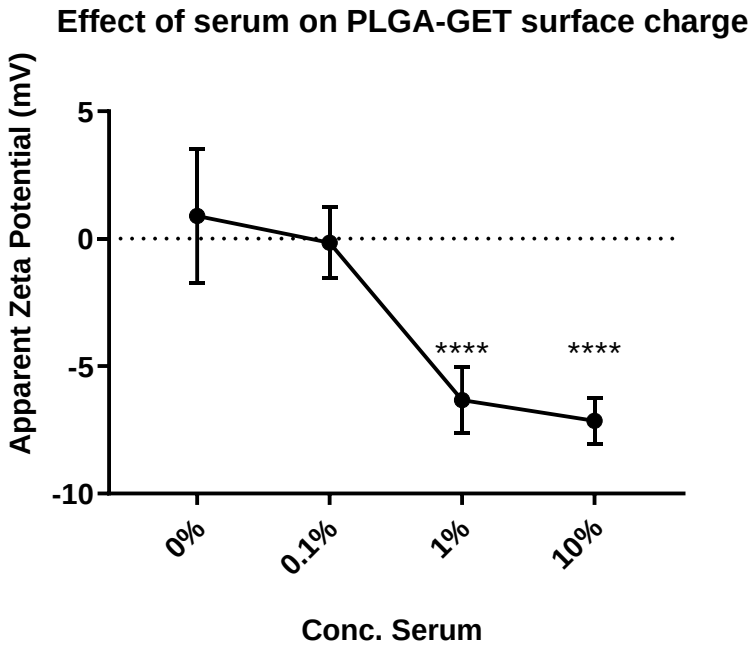

Figure 4-14 Effect of serum on PLGA-GET interaction. Change in the zeta potential of PLGA-GET MPs upon their incubation in increasing concentrations of FCS in SFM. The significant change in surface charge from neutral to negative Indicates serum albumin

electrostatic binding to GET on or distant from the surface of PLGA MPs. The reduction in Zeta potential is proportional to the amount of FCS content in the media.

4.12 The colloidal stability of PLGA-GET MPs

The assessment of the colloidal stability and aggregation behaviours of PLGA-GET MPs is an important step in characterising MPs for successful gene delivery outcomes. Highly negative or positively charged MPs are the most colloidally stable MPs due to the repulsive forces between like-charged MPs that prevent them from settlement and subsequent aggregation with each other (Carvalho *et al*., 2018, Moore *et al*., 2015). Due to the fact that these PLGA-GET MPs were neutrally charged, the aggregation behaviour of these MPs in GM (mimicking the cell culture conditions) was assessed by measuring of the size of the PLGA-GET MPs five hours after incubation, as this is the time during which the majority of MP uptake occurs in *in vitro* transfection studies (Park *et al*., 2011, Kang *et al*., 2012, Sahin *et al*., 2017). The measurements of MP size indicated a growth in the size of these GET complexed PLGA MPs in comparison to colloidally stable, non-complexed PLGA MPs. Moreover, the difficulty of removing these PLGA MPs during the washing steps of cultured cells in transduction and transfection studies could be due to the aggregation of these MPs. Figure 4-15 shows the presence of three peaks in the PLGA-GET MP population that were present in the Zetasizer reports. Peaks of small sized NPs in the range of 10 nm possibly indicate the complexation of GET with Albumin in GM. A second peak, which

forms the majority of the particle population according to the percentage given by the Zetasizer, indicates stable, non-aggregated PLGA-GET MPs, and the third peak indicates a small population of grown PLGA-GET MPs in a range of micro meters.

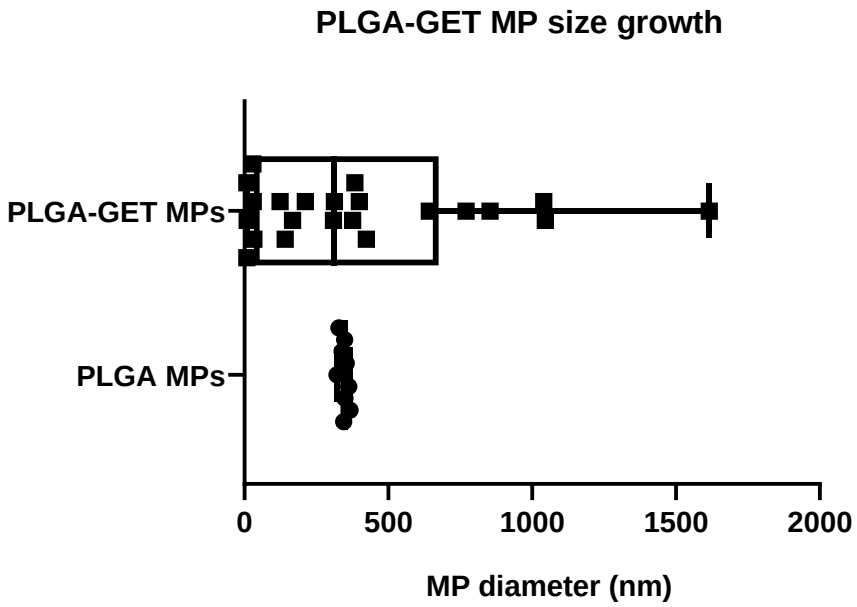

Figure 4-15 Growth of PLGA MPs in size after complexation with GET peptides and incubation in GM for 5 hr. The size of non-complexed PLGA-GET MPs is stable over the period of GM incubation compared to the size PLGA-GET MPs. The majority percentage of the PLGA-GET MPs were in the range of the non-complexed PLGA MPs of a around mean diameter of 0.35 µm however, the presence of other peaks of large particles in range of micro meter and smaller NPs in arrange of 10 nm was also present in the PLGA-GET MP population.

4.13 Further characterisation of PLGA-GET MPs

4.13.1 pDNA-PLL NPs do not sediment during the preparation of pDNA encapsulated PLGA MPs

In an attempt to determine whether the pDNA-PLL NPs were encapsulated in the PLGA MPs and to add to other characterisation steps detailed in Chapter 3 Section 3.7.2, the sedimentation of pDNA-PLL NPs during centrifugation in the process of pDNA encapsulation by double emulsion method was checked. For that, pDNA-PLL NPs were passed through the process of double emulsion, but without the PLGA. As a result, no pellet of pDNA-PLL was found by centrifugation, and these samples were used as controls in both measurements of the EE % by PicoGreen assay and complexed with PLR peptides for the transfection of NIH3T3 cells (Figure 4-16). As a result, these 'pDNA-PLL-PLR' did not produce any levels of transfection when compared to pDNA encapsulated PLGA MPs. These controls (in conjugation with Section 3.7.2) confirmed that pDNA-PLL NPs do not attach significantly to the surface of PLGA MPs, and do not sediment during the formulation process. Therefore, almost all the transfection is due to the pDNA encapsulated within the PLGA MPs, and the non-encapsulated pDNA is lost during the washing steps in the double emulsion process.

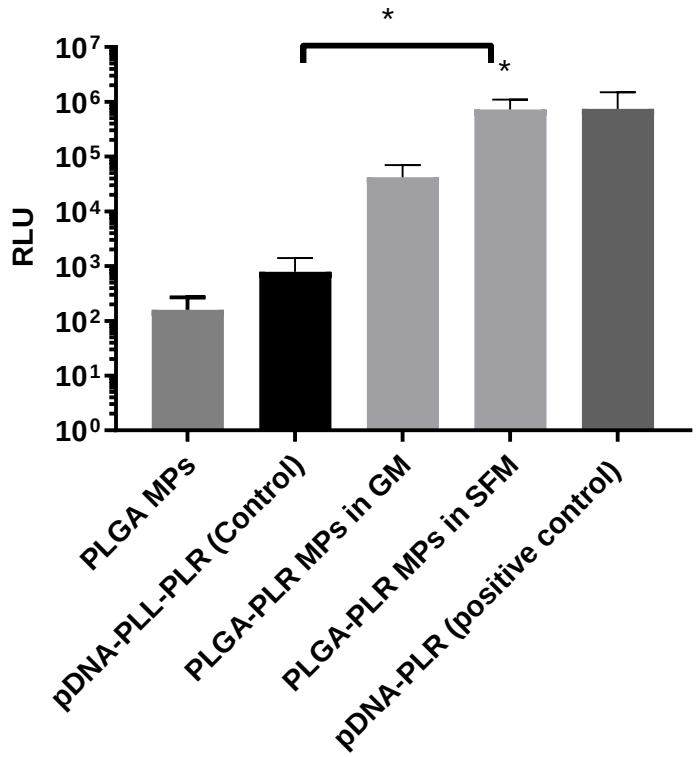

Figure 4-16 Localisation of the pDNA-PLL NPs. Transfection of pDNA encapsulated PLGA-PLR MPs was compared to controls (non-complexed PLGA MPs and pDNA-PLL NPs passed through the double emulsion process without PLGA). Complexation of PLR to PLGA MPs enhances the transfection in NIH3T3 cells. No transfection was detected in DNA-PLL NPs controls when complexed with the same dose of 4 µM PLR (pDNA-PLL-PLR). The data is represented as mean ± SD.

4.13.2 Assessment of the effect of PLL on transfection

To determine whether the PLL used in the condensation process of pDNA has contributed to the enhanced transfection of pDNA encapsulated PLGA MPs or the enhanced transfection was entirely due to the action of GET, the transfection levels of pDNA-PLL NPs (without encapsulation in PLGA) with or without PLR was tested in cultured NIH3T3 in GM. The result showed that pDNA-PLL NPs did not transfect the cells on their own and the luminescence

units were comparable to the background. On the other hand, when complexed with PLR (pDNA-PLL-PLR NPs), pDNA-PLL NPs resulted in fair levels of transfection, although these were not significant (Figure 4-17) and were lower by one order of magnitude than were the transfection levels produced from the same amount of pDNA (1 μg) when encapsulated in PLGA MPs and complexed with PLR (Section 4.6 and 4.13.1). To determine the interaction of pDNA-PLL NPs with PLR and the effect of serum Albumin on this interaction, pDNA-PLL-PLR NPs was transfected in SFM with an added 3mg/ml or 10 mg/ml of Bovine Serum Albumin (BSA). The higher Albumin content (compared to GM Albumin content of 3 mg/ml) increased the transfection levels of pDNA-PLL-PLR NPs significantly.

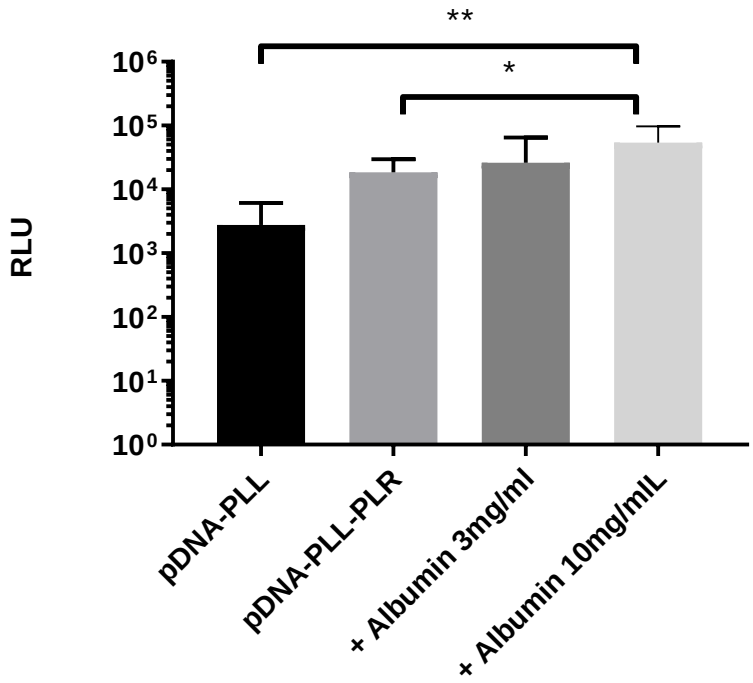

Figure 4-20 Determining the effect of PLL on transfection. pDNA-PLL NPs resulted in low levels of transfection using pGluc in NIH3T3 cells. Addition of PLR caused non-significant increase in the levels of transfection. Transfection in higher than physiological concentrations of Albumin in SFM increased the levels of transfections of these NPs significantly**.** The data is presented as mean ± SD. Where significance was *or ** P value was 0.0332 or 0.0021 respectively.

4.14 Comparison of GET with non-modified CPP

To confirm that the enhanced transduction characteristics of GET peptides was due to the presence of the heparin binding domain (HBD), P21 and FGF2B, their transduction and transfection levels were compared to their non-modified corresponding CPP and the most widely used TAT peptide (Table2) (Prochiantz, 2000, Koren *et al*., 2011). In this regard, the optimised 4 µM concentration of GET peptide was used to complex PLGA MPs with non-modified CPP in the Zeta potential, transduction and transfection studies.

Table 2: sequence and net charge of GET peptides and their non-modified correspondent CPPs.

Peptide	Amino acid sequence	Net charge
P21	KRKKKGKGLGKKRDPCLRKYK	11
8R	RRRRRRRR	8
P218R	KRKKKGKGLGKKRDPCLRKYK RRRRRRRR	19
LK15	KLLKLLLKLLLKLLK	5
P21LK15	KRKKKGKGLGKKRDPCLRKYK KLLKLLLKLLLKLLK	16
LK158R	KLLKLLLKLLLKLLK RRRRRRRR	13
P21LK158R	KRKKKGKGLGKKRDPCLRKYK KLLKLLLKLLLKLLK RRRRRRR	24
FGF2B	TYRSRKYTSWYVALKR	5
FGF2BLK158R	TYRSRKYTSWYVALKR KLLKLLLKLLLKLLK RRRRRRRR	18
TAT	YGRKKRRQRRR	8

4.14.1 Complexation of non-modified CPPs with PLGA MPs

Similar to the Zeta potential studies described in Section 4.2, in order to confirm the electrostatic complexation of the non-modified CPPs with PLGA MPs, the shift in surface charge of these MPs was measured after complexation and was compared to PLGA-GET MPs. Figure 4-18 demonstrates the electrostatic binding of these non-modified CPPs to PLGA MPs to form PLGA-non-modified CPP MPs.

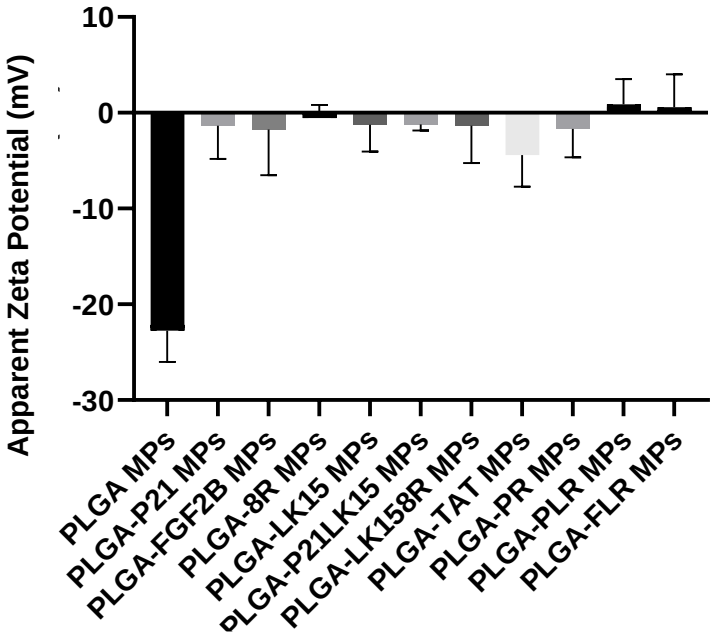

Figure 4-23 Surface charge shift of PLGA MPs coated with GET peptides and non-modified CPPs. coating of PLGA MPs with non-modified CPPs affects their surface charge indicating the electrostatic attachment of these peptides on the surface of PLGA MPs. Similar to complexation with GET peptides, Zeta potential of PLGA MPs changes from ~ -25mv to almost neutrally charged MPs upon complexation with the non-modified CPPs. Measurements were carried out 15 min. after complexation. Data is presented as mean ± SD.

4.14.2 Transduction of PLGA-non-modified CPP MPs

Following the confirmation of PLGA-non-modified CPP MP formation, their transduction levels were compared to that of PLGA-GET MPs in HIN3T3 cells using quantitative flow cytometry analysis. Figure 4-19 demonstrates the enhanced levels of transduction of GET peptides over the non-modified CPPs. In this study, two folds of 8R and four folds of each of P21LK15 and LK158R increase in fluorescence intensity were recorded in comparison to five and seven folds in PLR and FLR, respectively.

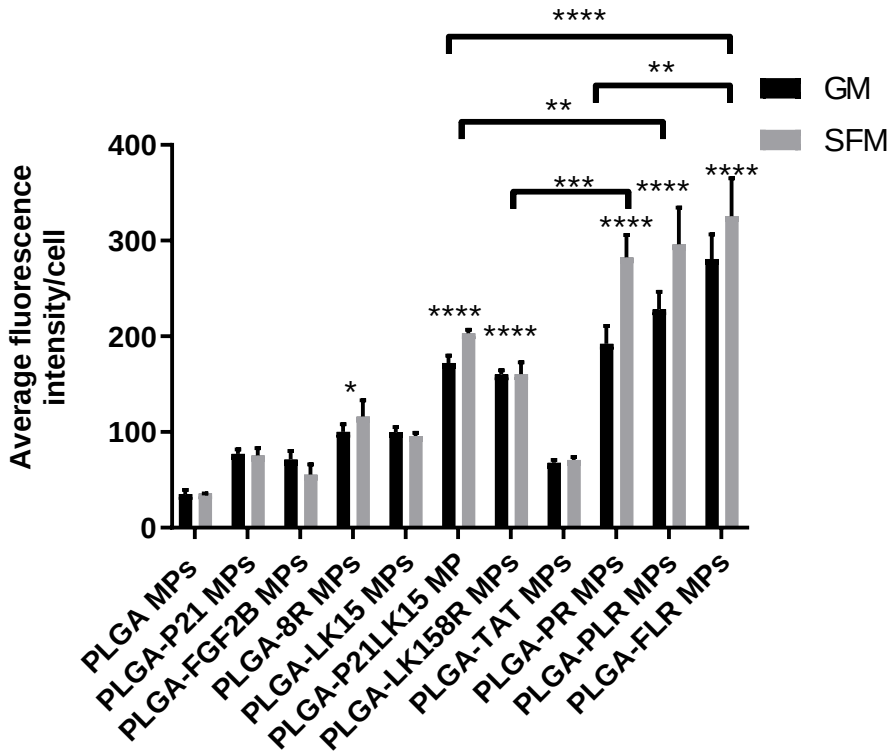

Figure 4-26 Comparison of transduction levels of PLGA-GET to PLGA-non-modified CPP MPs. Increase in the intercellular levels of PLGA MPs was recorded upon their complexation with the non-modified CPPs and HBDs. Significant two-fold increase in 8R and almost four folds in P21LK15 and LK158R complexed PLGA MPs was observed. Fold increase in fluorescence intensity was not significant in LK15, TAT, P21 or FGF2B complexed PLGA MPs. Levels of enhancement in FLR was higher significantly than all the non-modified CPP and HBD, P value >0.0001. PLR was significant to all the non-modified CPP and HBD. PR was significant to each of 8R, LK15, LK18R and TAT and the HBD, P= 0.0002. The asterisk over the bars indicate significance to control (PLGA MPs), the asterisk over the lines indicate significance between groups. Two-way Anova statistical analysis was used to generate the graph followed by Tukey test to determine significant differences between each mean. Data is presented as mean ± SD.

4.14.3 Transfection levels of PLGA-non-modified CPP MPs

CPPs have long been used as gene delivery tools to enhance the transfection of nucleic acid (Lehto *et al*., 2012, Liu *et al*., 2013a). Following the previous study (Section 4.12.2), the aim of the current study was to compare the transfection levels of GET complexed PLGA MPs to the non-modified CPP and HBD. Therefore, similar to the transfection studies in Section 4.6, these complexes were transfected into NIH3T3 cells overnight, and luminescence units were compared (Figure 4-20). The transfection level of FLR complexed PLGA MPs was significantly higher than was the best transfection level of non-modified CPPs recorded using P21LK15, LK158R and TAT complexed PLGA MPs. Moreover, PLGA-PLR MPs recorded more than one order of magnitude higher transfection when compared to P21LK15, LK158R and TAT complexed PLGA MPs. Interestingly, all LK15 containing peptides enhanced the transfection of pDNA encapsulated PLGA MPs.

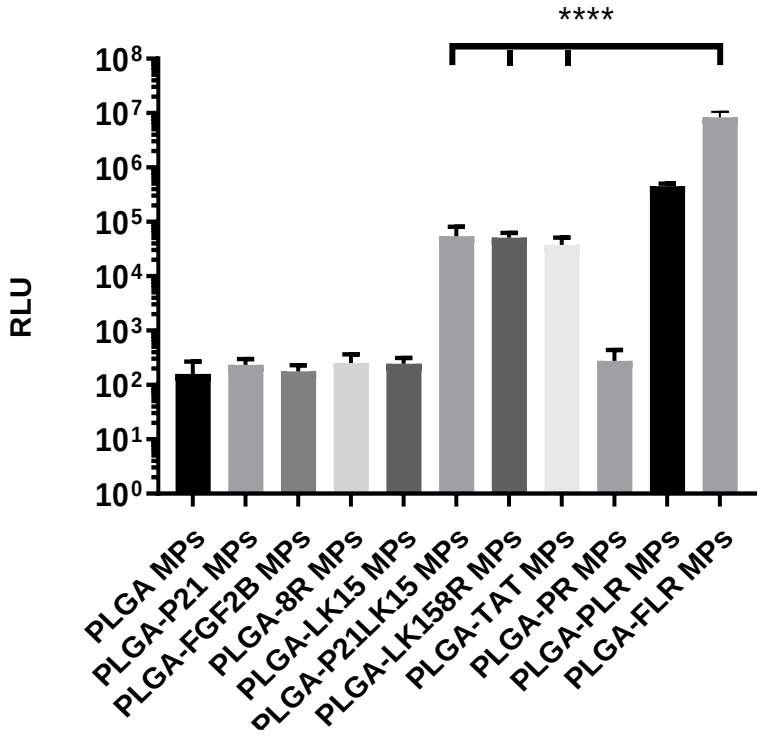

Figure 4-29 Comparison of transfection levels of PLGA-GET to PLGA-non-modified CPP MPs. Increase in transfection levels of PLGA MPs was recorded upon their complexation with the non-modified CPPs and HBDs. Transfection with FLR complexed PLGA MPs was significantly higher than with the non-modified CPPs and HBDs. PLR complexed PLGA MPs transfection was one order of magnitude higher than the highest transfection of the non-modified CPPs such as P21LK15, LK158R and TAT complexed PLGA MPs. pGluc was used for overnight transfection of NIH3T3. One-way Anova statistical analysis was used to generate the graph followed by Tukey test to determine significant differences between each mean. P value < 0.0001. Data is presented as mean ± SD.

4.15 Discussion

Enhancing the transduction and transfection efficiencies of the current gene delivery agents is crucial for harnessing the potential of non-viral gene delivery vectors. CPPs with cationic, neutral or even anionic poly peptide sequences have been used in the delivery of non-viral vectors with improved intracellular delivery properties (Scheller *et al*., 1999, Oess and Hildt, 2000, Li *et al*., 2004, Milletti, 2012). However, these levels of transfections are still not sufficient for the therapeutic application of these non-viral vectors. Other highly positively charged transfection tools, such as PEI, high molecular weight PLL and Lipofectamine compromise on cell viability to produce elevated levels of transfections (Breunig *et al*., 2007). Therefore, a balance between enhanced transfection and cell viability is crucial, and should be considered as the starting point for developing gene delivery vectors.

HS receptors are universal and have diverse structures and functions (Gallagher *et al*., 1986, Munoz and Linhardt, 2004). Targeting HS receptors on the cell surfaces offer a considerable advantage in gene delivery. GET peptides consist of a multi domain protein, which is an HS receptor binding motif that reacts with HS receptors on the cell surfaces and a CPP for the synergistic delivery of biological molecules. CPPs are known for their satisfactory cell viability outcomes in comparison to PEI, high molecular weight PLL and Lipofectamine, as well as the improved cellular delivery of

cargos such as small drug molecules, and biological macromolecules such as proteins and nucleic acids (Ciobanasu *et al*., 2009, Farkhani *et al*., 2014). Moreover, the presence of these HS binding motifs in GET allows for the concentration of the GET complexed cargo at the cell membrane for superior intracellular delivery of the cargos and subsequent enhanced transfections

(Dixon *et al*., 2016, Eltaher *et al*., 2016, Thiagarajan *et al*., 2017, Spiliotopoulos *et al*., 2019, Osman *et al*., 2018, Raftery *et al*., 2019, Abu-Awwad *et al*., 2017).

This chapter, therefore, demonstrated the use of GET peptides for the efficient delivery and transfection of pDNA encapsulated PLGA MPs. Moreover, the effect of the GET peptide sequence on the enhanced delivery and transfection characteristics of individual peptides has been determined. Furthermore, PLGA-GET complexes have been characterised in terms of surface charge and colloidal stability during the course of transfection. The dose of PLGA-GET was optimised based on cell viability, cellular delivery and transfection levels. Finally, the enhanced transduction and transfection levels of GET was compared to that of its non-modified CPP analogues.

4.15.1 Interaction of PLGA MPs with GET peptides and other ionised molecules

In order to characterise the enhanced intracellular delivery and transfection properties of GET peptides, negatively charged blank or pDNA encapsulated PLGA MPs were complexed with positively charged GET peptides (PR, PLR or

FLR) to form PLGA-GET MPs. Based on the shift in the surface charge of PLGA MPs upon complexation with GET peptides, the interaction of PLGA MPs and GET peptide is most likely to be electrostatic (Mishra *et al*., 2011, Sah *et al*., 2013, Abu-Awwad *et al*., 2017).

This electrostatic nature of the interaction could be demonstrated further by the interaction of FCS with the PLGA-GET complex. Mimicking cell culture conditions, the incubation of PLGA-GET MPs with increasing concentrations of FCS shifted the Zeta potential of PLGA-GET MP from neutral to negatively charged MPs proportional to the FCS content. Serum is a mixture of proteins and amino acids, with Albumin being the most abundant protein component. Albumin is a negatively charged 66 KD macromolecule (Wiig *et al*., 2003). It is possible that this negatively charged protein is complexed with positively charged GET peptides either on the surface of PLGA-GET MPs or away from the PLGA-GET MPs by drawing the GET peptides away from the surface of PLGA-GET MPs to form separate Albumin-GET complexes. The second assumption is more likely to occur due to the presence of small peaks in the range of 1-10 nm in the corresponding NP size measurement reports. These small peaks are likely to be due to the presence of small sized Albumin-GET NPs. Proteins have typical dimensions of 5−20 nm or less when complexed with other proteins in a NP (Kopp *et al*., 2017, Erickson, 2009). (Chen *et al*., 2015a) reported the size of BSA-complexed with RGD (CPP) peptides to be around 10 nm in diameter. However, not all the sample reports in the current study showed this peak, possibly due to the less

contribution of these small sized NPs to the total intensity produced by the various sized particles in the mixture. Moreover, the large PDI is indicative of the presence of mixed population of particles.

The interaction of PLGA-GET MPs with serum Albumin was reflected in their transduction levels in GM. In general, the transduction levels of PLGA-GET was higher in SFM, possibly due to a stronger PLGA-GET interaction in the absence of Albumin. The experimented doses of PLR and FLR in the transduction studies showed enhanced transduction in SFM in comparison to GM. Consequently, the higher levels of transduction in SFM were reflected directly in higher transfection in the same media. Nevertheless, the transfections in GM were present in very useful levels, and this FCS containing media was used in the bone differentiation studies (Chapter 5).

4.15.2 Enhanced cellular transduction and transfection of PLGA-GET MPs

The enhanced delivery and transfection of PLGA were due to the electrostatic complexation of PLGA MP with GET peptides. Nucleic acid encapsulated PLGA MPs, if delivered alone, are not usually efficient in terms of transfection. At the cellular level, PLGA MPs internalise primarily through a process known as macropinocytosis. This process is followed by the endosomal entrapment of PLGA MPs. The endosome is a cellular compartment in which most of the gene delivery vectors, if they have not escaped, are transported to lysosomes and degraded (Hillaireau and

Couvreur, 2009, Khalil *et al*., 2006). PLGA MPs are not efficient in terms of escaping the endosome. Therefore, the DNA is either to be released from the PLGA MPs before their application to cells for transfection (Hirosue *et al*., 2001), or PLGA MPs need to be complexed with transfection agents such as CPP, PEI or endosomal escape moieties (Chumakova *et al*., 2008, Kim *et al*., 2005, Makadia and Siegel, 2011). In the current studies, pDNA encapsulated PLGA MPs delivered alone did not result in transfection and their levels were comparable to the background, possibly due to endosomal entrapment. However, when complexed with PLR and FLR, pDNA encapsulated PLGA MPs produced higher transfection levels of up to five orders of magnitude than did the non-complexed PLGA MPs. However, PR complexed PLGA MPs resulted in poor transfection levels, with only one order of magnitude higher than that of the background.

Zeta potential studies give useful indications of a successful gene delivery vectors. Positively charged vectors interact better with negatively charged cell membranes than do neutral or negatively charged vectors. PLR has the highest value of net positive charge in its sequence in comparison to PR or FLR (Table 2, Section 4.14). Complexing PLGA MPs with a same molar ratio of the GET peptides would result in the presence of higher numbers of positively charged amino acids that could increase the overall Zeta potential of PLGA-PLR MPs in comparison to PLGA-PR or PLGA-FLR MPs. In the Zeta potential measurement studies of the three PLGA-GET MPs, an increase in Zeta potential values of PLGA-PLR MPs was recorded in comparison to either

PLGA-PR or PLGA-FLR which was significant in case of PLGA-PR MPs. However, this increase in Zeta potential did not contribute to higher transfection efficiency than that of PLGA-PR. This could be explained by the fact that the differences in the Zeta potential between PLGA-PLR and PLGA-FLR were not significant. However, the transduction and transfection levels of PLGA-FLR were significantly higher than PLGA-PLR MPs in NIH3T3 cells. Moreover, no significant difference in the Zeta potential between PLGA-FLR and PLGA-PR was found. However, the transfection of PLGA-FLR was significantly higher than that of PLGA-PR MPs. Therefore, based on these results, a comparison of transduction and transfection efficiencies amongst GET peptide variants on the basis of their molar ratio complexation to a constant amount of PLGA MPs was considered to be a valid method. Moreover, I do not believe that these levels of differences in the Zeta potential could lead to significant differences in transfection outcomes between PLGA-PR and PLGA-PLR or PLGA-FLR MPs.

Increasing the cellular levels of a transgene has a direct relationship with enhancing the transfection and gene delivery outcomes; however, this is not the only factor. The outcome of transfection depends on many steps that a vector undergoes during the transfection process. The first step in transfection is the interaction and fusion of a gene delivery vector with the cellular membranes, followed by cellular internalisation and endosomal entrapment as a result of this fusion (Hahn and Scanlan, 2010, Slivac *et al*., 2017, Vercauteren *et al*., 2012). Up to this stage, increased transduction

could lead to increased transfection. However, the following step in a successful transfection process is the ability of the transfecting agent to escape the endosomal entrapment. PR peptide has been used previously to deliver many cargos such as mRFP, magnetic NPs (Dixon *et al*., 2016, Spiliotopoulos *et al*., 2019), runt-related transcription factor RUNX2 (Thiagarajan *et al*., 2017) and MYOD for zonal myogenesis (Eltaher *et al*., 2016) intracellularly and results in transduced cells. However, when employed in the delivery of nucleic acids, due to the lack of LK15, the endosomal escape motif (Saleh *et al*., 2010, Alkotaji *et al*., 2014, Ahmed, 2017), PR is not sufficient to produce transfection despite its enhanced delivery characteristics. Therefore, transfection occurs as a result of the interplay of various factors. These results are most likely to be due to the lack of the endosomal escape moiety LK15 rather than to the lower surface charge in comparison to PLR. This could also be confirmed by the enhanced transfection of P21 or 8R via the addition of LK15 in P21LK15 and LK158R peptides in the comparison studies of the transduction and transfection efficiencies of GET and non-modified CPPs (Figure 4-19 and 4-20, respectively. Moreover, experiments concerning the delivery of pDNA-PR in comparison to pDNA-PLR NPs revealed that both NPs were up taken efficiently into NIH3T3 cells at comparable levels confirmed by the flow cytometry quantification as well as fluorescent microscopy images (Figure 4-8). However, pDNA-PR NPs resulted in significantly less luminescence units than pDNA-PLR NPs indicating potential endosomal entrapment of these

MPs. Although the microscopic images showed some levels of DNA-PR NP entrapment potentially in the endosome, however, they were not conclusive and not directly indicative of endosomal entrapment of DNA-PR NP. Endosomal inhibitors as well as endo lysosomal tracker dyes (Liu *et al*., 2013b, Najjar *et al*., 2017) could have been used to confirm this hypothesis. However, these results conclusively indicate that lack of LK15 in PR is potentially the main reason of their low transfection efficiency.

4.15.3 Transfection are not caused by high positive charges

Unlike other gene delivery tools that rely on high positive charges to enhance gene transfection, these PLGA-GET MPs are neutrally charged, and therefore eliminate the aspect of toxicity due to the extremely high positive charges of cationic vectors. Considering the cytotoxic effects of gene delivery vectors is one of the fundamental aspects during their developmental processes particularly for *in vivo* applications (Senior *et al*., 1991, Sakurai *et al*., 2001, Filion and Phillips, 1997). Increasing the transfection levels of non-viral vectors, which is usually achieved by increasing the amount of the positively charged transfection agent and results in increased levels of free positive charges, is related directly to increased levels of cellular toxicity (Lv *et al*., 2006). However, and in contrast to Lipofectamine, increasing the concentrations of GET peptides and their enhanced transfection properties did not affect cell viability in the present studies, even in highly susceptible cells such as IHMSCs in GM. Doses as high

as 20 µM of FLR could be safely used to enhanced transfection (Figure 4-13). However, Cell viability was compromised in SFM, possibly due to the increase in the free positive charges and reduced complexation of FLR with Albumin in the absence of serum. Although, SFM conditions are only used for the *in vitro* characterisation of non-viral vectors and are not designed to mimic the *in vivo* conditions, understanding gene delivery vector-environmental factors interaction is key in designing non-viral gene delivery vectors. Conclusively, GET peptides as non-viral gene delivery vectors achieves a balance between efficacy and safety.

PLR is Recognised as having transfection levels that are comparable to those of Lipofectamine (Osman *et al*., 2018). However, a larger amount of pDNA was required in the transfection studies by Dixon *et al*., 2016. Therefore, improved versions of GET peptides such as FLR was developed by our group and were used in *in vivo* lung gene transfection (Osman *et al*., 2018) and *in vivo* gene activated scaffold bone regeneration (Raftery *et al*., 2019) with much lower pDNA quantities than were used with PLR.

The surface charge of GET peptide complexed PLGA MPs and their interaction could be increased to enhance the transfection properties of GET peptides, possibly via covalent conjugation of the GET peptides with the PLGA MPs. According to the existing literature, covalent binding of the transfection agents to gene encapsulated nano-carriers is the method that is used most frequently to deliver non-viral vectors to produce stable MPs

(Mann *et al*., 2008b, Madaan *et al*., 2014, Doane and Burda, 2013, Zhang *et al*., 2008). However, for the purpose of this study and to demonstrate of the ability of GET peptides to enhance the delivery and transfection of PLGA MPs, electrostatic interaction was considered to be a simple process that did not require time-consuming optimisation procedures.

4.15.4 PLL does not contribute to transfection

In order to determine whether the enhanced transfection of PLGA-GET MPs was mainly due to the effect of GET peptides, and not due to the presence of PLL in the pDNA encapsulated PLGA-GET MPs, pDNA-PLL NPs were transfected in NIH3T3 cells in GM. The transfection level of these NPs was very low, which indicated that PLL had no effect on transfection (Section 4.13.2). Low Mw PLL is known for its low transfection efficiency in comparison to higher Mw PLL, possibly due to the lack of the proton-sponge effect necessary for endosomal escape (Mannisto *et al*., 2002, Arbab *et al*., 2004). The effect of reduced endosomal escape was also seen in other cationic polymers, such as PEI, when lower Mw variants were used (Bettinger *et al*., 2001, Lee *et al*., 2003). The decreased transfection of these low Mw polypeptides also results in their reduced cytotoxicity effects (Jin *et al*., 2014). Therefore, the only function of PLL in the pDNA encapsulated PLGA-GET MPs is the enhancement of the encapsulation of pDNA in PLGA MPs by means of pDNA condensation. Moreover, the use of low Mw PLL has the added advantage of improving the safety of the system.

To further confirm that the enhanced transfection of the pDNA encapsulated PLGA-GET MPs is due to the presence of GET peptides in the MPs system and determine whether the enhanced transfection effect of PLR could enhance the transection of these pDNA-PLL NPs, these pDNA-PLL NPs were complexed with PLR (to form pDNA-PLL-PLR) (Figure 4-17). The transfection of pDNA-PLL NPs increased when complexed with PLR. However, the transfection levels were non-significant and were lower than the pDNA encapsulated in PLGA MPs (same dose of 1 µg of pDNA was used). It appeared that the electrostatic interaction between positively charged pDNA-PLL NPs and PLR was weak, possibly due to both being positively charged. It was hypothesised that the presence of Albumin in the media could improve the transfection by interacting with positively charged pDNA-PLL NPs by surface adsorption (to form pDNA-PLL-Albumin) to produce overall negatively charged NPs that could enhance the attraction of positively charged PLR to the surface to pDNA-PLL-Albumin and form an Albumin sandwich between the two positive charges. To do this, pDNA-PLL and PLR were transfected in SFM and the addition of higher concentrations of Albumin than were present in GM. This procedure increased the transfection of pDNA-PLL-PLR NPs significantly, thus emphasising the enhanced transfection properties of PLR and the lack of the effect of PLL on transfection. Moreover, is important to understand the interaction of GET peptides with vectors/MPs in order to demonstrate the enhanced transfection propertied of these peptides.

4.15.5 The enhanced transfection effects of GET are due to HS domains (HBD)

GET peptide complexed PLGA MPs have been shown to be superior in terms of the enhanced delivery and transfection of PLGA MPs. To demonstrate the effect of HSD on the enhanced transfection characteristics of GET peptides, their transduction levels were compared to those of the original, non-modified CPPs from which the GET peptides were originally derived. All the GET peptides recorded higher transduction and transfection levels in comparison to their analogues (Figure 4-19). For example, PLGA-PR recorded higher transduction levels than PLGA-8R and PLGA-P21. Furthermore, PLGA-PR also recorded higher transduction levels than other CPPs such as PLGA-LK15, -LK158R, -P21LK15. However, similar low transfection levels of PR and 8R complexed PLGA MPs were observed due to the lack of LK15 in PR and 8R, as discussed previously. Moreover, PLR and FLR complexed PLGA MPs exhibited a similar effect of enhanced transduction to that of PR compared to their analogues, P21, FGF2B, 8R, LK15, P21LK15 and LK158R complexed PLGA MPs. Moreover, these GET peptides recorded significantly higher transfections of PLGA MPs than their analogues. Interestingly, P21 and FGF2B did not have any enhanced transduction or transfection effects on their own. Therefore, it can be concluded that the enhanced transduction and transfection effects of GET peptides are due to the presence of the P21 or FGF2B in the GET peptide chain, and the HS receptor binding effects. These enhancement in transduction and transfection efficiencies of GET

peptides are less likely to be due to increasing in the overall positive charge due to the addition of P21 and FGF2B in the sequence of GET peptides in comparison to the non-modified CPPs. These assumptions could be justified by the fact that these GET and non-modified CPPs complexed PLGA MPs exhibit the same Zeta potential but differ in their levels of transduction and transfection activities. Moreover, contrary to the general concept of enhanced transfection as a result of enhanced transduction, PLGA-PR recorded higher transduction activities than PLGA-TAT, PLGA-P21LK15 and PLGA-LK158R. However, their transfection activities were higher than PLGA-PR. Therefore, transfection occurs as a result of a combination of factors including cellular internalisation and endosomal escape as discussed previously.

There are other methods to confirm that the enhanced transfection effects of GET peptides are the result of the activation of HS receptors. One method is to block the HS receptors by the competitive effect of Heparin. However, due to the counter charge of Heparin to positively charged GET peptides, it would have been difficult to confirm that the reduced intracellular delivery and transfection of MPs was due to the competitive blockage of these receptors by Heparin rather than the complexation of Heparin with GET via electrostatic reactions, thus decreasing the availability of GET for receptor binding. Sodium perchlorate is another competitive inhibitor of HS receptors that could block the action of GET through the inhibition of the sulphation of proteoglycans on cell surfaces (Lefebvre *et al*., 1996), However, its

detrimental effects on cell viability could produce false positive results Indicating the decrease in the intercellular delivery and transfection of MPs, thus indicating that the reduced GET effects were due to HS receptor inactivation (Safaiyan *et al*., 1999, Lin and Perrimon, 2000). Other methods such as the use of mutant Chinese hamster ovary (CHO) cells deficient in HS production and heparinase are also possible (Higashiyama *et al*., 1993).

4.15.6 Colloidal stability of PLGA-GET

Due to the neutral surface charge of PLGA-GET MPs, it was assumed that these MPs would become colloidally unstable if they were to be incubated for a long time. Therefore, to demonstrate the stability of these MPs during cell culture in the transduction and transfection studies, these MPs were incubated in GM for five hours, which is the maximum time in which the majority of these MPs are taken up by the cells (Park *et al*., 2011, Kang *et al*., 2012). This experiment demonstrated some growth in the PLGA MPs' size, which is expected for neutrally charged MPs. Moreover, there was some difficulty in removing these PLGA MPs during the washing steps in cell culture. However, the effect of the sedimentation of these MPs on the transduction and transfection studies was eliminated by extensive washing of the cultured cells. The PLGA MPs were visible during the removal stages. Moreover, it is widely accepted that trypsinisation removes the majority of surface bound PLGA MPs, when samples are analysed via a flow cytometry

analysis (Phelan, 2007, Zeng *et al*., 2014, Phelan and May, 2015, Phelan and May, 2016).

Therefore, improving the stability of these MPs is necessary for their future use. If the stability of these PLGA-GET peptides can be improved, perhaps via the covalent conjugation of these GET peptides on the surface of the PLGA MPs, this could further enhance their transduction and transfection efficiency.

4.16 Chapter summary

1. The interaction of PLGA MPs with GET peptides could be characterised by Zeta potential measurements. PLGA MPs interact with GET peptides by electrostatic means.
2. All variants of GET peptides significantly enhanced the transduction levels of PLGA MPs with further enhanced transduction in PLR and FLR complexed PLGA MPs in comparison to non-complexed MPs.
3. PLR and FLR complexed PLGA MPs significantly enhanced the transfection levels of PLGA MPs in comparison to non-complexed PLGA MPs.
4. PR complexed PLGA MPs are associated with enhanced transduction however this does not result in enhanced transfection.
5. The poor transfection property of PR peptide is not related to the non-significant reduced levels of transduction in comparison to PLR.

6. Higher positive charges of PLGA-PLR in comparison to PLGA-PR is not related to enhanced transfection levels of PLR in comparison to PR complexed PLGA MPs. these assumptions could be further confirmed by the PLGA-FLR MPs with its lower positive charges and the significant increase in transduction and transfection levels in comparison to more positively charged PLGA-PLR MPs.
7. Lack of endosomal escape peptide LK15 in PR is potentially the major reason for its poor transfection properties.
8. Lack of LK15 resulted in endosomal entrapment of pDNA-PR in comparison to pDNA-PLR which resulted in significant lower transfection levels.
9. Enhanced transduction and transfection levels of GET peptides in comparison to their non-modified CPP analogues are due to the HBD and their specific interaction with HS receptors on the cell membrane.
10. Enhanced transduction and transfection levels of FLR in comparison to PLR are most possibly due to the substitution of P21 with FGF2B.
11. Increase in the dose of the GET peptides was directly related to enhancement in transduction levels of GET complexed PLGA MPs.
12. Increase in transduction levels of GET peptides complexed PLGA MPs was directly reflected in increased transfection levels of these MPs.
13. GET peptides are associated with improved cellular viability outcomes even in high doses of the peptide in comparison

commercially available gene transfection vectors such as Lipofectamine and could easily be used to transfect highly susceptible cell lines such as IHMSCs.

14. GET peptides are considered efficient gene delivery vectors due to the combination of enhanced transfection and improved cellular viability properties.
15. The efficiency of GET peptides could be further improved possibly by further enhancement in transfection levels through the employment of specialised chemical conjugation procedures to produce stable GET complexed MPs.
16. Moreover, these specialised conjugation procedures will eliminate the effect of environmental factors on the stability of GET complexed vectors.

Chapter 5.

Biomedical Applications Bone Differentiation

5.1 Introduction

Bone tissue regeneration through the delivery of recombinant human Bone Morphogenic Protein (rhBMP2) such as commercially available INFUSE® Bone Graft is a well-established method for spinal fusion and off-label applications. However, protein instability (with degradation soon after administration) (James *et al*., 2016, Shields *et al*., 2006) means there is a need to apply supra-physiological concentrations to maintain efficacy within the therapeutic window. These high levels of BMP2 are associated with serious side effects such as ectopic bone formation, osteolysis, aberrant immune responses and neurotoxicity (Lewandrowski *et al*., 2007, Tannoury and An, 2014). Therefore, there is a need to develop novel strategies to apply the activity of BMP2 more safely, physiologically and cost-effectively to promote bone healing in challenging and critical-sized bone traumas. Triggering MSCs to produce elevated but not supra-physiological levels of BMP2 via delivered ectopic transgenes is an alternative approach which does not rely on recombinant proteins. This can be achieved by gene delivery to express new BMP2 copies. In this case, the lower level of produced protein from transfected cells is more physiologically relevant than current approaches resulting in minimal or no off-target effects when applied *in vivo* (Raftery *et al*., 2019).

In this chapter, pBMP2 encapsulated PLGA-FLR MPs were employed to enhance bone differentiation in MSC. Encapsulated pBMP2 could be as

effective as non-encapsulated pBMP2 (Raftery *et al*., 2019) in inducing MSCs to differentiate to bone lineages. Cell culture conditions in terms of cell seeding density and pBMP2 dose were specifically optimised for the use of these PLGA MPs and IHMSCs in the context of the current study. Cell viability studies exhibit good tolerance of the system by the MSCs. Bone differentiation studies were confirmed change in morphology of the cells, deposition of dense calcium nodules, Alizarin Red staining and upregulation of osteogenic genes in transfected cultures in comparison to controls.

5.2 Optimisation of cell culture conditions

Before beginning the bone differentiation process with gene delivery, and in order to confirm the potency of the IHMSCs to differentiate into osteogenic lineages (Pittenger *et al*., 1999, Meyer *et al*., 2016), conventional Osteoinductive (OI) media containing Dexamethasone (Dex) was used (Yuasa *et al*., 2015, Moretti *et al*., 2017, Lukasova *et al*., 2018, Solchaga *et al*., 1998). To do this, cells were seeded at 4k cells/cm^2 in 24-well plate format (8k cells) (Siddappa *et al*., 2007, Mendes *et al*., 2004). Moreover, the two most frequently cited OI concentrations of Dex, 10, and 100 nM, were tested. The IHMSCs were fed these concentrations of Dex for four weeks, and the media were changed twice a week. IHMSCs cultured in expansion and basal media were used as controls. During the course of differentiation, no mineral was observed in cultures treated with any of the concentrations

of Dex using light microscopy. Moreover, no stained bone nodules were detected when stained with Alizarin Red (Figure 5-1).

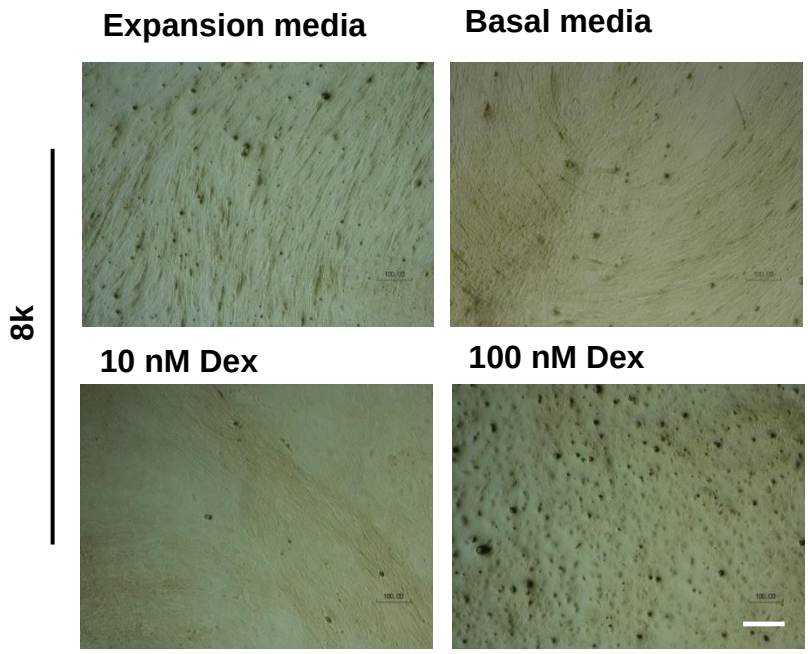

Figure 5-2 Optimisation of osteogenic differentiation of IHMSCs in OI media. Incubation of IHMSCs with 10 or 100 nm Dex for 4 weeks did not induce bone differentiation by Alizarin Red staining. Cells were seeded at 8k cell seeding density. Scale bar 100 µm.

5.3 Assessment of seeding density and Dex concentration on bone differentiation

Bone differentiation *in vitro* requires a confluent layer of adherent cells. In contrast to primary human mesenchymal stem cells (hMSCs) (Siddappa *et al*., 2007, Mendes *et al*., 2004), the 8k cell seeding density of IHMSCs in the previous experiment did not generate a confluent layer after an overnight incubation period. Therefore, the cell culture conditions were optimised in

terms of seeding density to achieve a confluent layer of IHMSCs. Moreover, the same concentrations of Dex as in the previous study were also applied to each seeding density. To start the differentiation with a more confluent layer of cells, the cell seeding density was increased to 15, 35 or 60k cell per well (1.9 cm^2) in a 24-well plate. The cell seeding density had a profound effect on the lineage commitment of these cells towards bone differentiation. Alizarin Red stained bone nodules were detected in confluent cells of 15 and 35k cells. Moreover, the bone nodules staining enhanced when the seeding density was increased, except for too confluent cell layers of 60k that did not differentiate to bone lineages. Moreover, the concentration of Dex affected the mineral deposition by these cells markedly. 10 nM Dex changed the morphology of the cells from fibroblastic to polygonal (Lou *et al*., 2017). However, this concentration of Dex was not sufficient to mineralise the matrix. Dex concentration of 100 nM was required to drive IHMSCs to differentiate into osteoblasts (Figure 5-2). Therefore, 35k cells and 100 nM Dex were chosen as the optimal conditions for the bone differentiation of IHMSCs. These conditions were applied as a positive control in the later studies of bone differentiation, and the media contained a high dose (100 nM) of Dex called OI. As 10 nM Dex did not result in differentiation, it was not considered to be an independent OI in these experiments.

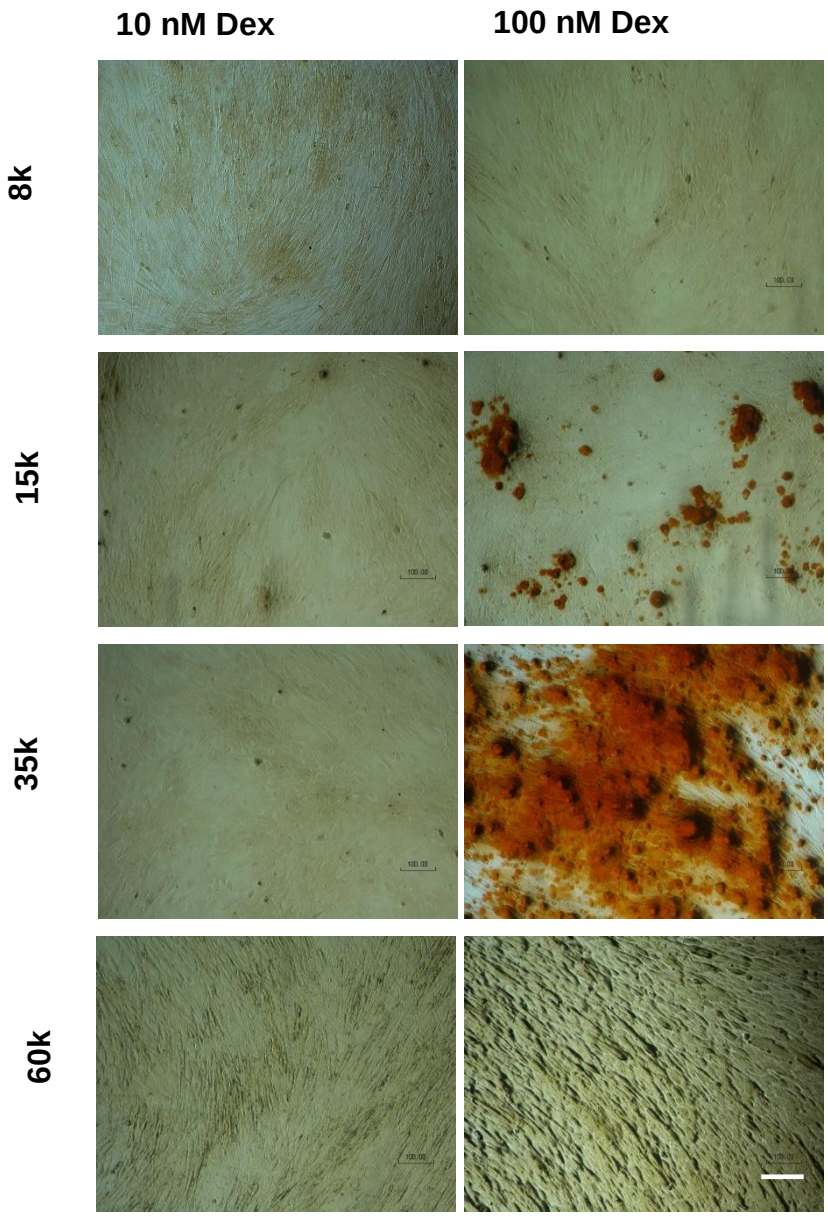

Figure 5-4 Effect of cell seeding density and Dex concentration on bone differentiation of IHMSCs. Different seeding denisties; 8, 15, 35 or 60K and two different contrations of Dex; 10 or 100 nM was applied. Differentiation was enhanced with increasing cell density except in over-confluent cell monolayer at 60k cell seeding density. Highest differentiation levels was observed in 35k cell seeding density and 100 nM Dex treated cells. 10 nM Dex did not induce bone differentiation at all cell seeding densities. Scale bar 100 μm.

5.4 Application of pBMP2-FLR NPs in bone differentiation

As a step-by-step control for the process and prior to beginning the bone differentiation studies with pBMP2 encapsulated PLGA-FLR MPs, the efficacy of pBMP2 and FLR peptide was tested in bone differentiation in IHMSCs. To do so, the previously published pBMP2-FLR NPs (Raftery *et al*., 2019) and the above optimised cell seeding density in the present bone differentiation assays were recapitulated. These pBMP2-FLR NPs were characterised in terms of size, charge and morphology to assess their suitability for intracellular delivery.

5.4.1 Characterisation of pBMP2-FLR NPs

5.4.1.1 Size and morphology

The formation of nano/microparticle sized polyplexes is key to determining successful cellular internalisation and gene delivery. As in the previous section (3.4.1), the hydrodynamic size of the pBMP2-FLR NPs was measured using dynamic light scattering (DLS) and Zetasizer Nano Zs. These NPs were prepared at the charge ratio of (+/-) 6. The mean size of these NPs was 76.9 ± 5.3 (mean ± SD) (Figure 5-3A and Appendix 1 Section 8.1.6.2). The PDI value of 0.24 ± 0.03 (mean ± SD) shows the homogenous population of the NPs. The size of these NPs was also confirmed by TEM imaging. These NPs were spherical in morphology (Figure 5-3B and Appendix 1 Section 8.1.6.1).

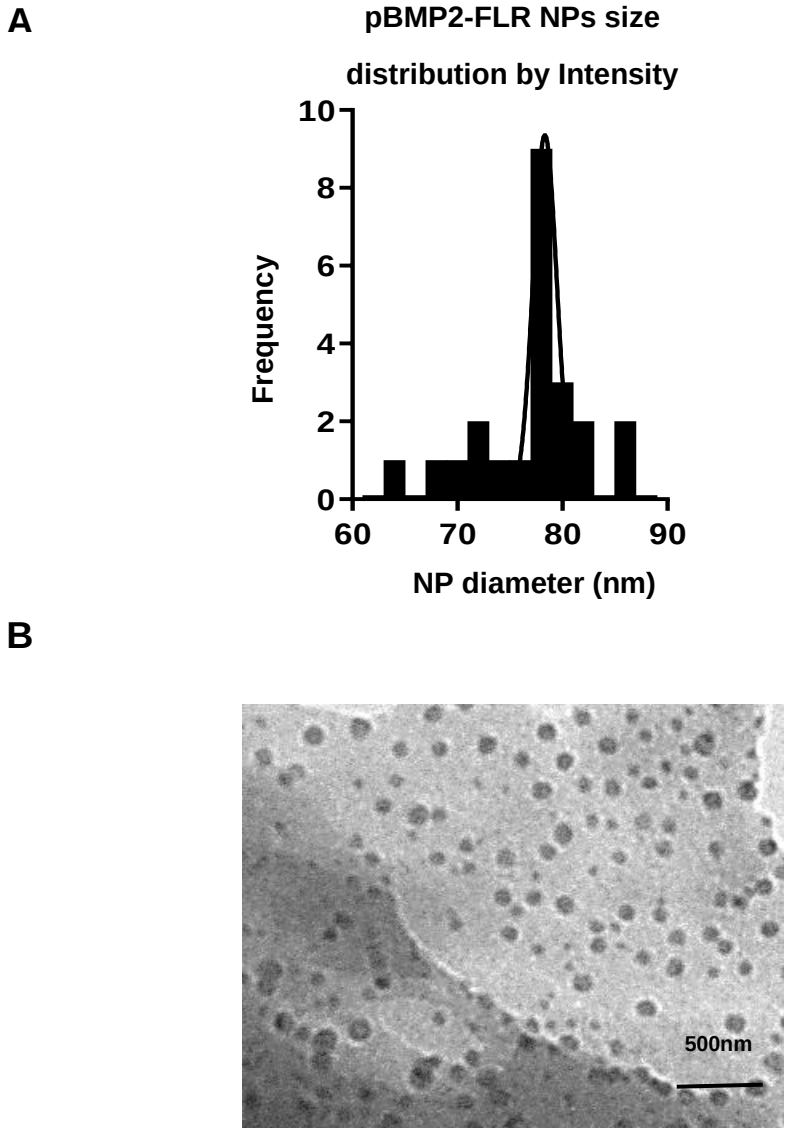

Figure 5-8 Size and morphology of pBMP2-FLR NPs at charge ratio of 6. (A) Size distribution of the pBMP2-FLR NPs measured with Zetasizer Nano Zs shows relatively small and homogenous NPs with a mean diameter of 76.9 nm. (B) TEM images demonstrates spherical NPs and further confirms the size of the same NPs.

5.4.1.2 pBMP2-FLR NPs charge

The Zeta potential of pDNA NPs could influence the interaction between the NPs and the cellular membrane. Positively charged pDNA NPs interact better

with negatively charged cellular membranes for enhanced cellular internalisation. In order to detect the formation of pBMP2-FLR NPs and to predict their interaction with cellular boundaries during delivery, the Zeta potential of these NPs was measured after complexation using Malvern Zetasizer Nano Zs. The mean Zeta potential of these NPs was 34 ± 3.6 mV (mean ± SD) (Figure 5-4 and Appendix 1 Section 8.1.6.3).

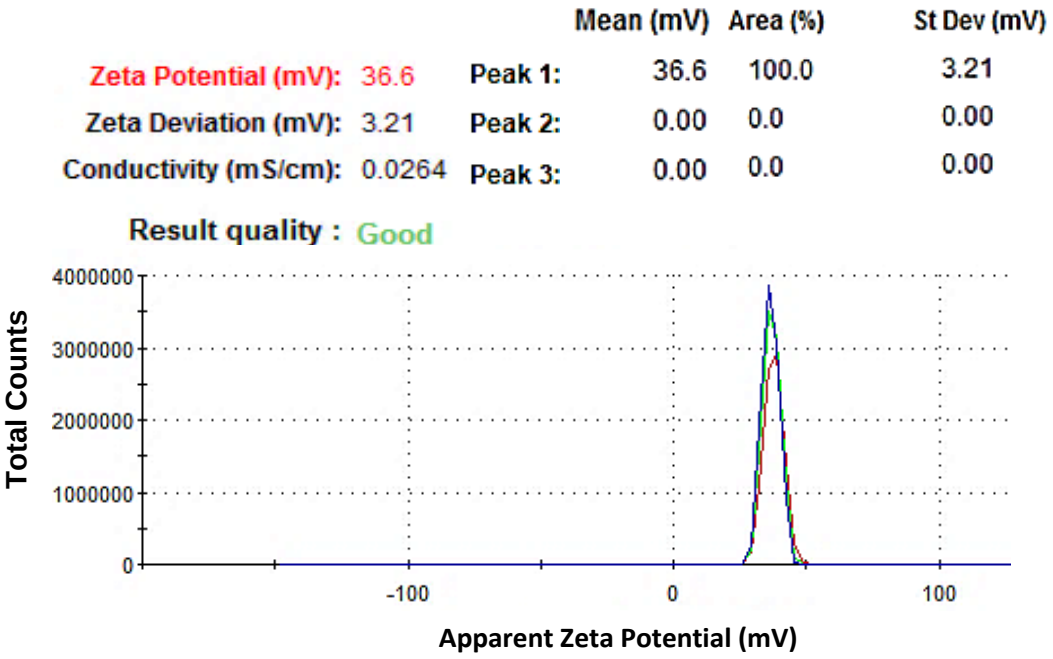

Figure 5-10 Zeta potential measurements of pBMP2-FLR NPs. Zetasizer report shows homogenous population of highly positively charged NPs. The report has passed the quality criteria. Mean Zeta potential value of 36.6 mV, with zeta deviation of 3.21 mV and conductivity of 0.0264 (mS/cm) exhibits good quality and colloidally stable pBMP2-FLR NPs.

5.4.2 Optimisation of dose of pBMP2-FLR

To determine the minimum dose of pBMP2-FLR required for bone differentiation, different doses of pBMP2-FLR NPs were tested. A dose of 1 µg pBMP2 complexed with 4 µM total concentration of FLR NPs was set as

1X dose. Other doses of 0.5, 0.25 and 0.125X were also tested. The IHMSCs transfected with any of the doses of pBMP2-FLR NPs did not result in differentiation. Moreover, the morphology of these cells did not change from fibroblastic to polygonal. Serial transfection twice a week for one week was also implemented o enhance the effect of pBMP2-FLR NPs transfection. In both cases, namely single and serial transfection, the cells did not show signs of bone differentiation such as a change in morphology or the deposition of matrix and calcium nodules. The effect of these transfections and doses of pBMP2-FLR NPs on cell viability was assessed during the highest transfection and toxicity levels on the third day (Duran *et al*., 2011) after single and second transfections (Figure 5-5). The cell viability assay indicated good compatibility of pBMP2-FLR NPs with IHMSCs, particularly in the single transfection studies. The cell viability was affected slightly more on the third day after the second transfection. However, in both single and serially transfected cells, the lack of bone differentiation was less likely to have been caused by these cell viability outcomes.

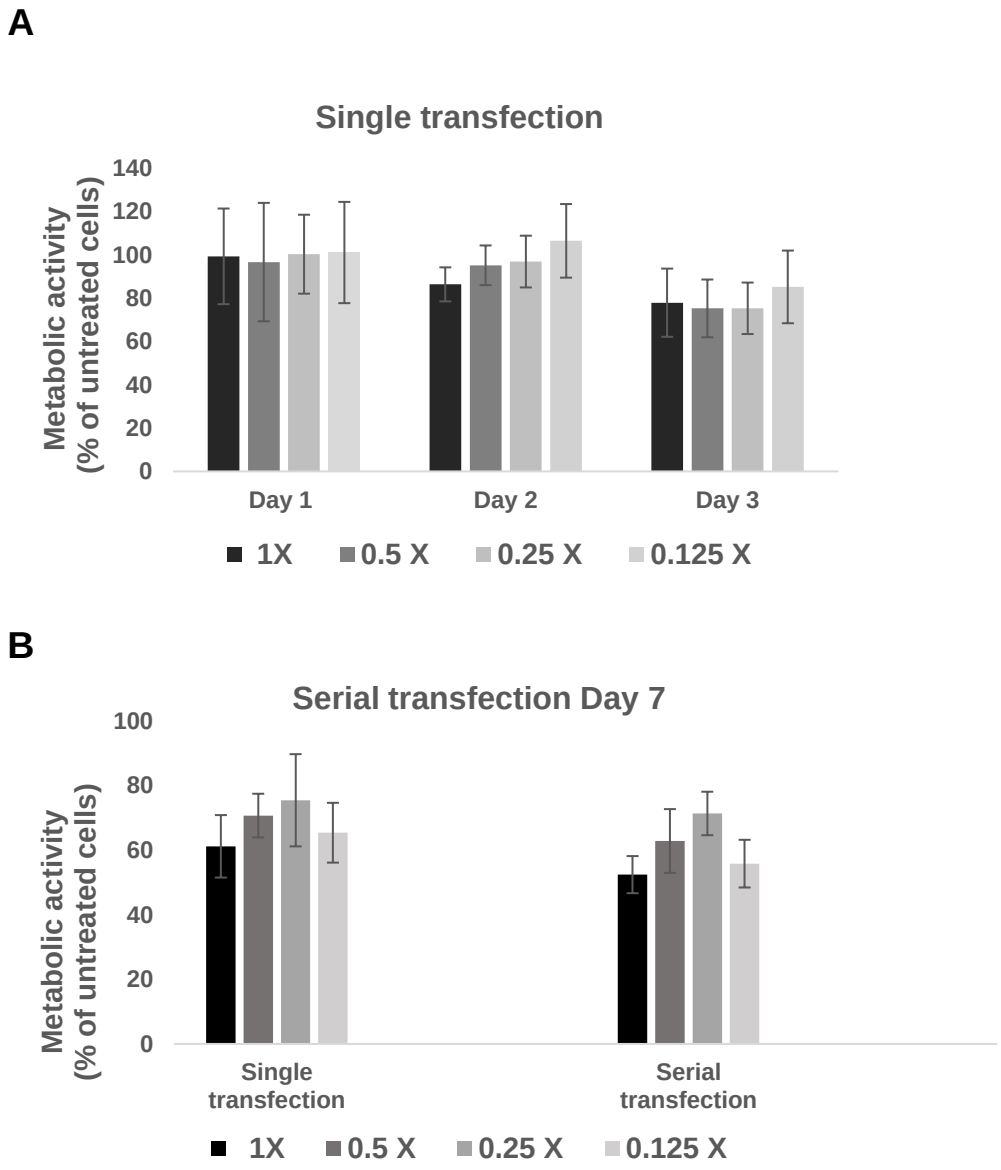

Figure 5-13 Cell metabolic activities in response to transfection with pBMP2-FLR NPs. IHMSCs transfected with the highest dose of pBMP2-FLR NPs (1 µg pBMP2 and 4 µM total concentration of FLR) showed a minimum of 75 % viable cells during the highest transfection activity of pBMP-FLR NPs at day 2 and 3 (A). Serially transfected cells (B) showed slight reduction in cell viability in comparison to cells transfected with a single dose of pBMP2-FLR NPs (A) on the third day after the second transfection. The transfections were carried out in GM. The percentage metabolic activity was calculated in comparison to non-transfected cells which was normalised to 100 %. The data is presented as mean ± SD.

5.4.3 Addition of Dexamethasone

During development, the process of bone differentiation occurs as a result of a delicate balance of the actions of multiple factors such as growth factors (GF), morphogens and inducer molecules. Most of these factors do not induce bone differentiation if applied individually, particularly in *in vitro* conditions (Andrades *et al*., 2013). The presence of Dex has a profound impact on the process of bone differentiation *in vivo*, although its exact mechanism is unknown. Dex has also been the subject of much research on enhanced bone differentiation *in vitro* (Roberts *et al*., 2011). In the present study, in order to enhance the OI effect of pBMP2 in bone differentiation, a low non-osteoinductive concentration of Dex (10 nM) was used. The incubation of IHMSCs in 10 nM Dex containing media after their transfection with pBMP2-FLR NPs enhanced the bone differentiation capacity of the cells significantly. 10 nM Dex treated controls without pBMP2-FLR transfection did not result in bone differentiation (Figures 5-2 and 5-6A). Therefore, Dex was not considered to be osteoinductive at this concentration, and the media that contained a low dose of Dex (10 nM) is called Ostepermissive (OP) media hereafter. A single transfection of a 0.5X dose of pBMP2-FLR NPs (0.5 µg of pBMP2 and 2 µM final concentration of FLR) was sufficient to induce bone differentiation.

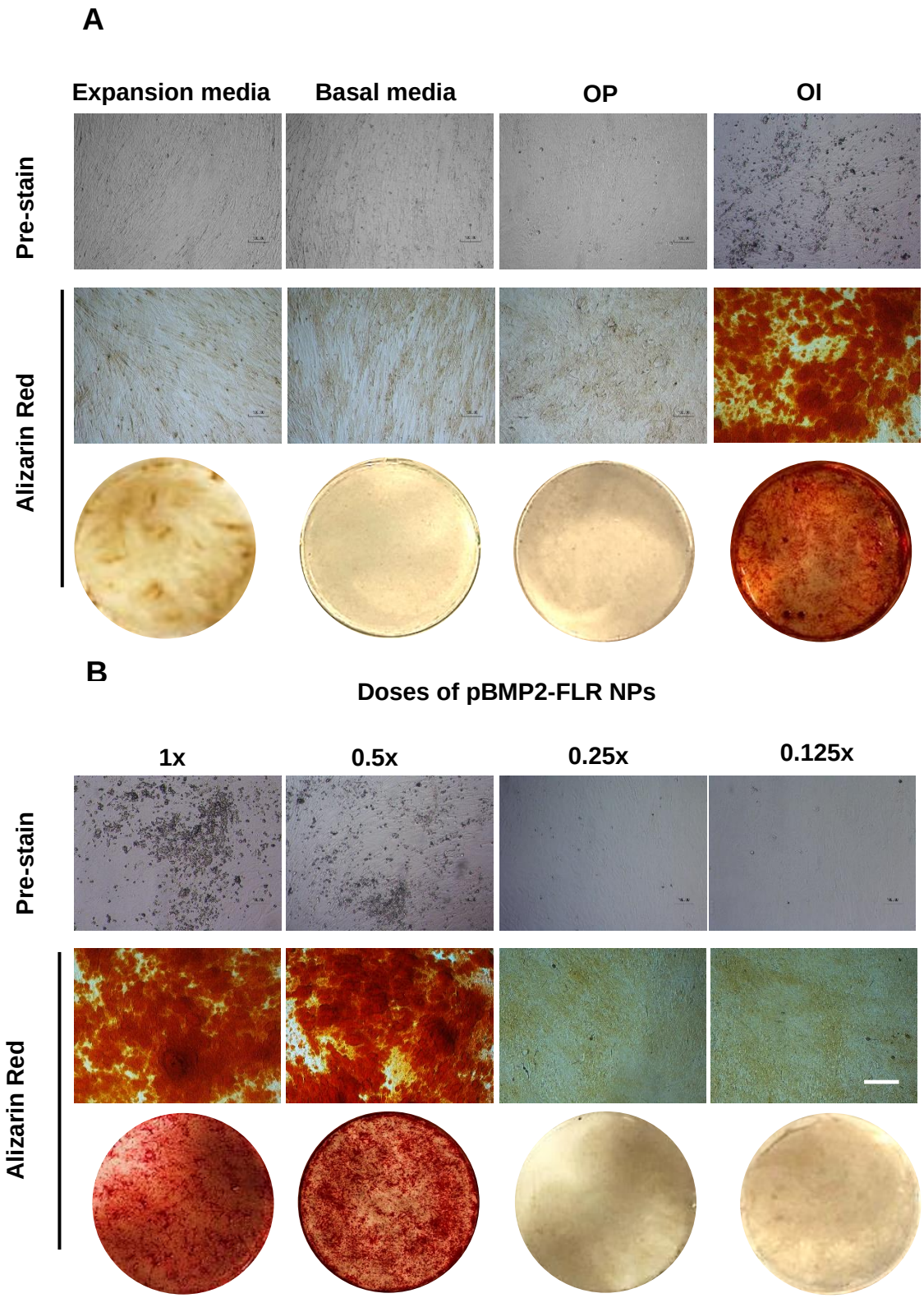
A
Expansion media
Basal media
OP
OI
Pre-stain
Alizarin Red
B
Doses of pBMP2-FLR NPs
1x
0.5x
0.25x
0.125x
Pre-stain
Alizarin Red

Figure 5-15 Osteogenic dfferentiation of IHMSCs as a result of pBMP2-FLR NPs transfection. (A) phase contrast microscopic images (pre-stain) and Alizarin Red stained microscopic and well plate images of control IHMSCs in expansion, basal, OP and OI media. (B) phase contrast microscopic images (pre-stain) and Alizarin Red stained microscopic and well plate images produced dense calcium deposits in cultures transfected with 1 or 0.5 µg of pBMP2-FLR NPs in comparison to controls. The bone differentiation was significantly enhanced with the addition of 10 nM Dex in comparison to cultures not conditioned with this concentration of Dex (images not shown). No differentiation was detected in cultures treated with OP media (containing 10 nM Dex) only without transfection. No spontaneous differentiation was detected in control cultures. Cells were cultured at 35k cells in 24-well plate format. Scale bar 100 µm.

5.5 Bone differentiation capacities of pBMP2 encapsulated PLGA-FLR MPs

Next, the efficacy of FLR complexed pBMP2 encapsulated PLGA MPs (pBMP2-PLGA-FLR MPs) was tested in bone differentiation assay, and the levels of bone induction were compared to those of the non-encapsulated pBMP2-FLR NPs in the previous study. During the transfection of IHMSCs with the same dose of encapsulated pBMP2 content of PLGA MPs (0.1 mg PLGA PMs) as the pBMP2-FLR NPs (0.5 µg of pBMP2), the levels of bone induction were less than those detected in pBMP2-FLR NPs transfected cultures (Figure 5-7B). Therefore, to obtain higher levels of bone differentiation, the dose of pBMP2 encapsulated PLGA-FLR MPs was increased to 0.2mg PLGA and a corresponding 1 µg pBMP2 content and 4 µM FLR concentration. IHMSCs initially changed in morphology from fibroblastic to polygonal cells in the early stages of differentiation (Week 1), followed by an increased deposition of extra cellular matric (ECM) and

calcium nodules forming on the cells observed using light microscopy starting from Week 3 (Figure 5-7B pre-stain).

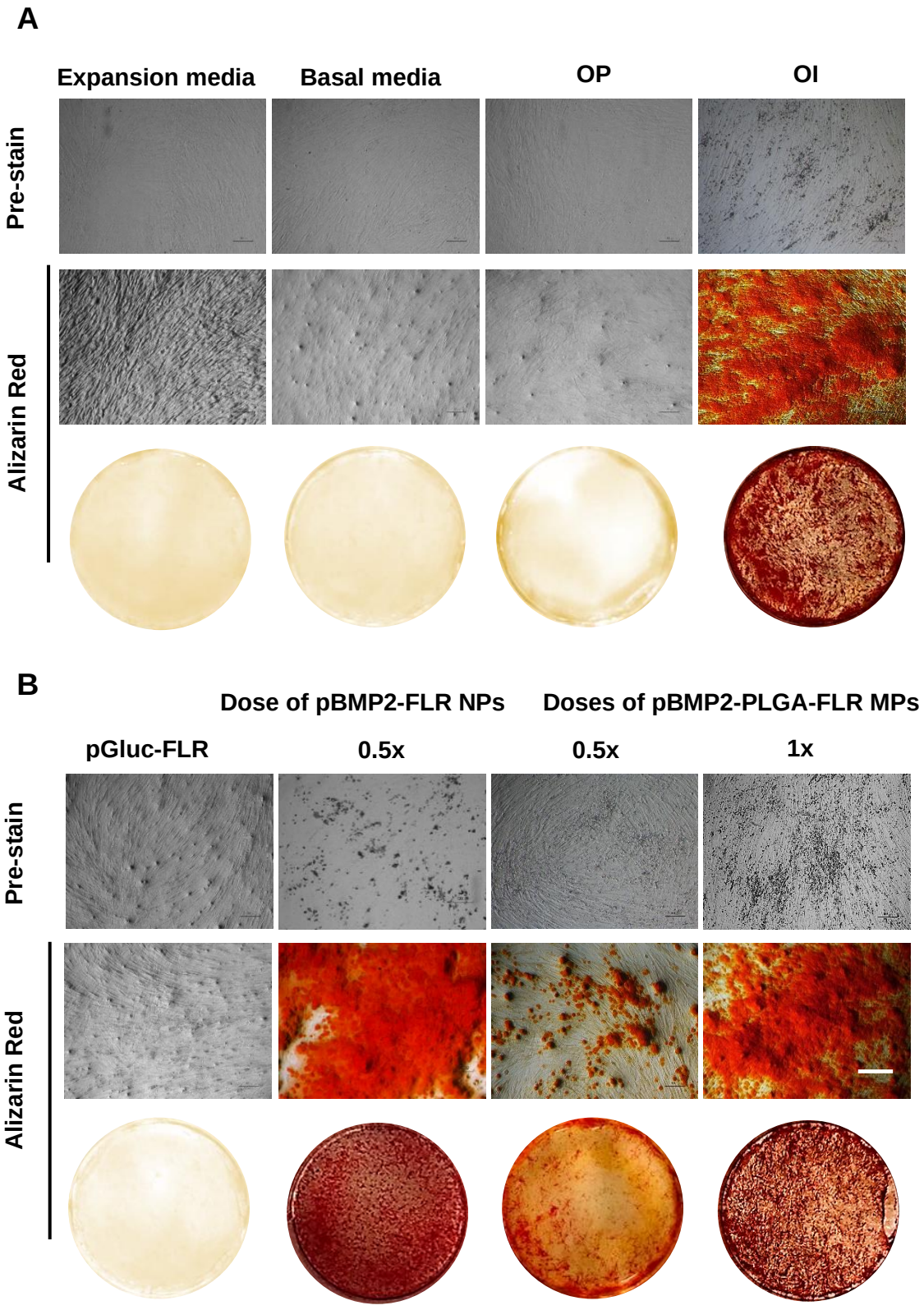

Figure 5-17 Osteogenic differentiation as a result of IHMSC transfection with both non-encapsulated pBMP2-FLR and pBMP2 encapsulated PLGA-FLR MPs. (A) phase contrast microscopic images (pre-stain) and Alizarin Red stained microscopic and well plate images of control IHMSCs in expansion, basal, OP and OI media. (B) phase contrast microscopic images (pre-stain) and Alizarin Red stained microscopic and well plate images produced dense calcium deposits in cultures transfected with pBMP2-FLR and pBMP2 encapsulated PLGA MPs in comparison to controls. The bone differentiation was significantly enhanced with increasing the dose of pBMP2-PLGA-FLR MPs to 1µg pBMP2 content. pGluc-FLR NP transfected cells and other controls confirm no spontaneous differentiation. Cells were cultured at 35k cells in 24-well plate format. Scale bar 100 µm.

5.6 Calcium Deposit Quantification

Alizarin Red stained calcium deposits could be extracted and quantified to determine the levels of differentiation and mineral deposition in the differentiated monolayers. In the present study, the extracted Alizarin Red from stained wells was used as a relative quantification method to confirm that both published pBMP2-FLR NPs (Raftery *et al*., 2019) and the pBMP2-PLGA-FLR MPs can induce similar levels of osteogenesis (Figure 5-8). A ten-fold increase in the molar concentration of the dye absorbed by the calcium nodules was recorded for the transfected cells in comparison to the controls. Cultures in basal media, OP, or transfected with pGluc instead of pBMP2 resulted in no spontaneous bone differentiation. Moreover, highly osteoinductive OI media with Dex (100 nM) produced similar levels of differentiation to those of the pBMP2 transfected samples.

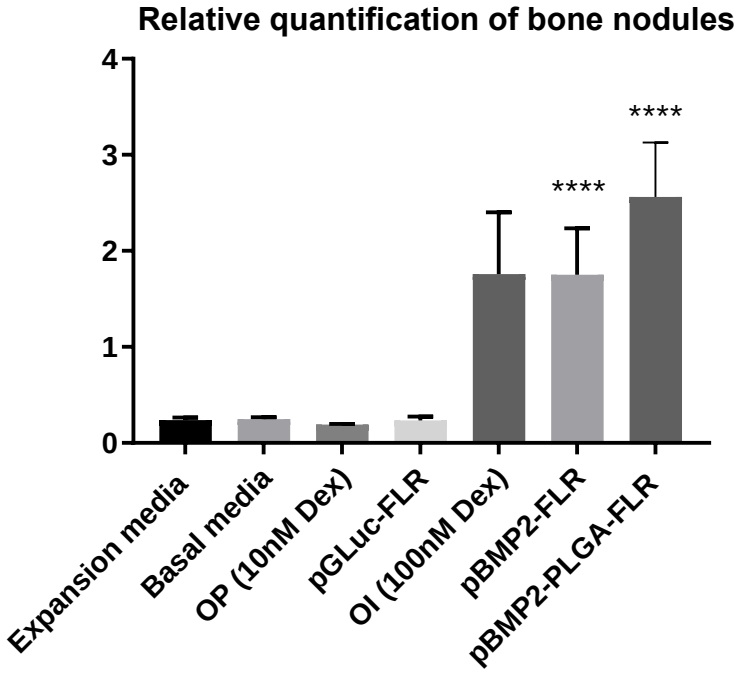

Figure 5-20 **Quantification of Alizarin Red stained calcium nodules.** (mM) fold increase of dye absorbed calcium nodules, indicates ten folds increase in calcified mineral deposition of pBMP2-FLR and pBMP2 encapsulated PLGA-FLR MP transfected IHMSCs in comparison to controls. OI media (100 nM Dex) treated cell was set as a positive control.

5.7 Gene expression analysis

As IHMSCs start to develop into bone precursor cells and eventually differentiate into mature osteoblasts, they express bone related gene markers. Some of these markers are bone lineage specific such as *BGLAP* also called Osteocalcin. Other genes could also be expressed in other tissues however, largely related to bone developmental stages such as *ALP*, *RUNX2* and *SPP1*. Quantitative Reverse Transcription-Polymerase Chain Reaction (QRT-PCR) analysis was employed to amplify expressed transcripts of osteogenic genes in these transfected cultures and these were compared to

untreated controls. The expression levels of all the assayed genes were upregulated in transfected samples in comparison to control samples. Non-specific *ALP* gene was highly expressed in both control and transfected samples. However, its level was significantly higher in transfected samples than in control samples. *ALP* level was higher in pBMP2-FLR transfected cells than control cells in basal media and OP media by 2.5 and 2.8 folds respectively. Likewise, *ALP* level of pBMP2 encapsulated PLGA-FLR MP transfected cultures was higher than that of the control cultures in basal and OP media by 3.2 and 3.6 folds respectively. Moreover, *RUNX2* transcription factor gene was also upregulated significantly in both transfected cells in comparison to controls. For example. *RUNX2* expression levels in pBMP2-FLR transfected cells was 4.1 and 4.4 folds higher than cells maintained in the basal and OP media respectively. The *RUNX2* fold increase of pBMP2 encapsulated PLGA-FLR MP transfected cells was 3.7 and 4 folds higher than the same controls respectively. Furthermore, *SPP1* gene level was upregulated by 2.8 and 5.5 folds in differentiated cells transfected with pBMP2 encapsulated PLGA MPs in comparison to cells maintained in basal and OP media respectively. Additionally, cells transfected with pBMP2-FLR NPs were also recorded an increase in this gene by 3 folds in comparison to each of the controls. Importantly, late osteogenic marker, matrix synthesis and mineralisation specific gene; *BGLAP* (Lian *et al*., 1989, Ryoo *et al*., 1997, Thiagarajan *et al*., 2017) was significantly upregulated in the transfected cells in comparison to the controls. pBMP2 encapsulated PLGA-FLR MP

transfected cells recorded 3.4 and 1.4 fold increase in *BGLAP* expression than cell cultured in basal and OP media respectively. Moreover, *BGLAP* expression level in pBMP2-FLR NP transfected cells was higher by 3.1 and 1.3 folds in comparison to the controls respectively (Figure 5-9).

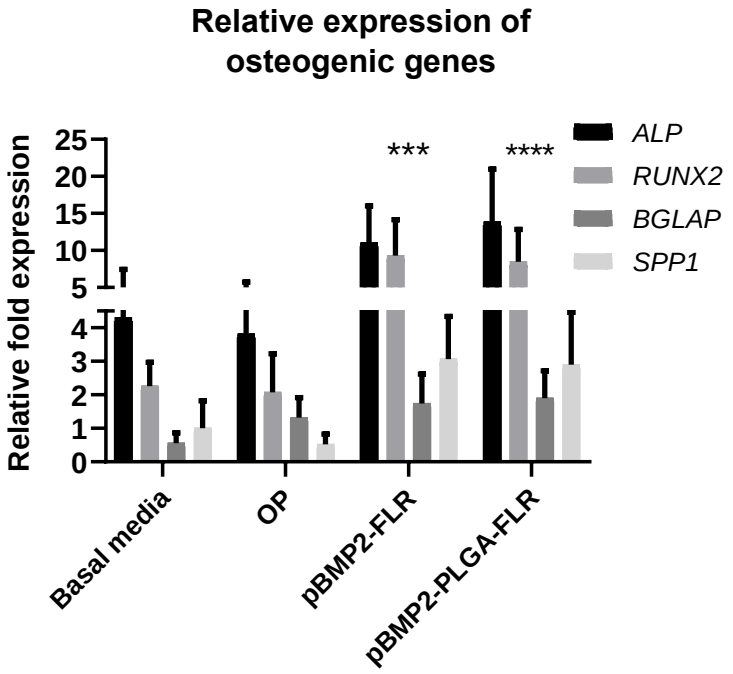

Figure 5-22 **Relative expression levels of osteogenic genes in transfected IHMSCs in comparison to control cells.** Significant activation of the osteogenic genes: *ALP* (Alkaline Phospahatese), *RUNX2* (Runt Related Transcription Factor 2), *BGLAP* (Bone Gamma-Carboxyglutamate Protein) also called Osteocalcin, and *SPP1* (Secreted Phosphoprotein 1) also called Osteopontin at week four of samples either transfected with pBMP2-FLR NPs or pBMP2-encapsulated PLGA-FLR MPs in comparison to non-transfected cells. The graph was plotted based on expression fold change to cells cultured in expansion media only. Two-way Anova statistical analysis was used to generate the graph. The data represented as mean ± SD. Where significance was *** or ****, P value was, 0.0002 or < 0.0001 respectively.

5.8 Metabolic activities of IHMSCs during bone differentiation

Cell viability studies were employed to determine the toxicity of pBMP2 encapsulated PLGA-FLR MPs during differentiation studies. As previously shown in section 4.10, FLR complexed pDNA encapsulated PLGA MPs demonstrated good compatibility with IHMSCs**.** Measuring cell viability of the transfected cells with the highest dose of 1 µg pBMP2 encapsulated PLGA-FLR MPs (0.2 mg pf PLGA and 4 µM FLR) the during differentiation study showed a minimum of 70 % viable cells during the first three days of highest transfection activities (Figure 5-10).

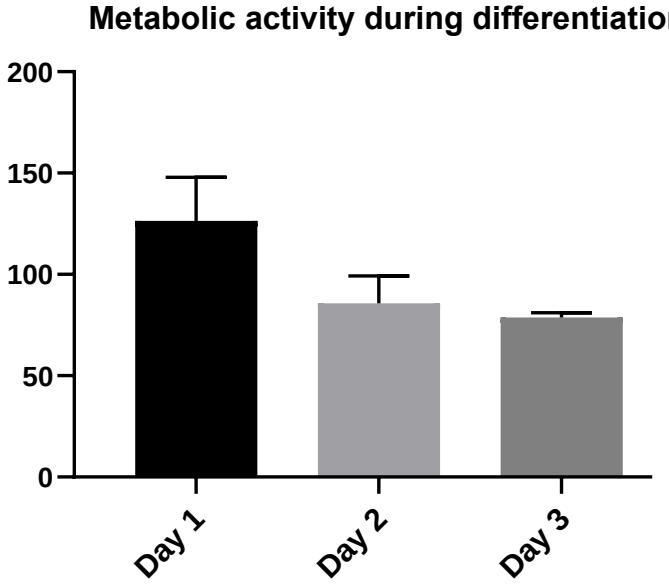

Figure 5-24 **Metabolic activity during differentiation.** Metabolic activity of the transfected cells during the first three days of differentiation. The cells have retained at least 70 % of viability during highest transfection activity (Day 2 & 3).

5.9 Discussion

A combination of gene delivery and cell therapy have been employed to maximise the therapeutic effect of each of the technologies. The transfection of Mesenchymal stem cells (MSCs) enhances their differentiation capacities and the overall therapeutic outcome in clinical settings (Partridge and Oreffo, 2004, Tsuda *et al*., 2003, Jeong *et al*., 2016, Gonzalez-Fernandez *et al*., 2017). Nevertheless, the amount of published work in this field is limited, mainly because MSCs are difficult to transfect and gene delivery is not translated easily, particularly *in vivo* (Wegman *et al*., 2011, Park *et al*., 2019, Lutz *et al*., 2008, Lee *et al*., 2010).

GET peptides have been used successfully to induce bone differentiation in gene activated scaffolds *in vitro* and *in vivo* (Raftery *et al*., 2019). However, as discussed in the previous chapters, cationic polymers (GET included) only partially encapsulate the nucleic acid, which results in poor protection against enzymatic differentiation. Therefore, in this study, the aim was to demonstrate the use of GET peptides in biomedical applications in combination with PLGA polymer nanotechnology for maximum DNase protection. Moreover, the effect of encapsulated pBMP2 in PLGA MPs on bone differentiation was compared to that of GET complexed pBMP2.

5.9.1 The use of IHMSC for bone differentiation

Human mesenchymal stem cells (hMSCs) are a population of multipotent stem cells derived from a variety of sources, mainly bone marrow. Other

sources of hMSC, such as adipose tissue, peripheral blood and cord blood, have also been investigated. hMSCs are known for their multilineage differentiation capacities, mainly to mesodermal lineages such as bone, adipose tissue and cartilage (Hass *et al*., 2011, Klingemann *et al*., 2008). However, their number in the body and their *in vitro* lifespan is limited (Bonab *et al*., 2006, Eggenhofer *et al*., 2014, Kim and Park, 2017). Immortalised hMSCs (IHMSCs) represent a valuable alternative to hMSCs in experimental settings. The use of IHMSCs provides access to a large number of cells, which is advantageous in terms of reducing donor-site morbidity, high cost, time for cell expansion and donor variability (Trounson and McDonald, 2015, Furukawa *et al*., 2015). Moreover, they have been well characterised and their multilineage differentiation capacities have been compared to those of hMSCs (Skarn *et al*., 2014, Galarza Torre *et al*., 2018).

Therefore, in the current study, IHMSCs were used to assess the bone differentiation potential of these pBMP2 encapsulated PLGA-FLR MPs.

5.9.2 Optimisation of cell culture conditions for bone differentiation

In order to test the osteogenic differentiation of IHMSCs, 4k cells/cm^2 were seeded and fed with 10 or 100 nM Dex for four weeks. However, these culture conditions did not result in any levels of osteogenic differentiation of the cells. Applying the above culture conditions when inducing primary hMSCs resulted in successful bone differentiation within three to four weeks

(Jarocha *et al*., 2008, Pilge *et al*., 2016). (Digirolamo *et al*., 1999) stated that, at the above seeding density cells are 70-90 % confluent. However, in the current studies, IHMSC cultures at the above seeding density were very sparse and were far below 70-90 % confluency after the overnight incubation of the cells. It was believed that these differences in the degree of confluency between the primary hMSCs and IHMSC cell lines at the same seeding density could be attributed to the difference in cell size and morphology between the two cell populations. Both primary hMSCs and IHMSCs are known as fibroblastic spindle-shaped cells. However, in contrast to IHMSCs, primary hMSCs inter senescence from the point of their *in vitro* cultivation and the occurrence of senescence increases upon multiple passages of the cells until almost the cells stop proliferating at later passages (Jiang *et al*., 2019, Li *et al*., 2017). As well as affecting differentiation potential, cell migration ability and immunomodulatory activities, cellular senescence affects the morphology and size of the cells (Wang *et al*., 2012, Turinetto *et al*., 2016). During senescence, hMSCs flatten and increase in size, which takes up more space in tissue culture plates (Lee *et al*., 2009, Yang *et al*., 2018b, Bruder *et al*., 1997, Bara *et al*., 2014, McKee and Chaudhry, 2017). This in turn affects confluency, cell-cell contact, cell signalling and MSC fate (Mao *et al*., 2016, Ball *et al*., 2004). This senescence related morphological changes have also been observed in other primary cells, such as primary human fibroblasts (Druelle *et al*., 2016) and endothelial cells (Johnson and Longenecker, 1982, Shi *et al*., 2004) during *in*

vitro expansion. Moreover, a cell count of hMSCs that was almost two-thirds lower than that of IHMSCs in direct relation to their larger size in comparison to IHMSCs at the same confluency and in the same size of culture dishes was experienced. By contrast, IHMSCs, as a result of their immortalisation, are driven to maintain stemness during their *in vitro* cell culture and do not inter senescence or change in size

5.9.3 Effect of cell density on osteoblastic differentiation and quantity of mineralised matrix

Following on from the process of optimising culture conditions to drive the IHMSCs to differentiate into osteogenic lineages, cell seeding density, among other factors, plays a critical role in the initial induction and quantity of calcified minerals during bone differentiation. (Abo-Aziza and A, 2017) studied the effect of hMSC monolayer percentage of confluency on their osteogenic differentiation efficiency, and found that cells that began with 80 % confluency had the highest mineralisation rate compared to sub-confluent monolayers at 50-70 % or too confluent monolayers at 100 % confluency. Low seeding density, which resulted in 20 % and 50 % confluency, did not cause a significant increase in Alizarin Red staining compared to cells cultured at 70 % and 80 % confluency. Moreover, increase in osteogenic genes has been correlated with an increase in cell seeding density. For example, the expression levels of *ALP* gene were found to be higher in denser cultures (Wang *et al*., 2010). These results could be attributed to the

influence of the initial seeding density on the commitment of the cells to either osteogenic or other mesodermal lineages (Ren *et al*., 2015).

In the present experiments, cultures with an initial seeding density of 35K and 80 % confluency (in 1.9 cm^2, 24-well plate) produced more mineral deposition than did cultures with initial cell seeding densities of 8k, 15k and 60k.

5.9.4 Osteoinductive properties of Dexamethasone are dose dependent

In vivo bone differentiation during development or injury is a highly regulated process that occurs as a result of the interplay of multiple endogenous factors. Therefore, mimicking this differentiation process *in vitro* requires the application of a balanced combination of these factors. In these experiments, as well as in others, gene delivery encapsulating a single factor such as pBMP2 did not result in bone differentiation (Lee *et al*., 2010, Wang *et al*., 2016, Raftery *et al*., 2017, Loozen *et al*., 2018). Therefore, the co-delivery of factors is necessary for *in vitro* bone differentiation. Dex is an osteoinductive glucocorticoid, and its use in *in vitro* culture has been adopted to mimic the *in vivo* conditions of the native glucocorticoids (Roberts *et al*., 2011, Raftery *et al*., 2017) that are essential for the morphological fibroblastic to polygonal changes reported previously (Jaiswal *et al*., 1997, Yamanouchi *et al*., 1997). In this assay, a minimal dose of Dex (10 nM) at sub-threshold levels (in OP) was used, which meant that, if

functional levels of BMP2 were expressed by gene delivery, this could induce significant osteogenesis. This was compared to high amounts of Dex (100 nM) in OI media, which are capable of inducing differentiation without BMP2 supplementation. As indicated by the controls in the present study, and as others have also concluded, Dex has no effect on osteogenesis at these sub-threshold concentrations, but only augments the osteogenic differentiation properties of pBMP2 (Roberts *et al*., 2011).

5.9.5 Efficient bone differentiation as a result of transfection with pBMP2-FLR and pBMP2 encapsulated PLGA-FLR MPs

To demonstrate the efficient delivery of pBMP2 encapsulated PLGA MPs complexed with FLR peptide, their biomedical applications in bone differentiation were tested and compared to the bone differentiation efficiency of previously published pBMP2-FLR NPs (Raftery *et al*., 2019). The dose of pBMP2-FLR NPs was optimised in the context of these experimental set up to determine the effective dose of encapsulated pBMP2 for bone differentiation. pBMP2 encapsulated PLGA MPs required higher doses than non-encapsulated pBMP2 to produce efficient bone differentiation. This could be explained by the possible partial association of pBMP2 with PLL used in the condensation of pBMP2 during the encapsulation process. This could consequently decrease the release of pBMP2 from pBMP2-PLL NPs encapsulated in PLGA MPs (Addi *et al*., 2017). The same effect of lower luciferase units was observed when pGluc encapsulated PLGA-PLR MPs were

compared to non-encapsulated pGluc-PLR NPs (positive control - see Section 4.13.1 Figure 4-16).

5.9.6 Osteogenic gene expression

The gene expression analysis studied the expression of bone specific and other highly associated osteogenic genes. For example, *ALP* is abundantly expressed in tissues other than bone. However, it is also highly upregulated in osteogenic differentiation. In the current studies, as well as increase in *ALP* levels in differentiated cultures transfected with encapsulated and non-encapsulated pBMP2, an increase in *ALP* expression levels was seen in cultures treated with media conditioned with osteogenic supplements such as ascorbic acid and b-glycerophosphate (Basal media), or media with added non-osteoinductive concentrations of Dexamethasone (OP media) in comparison to cultures maintained in expansion media. These cultures did not show any signs of osteogenic differentiation. However, the *ALP* level was three folds higher in these cultures in comparison to cultures maintained in expansion media. This increase in *ALP* due to the addition of bone supplements was also seen in (Rabadan-Ros *et al*., 2018) suggesting its osteoblast maturation role during the early stages of preosteoblast differentiation (Yohay *et al*., 1994). Moreover, bone transcription factor gene *RUNX2* is mediating the final stages of osteoblast maturation and lack of *RUNX2* in mutant animals has resulted in complete inhibition of bone formation (Choi *et al*., 2001, Lou *et al*., 2009) . in the current study, *RUNX2*

gene was significantly upregulated in transfected cultures in comparison to non-transfected control cultures. However, there was also a two-fold increase in *RUNX2* levels in the non-transfected cultured in comparison to cultures maintained in expansion media. This could also be explained by the cell growth regulatory roles of *RUNX2* during early preosteoblast proliferative expansion (Pratap *et al*., 2003). Furthermore, the upregulation of Osteopontin or *SPP1* is highly associated with differentiated osteoblasts. Hence, higher levels of *SPP1* in the current differentiated cultures were observed in compassion to undifferenced cultures. However, lower levels of increase could also be seen in undifferentiated preosteoblasts in basal and OP media (Sodek *et al*., 1995) due to its crucial role in the regulation of *ALP* expression during early differentiation (Liu *et al*., 1997). Late-stage osteogenic specific and matrix mineralisation gene; *BGLAP* expression was less seen in undifferentiated cultures in basal and OP media and increased significantly in differentiated cultures as a result of pBMP2-FLR and pBMP2 encapsulated PLGA-FLR MPs transfection strongly indicating successful differentiation of transfected cultures.

5.10 Chapter summary

1. Well-characterised, immortalised stem cell lines could be used as an alternative model for primary cells in *in vitro* differentiation assays due to their availability in large numbers, ability to be maintained to relatively higher passage numbers, and decreasing the effect of long-term, culture-related senescence and resulting morphological changes and their possible influence on differentiation capacities.
2. Optimisation of the cell culture is required to decrease the effect of various culture conditions, cell behaviour on differentiation outcomes.
3. Cell seeding density is an important variable that could directly affect lineage commitment of the cultured cells.
4. Osteoinductive properties of Dexamethasone is varied and dependent on its concentration and the cell source.
5. Unlike i*n vivo* conditions, combination of factors is required to induce bone differentiation *in vitro.*
6. Bone differentiation using encapsulated pBMP2 could require higher doses than the non-encapsulated form of the plasmid due to the complexity of the system which might affect the release of the encapsulated pBMP2.

Chapter 6.

Conclusions

6.1 Conclusions

In this study pDNA was encapsulated in PLGA MPs to protect the encapsulated pDNA form enzymatic degradation encountered by condensing polycation-based non-viral gene delivery vectors. This system has many other advantages compared to the current non-viral gene delivery vectors as it combines the benefits of scalability, potential for prolonged storage and stability. These attributes are significant when developing and translating a pharmaceutical gene delivery product. Moreover, for enhanced intracellular delivery characteristics, variants of GET peptides were complexed with the pDNA encapsulated PLGA MPs to form PLGA-GET MPs. Qualitative and quantitative analyses by fluorescence microscopy and flow cytometry demonstrated the enhanced intracellular delivery of the PLGA-GET MPs in comparison to non-complexed PLGA MPs. To determine whether the enhanced intracellular delivery of these MPs will enhance their transfection efficiencies, pGluc encapsulated PLGA-GET MPs were transfected into mammalian cells. LK15 containing GET peptides displayed enhanced transfection of these MPs as a direct result of enhanced transduction. These enhanced transfection properties of PLGA-GET MPs are functionally useful for biomedical applications.

The key points encountered in this study were:

6.1.1 Encapsulation of pDNA in PLGA MPs

In order to protect the encapsulated pDNA form environmental DNase enzymatic degradation, PLGA polymer was employed. Condensation of pDNA was required to enhance its encapsulation in polymer MPs. The findings in chapter 3 revealed that percentage of Encapsulation Efficiency (EE %) was much higher when pDNA was complexed with PLL to form pDNA-PLL NPs in comparison to naked pDNA; the EE% of pDNA-PLL NPs increased to 30 % in comparison to only 2-3 % of naked pDNA measured by the direct method. Moreover, the method by which PLGA MPs were fabricated largely affected the EE %. Results in this chapter suggest that modification of nanoprecipitation technique is not efficient for the encapsulation of hydrophilic pDNA in contrast to the double emulsion method.

It is imperative that pDNA encapsulated PLGA MPs are well characterised to evaluate the possibility of unfavourable surface attachment of positively charged pDNA-PLL NPs on the negatively charged PLGA MPs by electrostatic interaction during the process of double emulsion. Such characterisation includes Zeta potential measurements, exposure to DNases of the pDNA encapsulated PLGA MPs and comparison to blank PLGA MPs. In the present study, the Zeta potential measurements of the pDNA encapsulated PLGA MPs was compared to that of blank PLGA MPs. Moreover, controlling for the sedimentation of non-encapsulated pDNA-PLL NPs during centrifugation in the double emulsion method was also carried out to ensure transfection is

due the encapsulated and not surface contaminated DNA. Lastly, improved DNase protection ability of the encapsulated pDNA was demonstrated as function of its EE.

6.1.2 Complexation of GET peptides with PLGA MPs

Zeta potential measurements was indicative of electrostatic binding between the GET peptides and PLGA MPs. The Zeta potential of PLGA MPs changed significantly from highly negative to neutral or slightly positive MPs upon their complexation with PR, PLR or FLR variants of GET peptide. Transduction efficiencies of PLGA MPs was increased as a result of their complexation with GET peptides in comparison to PLGA MPs delivered alone. FLR complexed PLGA MPs recorded the highest transduction and transfection activities which were higher than the non-complexed PLGA MPs by seven folds and five orders of magnitude respectively. Moreover, the transduction and transfection efficiencies of FLR complexed PLGA MPs were two folds and almost one order of magnitude higher than PLR complexed PLGA MPs. The enhancement in both transduction and transfection was dose responsive up to saturation. These enhanced activities were confirmed to be not due to excessive positive charge of the PLGA-GET MPs as it is associated with other non–viral gene delivery vectors. Indeed these PLGA-GET MPs are neutrally charged and the enhanced transfection is entirely mediated by the delivery characteristics of GET peptide, including the requirement for effective endosomal escape activity due to the prescence of endosomal escpae moitiy; LK15. This system exhibited improved

transfcetion efifceincies and cell viability in comparison to other non-modified CPPs.

Moreover, the enhanced trafection efficies were confirmed to be entirely due to GET peptides and low molecular PLL does not exhibit any transfcetion activity. The main disadvantage of the system however, is the electrosatic complexation between the PLGA MPs and the GET peptides. Such complexation does not allow the production of colloidally stable MPs. Moreover, the stability of these MPs are compromised. Despite that, the PLGA-GET MPs was able to show improved levels of transfection as a direct result to their enhanced transduction properties.

6.1.3 Biomedical applications; Bone differentiation studies

To demonstrate the applicability of the enhanced transduction and transfection properties of PLGA-GET MPs in bone differentiation, the system was employed to transfect MSC *in vitro*. Results in chapter 4 revealed transfection efficiencies as high as 15 % could be achieved in MSC using this system which are considered as hard to transfect cells. The dose of BMP2 is critical to induce the MSC to bone lineages. pDNA encapsulated in PLGA MP exhibited lower luminescence units as well as transfection efficiencies when compared to non-encapsulated pDNA which resulted into higher dose of PLGA MPs to be applied in the bone differentiation assays to achieve the same effect by non-encapsulated pDNA.

6.2 Limitations of the study

The current study demonstrates efficient cellular internalisation of pDNA encapsulated PLGA MPs through the electrostatic complexation of GET peptides. Transduction and transfection levels of these PLGA MPs in optimal experimental conditions i.e. growth media which also resembles *in vivo* conditions are in useful levels and serves as good laboratory tools to assess the efficiency of these non-viral vectors. However, the therapeutic applications of the system are limited due instability of the electrostatic nature of the complex. To address this limitation, these GET peptides could be covalently attached on the surface of PLGA MPs. The process is carried out by carbodiimide EDC-NHS chemistry which is a specialised reaction that functionalises MPs through the activation of carboxyl groups on the surface of PLGA MPs and produce a linker to bind to the amine group in GET peptides. The finished product could be then characterised to confirm the presence of nitrogen group from the peptide on the surface of the PLGA MPs. Moreover, covalent binding of the GET peptides could allow maximise the number of GET peptides on the surface of the PLGA MPs and could potentially produce positively charged PLGA-GET MPs instead of neutral PLGA-GET MPs achieved with the electrostatic complexation. This in turn will increase the transduction and transfection activities of GET peptide. Furthermore, this will solve another limitation of the study which is the colloidal stability of these MPs and prevent their interaction with serum Albumin and other cell culture media components.

This study is also limited in terms of the level of transfection that pDNA encapsulated PLGA MP produce in comparison to non-encapsulated pDNA using pGluc in NIH3T3 cell line. Moreover, higher dose of pBMP2 encapsulated PLGA MPs is needed in comparison to non-encapsulated pBMP2 in the bone differentiation studies. It was speculated that these pDNA encapsulated PLGA MPs would produce higher or at least the same level of transfection as the non-encapsulated pDNA due to higher degree of nuclease protection *in vitro*. This could have occurred due to suboptimal release of the encapsulated pDNA from PLGA MPs due to the interaction between the positively charged pDNA-PLL NPs and the negatively charged PLGA MPs. This interaction could be possibly addressed by the addition of a positively charged excipient (Abu-Awwad *et al*., 2017) during the encapsulation process of pDNA in double emulsion which will potentially compete with the pDNA-PLL for PLGA binding to facilitate the release process. Moreover, these lower transfection levels could also be due to the better interaction of GET with highly negatively charged pDNA of -80 mV (Takeshita *et al*., 2013) in pDNA-PLR or pDNA-FLR NPs than with weekly negatively charged PLGA MPs (-23 mV). This could be addressed by the use of a negatively charged surfactants such as carboxymethyl dextran as a stabiliser (Sun *et al*., 2016, Vasić *et al*., 2020) in the double emulsion process which is going to increase the density of negatively charged carboxyl groups on the surface of PLGA MPs for better GET interaction instead of PVA which is a non-ionic surfactant and masks the carboxyl groups on the PLGA which intern results in poor electrostatic interaction between GET and PLGA MPs.

the substitution of PVA with carboxymethyl dextran could also enhance the covalent attachment of GET peptides if these MPs were to covalently attach to GET peptides.

6.3 Future perspective

This study focused on the enhancement of intracellular delivery and transfection of pDNA encapsulated PLGA MPs complexed with GET peptides. The findings presented in this thesis provide a body of data regarding the characterisation of pDNA NP prior to their encapsulation in PLGA MPs, characterisation of pDNA encapsulated PLGA MPs, characterisation of PLGA-GET MPs and biomedical application of PLGA-GET MPs. Improving the stability of the PLGA-GET MP system could lead to further improved transfection characteristics for biomedical applications.

Strategies to deliver the therapeutic effect of BMP2 in a safe way that eliminates the side effects associated with the current BMP2 protein (rhBMP2) delivery methods due to the application of high concentrations of BMP2, could be of great advantage in the field of bone regeneration. These pBMP2 encapsulated PLGA-GET MPs could be incorporated into tissue engineering constructs to produce physiologically relevant levels of BMP2 directly from transfected MSC *in vivo* or *ex vivo*.

For the full potential of this system to be realised, more physically stable freeze-dried PLGA-GET MPs must be developed though covalent attachment of the GET peptide on the surface PLGA MPs. Moreover, the process of the release of the encapsulated pDNA and/or enhancement of its encapsulation

efficiency has to be optimised to further improve the transfection efficiency outcomes of these PLGA-GET MPs.

Chapter 7.

References

ABBAS, A. O., DONOVAN, M. D. & SALEM, A. K. 2008. Formulating poly(lactide-co-glycolide) particles for plasmid DNA delivery. *J Pharm Sci,* 97**,** 2448-61.

ABO-AZIZA, F. A. M. & A, A. Z. 2017. The Impact of Confluence on Bone Marrow Mesenchymal Stem (BMMSC) Proliferation and Osteogenic Differentiation. *Int J Hematol Oncol Stem Cell Res,* 11**,** 121-132.

ABU-AWWAD, H. A. M., THIAGARAJAN, L. & DIXON, J. E. 2017. Controlled release of GAG-binding enhanced transduction (GET) peptides for sustained and highly efficient intracellular delivery. *Acta Biomater,* 57**,** 225-237.

ADDI, C., MURSCHEL, F., LIBERELLE, B., RIAHI, N. & DE CRESCENZO, G. 2017. A highly versatile adaptor protein for the tethering of growth factors to gelatin-based biomaterials. *Acta Biomater,* 50**,** 198-206.

ADEBILEJE, T., VALIZADEH, A. & AMANI, A. 2017. Effect of formulation parameters on the size of PLGA nanoparticles encapsulating bovine serum albumin: a response surface methodology. *Journal of Contemporary Medical Sciences* 3**,** 306–312

ADEREM, A. & UNDERHILL, D. M. 1999. Mechanisms of phagocytosis in macrophages. *Annu Rev Immunol,* 17**,** 593-623.

ADOLPH, E. J., NELSON, C. E., WERFEL, T. A., GUO, R., DAVIDSON, J. M., GUELCHER, S. A. & DUVALL, C. L. 2014. Enhanced Performance of Plasmid DNA Polyplexes Stabilized by a Combination of Core Hydrophobicity and Surface PEGylation. *J Mater Chem B,* 2**,** 8154-8164.

AHMED, M. 2017. Peptides, polypeptides and peptide-polymer hybrids as nucleic acid carriers. *Biomater Sci,* 5**,** 2188-2211.

AKINC, A., THOMAS, M., KLIBANOV, A. M. & LANGER, R. 2005. Exploring polyethylenimine-mediated DNA transfection and the proton sponge hypothesis. *J Gene Med,* 7**,** 657-63.

ALBANESE, A., TANG, P. S. & CHAN, W. C. 2012. The effect of nanoparticle size, shape, and surface chemistry on biological systems. *Annu Rev Biomed Eng,* 14**,** 1-16.

ALHAKAMY, N. A. & BERKLAND, C. J. 2013. Polyarginine molecular weight determines transfection efficiency of calcium condensed complexes. *Mol Pharm,* 10**,** 1940-8.

ALKOTAJI, M., PLUEN, A., ZINDY, E., HAMRANG, Z. & AOJULA, H. 2014. On the cellular uptake and membrane effect of the multifunctional peptide, TatLK15. *J Pharm Sci,* 103**,** 293-304.

AMINI, A. R., LAURENCIN, C. T. & NUKAVARAPU, S. P. 2012. Bone tissue engineering: recent advances and challenges. *Crit Rev Biomed Eng,* 40**,** 363-408.

AN, H. & JIN, B. 2012. Prospects of nanoparticle-DNA binding and its implications in medical biotechnology. *Biotechnol Adv,* 30**,** 1721-32.

ANDRADES, J., A.,, NARVÁEZ-LEDESMA, L., CERÓN-TORRES, L., CRUZ-AMAYA, A., P.,, LÓPEZ-GUILLÉN, D., MESA- ALMAGRO, M., L., & MORENO-MORENO, J., A. 2013. Bone Engineering: A Matter of Cells, Growth Factors and Biomaterials. *Regenerative Medicine and Tissue Engineering.* IntechOpen.

ARAKHA, M., PAL, S., SAMANTARRAI, D., PANIGRAHI, T. K., MALLICK, B. C., PRAMANIK, K., MALLICK, B. & JHA, S. 2015. Antimicrobial activity of iron oxide nanoparticle upon modulation of nanoparticle-bacteria interface. *Sci Rep,* 5**,** 14813.

ARBAB, A. S., YOCUM, G. T., WILSON, L. B., PARWANA, A., JORDAN, E. K., KALISH, H. & FRANK, J. A. 2004. Comparison of transfection agents in forming

complexes with ferumoxides, cell labeling efficiency, and cellular viability. *Mol Imaging,* 3**,** 24-32.

ARIKAWA, T., OMURA, K. & MORITA, I. 2004. Regulation of bone morphogenetic protein-2 expression by endogenous prostaglandin E2 in human mesenchymal stem cells. *J Cell Physiol,* 200**,** 400-6.

ARSCOTT, P. G., LI, A. Z. & BLOOMFIELD, V. A. 1990. Condensation of DNA by trivalent cations. 1. Effects of DNA length and topology on the size and shape of condensed particles. *Biopolymers,* 30**,** 619-30.

AUBIN, J. E. 1998. Advances in the osteoblast lineage. *Biochem Cell Biol,* 76**,** 899-910.

BADDING, M. A., VAUGHAN, E. E. & DEAN, D. A. 2012. Transcription factor plasmid binding modulates microtubule interactions and intracellular trafficking during gene transfer. *Gene Ther,* 19**,** 338-46.

BAI, H., LESTER, G. M. S., PETISHNOK, L. C. & DEAN, D. A. 2017. Cytoplasmic transport and nuclear import of plasmid DNA. *Biosci Rep,* 37.

BAIN, G., MULLER, T., WANG, X. & PAPKOFF, J. 2003. Activated beta-catenin induces osteoblast differentiation of C3H10T1/2 cells and participates in BMP2 mediated signal transduction. *Biochem Biophys Res Commun,* 301**,** 84-91.

BALL, S. G., SHUTTLEWORTH, A. C. & KIELTY, C. M. 2004. Direct cell contact influences bone marrow mesenchymal stem cell fate. *Int J Biochem Cell Biol,* 36**,** 714-27.

BALMAYOR, E. R. & VAN GRIENSVEN, M. 2015. Gene therapy for bone engineering. *Front Bioeng Biotechnol,* 3**,** 9.

BARA, J. J., RICHARDS, R. G., ALINI, M. & STODDART, M. J. 2014. Concise review: Bone marrow-derived mesenchymal stem cells change phenotype following in vitro culture: implications for basic research and the clinic. *Stem Cells,* 32**,** 1713-23.

BARNARD, A. R., GROPPE, M. & MACLAREN, R. E. 2014. Gene therapy for choroideremia using an adeno-associated viral (AAV) vector. *Cold Spring Harb Perspect Med,* 5**,** a017293.

BARTHOLOMEW, A., STURGEON, C., SIATSKAS, M., FERRER, K., MCINTOSH, K., PATIL, S., HARDY, W., DEVINE, S., UCKER, D., DEANS, R., MOSELEY, A. & HOFFMAN, R. 2002. Mesenchymal stem cells suppress lymphocyte proliferation in vitro and prolong skin graft survival in vivo. *Exp Hematol,* 30**,** 42-8.

BAYLINK, D. J., FINKELMAN, R. D. & MOHAN, S. 1993. Growth factors to stimulate bone formation. *J Bone Miner Res,* 8 Suppl 2**,** S565-72.

BETANCOURT, T., BROWN, B. & BRANNON-PEPPAS, L. 2007. Doxorubicin-loaded PLGA nanoparticles by nanoprecipitation: preparation, characterization and in vitro evaluation. *Nanomedicine (Lond),* 2**,** 219-32.

BETKER, J. L. & ANCHORDOQUY, T. J. 2015. Relating toxicity to transfection: using sphingosine to maintain prolonged expression in vitro. *Mol Pharm,* 12**,** 264-73.

BETTINGER, T., CARLISLE, R. C., READ, M. L., OGRIS, M. & SEYMOUR, L. W. 2001. Peptide-mediated RNA delivery: a novel approach for enhanced transfection of primary and post-mitotic cells. *Nucleic Acids Res,* 29**,** 3882-91.

BHAVSAR, M. D. & AMIJI, M. M. 2008. Development of novel biodegradable polymeric nanoparticles-in-microsphere formulation for local plasmid DNA delivery in the gastrointestinal tract. *AAPS PharmSciTech,* 9**,** 288-94.

BILATI, U., ALLEMANN, E. & DOELKER, E. 2005a. Development of a nanoprecipitation method intended for the entrapment of hydrophilic drugs into nanoparticles. *Eur J Pharm Sci,* 24**,** 67-75.

BILATI, U., ALLEMANN, E. & DOELKER, E. 2005b. Nanoprecipitation versus emulsion-based techniques for the encapsulation of proteins into biodegradable nanoparticles and process-related stability issues. *AAPS PharmSciTech,* 6**,** E594-604.

BLANCO, E., SHEN, H. & FERRARI, M. 2015. Principles of nanoparticle design for overcoming biological barriers to drug delivery. *Nat Biotechnol,* 33**,** 941-51.

BLEEKER, E. A., DE JONG, W. H., GEERTSMA, R. E., GROENEWOLD, M., HEUGENS, E. H., KOERS-JACQUEMIJNS, M., VAN DE MEENT, D., POPMA, J. R., RIETVELD, A. G., WIJNHOVEN, S. W., CASSEE, F. R. & OOMEN, A. G. 2013. Considerations on the EU definition of a nanomaterial: science to support policy making. *Regul Toxicol Pharmacol,* 65**,** 119-25.

BLOOMFIELD, V. A. 1991. Condensation of DNA by multivalent cations: considerations on mechanism. *Biopolymers,* 31**,** 1471-81.

BLOOMFIELD, V. A. 1996. DNA condensation. *Curr Opin Struct Biol,* 6**,** 334-41.

BLOOMFIELD, V. A. 1997. DNA condensation by multivalent cations. *Biopolymers,* 44**,** 269-82.

BONAB, M. M., ALIMOGHADDAM, K., TALEBIAN, F., GHAFFARI, S. H., GHAVAMZADEH, A. & NIKBIN, B. 2006. Aging of mesenchymal stem cell in vitro. *BMC Cell Biol,* 7**,** 14.

BOSTROM, M., WILLIAMS, D. R. & NINHAM, B. W. 2001. Specific ion effects: why DLVO theory fails for biology and colloid systems. *Phys Rev Lett,* 87**,** 168103.

BOUARD, D., ALAZARD-DANY, D. & COSSET, F. L. 2009. Viral vectors: from virology to transgene expression. *Br J Pharmacol,* 157**,** 153-65.

BREUNIG, M., LUNGWITZ, U., LIEBL, R. & GOEPFERICH, A. 2007. Breaking up the correlation between efficacy and toxicity for nonviral gene delivery. *Proc Natl Acad Sci U S A,* 104**,** 14454-9.

BRGLES, M., SANTAK, M., HALASSY, B., FORCIC, D. & TOMASIC, J. 2012. Influence of charge ratio of liposome/DNA complexes on their size after extrusion and transfection efficiency. *Int J Nanomedicine,* 7**,** 393-401.

BRUDER, S. P., JAISWAL, N. & HAYNESWORTH, S. E. 1997. Growth kinetics, self-renewal, and the osteogenic potential of purified human mesenchymal stem cells during extensive subcultivation and following cryopreservation. *J Cell Biochem,* 64**,** 278-94.

BUKHARI, A., IDRIS, A. & ATTA, M. 2014. Effect of organic and aqueous dispersion medium on the development of polystyrene nanoparticles in nanoprecipitation method. *Malaysian Journal of Fundamental and Applied Sciences,* 10**,** 28-32.

BUTTERY, L. D., BOURNE, S., XYNOS, J. D., WOOD, H., HUGHES, F. J., HUGHES, S. P., EPISKOPOU, V. & POLAK, J. M. 2001. Differentiation of osteoblasts and in vitro bone formation from murine embryonic stem cells. *Tissue Eng,* 7**,** 89-99.

CAFFERY, B., LEE, J. S. & ALEXANDER-BRYANT, A. A. 2019. Vectors for Glioblastoma Gene Therapy: Viral & Non-Viral Delivery Strategies. *Nanomaterials (Basel),* 9.

CAPAN, Y., WOO, B. H., GEBREKIDAN, S., AHMED, S. & DELUCA, P. P. 1999a. Influence of formulation parameters on the characteristics of poly(D, L-

lactide-co-glycolide) microspheres containing poly(L-lysine) complexed plasmid DNA. *J Control Release,* 60**,** 279-86.

CAPAN, Y., WOO, B. H., GEBREKIDAN, S., AHMED, S. & DELUCA, P. P. 1999b. Preparation and characterization of poly (D,L-lactide-co-glycolide) microspheres for controlled release of poly(L-lysine) complexed plasmid DNA. *Pharmaceutical Research,* 16**,** 509-513.

CAPLAN, A. I. 1991. Mesenchymal stem cells. *J Orthop Res,* 9**,** 641-50.

CARTIERA, M. S., JOHNSON, K. M., RAJENDRAN, V., CAPLAN, M. J. & SALTZMAN, W. M. 2009. The uptake and intracellular fate of PLGA nanoparticles in epithelial cells. *Biomaterials,* 30**,** 2790-8.

CARVALHO, M., SEPODES, B. & MARTINS, A. P. 2017. Regulatory and Scientific Advancements in Gene Therapy: State-of-the-Art of Clinical Applications and of the Supporting European Regulatory Framework. *Front Med (Lausanne),* 4**,** 182.

CARVALHO, P. M., FELICIO, M. R., SANTOS, N. C., GONCALVES, S. & DOMINGUES, M. M. 2018. Application of Light Scattering Techniques to Nanoparticle Characterization and Development. *Front Chem,* 6**,** 237.

CASETTARI, L., CASTAGNINO, E., STOLNIK, S., LEWIS, A., HOWDLE, S. M. & ILLUM, L. 2011. Surface characterisation of bioadhesive PLGA/chitosan microparticles produced by supercritical fluid technology. *Pharm Res,* 28**,** 1668-82.

CHANG, Y. L., STANFORD, C. M. & KELLER, J. C. 2000. Calcium and phosphate supplementation promotes bone cell mineralization: implications for hydroxyapatite (HA)-enhanced bone formation. *J Biomed Mater Res,* 52**,** 270-8.

CHAUDHURY, S. 2012. Mesenchymal stem cell applications to tendon healing. *Muscles Ligaments Tendons J,* 2**,** 222-9.

CHEN, B., HE, X. Y., YI, X. Q., ZHUO, R. X. & CHENG, S. X. 2015a. Dual-peptide-functionalized albumin-based nanoparticles with ph-dependent self-assembly behavior for drug delivery. *ACS Appl Mater Interfaces,* 7**,** 15148-53.

CHEN, J., GUO, Z., TIAN, H. & CHEN, X. 2016. Production and clinical development of nanoparticles for gene delivery. *Mol Ther Methods Clin Dev,* 3**,** 16023.

CHEN, W., BAYLINK, D. J., BRIER-JONES, J., NEISES, A., KIROYAN, J. B., RUNDLE, C. H., LAU, K. H. & ZHANG, X. B. 2015b. PDGFB-based stem cell gene therapy increases bone strength in the mouse. *Proc Natl Acad Sci U S A,* 112**,** E3893-900.

CHENG, C. J., TIETJEN, G. T., SAUCIER-SAWYER, J. K. & SALTZMAN, W. M. 2015. A holistic approach to targeting disease with polymeric nanoparticles. *Nat Rev Drug Discov,* 14**,** 239-47.

CHIDAMBARAM, M. & KRISHNASAMY, K. 2014. Modifications to the conventional nanoprecipitation technique: an approach to fabricate narrow sized polymeric nanoparticles. *Adv Pharm Bull,* 4**,** 205-8.

CHO, E. J., HOLBACK, H., LIU, K. C., ABOUELMAGD, S. A., PARK, J. & YEO, Y. 2013. Nanoparticle characterization: state of the art, challenges, and emerging technologies. *Mol Pharm,* 10**,** 2093-110.

CHO, T. J., GERSTENFELD, L. C. & EINHORN, T. A. 2002. Differential temporal expression of members of the transforming growth factor beta superfamily during murine fracture healing. *J Bone Miner Res,* 17**,** 513-20.

CHOI, J. Y., PRATAP, J., JAVED, A., ZAIDI, S. K., XING, L., BALINT, E., DALAMANGAS, S., BOYCE, B., VAN WIJNEN, A. J., LIAN, J. B., STEIN, J. L., JONES, S. N. &

STEIN, G. S. 2001. Subnuclear targeting of Runx/Cbfa/AML factors is essential for tissue-specific differentiation during embryonic development. *Proc Natl Acad Sci U S A,* 98**,** 8650-5.

CHOUDHERY, M. S., BADOWSKI, M., MUISE, A., PIERCE, J. & HARRIS, D. T. 2014. Donor age negatively impacts adipose tissue-derived mesenchymal stem cell expansion and differentiation. *J Transl Med,* 12**,** 8.

CHRISTIE, R. J., NISHIYAMA, N. & KATAOKA, K. 2010. Delivering the code: polyplex carriers for deoxyribonucleic acid and ribonucleic acid interference therapies. *Endocrinology,* 151**,** 466-73.

CHUA, C. C., RAHIMI, N., FORSTEN-WILLIAMS, K. & NUGENT, M. A. 2004. Heparan sulfate proteoglycans function as receptors for fibroblast growth factor-2 activation of extracellular signal-regulated kinases 1 and 2. *Circ Res,* 94**,** 316-23.

CHUGH, A., EUDES, F. & SHIM, Y. S. 2010. Cell-penetrating peptides: Nanocarrier for macromolecule delivery in living cells. *IUBMB Life,* 62**,** 183-93.

CHUMAKOVA, O. V., LIOPO, A. V., ANDREEV, V. G., CICENAITE, I., EVERS, B. M., CHAKRABARTY, S., PAPPAS, T. C. & ESENALIEV, R. O. 2008. Composition of PLGA and PEI/DNA nanoparticles improves ultrasound-mediated gene delivery in solid tumors in vivo. *Cancer Lett,* 261**,** 215-25.

CIOBANASU, C., HARMS, E., TUNNEMANN, G., CARDOSO, M. C. & KUBITSCHECK, U. 2009. Cell-penetrating HIV1 TAT peptides float on model lipid bilayers. *Biochemistry,* 48**,** 4728-37.

CLAMME, J. P., KRISHNAMOORTHY, G. & MELY, Y. 2003. Intracellular dynamics of the gene delivery vehicle polyethylenimine during transfection: investigation by two-photon fluorescence correlation spectroscopy. *Biochim Biophys Acta,* 1617**,** 52-61.

COHEN-SELA, E., CHORNY, M., KOROUKHOV, N., DANENBERG, H. D. & GOLOMB, G. 2009. A new double emulsion solvent diffusion technique for encapsulating hydrophilic molecules in PLGA nanoparticles. *J Control Release,* 133**,** 90-5.

COHEN, H., LEVY, R. J., GAO, J., FISHBEIN, I., KOUSAEV, V., SOSNOWSKI, S., SLOMKOWSKI, S. & GOLOMB, G. 2000. Sustained delivery and expression of DNA encapsulated in polymeric nanoparticles. *Gene Ther,* 7**,** 1896-905.

COHEN, R. N., VAN DER AA, M. A., MACARAEG, N., LEE, A. P. & SZOKA, F. C., JR. 2009. Quantification of plasmid DNA copies in the nucleus after lipoplex and polyplex transfection. *J Control Release,* 135**,** 166-74.

COLSON, Y. L. & GRINSTAFF, M. W. 2012. Biologically responsive polymeric nanoparticles for drug delivery. *Adv Mater,* 24**,** 3878-86.

CROTTS, G. & PARK, T. G. 1998. Protein delivery from poly(lactic-co-glycolic acid) biodegradable microspheres: release kinetics and stability issues. *J Microencapsul,* 15**,** 699-713.

CRUZ, L., SOARES, L. U., COSTA, T. D., MEZZALIRA, G., DA SILVEIRA, N. P., GUTERRES, S. S. & POHLMANN, A. R. 2006. Diffusion and mathematical modeling of release profiles from nanocarriers. *Int J Pharm,* 313**,** 198-205.

CUN, D., JENSEN, D. K., MALTESEN, M. J., BUNKER, M., WHITESIDE, P., SCURR, D., FOGED, C. & NIELSEN, H. M. 2011. High loading efficiency and sustained release of siRNA encapsulated in PLGA nanoparticles: quality by design optimization and characterization. *Eur J Pharm Biopharm,* 77**,** 26-35.

DAMS, E. T., LAVERMAN, P., OYEN, W. J., STORM, G., SCHERPHOF, G. L., VAN DER MEER, J. W., CORSTENS, F. H. & BOERMAN, O. C. 2000. Accelerated blood

clearance and altered biodistribution of repeated injections of sterically stabilized liposomes. *J Pharmacol Exp Ther,* 292**,** 1071-9.

DANHIER, F., ANSORENA, E., SILVA, J. M., COCO, R., LE BRETON, A. & PREAT, V. 2012. PLGA-based nanoparticles: an overview of biomedical applications. *J Control Release,* 161**,** 505-22.

DAVIS, M. E. 2002. Non-viral gene delivery systems. *Curr Opin Biotechnol,* 13**,** 128-31.

DEAN, D. A., DEAN, B. S., MULLER, S. & SMITH, L. C. 1999. Sequence requirements for plasmid nuclear import. *Exp Cell Res,* 253**,** 713-22.

DERAKHSHANKHAH, H. & JAFARI, S. 2018. Cell penetrating peptides: A concise review with emphasis on biomedical applications. *Biomed Pharmacother,* 108**,** 1090-1096.

DI NICOLA, M., CARLO-STELLA, C., MAGNI, M., MILANESI, M., LONGONI, P. D., MATTEUCCI, P., GRISANTI, S. & GIANNI, A. M. 2002. Human bone marrow stromal cells suppress T-lymphocyte proliferation induced by cellular or nonspecific mitogenic stimuli. *Blood,* 99**,** 3838-43.

DIGIROLAMO, C. M., STOKES, D., COLTER, D., PHINNEY, D. G., CLASS, R. & PROCKOP, D. J. 1999. Propagation and senescence of human marrow stromal cells in culture: a simple colony-forming assay identifies samples with the greatest potential to propagate and differentiate. *Br J Haematol,* 107**,** 275-81.

DIMITRIOU, R., JONES, E., MCGONAGLE, D. & GIANNOUDIS, P. V. 2011. Bone regeneration: current concepts and future directions. *BMC Med,* 9**,** 66.

DINARVAND, R., SEPEHRI, N., MANOOCHEHRI, S., ROUHANI, H. & ATYABI, F. 2011. Polylactide-co-glycolide nanoparticles for controlled delivery of anticancer agents. *Int J Nanomedicine,* 6**,** 877-95.

DING, D. C., CHOU, H. L., HUNG, W. T., LIU, H. W. & CHU, T. Y. 2013. Human adipose-derived stem cells cultured in keratinocyte serum free medium: Donor's age does not affect the proliferation and differentiation capacities. *J Biomed Sci,* 20**,** 59.

DIXON, J. E., OSMAN, G., MORRIS, G. E., MARKIDES, H., ROTHERHAM, M., BAYOUSSEF, Z., EL HAJ, A. J., DENNING, C. & SHAKESHEFF, K. M. 2016. Highly efficient delivery of functional cargoes by the synergistic effect of GAG binding motifs and cell-penetrating peptides. *Proc Natl Acad Sci U S A,* 113**,** E291-9.

DIZAJ, S. M., JAFARI, S. & KHOSROUSHAHI, A. Y. 2014. A sight on the current nanoparticle-based gene delivery vectors. *Nanoscale Res Lett,* 9**,** 252.

DOANE, T. & BURDA, C. 2013. Nanoparticle mediated non-covalent drug delivery. *Adv Drug Deliv Rev,* 65**,** 607-21.

DOMINICI, M., LE BLANC, K., MUELLER, I., SLAPER-CORTENBACH, I., MARINI, F., KRAUSE, D., DEANS, R., KEATING, A., PROCKOP, D. & HORWITZ, E. 2006. Minimal criteria for defining multipotent mesenchymal stromal cells. The International Society for Cellular Therapy position statement. *Cytotherapy,* 8**,** 315-7.

DORDELMANN, G., KOZLOVA, D., KARCZEWSKI, S., LIZIO, R., KNAUER, S. & EPPLE, M. 2014. Calcium phosphate increases the encapsulation efficiency of hydrophilic drugs (proteins, nucleic acids) into poly(d,l-lactide-co-glycolide acid) nanoparticles for intracellular delivery. *J Mater Chem B,* 2**,** 7250-7259.

DOW, S. W., FRADKIN, L. G., LIGGITT, D. H., WILLSON, A. P., HEATH, T. D. & POTTER, T. A. 1999. Lipid-DNA complexes induce potent activation of

innate immune responses and antitumor activity when administered intravenously. *J Immunol,* 163**,** 1552-61.

DRAGAN, A. I., CASAS-FINET, J. R., BISHOP, E. S., STROUSE, R. J., SCHENERMAN, M. A. & GEDDES, C. D. 2010. Characterization of PicoGreen interaction with dsDNA and the origin of its fluorescence enhancement upon binding. *Biophys J,* 99**,** 3010-9.

DRUELLE, C., DRULLION, C., DESLE, J., MARTIN, N., SAAS, L., CORMENIER, J., MALAQUIN, N., HUOT, L., SLOMIANNY, C., BOUALI, F., VERCAMER, C., HOT, D., POURTIER, A., CHEVET, E., ABBADIE, C. & PLUQUET, O. 2016. ATF6alpha regulates morphological changes associated with senescence in human fibroblasts. *Oncotarget,* 7**,** 67699-67715.

DURAN, M. C., WILLENBROCK, S., BARCHANSKI, A., MULLER, J. M., MAIOLINI, A., SOLLER, J. T., BARCIKOWSKI, S., NOLTE, I., FEIGE, K. & MURUA ESCOBAR, H. 2011. Comparison of nanoparticle-mediated transfection methods for DNA expression plasmids: efficiency and cytotoxicity. *J Nanobiotechnology,* 9**,** 47.

DURYMANOV, M. & REINEKE, J. 2018. Non-viral Delivery of Nucleic Acids: Insight Into Mechanisms of Overcoming Intracellular Barriers. *Front Pharmacol,* 9**,** 971.

EDWARDS, S. A. & WILLIAMS, D. R. 2004. Double layers and interparticle forces in colloid science and biology: analytic results for the effect of ionic dispersion forces. *Phys Rev Lett,* 92**,** 248303.

EGGENHOFER, E., LUK, F., DAHLKE, M. H. & HOOGDUIJN, M. J. 2014. The life and fate of mesenchymal stem cells. *Front Immunol,* 5**,** 148.

EINHORN, T. A. 1998. The cell and molecular biology of fracture healing. *Clin Orthop Relat Res***,** S7-21.

ELOUAHABI, A. & RUYSSCHAERT, J. M. 2005. Formation and intracellular trafficking of lipoplexes and polyplexes. *Mol Ther,* 11**,** 336-47.

ELTAHER, H. M., YANG, J., SHAKESHEFF, K. M. & DIXON, J. E. 2016. Highly efficient intracellular transduction in three-dimensional gradients for programming cell fate. *Acta Biomater,* 41**,** 181-92.

ERICKSON, H. P. 2009. Size and shape of protein molecules at the nanometer level determined by sedimentation, gel filtration, and electron microscopy. *Biol Proced Online,* 11**,** 32-51.

ESTÉVEZ-TORRES, A. & BAIGL, D. 2011. DNA compaction: fundamentals and applications. *Soft Matter,* 7**,** 6746.

EU 2011. COMMISSION RECOMMENDATION of 18 October 2011 on the definition of nanomaterial. *Official Journal of the European Union,* (2011/696/EU).

EVANS, C. H. 2012. Gene delivery to bone. *Adv Drug Deliv Rev,* 64**,** 1331-40.

FARKHANI, S. M., VALIZADEH, A., KARAMI, H., MOHAMMADI, S., SOHRABI, N. & BADRZADEH, F. 2014. Cell penetrating peptides: efficient vectors for delivery of nanoparticles, nanocarriers, therapeutic and diagnostic molecules. *Peptides,* 57**,** 78-94.

FATHI-ACHACHELOUEI, M., KNOPF-MARQUES, H., RIBEIRO DA SILVA, C. E., BARTHES, J., BAT, E., TEZCANER, A. & VRANA, N. E. 2019. Use of Nanoparticles in Tissue Engineering and Regenerative Medicine. *Front Bioeng Biotechnol,* 7**,** 113.

FECZKÓ, T., TOTH, J., DÓSA, G. & GYENIS, J. 2011. Influence of process conditions on the mean size of PLGA nanoparticles. *Chemical Engineering and Processing* 50**,** 50.

FERENCIK, M., LACKO, I. & DEVINSKY, F. 1990. Amine Oxides and Quaternary Ammonium-Salts .34.35. Immunomodulatory Activity of Some Amphiphilic Compounds. *Pharmazie,* 45**,** 695-696.

FESSI, H., PUISIEUX, F., DEVISSAGUET, J., AMMOURY, N. & BENITA, S. 1989a. Nanocapsule formation by interfacial polymer deposition following solvent displacement. *International Journal of Pharmaceutics,* 55**,** R1–R4.

FESSI, H., PUISIEUX, F., DEVISSAGUET, J. P., AMMOURY, N. & BENITA, S. 1989b. Nanocapsule formation by interfacial polymer deposition following solvent displacement. *International Journal of Pharmaceutics,* 55**,** R1-R4.

FEYNMAN, R. P. 1960. There's plenty of room at the bottom. An invitation to enter a new field of physics. *Engineering and Science (Caltech),* 23**,** 22-36.

FIHURKA, O., SANCHEZ-RAMOS, J. & SAVA, V. 2018. Optimizing Nanoparticle Design for Gene Therapy: Protection of Oligonucleotides from Degradation Without Impeding Release of Cargo. *Nanomed Nanosci Res,* 2.

FILION, M. C. & PHILLIPS, N. C. 1997. Toxicity and immunomodulatory activity of liposomal vectors formulated with cationic lipids toward immune effector cells. *Biochimica Et Biophysica Acta-Biomembranes,* 1329**,** 345-356.

FISHER, K. D., ULBRICH, K., SUBR, V., WARD, C. M., MAUTNER, V., BLAKEY, D. & SEYMOUR, L. W. 2000. A versatile system for receptor-mediated gene delivery permits increased entry of DNA into target cells, enhanced delivery to the nucleus and elevated rates of transgene expression. *Gene Ther,* 7**,** 1337-43.

FOROOZANDEH, P. & AZIZ, A. A. 2018. Insight into Cellular Uptake and Intracellular Trafficking of Nanoparticles. *Nanoscale Res Lett,* 13**,** 339.

FORREST, M. L. & PACK, D. W. 2002. On the kinetics of polyplex endocytic trafficking: implications for gene delivery vector design. *Mol Ther,* 6**,** 57-66.

FRANCESCHI, R. T., YANG, S., RUTHERFORD, R. B., KREBSBACH, P. H., ZHAO, M. & WANG, D. 2004. Gene therapy approaches for bone regeneration. *Cells Tissues Organs,* 176**,** 95-108.

FREITAS, S., MERKLE, H. P. & GANDER, B. 2005. Microencapsulation by solvent extraction/evaporation: reviewing the state of the art of microsphere preparation process technology. *J Control Release,* 102**,** 313-32.

FRIEDENSTEIN, A. J., CHAILAKHYAN, R. K. & GERASIMOV, U. V. 1987. Bone marrow osteogenic stem cells: in vitro cultivation and transplantation in diffusion chambers. *Cell Tissue Kinet,* 20**,** 263-72.

FRIEDLAENDER, G. E. 2004. Osteogenic protein-1 in treatment of tibial nonunions: current status. *Surg Technol Int,* 13**,** 249-52.

FU, C., YANG, X., TAN, S. & SONG, L. 2017. Enhancing Cell Proliferation and Osteogenic Differentiation of MC3T3-E1 Pre-osteoblasts by BMP-2 Delivery in Graphene Oxide-Incorporated PLGA/HA Biodegradable Microcarriers. *Sci Rep,* 7**,** 12549.

FURUKAWA, S., KUWAJIMA, Y., CHOSA, N., SATOH, K., OHTSUKA, M., MIURA, H., KIMURA, M., INOKO, H., ISHISAKI, A., FUJIMURA, A. & MIURA, H. 2015. Establishment of immortalized mesenchymal stem cells derived from the submandibular glands of tdTomato transgenic mice. *Exp Ther Med,* 10**,** 1380-1386.

GALARZA TORRE, A., SHAW, J. E., WOOD, A., GILBERT, H. T. J., DOBRE, O., GENEVER, P., BRENNAN, K., RICHARDSON, S. M. & SWIFT, J. 2018. An immortalised mesenchymal stem cell line maintains mechano-responsive

behaviour and can be used as a reporter of substrate stiffness. *Sci Rep,* 8**,** 8981.

GALLAGHER, J. T., LYON, M. & STEWARD, W. P. 1986. Structure and function of heparan sulphate proteoglycans. *Biochem J,* 236**,** 313-25.

GAO, X. & HUANG, L. 1996. Potentiation of cationic liposome-mediated gene delivery by polycations. *Biochemistry,* 35**,** 1027-36.

GASCÓN, A., R.,, POZO-RODRÍGUEZ, A. & SOLINÍS, M., A. 2013. Non-Viral Delivery Systems in Gene Therapy. *Gene Therapy - Tools and Potential Applications, Francisco Martin Molina, IntechOpen.* Gene Therapy - Tools and Potential Applications, Francisco Martin Molina, IntechOpen.

GASMI, H., SIEPMANN, F., HAMOUDI, M. C., DANEDE, F., VERIN, J., WILLART, J. F. & SIEPMANN, J. 2016. Towards a better understanding of the different release phases from PLGA microparticles: Dexamethasone-loaded systems. *Int J Pharm,* 514**,** 189-199.

GEBREKIDAN, S., WOO, B. H. & DELUCA, P. P. 2000. Formulation and in vitro transfection efficiency of poly (D, L-lactide-co-glycolide) microspheres containing plasmid DNA for gene delivery. *AAPS PharmSciTech,* 1**,** E28.

GEHR, P. 2018. Interaction of nanoparticles with biological systems. *Colloids Surf B Biointerfaces,* 172**,** 395-399.

GHALI, O., BROUX, O., FALGAYRAC, G., HAREN, N., VAN LEEUWEN, J. P., PENEL, G., HARDOUIN, P. & CHAUVEAU, C. 2015. Dexamethasone in osteogenic medium strongly induces adipocyte differentiation of mouse bone marrow stromal cells and increases osteoblast differentiation. *BMC Cell Biol,* 16**,** 9.

GIRDLESTONE, J. 2016. Mesenchymal stromal cells with enhanced therapeutic properties. *Immunotherapy,* 8**,** 1405-1416.

GLOVER, D. J., LEYTON, D. L., MOSELEY, G. W. & JANS, D. A. 2010. The efficiency of nuclear plasmid DNA delivery is a critical determinant of transgene expression at the single cell level. *J Gene Med,* 12**,** 77-85.

GOMES DOS REIS, L., LEE, W. H., SVOLOS, M., MOIR, L. M., JABER, R., WINDHAB, N., YOUNG, P. M. & TRAINI, D. 2019. Nanotoxicologic Effects of PLGA Nanoparticles Formulated with a Cell-Penetrating Peptide: Searching for a Safe pDNA Delivery System for the Lungs. *Pharmaceutics,* 11.

GONZALEZ-FERNANDEZ, T., SATHY, B. N., HOBBS, C., CUNNIFFE, G. M., MCCARTHY, H. O., DUNNE, N. J., NICOLOSI, V., O'BRIEN, F. J. & KELLY, D. J. 2017. Mesenchymal stem cell fate following non-viral gene transfection strongly depends on the choice of delivery vector. *Acta Biomater,* 55**,** 226-238.

GOODMAN, C. M., MCCUSKER, C. D., YILMAZ, T. & ROTELLO, V. M. 2004. Toxicity of gold nanoparticles functionalized with cationic and anionic side chains. *Bioconjug Chem,* 15**,** 897-900.

GOSWAMI, R., SUBRAMANIAN, G., SILAYEVA, L., NEWKIRK, I., DOCTOR, D., CHAWLA, K., CHATTOPADHYAY, S., CHANDRA, D., CHILUKURI, N. & BETAPUDI, V. 2019. Gene Therapy Leaves a Vicious Cycle. *Front Oncol,* 9**,** 297.

GOTTFRIED, L., F., & DEAN, D., A. 2012. Extracellular and Intracellular Barriers to Non-Viral Gene Transfer. IntechOpen.

GOVENDER, T., STOLNIK, S., GARNETT, M. C., ILLUM, L. & DAVIS, S. S. 1999. PLGA nanoparticles prepared by nanoprecipitation: drug loading and release studies of a water soluble drug. *J Control Release,* 57**,** 171-85.

GRABOWSKA, M., GRZESKOWIAK, B. F., SZUTKOWSKI, K., WAWRZYNIAK, D., GLODOWICZ, P., BARCISZEWSKI, J., JURGA, S., ROLLE, K. & MROWCZYNSKI, R. 2019. Nano-mediated delivery of double-stranded RNA for gene therapy of glioblastoma multiforme. *PLoS One,* 14**,** e0213852.

GRANT, S. R., PAGE, C. M., DIAZ, I., BUSH, S., BISTA, T., TURNER, L. M. & WALKER, G. V. 2018. The great esophageal escape: A case of extreme esophageal interfraction motion during neoadjuvant chemoradiation therapy. *Pract Radiat Oncol,* 8**,** e251-e254.

GREB-MARKIEWICZ, B., ZAREBSKI, M. & OZYHAR, A. 2018. Multiple sequences orchestrate subcellular trafficking of neuronal PAS domain-containing protein 4 (NPAS4). *J Biol Chem,* 293**,** 11255-11270.

GREGORY, C. A., GUNN, W. G., PEISTER, A. & PROCKOP, D. J. 2004. An Alizarin red-based assay of mineralization by adherent cells in culture: comparison with cetylpyridinium chloride extraction. *Anal Biochem,* 329**,** 77-84.

GRIESENBACH, U. & ALTON, E. W. 2012. Progress in gene and cell therapy for cystic fibrosis lung disease. *Curr Pharm Des,* 18**,** 642-62.

GRIGSBY, C. L. & LEONG, K. W. 2010. Balancing protection and release of DNA: tools to address a bottleneck of non-viral gene delivery. *J R Soc Interface,* 7 Suppl 1**,** S67-82.

GULDBERG, R. E., OEST, M. E., DUPONT, K., PEISTER, A., DEUTSCH, E., KOLAMBKAR, Y. & MOONEY, D. 2007. Biologic augmentation of polymer scaffolds for bone repair. *J Musculoskelet Neuronal Interact,* 7**,** 333-4.

GUTERRES, S. S., ALVES, M. P. & POHLMANN, A. R. 2007. Polymeric nanoparticles, nanospheres and nanocapsules, for cutaneous applications. *Drug Target Insights,* 2**,** 147-57.

HABAULT, J. & POYET, J. L. 2019. Recent Advances in Cell Penetrating Peptide-Based Anticancer Therapies. *Molecules,* 24.

HACOBIAN, A. & HERCHER, D. 2018. Pushing the Right Buttons: Improving Efficacy of Therapeutic DNA Vectors. *Tissue Eng Part B Rev,* 24**,** 226-239.

HAHN, P. & SCANLAN, E. 2010. Gene delivery into mammalian cells: an overview on existing approaches employed in vitro and in vivo. *Top Curr Chem. 2010;,* 296**,** 1-13.

HALL, A., LACHELT, U., BARTEK, J., WAGNER, E. & MOGHIMI, S. M. 2017. Polyplex Evolution: Understanding Biology, Optimizing Performance. *Mol Ther,* 25**,** 1476-1490.

HAMIDOUCHE, Z., FROMIGUE, O., RINGE, J., HAUPL, T., VAUDIN, P., PAGES, J. C., SROUJI, S., LIVNE, E. & MARIE, P. J. 2009. Priming integrin alpha5 promotes human mesenchymal stromal cell osteoblast differentiation and osteogenesis. *Proc Natl Acad Sci U S A,* 106**,** 18587-91.

HAN, S., MAHATO, R. I., SUNG, Y. K. & KIM, S. W. 2000. Development of biomaterials for gene therapy. *Mol Ther,* 2**,** 302-17.

HARDEE, C. L., AREVALO-SOLIZ, L. M., HORNSTEIN, B. D. & ZECHIEDRICH, L. 2017. Advances in Non-Viral DNA Vectors for Gene Therapy. *Genes (Basel),* 8.

HARRIS, S. E., GUO, D., HARRIS, M. A., KRISHNASWAMY, A. & LICHTLER, A. 2003. Transcriptional regulation of BMP-2 activated genes in osteoblasts using gene expression microarray analysis: role of Dlx2 and Dlx5 transcription factors. *Front Biosci,* 8**,** s1249-65.

HARRISON, R. L., BYRNE, B. J. & TUNG, L. 1998. Electroporation-mediated gene transfer in cardiac tissue. *FEBS Lett,* 435**,** 1-5.

HASAN, A., MORSHED, M., MEMIC, A., HASSAN, S., WEBSTER, T. J. & MAREI, H. E. 2018. Nanoparticles in tissue engineering: applications, challenges and prospects. *Int J Nanomedicine,* 13**,** 5637-5655.

HASS, R., KASPER, C., BOHM, S. & JACOBS, R. 2011. Different populations and sources of human mesenchymal stem cells (MSC): A comparison of adult and neonatal tissue-derived MSC. *Cell Commun Signal,* 9**,** 12.

HATA, R. & SENOO, H. 1989. L-ascorbic acid 2-phosphate stimulates collagen accumulation, cell proliferation, and formation of a three-dimensional tissuelike substance by skin fibroblasts. *J Cell Physiol,* 138**,** 8-16.

HE, Q., LIU, J., SUN, X. & ZHANG, Z. R. 2004. Preparation and characteristics of DNA-nanoparticles targeting to hepatocarcinoma cells. *World J Gastroenterol,* 10**,** 660-3.

HEINONEN, K., RAO, P. N., SLACK, J. L., CRUZ, J., BLOOMFIELD, C. D. & MROZEK, K. 1996. Isochromosome 12p in two cases of acute myeloid leukaemia without evidence of germ cell tumour. *Br J Haematol,* 93**,** 677-80.

HERBERTS, C. A., KWA, M. S. & HERMSEN, H. P. 2011. Risk factors in the development of stem cell therapy. *J Transl Med,* 9**,** 29.

HEWLETT, L. J., PRESCOTT, A. R. & WATTS, C. 1994. The coated pit and macropinocytic pathways serve distinct endosome populations. *J Cell Biol,* 124**,** 689-703.

HIGASHIYAMA, S., ABRAHAM, J. A. & KLAGSBRUN, M. 1993. Heparin-binding EGF-like growth factor stimulation of smooth muscle cell migration: dependence on interactions with cell surface heparan sulfate. *J Cell Biol,* 122**,** 933-40.

HILLAIREAU, H. & COUVREUR, P. 2009. Nanocarriers' entry into the cell: relevance to drug delivery. *Cell Mol Life Sci,* 66**,** 2873-96.

HIROSUE, S., MULLER, B. G., MULLIGAN, R. C. & LANGER, R. 2001. Plasmid DNA encapsulation and release from solvent diffusion nanospheres. *J Control Release,* 70**,** 231-42.

HISHIKAWA, K., MIURA, S., MARUMO, T., YOSHIOKA, H., MORI, Y., TAKATO, T. & FUJITA, T. 2004. *Gene expression profile of human mesenchymal stem cells during osteogenesis in three-dimensional thermoreversible gelation polymer*.

HOFLAND, H. E., SHEPHARD, L. & SULLIVAN, S. M. 1996. Formation of stable cationic lipid/DNA complexes for gene transfer. *Proc Natl Acad Sci U S A,* 93**,** 7305-9.

HONG, D., CHEN, H., XUE, Y. & LI, D. 2009a. Osteoblastogenic effects of dexamethasone through upregulation of TAZ expression in rat mesenchymal stem cells. *Seroid biochemistry and molecular biology* 116**,** 86-92.

HONG, D., CHEN, H. X., XUE, Y., LI, D. M., WAN, X. C., GE, R. & LI, J. C. 2009b. Osteoblastogenic effects of dexamethasone through upregulation of TAZ expression in rat mesenchymal stem cells. *J Steroid Biochem Mol Biol,* 116**,** 86-92.

HORNIG, S., HEINZE, T., BECERBC, C., R. & SCHUBERT, U., S 2009. Synthetic polymeric nanoparticles by nanoprecipitation. *Journal of Materials Chemistry,* 19**,** 3838-3840.

HOUK, B. E., HOCHHAUS, G. & HUGHES, J. A. 1999. Kinetic modeling of plasmid DNA degradation in rat plasma. *AAPS PharmSci,* 1**,** E9.

HOUK, B. E., MARTIN, R., HOCHHAUS, G. & HUGHES, J. A. 2001. Pharmacokinetics of plasmid DNA in the rat. *Pharm Res,* 18**,** 67-74.

HU, J., ZHU, M., LIU, K., FAN, H., ZHAO, W., MAO, Y. & ZHANG, Y. 2016. A Biodegradable Polyethylenimine-Based Vector Modified by Trifunctional Peptide R18 for Enhancing Gene Transfection Efficiency In Vivo. *PLoS One,* 11**,** e0166673.

HU, L., MAO, Z. & GAO, C. 2009. Colloidal particles for cellular uptake and delivery. *Journal of Materials Chemistry,* 19**,** 3108–3115.

HUANG, W. & ZHANG, C. 2018. Tuning the size of poly(lactic-co-glycolic acid) (PLGA) nanoparticles fabricated by nanoprecipitation. *Biotechnology journal,* 13.

HUTH, S., HOFFMANN, F., VON GERSDORFF, K., LANER, A., REINHARDT, D., ROSENECKER, J. & RUDOLPH, C. 2006. Interaction of polyamine gene vectors with RNA leads to the dissociation of plasmid DNA-carrier complexes. *J Gene Med,* 8**,** 1416-24.

INODA, H., YAMAMOTO, G. & HATTORI, T. 2004. Histological investigation of osteoinductive properties of rh-BMP2 in a rat calvarial bone defect model. *J Craniomaxillofac Surg,* 32**,** 365-9.

INTRA, J. & SALEM, A. K. 2010. Fabrication, characterization and in vitro evaluation of poly(D,L-lactide-co-glycolide) microparticles loaded with polyamidoamine-plasmid DNA dendriplexes for applications in nonviral gene delivery. *J Pharm Sci,* 99**,** 368-84.

IQBAL, M., ZAFAR, N., FESSI, H. & ELAISSARI, A. 2015. Double emulsion solvent evaporation techniques used for drug encapsulation. *Int J Pharm,* 496**,** 173-90.

JAISWAL, N., HAYNESWORTH, S. E., CAPLAN, A. I. & BRUDER, S. P. 1997. Osteogenic differentiation of purified, culture-expanded human mesenchymal stem cells in vitro. *J Cell Biochem,* 64**,** 295-312.

JAMES, A. W., LACHAUD, G., SHEN, J., ASATRIAN, G., NGUYEN, V., ZHANG, X., TING, K. & SOO, C. 2016. A Review of the Clinical Side Effects of Bone Morphogenetic Protein-2. *Tissue Eng Part B Rev,* 22**,** 284-97.

JAROCHA, D., LUKASIEWICZ, E. & MAJKA, M. 2008. Adventage of mesenchymal stem cells (MSC) expansion directly from purified bone marrow CD105+ and CD271+ cells. *Folia Histochem Cytobiol,* 46**,** 307-14.

JEONG, C., YOO, J., LEE, D. & KIM, Y. C. 2016. A branched TAT cell-penetrating peptide as a novel delivery carrier for the efficient gene transfection. *Biomater Res,* 20**,** 28.

JEONG, J. H. & PARK, T. G. 2002. Poly(L-lysine)-g-poly(D,L-lactic-co-glycolic acid) micelles for low cytotoxic biodegradable gene delivery carriers. *J Control Release,* 82**,** 159-66.

JIANG, T., XU, G., WANG, Q., YANG, L., ZHENG, L., ZHAO, J. & ZHANG, X. 2019. Correction: In vitro expansion impaired the stemness of early passage mesenchymal stem cells for treatment of cartilage defects. *Cell Death Dis,* 10**,** 716.

JIN, L., ZENG, X., LIU, M., DENG, Y. & HE, N. 2014. Current progress in gene delivery technology based on chemical methods and nano-carriers. *Theranostics,* 4**,** 240-55.

JOHNSON, E. E., URIST, M. R. & FINERMAN, G. A. 1992. Resistant nonunions and partial or complete segmental defects of long bones. Treatment with implants of a composite of human bone morphogenetic protein (BMP) and autolyzed, antigen-extracted, allogeneic (AAA) bone. *Clin Orthop Relat Res***,** 229-37.

JOHNSON, L. K. & LONGENECKER, J. P. 1982. Senescence of aortic endothelial cells in vitro: influence of culture conditions and preliminary characterization of the senescent phenotype. *Mech Ageing Dev,* 18**,** 1-18.

JONES, C. H., CHEN, C. K., RAVIKRISHNAN, A., RANE, S. & PFEIFER, B. A. 2013. Overcoming nonviral gene delivery barriers: perspective and future. *Mol Pharm,* 10**,** 4082-98.

JONES, D. H., CORRIS, S., MCDONALD, S., CLEGG, J. C. & FARRAR, G. H. 1997. Poly(DL-lactide-co-glycolide)-encapsulated plasmid DNA elicits systemic and mucosal antibody responses to encoded protein after oral administration. *Vaccine,* 15**,** 814-7.

JUNG, S. H., LEE, H. C., YU, D. M., KIM, B. C., PARK, S. M., LEE, Y. S., PARK, H. J., KO, Y. G. & LEE, J. S. 2016. Heparan sulfation is essential for the prevention of cellular senescence. *Cell Death Differ,* 23**,** 417-29.

KADLECOVA, Z., BALDI, L., HACKER, D., WURM, F. M. & KLOK, H. A. 2012. Comparative study on the in vitro cytotoxicity of linear, dendritic, and hyperbranched polylysine analogues. *Biomacromolecules,* 13**,** 3127-37.

KADLECOVA, Z., RAJENDRA, Y., MATASCI, M., BALDI, L., HACKER, D. L., WURM, F. M. & KLOK, H. A. 2013. DNA delivery with hyperbranched polylysine: a comparative study with linear and dendritic polylysine. *J Control Release,* 169**,** 276-88.

KAKRAN, M. & ANTIPINA, M. N. 2014. Emulsion-based techniques for encapsulation in biomedicine, food and personal care. *Curr Opin Pharmacol,* 18**,** 47-55.

KANG, H. C., SAMSONOVA, O., KANG, S. W. & BAE, Y. H. 2012. The effect of environmental pH on polymeric transfection efficiency. *Biomaterials,* 33**,** 1651-62.

KATZ, M. G., FARGNOLI, A. S., WILLIAMS, R. D. & BRIDGES, C. R. 2013. Gene therapy delivery systems for enhancing viral and nonviral vectors for cardiac diseases: current concepts and future applications. *Hum Gene Ther,* 24**,** 914-27.

KAY, M. A., GLORIOSO, J. C. & NALDINI, L. 2001. Viral vectors for gene therapy: the art of turning infectious agents into vehicles of therapeutics. *Nat Med,* 7**,** 33-40.

KELES, E., SONG, Y., DU, D., DONG, W. J. & LIN, Y. 2016. Recent progress in nanomaterials for gene delivery applications. *Biomater Sci,* 4**,** 1291-309.

KEUM, C. G., NOH, Y. W., BAEK, J. S., LIM, J. H., HWANG, C. J., NA, Y. G., SHIN, S. C. & CHO, C. W. 2011. Practical preparation procedures for docetaxel-loaded nanoparticles using polylactic acid-co-glycolic acid. *Int J Nanomedicine,* 6**,** 2225-34.

KHALIL, I. A., KOGURE, K., AKITA, H. & HARASHIMA, H. 2006. Uptake pathways and subsequent intracellular trafficking in nonviral gene delivery. *Pharmacol Rev,* 58**,** 32-45.

KICHLER, A., LEBORGNE, C., COEYTAUX, E. & DANOS, O. 2001. Polyethylenimine-mediated gene delivery: a mechanistic study. *J Gene Med,* 3**,** 135-44.

KIM, H. J. & PARK, J. S. 2017. Usage of Human Mesenchymal Stem Cells in Cell-based Therapy: Advantages and Disadvantages. *Dev Reprod,* 21**,** 1-10.

KIM, I. S., LEE, S. K., PARK, Y. M., LEE, Y. B., SHIN, S. C., LEE, K. C. & OH, I. J. 2005. Physicochemical characterization of poly(L-lactic acid) and poly(D,L-lactide-co-glycolide) nanoparticles with polyethylenimine as gene delivery carrier. *Int J Pharm,* 298**,** 255-62.

KIM, J. H., PARK, J. S., YANG, H. N., WOO, D. G., JEON, S. Y., DO, H. J., LIM, H. Y., KIM, J. M. & PARK, K. H. 2011. The use of biodegradable PLGA nanoparticles to mediate SOX9 gene delivery in human mesenchymal stem cells (hMSCs) and induce chondrogenesis. *Biomaterials,* 32**,** 268-78.

KIM, K. T., LEE, J. Y., KIM, D. D., YOON, I. S. & CHO, H. J. 2019. Recent Progress in the Development of Poly(lactic-co-glycolic acid)-Based Nanostructures for Cancer Imaging and Therapy. *Pharmaceutics,* 11.

KIM, T. K. & EBERWINE, J. H. 2010. Mammalian cell transfection: the present and the future. *Anal Bioanal Chem,* 397**,** 3173-8.

KLINGEMANN, H., MATZILEVICH, D. & MARCHAND, J. 2008. Mesenchymal Stem Cells - Sources and Clinical Applications. *Transfus Med Hemother,* 35**,** 272-277.

KOFRON, M. D. & LAURENCIN, C. T. 2006. Bone tissue engineering by gene delivery. *Adv Drug Deliv Rev,* 58**,** 555-76.

KOLAMBKAR, Y. M., DUPONT, K. M., BOERCKEL, J. D., HUEBSCH, N., MOONEY, D. J., HUTMACHER, D. W. & GULDBERG, R. E. 2011. An alginate-based hybrid system for growth factor delivery in the functional repair of large bone defects. *Biomaterials,* 32**,** 65-74.

KOLTOVER, I., SALDITT, T., RADLER, J. O. & SAFINYA, C. R. 1998. An inverted hexagonal phase of cationic liposome-DNA complexes related to DNA release and delivery. *Science,* 281**,** 78-81.

KOMMAREDDY, S. & AMIJI, M. 2005. Preparation and evaluation of thiol-modified gelatin nanoparticles for intracellular DNA delivery in response to glutathione. *Bioconjug Chem,* 16**,** 1423-32.

KOPP, M., KOLLENDA, S. & EPPLE, M. 2017. Nanoparticle-Protein Interactions: Therapeutic Approaches and Supramolecular Chemistry. *Acc Chem Res,* 50**,** 1383-1390.

KOREN, E., APTE, A., SAWANT, R. R., GRUNWALD, J. & TORCHILIN, V. P. 2011. Cell-penetrating TAT peptide in drug delivery systems: proteolytic stability requirements. *Drug Deliv,* 18**,** 377-84.

KOU, L., SUN, J., ZHAI, Y. & HEA, Z. 2013. The endocytosis and intracellular fate of nanomedicines: Implication for rational design. *Asian Journal of Pharmaceutical Sciences,* 8**,** 1-10.

KOYNOVA, R., TARAHOVSKY, Y. S., WANG, L. & MACDONALD, R. C. 2007. Lipoplex formulation of superior efficacy exhibits high surface activity and fusogenicity, and readily releases DNA. *Biochim Biophys Acta,* 1768**,** 375-86.

KREBSBACH, P. H., GU, K., FRANCESCHI, R. T. & RUTHERFORD, R. B. 2000. Gene therapy-directed osteogenesis: BMP-7-transduced human fibroblasts form bone in vivo. *Hum Gene Ther,* 11**,** 1201-10.

KREISS, P., CAMERON, B., RANGARA, R., MAILHE, P., AGUERRE-CHARRIOL, O., AIRIAU, M., SCHERMAN, D., CROUZET, J. & PITARD, B. 1999. Plasmid DNA size does not affect the physicochemical properties of lipoplexes but modulates gene transfer efficiency. *Nucleic Acids Res,* 27**,** 3792-8.

KRIEGEL, C. & AMIJI, M. 2011. Oral TNF-alpha gene silencing using a polymeric microsphere-based delivery system for the treatment of inflammatory bowel disease. *J Control Release,* 150**,** 77-86.

KRUKEMEYER, M. G., KRENN, V., HUEBNER, F., WAGNER, W. & RESCH, R. 2015. History and Possible Uses of Nanomedicine Based on Nanoparticles and Nanotechnological Progress. *Journal of Nanomedicine & Nanotechnology,* 6.

LACHELT, U. & WAGNER, E. 2015. Nucleic Acid Therapeutics Using Polyplexes: A Journey of 50 Years (and Beyond). *Chem Rev,* 115**,** 11043-78.

LAEMMLI, U. K. 1975. Characterization of DNA condensates induced by poly(ethylene oxide) and polylysine. *Proc Natl Acad Sci U S A,* 72**,** 4288-92.

LANGENBACH, F. & HANDSCHEL, J. 2013. Effects of dexamethasone, ascorbic acid and beta-glycerophosphate on the osteogenic differentiation of stem cells in vitro. *Stem Cell Res Ther,* 4**,** 117.

LEBOY, P. S., BERESFORD, J. N., DEVLIN, C. & OWEN, M. E. 1991. Dexamethasone induction of osteoblast mRNAs in rat marrow stromal cell cultures. *J Cell Physiol,* 146**,** 370-8.

LECHARDEUR, D. & LUKACS, G. L. 2002. Intracellular barriers to non-viral gene transfer. *Curr Gene Ther,* 2**,** 183-94.

LECHARDEUR, D., SOHN, K. J., HAARDT, M., JOSHI, P. B., MONCK, M., GRAHAM, R. W., BEATTY, B., SQUIRE, J., O'BRODOVICH, H. & LUKACS, G. L. 1999. Metabolic instability of plasmid DNA in the cytosol: a potential barrier to gene transfer. *Gene Ther,* 6**,** 482-97.

LECHARDEUR, D., VERKMAN, A. S. & LUKACS, G. L. 2005. Intracellular routing of plasmid DNA during non-viral gene transfer. *Adv Drug Deliv Rev,* 57**,** 755-67.

LEE, J. S., LEE, M. O., MOON, B. H., SHIM, S. H., FORNACE, A. J., JR. & CHA, H. J. 2009. Senescent growth arrest in mesenchymal stem cells is bypassed by Wip1-mediated downregulation of intrinsic stress signaling pathways. *Stem Cells,* 27**,** 1963-75.

LEE, J. Y., CHOO, J. E., CHOI, Y. S., LEE, K. Y., MIN, D. S., PI, S. H., SEOL, Y. J., LEE, S. J., JO, I. H., CHUNG, C. P. & PARK, Y. J. 2007. Characterization of the surface immobilized synthetic heparin binding domain derived from human fibroblast growth factor-2 and its effect on osteoblast differentiation. *J Biomed Mater Res A,* 83**,** 970-9.

LEE, M., RENTZ, J., HAN, S. O., BULL, D. A. & KIM, S. W. 2003. Water-soluble lipopolymer as an efficient carrier for gene delivery to myocardium. *Gene Ther,* 10**,** 585-93.

LEE, S. H., LEE, J. B., BAE, M. S., BALIKOV, D. A., HWANG, A., BOIRE, T. C., KWON, I. K., SUNG, H. J. & YANG, J. W. 2015. Current progress in nanotechnology applications for diagnosis and treatment of kidney diseases. *Adv Healthc Mater,* 4**,** 2037-45.

LEE, S. J., KANG, S. W., DO, H. J., HAN, I., SHIN, D. A., KIM, J. H. & LEE, S. H. 2010. Enhancement of bone regeneration by gene delivery of BMP2/Runx2 bicistronic vector into adipose-derived stromal cells. *Biomaterials,* 31**,** 5652-9.

LEFEBVRE, F., PILET, P., BONZON, N., DACULSI, G. & RABAUD, M. 1996. New preparation and microstructure of the EndoPatch elastin-collagen containing glycosaminoglycans. *Biomaterials,* 17**,** 1813-8.

LEHTO, T., KURRIKOFF, K. & LANGEL, U. 2012. Cell-penetrating peptides for the delivery of nucleic acids. *Expert Opin Drug Deliv,* 9**,** 823-36.

LEITE, E. A., GRABE-GUIMARAES, A., GUIMARAES, H. N., MACHADO-COELHO, G. L., BARRATT, G. & MOSQUEIRA, V. C. 2007. Cardiotoxicity reduction induced by halofantrine entrapped in nanocapsule devices. *Life Sci,* 80**,** 1327-34.

LEVI, B., HYUN, J. S., MONTORO, D. T., LO, D. D., CHAN, C. K., HU, S., SUN, N., LEE, M., GROVA, M., CONNOLLY, A. J., WU, J. C., GURTNER, G. C., WEISSMAN, I. L., WAN, D. C. & LONGAKER, M. T. 2012. In vivo directed differentiation of

pluripotent stem cells for skeletal regeneration. *Proc Natl Acad Sci U S A,* 109**,** 20379-84.

LEWANDROWSKI, K. U., NANSON, C. & CALDERON, R. 2007. Vertebral osteolysis after posterior interbody lumbar fusion with recombinant human bone morphogenetic protein 2: a report of five cases. *Spine J,* 7**,** 609-14.

LI, W., NICOL, F. & SZOKA, F. C., JR. 2004. GALA: a designed synthetic pH-responsive amphipathic peptide with applications in drug and gene delivery. *Adv Drug Deliv Rev,* 56**,** 967-85.

LI, Y., WU, Q., WANG, Y., LI, L., BU, H. & BAO, J. 2017. Senescence of mesenchymal stem cells (Review). *Int J Mol Med,* 39**,** 775-782.

LIAN, J., STEWART, C., PUCHACZ, E., MACKOWIAK, S., SHALHOUB, V., COLLART, D., ZAMBETTI, G. & STEIN, G. 1989. Structure of the rat osteocalcin gene and regulation of vitamin D-dependent expression. *Proc Natl Acad Sci U S A,* 86**,** 1143-7.

LIEBERMAN, J. R., LE, L. Q., WU, L., FINERMAN, G. A., BERK, A., WITTE, O. N. & STEVENSON, S. 1998. Regional gene therapy with a BMP-2-producing murine stromal cell line induces heterotopic and orthotopic bone formation in rodents. *J Orthop Res,* 16**,** 330-9.

LIMA, A. C., ALVAREZ-LORENZO, C. & MANO, J. F. 2016. Design Advances in Particulate Systems for Biomedical Applications. *Adv Healthc Mater,* 5**,** 1687-723.

LIN, X. & PERRIMON, N. 2000. Role of heparan sulfate proteoglycans in cell-cell signaling in Drosophila. *Matrix Biol,* 19**,** 303-7.

LINARD, C., BRACHET, M., L'HOMME, B., STRUP-PERROT, C., BUSSON, E., BONNEAU, M., LATAILLADE, J. J., BEY, E. & BENDERITTER, M. 2018. Long-term effectiveness of local BM-MSCs for skeletal muscle regeneration: a proof of concept obtained on a pig model of severe radiation burn. *Stem Cell Res Ther,* 9**,** 299.

LIU, B. R., LIOU, J. S., CHEN, Y. J., HUANG, Y. W. & LEE, H. J. 2013a. Delivery of nucleic acids, proteins, and nanoparticles by arginine-rich cell-penetrating peptides in rotifers. *Mar Biotechnol (NY),* 15**,** 584-95.

LIU, B. R., LO, S. Y., LIU, C. C., CHYAN, C. L., HUANG, Y. W., ARONSTAM, R. S. & LEE, H. J. 2013b. Endocytic Trafficking of Nanoparticles Delivered by Cell-penetrating Peptides Comprised of Nona-arginine and a Penetration Accelerating Sequence. *PLoS One,* 8**,** e67100.

LIU, G., MOLAS, M., GROSSMANN, G. A., PASUMARTHY, M., PERALES, J. C., COOPER, M. J. & HANSON, R. W. 2001. Biological properties of poly-L-lysine-DNA complexes generated by cooperative binding of the polycation. *J Biol Chem,* 276**,** 34379-87.

LIU, M., TENG, C. P., WIN, K. Y., CHEN, Y., ZHANG, X., YANG, D. P., LI, Z. & YE, E. 2019. Polymeric Encapsulation of Turmeric Extract for Bioimaging and Antimicrobial Applications. *Macromol Rapid Commun,* 40**,** e1800216.

LIU, R., MA, G. H., WAN, Y. H. & SU, Z. G. 2005. Influence of process parameters on the size distribution of PLA microcapsules prepared by combining membrane emulsification technique and double emulsion-solvent evaporation method. *Colloids Surf B Biointerfaces,* 45**,** 144-53.

LIU, Y. K., UEMURA, T., NEMOTO, A., YABE, T., FUJII, N., USHIDA, T. & TATEISHI, T. 1997. Osteopontin involvement in integrin-mediated cell signaling and regulation of expression of alkaline phosphatase during early differentiation of UMR cells. *FEBS Lett,* 420**,** 112-6.

LOOZEN, L. D., VANDERSTEEN, A., KRAGTEN, A. H., ONER, F. C., DHERT, W. J., KRUYT, M. C. & ALBLAS, J. 2018. Bone formation by heterodimers through non-viral gene delivery of BMP-2/6 and BMP-2/7. *Eur Cell Mater,* 35**,** 195-208.

LOU, Y., JAVED, A., HUSSAIN, S., COLBY, J., FREDERICK, D., PRATAP, J., XIE, R., GAUR, T., VAN WIJNEN, A. J., JONES, S. N., STEIN, G. S., LIAN, J. B. & STEIN, J. L. 2009. A Runx2 threshold for the cleidocranial dysplasia phenotype. *Hum Mol Genet,* 18**,** 556-68.

LOU, Y. R., TOH, T. C., TEE, Y. H. & YU, H. 2017. 25-Hydroxyvitamin D3 induces osteogenic differentiation of human mesenchymal stem cells. *Sci Rep,* 7**,** 42816.

LU, J. M., WANG, X., MARIN-MULLER, C., WANG, H., LIN, P. H., YAO, Q. & CHEN, C. 2009. Current advances in research and clinical applications of PLGA-based nanotechnology. *Expert Rev Mol Diagn,* 9**,** 325-41.

LU, Y., WU, F., DUAN, W., MU, X., FANG, S., LU, N., ZHOU, X. & KONG, W. 2020. Engineering a "PEG-g-PEI/DNA nanoparticle-in- PLGA microsphere" hybrid controlled release system to enhance immunogenicity of DNA vaccine. *Mater Sci Eng C Mater Biol Appl,* 106**,** 110294.

LUAN, X. & BODMEIER, R. 2006. Modification of the tri-phasic drug release pattern of leuprolide acetate-loaded poly(lactide-co-glycolide) microparticles. *Eur J Pharm Biopharm,* 63**,** 205-14.

LUDTKE, J. J., SEBESTYEN, M. G. & WOLFF, J. A. 2002. The effect of cell division on the cellular dynamics of microinjected DNA and dextran. *Mol Ther,* 5**,** 579-88.

LUKASOVA, V., BUZGO, M., VOCETKOVA, K., KUBÍKOVÁ, T., TONAR, Z., DOUPNIK, M., BLAHNOVA, V., LITVINEC, A., SOVKOVA, V., VOLTROVÁ, B., STAFFA, A., SVORA, P., KRALICKOVA, M., AMLER, E., FILOVA, E., RUSTICHELLI, F. & RAMPICHOVA, M. 2018. Osteoinductive 3D scaffolds prepared by blend centrifugal spinning for long-term delivery of osteogenic supplements. *RSC Adv,* 8**,** 21889-21904.

LUO, D. & SALTZMAN, W. M. 2000. Synthetic DNA delivery systems. *Nat Biotechnol,* 18**,** 33-7.

LUQUE-ALCARAZ, A., G., LIZARDI-MENDOZA, J., GOYCOOLEA, F., M., HIGUERA-CIAPARAD, I. & ARGÜELLES-MONAL, W. 2016. Preparation of chitosan nanoparticles by nanoprecipitation and their ability as a drug nanocarrier. *RSC Adv,* 6**,** 59250-59256.

LUTZ, R., PARK, J., FELSZEGHY, E., WILTFANG, J., NKENKE, E. & SCHLEGEL, K. A. 2008. Bone regeneration after topical BMP-2-gene delivery in circumferential peri-implant bone defects. *Clin Oral Implants Res,* 19**,** 590-9.

LV, H. T., ZHANG, S. B., WANG, B., CUI, S. H. & YAN, J. 2006. Toxicity of cationic lipids and cationic polymers in gene delivery. *Journal of Controlled Release,* 114**,** 100-109.

MADAAN, K., KUMAR, S., POONIA, N., LATHER, V. & PANDITA, D. 2014. Dendrimers in drug delivery and targeting: Drug-dendrimer interactions and toxicity issues. *J Pharm Bioallied Sci,* 6**,** 139-50.

MADY, M., MOHAMMED, W., EL-GUENDY, N. M. & ELSAYED, A. 2011. Eeffect of the polymer molecular weight on the DNA/PEI polyplexes properties. *Rom J Biophys* 21**,** 151–165.

MAGADALA, P. & AMIJI, M. 2008. Epidermal growth factor receptor-targeted gelatin-based engineered nanocarriers for DNA delivery and transfection in human pancreatic cancer cells. *AAPS J,* 10**,** 565-76.

MAILANDER, V. & LANDFESTER, K. 2009. Interaction of nanoparticles with cells. *Biomacromolecules,* 10**,** 2379-400.

MAKADIA, H. K. & SIEGEL, S. J. 2011. Poly Lactic-co-Glycolic Acid (PLGA) as Biodegradable Controlled Drug Delivery Carrier. *Polymers (Basel),* 3**,** 1377-1397.

MANN, A., KHAN, M. A., SHUKLA, V. & GANGULI, M. 2007. Atomic force microscopy reveals the assembly of potential DNA "nanocarriers" by poly-L-ornithine. *Biophys Chem,* 129**,** 126-36.

MANN, A., RICHA, R. & GANGULI, M. 2008a. DNA condensation by poly-L-lysine at the single molecule level: role of DNA concentration and polymer length. *J Control Release,* 125**,** 252-62.

MANN, A., THAKUR, G., SHUKLA, V. & GANGULI, M. 2008b. Peptides in DNA delivery: current insights and future directions. *Drug Discov Today,* 13**,** 152-60.

MANN, A., THAKUR, G., SHUKLA, V., SINGH, A. K., KHANDURI, R., NAIK, R., JIANG, Y., KALRA, N., DWARAKANATH, B. S., LANGEL, U. & GANGULI, M. 2011. Differences in DNA condensation and release by lysine and arginine homopeptides govern their DNA delivery efficiencies. *Mol Pharm,* 8**,** 1729-41.

MANNISTO, M., VANDERKERKEN, S., TONCHEVA, V., ELOMAA, M., RUPONEN, M., SCHACHT, E. & URTTI, A. 2002. Structure-activity relationships of poly(L-lysines): effects of pegylation and molecular shape on physicochemical and biological properties in gene delivery. *J Control Release,* 83**,** 169-82.

MANOME, Y., NAKAMURA, M., OHNO, T. & FURUHATA, H. 2000. Ultrasound facilitates transduction of naked plasmid DNA into colon carcinoma cells in vitro and in vivo. *Hum Gene Ther,* 11**,** 1521-8.

MAO, A. S., SHIN, J. W. & MOONEY, D. J. 2016. Effects of substrate stiffness and cell-cell contact on mesenchymal stem cell differentiation. *Biomaterials,* 98**,** 184-91.

MARTINEZ RIVAS, C. J., TARHINI, M., BADRI, W., MILADI, K., GREIGE-GERGES, H., NAZARI, Q. A., GALINDO RODRIGUEZ, S. A., ROMAN, R. A., FESSI, H. & ELAISSARI, A. 2017. Nanoprecipitation process: From encapsulation to drug delivery. *Int J Pharm,* 532**,** 66-81.

MARTIS, E., BADVE, R. & DEGWEKAR, M. 2012. Nanotechnology based devices and applications in medicine: An overview. *Chronicles of Young Scientists,* 3**,** 68.

MASUDA-ROBENS, J. M., KUTNEY, S. N., QI, H. & CHOU, M. M. 2003. The TRE17 oncogene encodes a component of a novel effector pathway for Rho GTPases Cdc42 and Rac1 and stimulates actin remodeling. *Mol Cell Biol,* 23**,** 2151-61.

MCCULLOCH, C. A. & TENENBAUM, H. C. 1986. Dexamethasone induces proliferation and terminal differentiation of osteogenic cells in tissue culture. *Anat Rec,* 215**,** 397-402.

MCKEE, C. & CHAUDHRY, G. R. 2017. Advances and challenges in stem cell culture. *Colloids Surf B Biointerfaces,* 159**,** 62-77.

MEACHAM, J. M., DURVASULA, K., DEGERTEKIN, F. L. & FEDOROV, A. G. 2014. Physical methods for intracellular delivery: practical aspects from laboratory use to industrial-scale processing. *J Lab Autom,* 19**,** 1-18.

MELLMAN, I., FUCHS, R. & HELENIUS, A. 1986. Acidification of the endocytic and exocytic pathways. *Annu Rev Biochem,* 55**,** 663-700.

MELLOTT, A. J., FORREST, M. L. & DETAMORE, M. S. 2013. Physical non-viral gene delivery methods for tissue engineering. *Ann Biomed Eng,* 41**,** 446-68.

MENDES, S., C., TIBBLE, J., M., VEENHOF, M., BOTH, S., ONER, F., C., VAN BLITTERSWIJK, C. & DE BRUIJN, J., D. 2004. Relation between *in vivo* and *in vitro* osteogenic potentialof cultured human bone marrow stromal cells *Materilas Science: Materials in Medicine,* 15**,** 1123-1128.

MESIKA, A., KISS, V., BRUMFELD, V., GHOSH, G. & REICH, Z. 2005. Enhanced intracellular mobility and nuclear accumulation of DNA plasmids associated with a karyophilic protein. *Hum Gene Ther,* 16**,** 200-8.

MEYER, M. B., BENKUSKY, N. A., SEN, B., RUBIN, J. & PIKE, J. W. 2016. Epigenetic Plasticity Drives Adipogenic and Osteogenic Differentiation of Marrow-derived Mesenchymal Stem Cells. *J Biol Chem,* 291**,** 17829-47.

MIELE, E., SPINELLI, G. P., MIELE, E., DI FABRIZIO, E., FERRETTI, E., TOMAO, S. & GULINO, A. 2012. Nanoparticle-based delivery of small interfering RNA: challenges for cancer therapy. *Int J Nanomedicine,* 7**,** 3637-57.

MIKHONIN, A. V., MYSHAKINA, N. S., BYKOV, S. V. & ASHER, S. A. 2005. UV resonance Raman determination of polyproline II, extended 2.5(1)-helix, and beta-sheet Psi angle energy landscape in poly-L-lysine and poly-L-glutamic acid. *J Am Chem Soc,* 127**,** 7712-20.

MILLETTI, F. 2012. Cell-penetrating peptides: classes, origin, and current landscape. *Drug Discov Today,* 17**,** 850-60.

MILOSEVIC, M., STOJANOVIC, D., SIMIC, V., MILICEVIC, B., RADISAVLJEVIC, A., USKOKOVIC, P. & KOJIC, M. 2018. A Computational Model for Drug Release from PLGA Implant. *Materials (Basel),* 11.

MINAGAWA, K., MATSUZAWA, Y., YOSHIKAWA, K., MATSUMOTO, M. & DOI, M. 1991. Direct observation of the biphasic conformational change of DNA induced by cationic polymers. *FEBS Lett,* 295**,** 67-9.

MIR, M., AHMED, N. & REHMAN, A. U. 2017. Recent applications of PLGA based nanostructures in drug delivery. *Colloids Surf B Biointerfaces,* 159**,** 217-231.

MIRTIC, A. & GRDADOLNIK, J. 2013. The structure of poly-L-lysine in different solvents. *Biophys Chem,* 175-176**,** 47-53.

MISHRA, D., KANG, H. C. & BAE, Y. H. 2011. Reconstitutable charged polymeric (PLGA)(2)-b-PEI micelles for gene therapeutics delivery. *Biomaterials,* 32**,** 3845-54.

MISRA, R. & SAHOO, S. K. 2010. Intracellular trafficking of nuclear localization signal conjugated nanoparticles for cancer therapy. *Eur J Pharm Sci,* 39**,** 152-63.

MOGHIMI, S. M., SYMONDS, P., MURRAY, J. C., HUNTER, A. C., DEBSKA, G. & SZEWCZYK, A. 2005. A two-stage poly(ethylenimine)-mediated cytotoxicity: implications for gene transfer/therapy. *Mol Ther,* 11**,** 990-5.

MOK, H. & PARK, T. G. 2008. Direct plasmid DNA encapsulation within PLGA nanospheres by single oil-in-water emulsion method. *Eur J Pharm Biopharm,* 68**,** 105-11.

MOON, J. J., SUH, H., POLHEMUS, M. E., OCKENHOUSE, C. F., YADAVA, A. & IRVINE, D. J. 2012. Antigen-displaying lipid-enveloped PLGA nanoparticles as delivery agents for a Plasmodium vivax malaria vaccine. *PLoS One,* 7**,** e31472.

MOORE, T. L., RODRIGUEZ-LORENZO, L., HIRSCH, V., BALOG, S., URBAN, D., JUD, C., ROTHEN-RUTISHAUSER, B., LATTUADA, M. & PETRI-FINK, A. 2015. *Nanoparticle colloidal stability in cell culture media and impact on cellular interactions*.

MORA-HUERTAS, C. E., FESSI, H. & ELAISSARI, A. 2010. Polymer-based nanocapsules for drug delivery. *Int J Pharm,* 385**,** 113-42.

MORALES-CRUZ, M., FLORES-FERNANDEZ, G. M., MORALES-CRUZ, M., ORELLANO, E. A., RODRIGUEZ-MARTINEZ, J. A., RUIZ, M. & GRIEBENOW, K. 2012. Two-step nanoprecipitation for the production of protein-loaded PLGA nanospheres. *Results Pharma Sci,* 2**,** 79-85.

MORETTI, R. D. C., DUAILIBI, M. T., MARTINS, P. O., DOS SANTOS, J. A. & DUAILIBI, S. E. 2017. Osteoinductive effects of preoperative dexamethasone in human dental pulp stem cells primary culture. *Future Sci OA,* 3**,** FSO184.

MOSTAFA, N. Z., FITZSIMMONS, R., MAJOR, P. W., ADESIDA, A., JOMHA, N., JIANG, H. & ULUDAG, H. 2012. Osteogenic differentiation of human mesenchymal stem cells cultured with dexamethasone, vitamin D3, basic fibroblast growth factor, and bone morphogenetic protein-2. *Connect Tissue Res,* 53**,** 117-31.

MUMPER, R. J., DUGUID, J. G., ANWER, K., BARRON, M. K., NITTA, H. & ROLLAND, A. P. 1996. Polyvinyl derivatives as novel interactive polymers for controlled gene delivery to muscle. *Pharm Res,* 13**,** 701-9.

MUNDARGI, R. C., BABU, V. R., RANGASWAMY, V., PATEL, P. & AMINABHAVI, T. M. 2008. Nano/micro technologies for delivering macromolecular therapeutics using poly(D,L-lactide-co-glycolide) and its derivatives. *J Control Release,* 125**,** 193-209.

MUNDLOS, S., OTTO, F., MUNDLOS, C., MULLIKEN, J. B., AYLSWORTH, A. S., ALBRIGHT, S., LINDHOUT, D., COLE, W. G., HENN, W., KNOLL, J. H., OWEN, M. J., MERTELSMANN, R., ZABEL, B. U. & OLSEN, B. R. 1997. Mutations involving the transcription factor CBFA1 cause cleidocranial dysplasia. *Cell,* 89**,** 773-9.

MUNOZ, E. M. & LINHARDT, R. J. 2004. Heparin-binding domains in vascular biology. *Arterioscler Thromb Vasc Biol,* 24**,** 1549-57.

NAFEE, N., TAETZ, S., SCHNEIDER, M., SCHAEFER, U. F. & LEHR, C. M. 2007. Chitosan-coated PLGA nanoparticles for DNA/RNA delivery: Effect of the formulation parameters on complexation and transfection of antisense oligonucleotides. *Nanomedicine-Nanotechnology Biology and Medicine,* 3**,** 173-183.

NAJJAR, K., ERAZO-OLIVERAS, A., MOSIOR, J. W., WHITLOCK, M. J., ROSTANE, I., CINCLAIR, J. M. & PELLOIS, J. P. 2017. Unlocking Endosomal Entrapment with Supercharged Arginine-Rich Peptides. *Bioconjug Chem,* 28**,** 2932-2941.

NALDINI, L. 2015. Gene therapy returns to centre stage. *Nature,* 526**,** 351-60.

NAYEROSSADAT, N., MAEDEH, T. & ALI, P. A. 2012. Viral and nonviral delivery systems for gene delivery. *Adv Biomed Res,* 1**,** 27.

NAYVELT, I., THOMAS, T. & THOMAS, T. J. 2007. Mechanistic differences in DNA nanoparticle formation in the presence of oligolysines and poly-L-lysine. *Biomacromolecules,* 8**,** 477-84.

NEUMANN, A., CHRISTEL, A., KASPER, C. & BEHRENS, P. 2013. BMP2-loaded nanoporous silica nanoparticles promote osteogenic differentiation of human mesenchymal stem cells. *RSC Advances,* 3**,** 24222–24230.

NI, R., FENG, R. & CHAU, Y. 2019. Synthetic Approaches for Nucleic Acid Delivery: Choosing the Right Carriers. *Life (Basel),* 9.

NICHOLS, B. 2003. Caveosomes and endocytosis of lipid rafts. *J Cell Sci,* 116**,** 4707-14.

NIE, Y., ZHANG, Z. & DUAN, Y. 2008. Combined Use of Polycationic Peptide and Biodegradable Macromolecular Polymer as a Novel Gene Delivery System: A Preliminary Study. *Drug Delivery,* 13**,** 441–446.

NIIDOME, T., NAKASHIMA, K., TAKAHASHI, H. & NIIDOME, Y. 2004. Preparation of primary amine-modified gold nanoparticles and their transfection ability into cultivated cells. *Chem Commun (Camb)***,** 1978-9.

NIKALJE, A. P. 2015. Nanotechnology and its Applications in Medicine. *Medicinal Chemistry,* 5.

NIU, X., ZOU, W., LIU, C., ZHANG, N. & FU, C. 2009. Modified nanoprecipitation method to fabricate DNA-loaded PLGA nanoparticles. *Drug Dev Ind Pharm,* 35**,** 1375-83.

NIVEN, R., ZHANG, Y. & SMITH, J. 1997. Toward development of a non-viral gene therapeutic. *Adv Drug Deliv Rev,* 26**,** 135-150.

NOGUCHI, A., FURUNO, T., KAWAURA, C. & NAKANISHI, M. 1998. Membrane fusion plays an important role in gene transfection mediated by cationic liposomes. *FEBS Lett,* 433**,** 169-73.

NORONHA, N. C., MIZUKAMI, A., CALIARI-OLIVEIRA, C., COMINAL, J. G., ROCHA, J. L. M., COVAS, D. T., SWIECH, K. & MALMEGRIM, K. C. R. 2019. Priming approaches to improve the efficacy of mesenchymal stromal cell-based therapies. *Stem Cell Res Ther,* 10**,** 131.

OESS, S. & HILDT, E. 2000. Novel cell permeable motif derived from the PreS2-domain of hepatitis-B virus surface antigens. *Gene Ther,* 7**,** 750-8.

OKADA, H. & TOGUCHI, H. 1995. Biodegradable microspheres in drug delivery. *Crit Rev Ther Drug Carrier Syst,* 12**,** 1-99.

OSMAN, G., RODRIGUEZ, J., CHAN, S. Y., CHISHOLM, J., DUNCAN, G., KIM, N., TATLER, A. L., SHAKESHEFF, K. M., HANES, J., SUK, J. S. & DIXON, J. E. 2018. PEGylated enhanced cell penetrating peptide nanoparticles for lung gene therapy. *J Control Release,* 285**,** 35-45.

OSTER, C. G. & KISSEL, T. 2005. Comparative study of DNA encapsulation into PLGA microparticles using modified double emulsion methods and spray drying techniques. *J Microencapsul,* 22**,** 235-44.

OWEN, M. 1988. Marrow stromal stem cells. *J Cell Sci Suppl,* 10**,** 63-76.

PACK, D. W., HOFFMAN, A. S., PUN, S. & STAYTON, P. S. 2005. Design and development of polymers for gene delivery. *Nat Rev Drug Discov,* 4**,** 581-93.

PALAMA, I. E., CORTESE, B., D'AMONE, S. & GIGLI, G. 2015. mRNA delivery using non-viral PCL nanoparticles. *Biomater Sci,* 3**,** 144-51.

PARK, J., WRZESINSKI, S. H., STERN, E., LOOK, M., CRISCIONE, J., RAGHEB, R., JAY, S. M., DEMENTO, S. L., AGAWU, A., LICONA LIMON, P., FERRANDINO, A. F., GONZALEZ, D., HABERMANN, A., FLAVELL, R. A. & FAHMY, T. M. 2012. Combination delivery of TGF-beta inhibitor and IL-2 by nanoscale liposomal polymeric gels enhances tumour immunotherapy. *Nat Mater,* 11**,** 895-905.

PARK, J. S., SURENDRAN, S., KAMENDULIS, L. M. & MORRAL, N. 2011. Comparative nucleic acid transfection efficacy in primary hepatocytes for gene silencing and functional studies. *BMC Res Notes,* 4**,** 8.

PARK, S. Y., KIM, K. H., KIM, S., LEE, Y. M. & SEOL, Y. J. 2019. BMP-2 Gene Delivery-Based Bone Regeneration in Dentistry. *Pharmaceutics,* 11.

PARK, T. G. 1995. Degradation of poly(lactic-co-glycolic acid) microspheres: effect of copolymer composition. *Biomaterials,* 16**,** 1123-30.

PARTRIDGE, K. A. & OREFFO, R. O. 2004. Gene delivery in bone tissue engineering: progress and prospects using viral and nonviral strategies. *Tissue Eng,* 10**,** 295-307.

PATIL, Y. & PANYAM, J. 2009. Polymeric nanoparticles for siRNA delivery and gene silencing. *Int J Pharm,* 367**,** 195-203.

PCHELINTSEV, N. A., ADAMS, P. D. & NELSON, D. M. 2016. Critical Parameters for Efficient Sonication and Improved Chromatin Immunoprecipitation of High Molecular Weight Proteins. *PLoS One,* 11**,** e0148023.

PEARSE, B. M. 1976. Clathrin: a unique protein associated with intracellular transfer of membrane by coated vesicles. *Proc Natl Acad Sci U S A,* 73**,** 1255-9.

PELTONEN, L., AITTA, J., HYVONEN, S., KARJALAINEN, M. & HIRVONEN, J. 2004. Improved entrapment efficiency of hydrophilic drug substance during nanoprecipitation of poly(l)lactide nanoparticles. *AAPS PharmSciTech,* 5**,** E16.

PENG, H., WRIGHT, V., USAS, A., GEARHART, B., SHEN, H. C., CUMMINS, J. & HUARD, J. 2002. Synergistic enhancement of bone formation and healing by stem cell-expressed VEGF and bone morphogenetic protein-4. *J Clin Invest,* 110**,** 751-9.

PEREZ-MARTINEZ, F. C., GUERRA, J., POSADAS, I. & CENA, V. 2011. Barriers to non-viral vector-mediated gene delivery in the nervous system. *Pharm Res,* 28**,** 1843-58.

PEREZ, R. A., WON, J. E., KNOWLES, J. C. & KIM, H. W. 2013. Naturally and synthetic smart composite biomaterials for tissue regeneration. *Adv Drug Deliv Rev,* 65**,** 471-96.

PHELAN, K. & MAY, K. M. 2015. Basic techniques in mammalian cell tissue culture. *Curr Protoc Cell Biol,* 66**,** 1 1 1-1 1 22.

PHELAN, K. & MAY, K. M. 2016. Basic Techniques in Mammalian Cell Tissue Culture. *Curr Protoc Toxicol,* 70**,** A 3B 1-A 3B 22.

PHELAN, M. C. 2007. Basic techniques in mammalian cell tissue culture. *Curr Protoc Cell Biol,* Chapter 1**,** Unit 1 1.

PIETTE, E., REYCHLER, H. & VIDAL, E. 1985. [Introduction to the biology of bone grafts]. *Acta Stomatol Belg,* 82**,** 27-39.

PILGE, H., FROBEL, J., MROTZEK, S. J., FISCHER, J. C., PRODINGER, P. M., ZILKENS, C., BITTERSOHL, B. & KRAUSPE, R. 2016. Effects of thromboprophylaxis on mesenchymal stromal cells during osteogenic differentiation: an in-vitro study comparing enoxaparin with rivaroxaban. *BMC Musculoskelet Disord,* 17**,** 108.

PITTENGER, M. F., MACKAY, A. M., BECK, S. C., JAISWAL, R. K., DOUGLAS, R., MOSCA, J. D., MOORMAN, M. A., SIMONETTI, D. W., CRAIG, S. & MARSHAK, D. R. 1999. Multilineage potential of adult human mesenchymal stem cells. *Science,* 284**,** 143-7.

POLA, E., GAO, W., ZHOU, Y., POLA, R., LATTANZI, W., SFEIR, C., GAMBOTTO, A. & ROBBINS, P. D. 2004. Efficient bone formation by gene transfer of human LIM mineralization protein-3. *Gene Ther,* 11**,** 683-93.

PRABHA, S., ARYA, G., CHANDRA, R., AHMED, B. & NIMESH, S. 2016. Effect of size on biological properties of nanoparticles employed in gene delivery. *Artif Cells Nanomed Biotechnol,* 44**,** 83-91.

PRAMOD, P. S., TAKAMURA, K., CHAPHEKAR, S., BALASUBRAMANIAN, N. & JAYAKANNAN, M. 2012. Dextran vesicular carriers for dual encapsulation of hydrophilic and hydrophobic molecules and delivery into cells. *Biomacromolecules,* 13**,** 3627-40.

PRATAP, J., GALINDO, M., ZAIDI, S. K., VRADII, D., BHAT, B. M., ROBINSON, J. A., CHOI, J. Y., KOMORI, T., STEIN, J. L., LIAN, J. B., STEIN, G. S. & VAN WIJNEN, A. J. 2003. Cell growth regulatory role of Runx2 during proliferative expansion of preosteoblasts. *Cancer Res,* 63**,** 5357-62.

PROCHIANTZ, A. 2000. Messenger proteins: homeoproteins, TAT and others. *Curr Opin Cell Biol,* 12**,** 400-6.

PUN, S., H. & HOFFMAN, A. S. 2013. Nucleic Acid Delivery

In: RATNER, B., D., HOFFMAN, A., S. & LEMONS, J., E. (eds.) *Biomaterials Science (Third Edition) An Introduction to Materials in Medicine.* Academic Press AP.

RABADAN-ROS, R., REVILLA-NUIN, B., MAZÓN, P., AZNAR-CERVANTES, S., ROS-TARRAGA, P., DE AZA PIEDAD, N. & MESEGUER-OLMO, L. 2018. Impact of a Porous Si-Ca-P Monophasic Ceramic on Variation of Osteogenesis-Related Gene Expression of Adult Human Mesenchymal Stem Cells. *Applied Sciences,* 8.

RAFTERY, R. M., MENCIA CASTANO, I., CHEN, G., CAVANAGH, B., QUINN, B., CURTIN, C. M., CRYAN, S. A. & O'BRIEN, F. J. 2017. Translating the role of osteogenic-angiogenic coupling in bone formation: Highly efficient chitosan-pDNA activated scaffolds can accelerate bone regeneration in critical-sized bone defects. *Biomaterials,* 149**,** 116-127.

RAFTERY, R. M., WALSH, D. P., BLOKPOEL FERRERAS, L., MENCIA CASTANO, I., CHEN, G., LEMOINE, M., OSMAN, G., SHAKESHEFF, K. M., DIXON, J. E. & O'BRIEN, F. J. 2019. Highly versatile cell-penetrating peptide loaded scaffold for efficient and localised gene delivery to multiple cell types: From development to application in tissue engineering. *Biomaterials,* 216**,** 119277.

RAMAMOORTH, M. & NARVEKAR, A. 2015. Non viral vectors in gene therapy- an overview. *J Clin Diagn Res,* 9**,** GE01-6.

RAWADI, G., VAYSSIERE, B., DUNN, F., BARON, R. & ROMAN-ROMAN, S. 2003. BMP-2 controls alkaline phosphatase expression and osteoblast mineralization by a Wnt autocrine loop. *J Bone Miner Res,* 18**,** 1842-53.

REGNSTROM, K., RAGNARSSON, E. G., KOPING-HOGGARD, M., TORSTENSSON, E., NYBLOM, H. & ARTURSSON, P. 2003. PEI - a potent, but not harmless, mucosal immuno-stimulator of mixed T-helper cell response and FasL-mediated cell death in mice. *Gene Ther,* 10**,** 1575-83.

REN, J., WANG, H., TRAN, K., CIVINI, S., JIN, P., CASTIELLO, L., FENG, J., KUZNETSOV, S. A., ROBEY, P. G., SABATINO, M. & STRONCEK, D. F. 2015. Human bone marrow stromal cell confluence: effects on cell characteristics and methods of assessment. *Cytotherapy,* 17**,** 897-911.

REZVANTALAB, S., DRUDE, N. I., MORAVEJI, M. K., GUVENER, N., KOONS, E. K., SHI, Y., LAMMERS, T. & KIESSLING, F. 2018. PLGA-Based Nanoparticles in Cancer Treatment. *Frontiers in Pharmacology,* 9.

RIBEIRO, S., HUSSAIN, N. & FLORENCE, A. T. 2005. Release of DNA from dendriplexes encapsulated in PLGA nanoparticles. *Int J Pharm,* 298**,** 354-60.

ROBERTS, S. J., CHEN, Y., MOESEN, M., SCHROOTEN, J. & LUYTEN, F. P. 2011. Enhancement of osteogenic gene expression for the differentiation of human periosteal derived cells. *Stem Cell Res,* 7**,** 137-44.

ROBISON, R. 1923. The Possible Significance of Hexosephosphoric Esters in Ossification. *Biochem J,* 17**,** 286-93.

ROBISON, R. & SOAMES, K. M. 1924. The Possible Significance of Hexosephosphoric Esters in Ossification: Part II. The Phosphoric Esterase of Ossifying Cartilage. *Biochem J,* 18**,** 740-54.

RODAN, G. A. 1992. Introduction to bone biology. *Bone,* 13 Suppl 1**,** S3-6.

ROMOREN, K., AABERGE, A., SMISTAD, G., THU, B. J. & EVENSEN, O. 2004. Long-term stability of chitosan-based polyplexes. *Pharm Res,* 21**,** 2340-6.

ROOINTAN A , S. K., FATEMEH MEMARI,MOLOOD GANDOMANI,SEYED MOHAMMAD GHEIBI HAYAT &SOLIMAN MOHAMMADI-SAMANI 2018. Poly(lactic-co-glycolic acid): The most ardent and flexible candidate in biomedicine! *International Journal of Polymeric Materials and Polymeric Biomaterials,* 67**,** 1028-1049.

ROY, I., MITRA, S., MAITRA, A. & MOZUMDAR, S. 2003. Calcium phosphate nanoparticles as novel non-viral vectors for targeted gene delivery. *Int J Pharm,* 250**,** 25-33.

RYOO, H. M., HOFFMANN, H. M., BEUMER, T., FRENKEL, B., TOWLER, D. A., STEIN, G. S., STEIN, J. L., VAN WIJNEN, A. J. & LIAN, J. B. 1997. Stage-specific expression of Dlx-5 during osteoblast differentiation: involvement in regulation of osteocalcin gene expression. *Mol Endocrinol,* 11**,** 1681-94.

SAFAIYAN, F., KOLSET, S. O., PRYDZ, K., GOTTFRIDSSON, E., LINDAHL, U. & SALMIVIRTA, M. 1999. Selective effects of sodium chlorate treatment on the sulfation of heparan sulfate. *J Biol Chem,* 274**,** 36267-73.

SAH, H., THOMA, L. A., DESU, H. R., SAH, E. & WOOD, G. C. 2013. Concepts and practices used to develop functional PLGA-based nanoparticulate systems. *Int J Nanomedicine,* 8**,** 747-65.

SAHIN, A., ESENDAGLI, G., YERLIKAYA, F., CABAN-TOKTAS, S., YOYEN-ERMIS, D., HORZUM, U., AKTAS, Y., KHAN, M., COUVREUR, P. & CAPAN, Y. 2017. A small variation in average particle size of PLGA nanoparticles prepared by nanoprecipitation leads to considerable change in nanoparticles' characteristics and efficacy of intracellular delivery. *Artif Cells Nanomed Biotechnol,* 45**,** 1657-1664.

SAKUMA, T., HIGASHIYAMA, S., HOSOE, S., HAYASHI, S. & TANIGUCHI, N. 1997. CD9 antigen interacts with heparin-binding EGF-like growth factor through its heparin-binding domain. *J Biochem,* 122**,** 474-80.

SAKURAI, F., NISHIOKA, T., SAITO, H., BABA, T., OKUDA, A., MATSUMOTO, O., TAGA, T., YAMASHITA, F., TAKAKURA, Y. & HASHIDA, M. 2001. Interaction between DNA-cationic liposome complexes and erythrocytes is an important factor in systemic gene transfer via the intravenous route in mice: the role of the neutral helper lipid. *Gene Therapy,* 8**,** 677-686.

SALEH, A. F., AOJULA, H., ARTHANARI, Y., OFFERMAN, S., ALKOTAJI, M. & PLUEN, A. 2010. Improved Tat-mediated plasmid DNA transfer by fusion to LK15 peptide. *J Control Release,* 143**,** 233-42.

SAMBROOK, J. & RUSSELL, D. W. 2006a. Fragmentation of DNA by sonication. *CSH Protoc,* 2006.

SAMBROOK, J. & RUSSELL, D. W. 2006b. Purification of nucleic acids by extraction with phenol:chloroform. *CSH Protoc,* 2006.

SATO, M., OHTSUKA, M., WATANABE, S. & GURUMURTHY, C. B. 2016. Nucleic acids delivery methods for genome editing in zygotes and embryos: the old, the new, and the old-new. *Biol Direct,* 11**,** 16.

SCHAFFER, D., V., FIDELMAN, N., A., DAN, N. & LAUFFENBURGER, D., A. 2000. Vector unpacking as a potential barrier for receptor-mediated polyplex gene delivery. *Biotechnol. Bioeng,* 67**,** 598-606.

SCHELLER, A., OEHLKE, J., WIESNER, B., DATHE, M., KRAUSE, E., BEYERMANN, M., MELZIG, M. & BIENERT, M. 1999. Structural requirements for cellular uptake of alpha-helical amphipathic peptides. *J Pept Sci,* 5**,** 185-94.

SCHLIECKER, G., SCHMIDT, C., FUCHS, S. & KISSEL, T. 2003. Characterization of a homologous series of D,L-lactic acid oligomers; a mechanistic study on the degradation kinetics in vitro. *Biomaterials,* 24**,** 3835-44.

SCHUBERT, S., DELANEY, J., T. & SCHUBERT, U., S. 2011. Nanoprecipitation and nanoformulation of polymers: from history to powerful possibilities beyond poly(lactic acid). *Soft Matter,* 7**,** 1581–1588.

SELBY, L. I., CORTEZ-JUGO, C. M., SUCH, G. K. & JOHNSTON, A. P. R. 2017. Nanoescapology: progress toward understanding the endosomal escape of polymeric nanoparticles. *Wiley Interdiscip Rev Nanomed Nanobiotechnol,* 9.

SENIOR, J. H., TRIMBLE, K. R. & MASKIEWICZ, R. 1991. Interaction of Positively-Charged Liposomes with Blood - Implications for Their Application Invivo. *Biochimica Et Biophysica Acta,* 1070**,** 173-179.

SHANG, L., NIENHAUS, K. & NIENHAUS, G. U. 2014. Engineered nanoparticles interacting with cells: size matters. *J Nanobiotechnology,* 12**,** 5.

SHARMA, D., KANCHI, S., BISETTYA, K. & NUTHALAPATI, V. N. 2016a. Perspective on Analytical Sciences and Nanotechnology. *In:* CHAUDHERY MUSTANSAR HUSSAIN, B. K. (ed.) *Advanced Environmental Analysis: Applications of Nanomaterials.*

SHARMA, R., AHMAD, G., ESTEVES, S. C. & AGARWAL, A. 2016b. Terminal deoxynucleotidyl transferase dUTP nick end labeling (TUNEL) assay using bench top flow cytometer for evaluation of sperm DNA fragmentation in fertility laboratories: protocol, reference values, and quality control. *J Assist Reprod Genet,* 33**,** 291-300.

SHI, J., VOTRUBA, A. R., FAROKHZAD, O. C. & LANGER, R. 2010. Nanotechnology in drug delivery and tissue engineering: from discovery to applications. *Nano Lett,* 10**,** 3223-30.

SHI, Q., AIDA, K., VANDEBERG, J. L. & WANG, X. L. 2004. Passage-dependent changes in baboon endothelial cells--relevance to in vitro aging. *DNA Cell Biol,* 23**,** 502-9.

SHI, Y. & WHETSTINE, J. R. 2007. *Dynamic regulation of histone lysine methylation by demethylases*.

SHIELDS, L. B., RAQUE, G. H., GLASSMAN, S. D., CAMPBELL, M., VITAZ, T., HARPRING, J. & SHIELDS, C. B. 2006. Adverse effects associated with high-dose recombinant human bone morphogenetic protein-2 use in anterior cervical spine fusion. *Spine (Phila Pa 1976),* 31**,** 542-7.

SIDDAPPA, R., LICHT, R., VAN BLITTERSWIJK, C. & DE BOER, J. 2007. Donor variation and loss of multipotency during in vitro expansion of human mesenchymal stem cells for bone tissue engineering. *J Orthop Res,* 25**,** 1029-41.

SILLER, A. F. & WHYTE, M. P. 2018. Alkaline Phosphatase: Discovery and Naming of Our Favorite Enzyme. *J Bone Miner Res,* 33**,** 362-364.

SILVA, G. A. 2004. Introduction to nanotechnology and its applications to medicine. *Surg Neurol,* 61**,** 216-20.

SIMOES, S., SLEPUSHKIN, V., PIRES, P., GASPAR, R., DE LIMA, M. P. & DUZGUNES, N. 1999. Mechanisms of gene transfer mediated by lipoplexes associated with targeting ligands or pH-sensitive peptides. *Gene Ther,* 6**,** 1798-807.

SINGER, V. L., JONES, L. J., YUE, S. T. & HAUGLAND, R. P. 1997. Characterization of PicoGreen reagent and development of a fluorescence-based solution assay for double-stranded DNA quantitation. *Anal Biochem,* 249**,** 228-38.

SINHA, V. R. & TREHAN, A. 2003. Biodegradable microspheres for protein delivery. *J Control Release,* 90**,** 261-80.

SKARN, M., NOORDHUIS, P., WANG, M. Y., VEUGER, M., KRESSE, S. H., EGELAND, E. V., MICCI, F., NAMLOS, H. M., HAKELIEN, A. M., OLAFSRUD, S. M., LORENZ, S., HARALDSEN, G., KVALHEIM, G., MEZA-ZEPEDA, L. A. & MYKLEBOST, O. 2014. Generation and characterization of an immortalized human mesenchymal stromal cell line. *Stem Cells Dev,* 23**,** 2377-89.

SLIVAC, I., GUAY, D., MANGION, M., CHAMPEIL, J. & GAILLET, B. 2017. Non-viral nucleic acid delivery methods. *Expert Opin Biol Ther,* 17**,** 105-118.

SMITH, B. C. & DENU, J. M. 2009. Chemical mechanisms of histone lysine and arginine modifications. *Biochim Biophys Acta,* 1789**,** 45-57.

SMITH, E. L., KANCZLER, J. M., GOTHARD, D., ROBERTS, C. A., WELLS, J. A., WHITE, L. J., QUTACHI, O., SAWKINS, M. J., PETO, H., RASHIDI, H., ROJO, L., STEVENS, M. M., EL HAJ, A. J., ROSE, F. R., SHAKESHEFF, K. M. & OREFFO, R. O. 2014. Evaluation of skeletal tissue repair, part 2: enhancement of skeletal tissue repair through dual-growth-factor-releasing hydrogels within an ex vivo chick femur defect model. *Acta Biomater,* 10**,** 4197-205.

SODEK, J., CHEN, J., NAGATA, T., KASUGAI, S., TODESCAN, R., JR., LI, I. W. & KIM, R. H. 1995. Regulation of osteopontin expression in osteoblasts. *Ann N Y Acad Sci,* 760**,** 223-41.

SOLCHAGA, L., A., CASSIEDE, P. & CAPLAN, A. I. 1998. Different response to osteo-inductive agents in bone marrow- and periosteum-derived cell preparations. *Acfa Orthop Scand,* 69**,** 426-432.

SPILIOTOPOULOS, A., BLOKPOEL FERRERAS, L., DENSHAM, R. M., CAULTON, S. G., MADDISON, B. C., MORRIS, J. R., DIXON, J. E., GOUGH, K. C. & DREVENY, I. 2019. Discovery of peptide ligands targeting a specific ubiquitin-like domain-binding site in the deubiquitinase USP11. *J Biol Chem,* 294**,** 424-436.

STEINBACH, J. M., SEO, Y. E. & SALTZMAN, W. M. 2016. Cell penetrating peptide-modified poly(lactic-co-glycolic acid) nanoparticles with enhanced cell internalization. *Acta Biomater,* 30**,** 49-61.

STERNLING, C., V. & SCRIVEN, L., E. 1959. Interfacial turbulence: hydrodynamic instability and the marangoni effect. *AIChE,* 5**,** 514–523.

STRECK, S., CLULOW, A. J., NIELSEN, H. M., RADES, T., BOYD, B. J. & MCDOWELL, A. 2019. The distribution of cell-penetrating peptides on polymeric nanoparticles prepared using microfluidics and elucidated with small angle X-ray scattering. *J Colloid Interface Sci,* 555**,** 438-448.

SUN, D., XUE, A., ZHANG, B., XUE, X., ZHANG, J. & LIU, W. 2016. Enhanced oral bioavailability of acetylpuerarin by poly(lactide-co-glycolide) nanoparticles optimized using uniform design combined with response surface methodology. *Drug Des Devel Ther,* 10**,** 2029-39.

SWANSON, J. A. & WATTS, C. 1995. Macropinocytosis. *Trends Cell Biol,* 5**,** 424-8.

TABATT, K., KNEUER, C., SAMETI, M., OLBRICH, C., MULLER, R. H., LEHR, C. M. & BAKOWSKY, U. 2004. Transfection with different colloidal systems: comparison of solid lipid nanoparticles and liposomes. *J Control Release,* 97**,** 321-32.

TAHARA, K., SAKAI, T., YAMAMOTO, H., TAKEUCHI, H. & KAWASHIMA, Y. 2008. Establishing chitosan coated PLGA nanosphere platform loaded with wide variety of nucleic acid by complexation with cationic compound for gene delivery. *Int J Pharm,* 354**,** 210-6.

TAHARA, K., YAMAMOTO, H., HIRASHIMA, N. & KAWASHIMA, Y. 2010. Chitosan-modified poly(D,L-lactide-co-glycolide) nanospheres for improving siRNA delivery and gene-silencing effects. *Eur J Pharm Biopharm,* 74**,** 421-6.

TAKAMIZAWA, S., MAEHATA, Y., IMAI, K., SENOO, H., SATO, S. & HATA, R. 2004. Effects of ascorbic acid and ascorbic acid 2-phosphate, a long-acting vitamin C derivative, on the proliferation and differentiation of human osteoblast-like cells. *Cell Biol Int,* 28**,** 255-65.

TAKEI, K. & HAUCKE, V. 2001. Clathrin-mediated endocytosis: membrane factors pull the trigger. *Trends Cell Biol,* 11**,** 385-91.

TAKESHITA, T., MATSUURA, Y., ARAKAWA, S. & OKAMOTO, M. 2013. Biomineralization of hydroxyapatite on DNA molecules in SBF: morphological features and computer simulation. *Langmuir,* 29**,** 11975-81.

TANG, J., CHEN, J. Y., LIU, J., LUO, M., WANG, Y. J., WEI, X. W., GAO, X., WANG, B. L., LIU, Y. B., YI, T., TONG, A. P., SONG, X. R., XIE, Y. M., ZHAO, Y., XIANG, M., HUANG, Y. & ZHENG, Y. 2012. Calcium phosphate embedded PLGA nanoparticles: a promising gene delivery vector with high gene loading and transfection efficiency. *Int J Pharm,* 431**,** 210-21.

TANNOURY, C. A. & AN, H. S. 2014. Complications with the use of bone morphogenetic protein 2 (BMP-2) in spine surgery. *Spine J,* 14**,** 552-9.

THIAGARAJAN, L., ABU-AWWAD, H. A. M. & DIXON, J. E. 2017. Osteogenic Programming of Human Mesenchymal Stem Cells with Highly Efficient Intracellular Delivery of RUNX2. *Stem Cells Transl Med,* 6**,** 2146-2159.

THOMAS, M. & KLIBANOV, A. M. 2003. Non-viral gene therapy: polycation-mediated DNA delivery. *Appl Microbiol Biotechnol,* 62**,** 27-34.

TIERNEY, E. G., DUFFY, G. P., HIBBITTS, A. J., CRYAN, S. A. & O'BRIEN, F. J. 2012. The development of non-viral gene-activated matrices for bone regeneration using polyethyleneimine (PEI) and collagen-based scaffolds. *J Control Release,* 158**,** 304-11.

TOMANKOVA, K., POLAKOVA, K., PIZOVA, K., BINDER, S., HAVRDOVA, M., KOLAROVA, M., KRIEGOVA, E., ZAPLETALOVA, J., MALINA, L., HORAKOVA, J., MALOHLAVA, J., KOLOKITHAS-NTOUKAS, A., BAKANDRITSOS, A., KOLAROVA, H. & ZBORIL, R. 2015. In vitro cytotoxicity analysis of doxorubicin-loaded/superparamagnetic iron oxide colloidal nanoassemblies on MCF7 and NIH3T3 cell lines. *Int J Nanomedicine,* 10**,** 949-61.

TROS DE ILARDUYA, C., SUN, Y. & DUZGUNES, N. 2010. Gene delivery by lipoplexes and polyplexes. *Eur J Pharm Sci,* 40**,** 159-70.

TROUNSON, A. & MCDONALD, C. 2015. Stem Cell Therapies in Clinical Trials: Progress and Challenges. *Cell Stem Cell,* 17**,** 11-22.

TSUDA, H., WADA, T., ITO, Y., UCHIDA, H., DEHARI, H., NAKAMURA, K., SASAKI, K., KOBUNE, M., YAMASHITA, T. & HAMADA, H. 2003. Efficient BMP2 gene

transfer and bone formation of mesenchymal stem cells by a fiber-mutant adenoviral vector. *Mol Ther,* 7**,** 354-65.

TSUJIYAMA, S., NITTA, T. & MAOKA, T. 2011. Biodegradation of polyvinyl alcohol by Flammulina velutipes in an unsubmerged culture. *J Biosci Bioeng,* 112**,** 58-62.

TURINETTO, V., VITALE, E. & GIACHINO, C. 2016. Senescence in Human Mesenchymal Stem Cells: Functional Changes and Implications in Stem Cell-Based Therapy. *Int J Mol Sci,* 17.

URIST, M. R. 1965. Bone: formation by autoinduction. *Science,* 150**,** 893-9.

URRUTIA, D. N., CAVIEDES, P., MARDONES, R., MINGUELL, J. J., VEGA-LETTER, A. M. & JOFRE, C. M. 2019. Comparative study of the neural differentiation capacity of mesenchymal stromal cells from different tissue sources: An approach for their use in neural regeneration therapies. *PLoS One,* 14**,** e0213032.

VALENTIN-OPRAN, A., WOZNEY, J., CSIMMA, C., LILLY, L. & RIEDEL, G. E. 2002. Clinical evaluation of recombinant human bone morphogenetic protein-2. *Clin Orthop Relat Res***,** 110-20.

VANDERVOORT, J. & LUDWIG, A. 2002. Biocompatible stabilizers in the preparation of PLGA nanoparticles: a factorial design study. *Int J Pharm,* 238**,** 77-92.

VARELA-RAMIREZ, A., ABENDROTH, J., MEJIA, A. A., PHAN, I. Q., LORIMER, D. D., EDWARDS, T. E. & AGUILERA, R. J. 2017. Structure of acid deoxyribonuclease. *Nucleic Acids Res,* 45**,** 6217-6227.

VASCONCELOS, A., VEGA, E., PEREZ, Y., GOMARA, M. J., GARCIA, M. L. & HARO, I. 2015. Conjugation of cell-penetrating peptides with poly(lactic-co-glycolic acid)-polyethylene glycol nanoparticles improves ocular drug delivery. *Int J Nanomedicine,* 10**,** 609-31.

VASIĆ, K., KNEZ, Z., KONSTANTINOVA, E., A., KOKORIN, A., I., GYERGYEK, S. & LEITGEB, M. 2020. Structural and magnetic characteristics of carboxymethyl dextran coated magnetic nanoparticles: From characterization to immobilization application. *Reactive and Functional Polymers,* 148.

VATER, C., KASTEN, P. & STIEHLER, M. 2011. Culture media for the differentiation of mesenchymal stromal cells. *Acta Biomater,* 7**,** 463-77.

VERCAUTEREN, D., REJMAN, J., MARTENS, T. F., DEMEESTER, J., DE SMEDT, S. C. & BRAECKMANS, K. 2012. On the cellular processing of non-viral nanomedicines for nucleic acid delivery: mechanisms and methods. *J Control Release,* 161**,** 566-81.

VILLANUEVA, A., CANETE, M., ROCA, A. G., CALERO, M., VEINTEMILLAS-VERDAGUER, S., SERNA, C. J., MORALES MDEL, P. & MIRANDA, R. 2009. The influence of surface functionalization on the enhanced internalization of magnetic nanoparticles in cancer cells. *Nanotechnology,* 20**,** 115103.

VON GERSDORFF, K., SANDERS, N. N., VANDENBROUCKE, R., DE SMEDT, S. C., WAGNER, E. & OGRIS, M. 2006. The internalization route resulting in successful gene expression depends on both cell line and polyethylenimine polyplex type. *Mol Ther,* 14**,** 745-53.

WAGNER, E., OGRIS, M. & ZAUNER, W. 1998. Polylysine-based transfection systems utilizing receptor-mediated delivery. *Adv Drug Deliv Rev,* 30**,** 97-113.

WALSH, S., JORDAN, G. R., JEFFERISS, C., STEWART, K. & BERESFORD, J. N. 2001. High concentrations of dexamethasone suppress the proliferation but not

the differentiation or further maturation of human osteoblast precursors in vitro: relevance to glucocorticoid-induced osteoporosis. *Rheumatology (Oxford),* 40**,** 74-83.

WALTER, E., DREHER, D., KOK, M., THIELE, L., KIAMA, S. G., GEHR, P. & MERKLE, H. P. 2001. Hydrophilic poly(DL-lactide-co-glycolide) microspheres for the delivery of DNA to human-derived macrophages and dendritic cells. *J Control Release,* 76**,** 149-68.

WANG, J., WANG, B. M. & SCHWENDEMAN, S. P. 2002. Characterization of the initial burst release of a model peptide from poly(D,L-lactide-co-glycolide) microspheres. *J Control Release,* 82**,** 289-307.

WANG, L., DORMER, N. H., BONEWALD, L. F. & DETAMORE, M. S. 2010. Osteogenic differentiation of human umbilical cord mesenchymal stromal cells in polyglycolic acid scaffolds. *Tissue Eng Part A,* 16**,** 1937-48.

WANG, X., ISHIDA, T. & KIWADA, H. 2007. Anti-PEG IgM elicited by injection of liposomes is involved in the enhanced blood clearance of a subsequent dose of PEGylated liposomes. *J Control Release,* 119**,** 236-44.

WANG, Y., HAN, Z. B., SONG, Y. P. & HAN, Z. C. 2012. Safety of mesenchymal stem cells for clinical application. *Stem Cells Int,* 2012**,** 652034.

WANG, Y., HE, T., LIU, J., LIU, H., ZHOU, L., HAO, W., SUN, Y. & WANG, X. 2016. Synergistic effects of overexpression of BMP2 and TGFbeta3 on osteogenic differentiation of bone marrow mesenchymal stem cells. *Mol Med Rep,* 14**,** 5514-5520.

WANG, Z., TIRUPPATHI, C., MINSHALL, R. D. & MALIK, A. B. 2009. Size and dynamics of caveolae studied using nanoparticles in living endothelial cells. *ACS Nano,* 3**,** 4110-6.

WEGMAN, F., BIJENHOF, A., SCHUIJFF, L., ONER, F. C., DHERT, W. J. & ALBLAS, J. 2011. Osteogenic differentiation as a result of BMP-2 plasmid DNA based gene therapy in vitro and in vivo. *Eur Cell Mater,* 21**,** 230-42; discussion 242.

WIIG, H., KOLMANNSKOG, O., TENSTAD, O. & BERT, J. L. 2003. Effect of charge on interstitial distribution of albumin in rat dermis in vitro. *J Physiol,* 550**,** 505-14.

WITTRUP, A., AI, A., LIU, X., HAMAR, P., TRIFONOVA, R., CHARISSE, K., MANOHARAN, M., KIRCHHAUSEN, T. & LIEBERMAN, J. 2015. Visualizing lipid-formulated siRNA release from endosomes and target gene knockdown. *Nat Biotechnol,* 33**,** 870-6.

WOLFERT, M. A., SCHACHT, E. H., TONCHEVA, V., ULBRICH, K., NAZAROVA, O. & SEYMOUR, L. W. 1996. Characterization of vectors for gene therapy formed by self-assembly of DNA with synthetic block co-polymers. *Hum Gene Ther,* 7**,** 2123-33.

WOLFERT, M. A. & SEYMOUR, L. W. 1996. Atomic force microscopic analysis of the influence of the molecular weight of poly(L)lysine on the size of polyelectrolyte complexes formed with DNA. *Gene Ther,* 3**,** 269-73.

WONG, J. K. L., MOHSENI, R., HAMIDIEH, A. A., MACLAREN, R. E., HABIB, N. & SEIFALIAN, A. M. 2017. Will Nanotechnology Bring New Hope for Gene Delivery? *Trends Biotechnol,* 35**,** 434-451.

WU, M. L., FREITAS, S. S., MONTEIRO, G. A., PRAZERES, D. M. & SANTOS, J. A. 2009. Stabilization of naked and condensed plasmid DNA against degradation induced by ultrasounds and high-shear vortices. *Biotechnol Appl Biochem,* 53**,** 237-46.

WU, P., CHEN, H., JIN, R., WENG, T., HO, J. K., YOU, C., ZHANG, L., WANG, X. & HAN, C. 2018. Non-viral gene delivery systems for tissue repair and regeneration. *J Transl Med,* 16**,** 29.

XIANG, S., TONG, H., SHI, Q., FERNANDES, J. C., JIN, T., DAI, K. & ZHANG, X. 2012. Uptake mechanisms of non-viral gene delivery. *J Control Release,* 158**,** 371-8.

XIE, H. & SMITH, J. W. 2010. Fabrication of PLGA nanoparticles with a fluidic nanoprecipitation system. *J Nanobiotechnology,* 8**,** 18.

XU, J. 2016. Synthesis of polymeric nanoparticles for the controlled release of hydrophobic and hydrophillic therapeutic compounds. Chemical Physics [physics.chem-ph]. Université de Bordeaux,.

XU, J., CHEN, Y., JIANG, X., GUI, Z. & ZHANG, L. 2019. Development of Hydrophilic Drug Encapsulation and Controlled Release Using a Modified Nanoprecipitation Method. *Processes,* 7.

XU, L., LIU, Y., SUN, Y., WANG, B., XIONG, Y., LIN, W., WEI, Q., WANG, H., HE, W., WANG, B. & LI, G. 2017. Tissue source determines the differentiation potentials of mesenchymal stem cells: a comparative study of human mesenchymal stem cells from bone marrow and adipose tissue. *Stem Cell Res Ther,* 8**,** 275.

XU, Q., CROSSLEY, A. & CZERNUSZKA, J. 2009. Preparation and characterization of negatively charged poly(lactic-co-glycolic acid) microspheres. *J Pharm Sci,* 98**,** 2377-89.

XU, Y., HUI, S. W., FREDERIK, P. & SZOKA, F. C., JR. 1999. Physicochemical characterization and purification of cationic lipoplexes. *Biophys J,* 77**,** 341-53.

YADAV, K. S. & SAWANT, K. K. 2010. Modified nanoprecipitation method for preparation of cytarabine-loaded PLGA nanoparticles. *AAPS PharmSciTech,* 11**,** 1456-65.

YAMANOUCHI, K., GOTOH, Y. & NAGAYAMA, M. 1997. Dexamethasone enhances differentiation of human osteoblastic cells in vitro. *Journal of Bone and Mineral Metabolism* 15**,** 23-29.

YANEZ-MUNOZ, R. J., BALAGGAN, K. S., MACNEIL, A., HOWE, S. J., SCHMIDT, M., SMITH, A. J., BUCH, P., MACLAREN, R. E., ANDERSON, P. N., BARKER, S. E., DURAN, Y., BARTHOLOMAE, C., VON KALLE, C., HECKENLIVELY, J. R., KINNON, C., ALI, R. R. & THRASHER, A. J. 2006. Effective gene therapy with nonintegrating lentiviral vectors. *Nat Med,* 12**,** 348-53.

YANG, W., WANG, F., FENG, L., YAN, S. & GUO, R. 2018a. Applications and Prospects of Non-viral Vectors in Bone Regeneration. *Curr Gene Ther,* 18**,** 21-28.

YANG, Y. K., OGANDO, C. R., WANG SEE, C., CHANG, T. Y. & BARABINO, G. A. 2018b. Changes in phenotype and differentiation potential of human mesenchymal stem cells aging in vitro. *Stem Cell Res Ther,* 9**,** 131.

YANG, Y. Y., CHUNG, T. S. & NG, N. P. 2001. Morphology, drug distribution, and in vitro release profiles of biodegradable polymeric microspheres containing protein fabricated by double-emulsion solvent extraction/evaporation method. *Biomaterials,* 22**,** 231-41.

YEO, Y. & PARK, K. 2004. Control of encapsulation efficiency and initial burst in polymeric microparticle systems. *Arch Pharm Res,* 27**,** 1-12.

YOHAY, D. A., ZHANG, J., THRAILKILL, K. M., ARTHUR, J. M. & QUARLES, L. D. 1994. Role of serum in the developmental expression of alkaline phosphatase in MC3T3-E1 osteoblasts. *J Cell Physiol,* 158**,** 467-75.

YOSHIDA, Y., KOBAYASHI, E., ENDO, H., HAMAMOTO, T., YAMANAKA, T., FUJIMURA, A. & KAGAWA, Y. 1997. Introduction of DNA into rat liver with a hand-held gene gun: distribution of the expressed enzyme, [32P]DNA, and Ca2+ flux. *Biochem Biophys Res Commun,* 234**,** 695-700.

YUAN, X., LOGAN, T. M. & MA, T. 2019. Metabolism in Human Mesenchymal Stromal Cells: A Missing Link Between hMSC Biomanufacturing and Therapy? *Front Immunol,* 10**,** 977.

YUASA, M., YAMADA, T., TANIYAMA, T., MASAOKA, T., XUETAO, W., YOSHII, T., HORIE, M., YASUDA, H., UEMURA, T., OKAWA, A. & SOTOME, S. 2015. Dexamethasone enhances osteogenic differentiation of bone marrow- and muscle-derived stromal cells and augments ectopic bone formation induced by bone morphogenetic protein-2. *PLoS One,* 10**,** e0116462.

YUE, J., WU, J., LIU, D., ZHAO, X. & LU, W. W. 2015. BMP2 gene delivery to bone mesenchymal stem cell by chitosan-g-PEI nonviral vector. *Nanoscale Res Lett,* 10**,** 203.

ZABNER, J., FASBENDER, A. J., MONINGER, T., POELLINGER, K. A. & WELSH, M. J. 1995. Cellular and molecular barriers to gene transfer by a cationic lipid. *J Biol Chem,* 270**,** 18997-9007.

ZENG, J., MOHAMMADREZA, A., GAO, W., MERZA, S., SMITH, D., KELBAUSKAS, L. & MELDRUM, D. R. 2014. A minimally invasive method for retrieving single adherent cells of different types from cultures. *Sci Rep,* 4**,** 5424.

ZHANG, N., CHITTASUPHO, C., DUANGRAT, C., SIAHAAN, T. J. & BERKLAND, C. 2008. PLGA nanoparticle--peptide conjugate effectively targets intercellular cell-adhesion molecule-1. *Bioconjug Chem,* 19**,** 145-52.

ZHANG, R., EDWARDS, J. R., KO, S. Y., DONG, S., LIU, H., OYAJOBI, B. O., PAPASIAN, C., DENG, H. W. & ZHAO, M. 2011. Transcriptional regulation of BMP2 expression by the PTH-CREB signaling pathway in osteoblasts. *PLoS One,* 6**,** e20780.

ZHANG, R., OYAJOBI, B. O., HARRIS, S. E., CHEN, D., TSAO, C., DENG, H. W. & ZHAO, M. 2013. Wnt/beta-catenin signaling activates bone morphogenetic protein 2 expression in osteoblasts. *Bone,* 52**,** 145-56.

ZHANG, S. X. A. X. 2013. *Cellular Uptake Mechanism of Non-Viral Gene Delivery and Means for Improving Transfection Efficiency*.

ZHAO, K., LI, W., HUANG, T., LUO, X., CHEN, G., ZHANG, Y., GUO, C., DAI, C., JIN, Z., ZHAO, Y., CUI, H. & WANG, Y. 2013. Preparation and efficacy of Newcastle disease virus DNA vaccine encapsulated in PLGA nanoparticles. *PLoS One,* 8**,** e82648.

ZHAO, M., HARRIS, S. E., HORN, D., GENG, Z., NISHIMURA, R., MUNDY, G. R. & CHEN, D. 2002. Bone morphogenetic protein receptor signaling is necessary for normal murine postnatal bone formation. *J Cell Biol,* 157**,** 1049-60.

ZHOU, H., COOPER, M. S. & SEIBEL, M. J. 2013. Endogenous Glucocorticoids and Bone. *Bone Res,* 1**,** 107-19.

Chapter 8.

Appendices

8.1 Appendix 1: Particle size and Zeta potential data of pDNA NP/MPs, PLGA NP/MPs

8.1.1 PLGA NP/MPs prepared by modified nanoprecipitation

8.1.1.1 PLGA MPs: 5% PLGA, Solvent: DMF

8.1.1.1.1 TEM

Batches

1

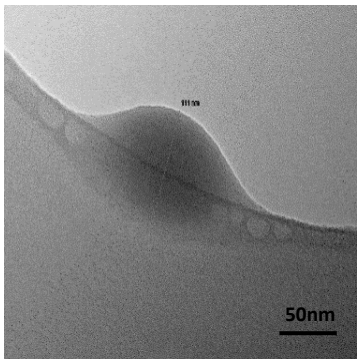

2

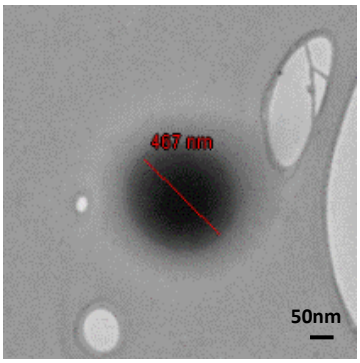

3

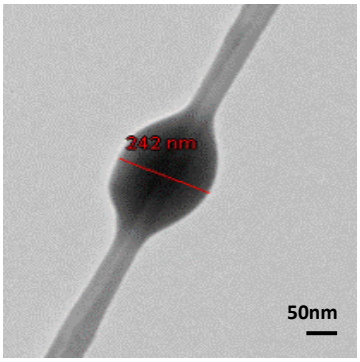

8.1.1.1.2 DLS

Batch 1

			Size (d.nm):	% Intensity:	St Dev (d.nm):
Z-Average (d.nm):	399.5	Peak 1:	115.7	100.0	15.75
PdI:	0.442	Peak 2:	0.000	0.0	0.000
Intercept:	1.03	Peak 3:	0.000	0.0	0.000

Result quality : Refer to quality report

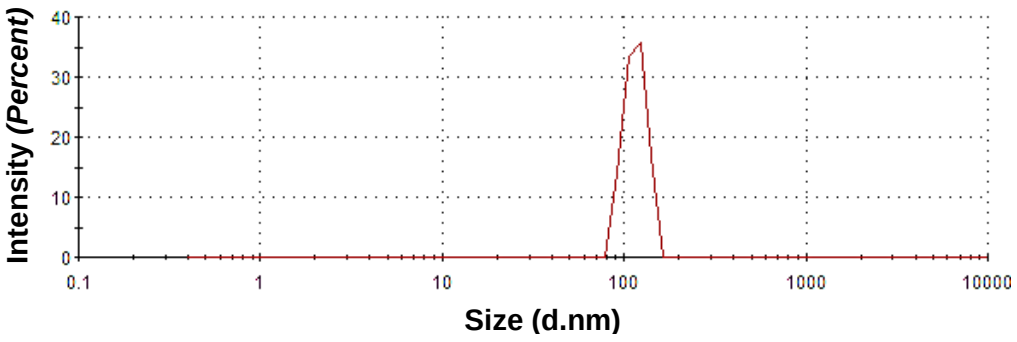

Batch 2

			Size (d.nm):	% Intensity:	St Dev (d.nm):
Z-Average (d.nm):	591.5	Peak 1:	260.2	100.0	27.61
PdI:	0.551	Peak 2:	0.000	0.0	0.000
Intercept:	1.01	Peak 3:	0.000	0.0	0.000

Result quality : Refer to quality report

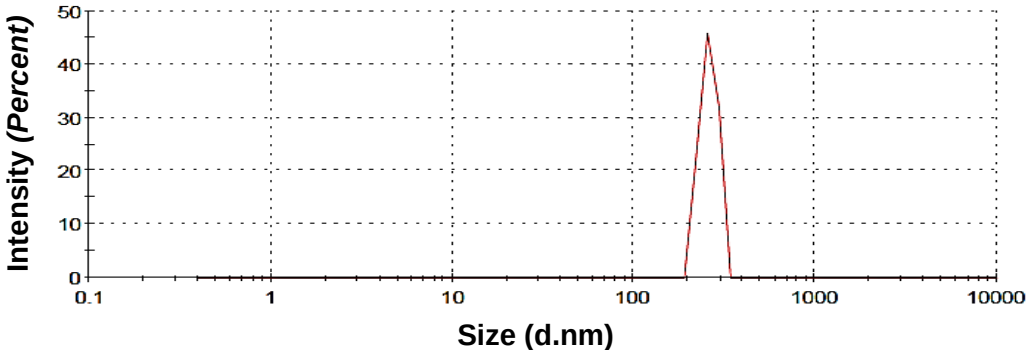

Batch 3

			Size (d.nm):	% Intensity:	St Dev (d.nm):
Z-Average (d.nm):	588.2	Peak 1:	237.2	100.0	27.89
PdI:	0.563	Peak 2:	0.000	0.0	0.000
Intercept:	1.03	Peak 3:	0.000	0.0	0.000

Result quality : Refer to quality report

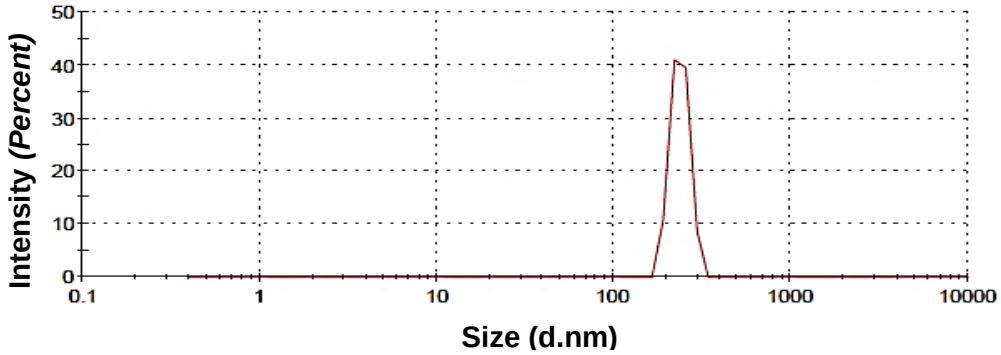

8.1.1.2 PLGA NPs: 2% PLGA, Solvent: DMSO

8.1.1.2.1 TEM

Batches

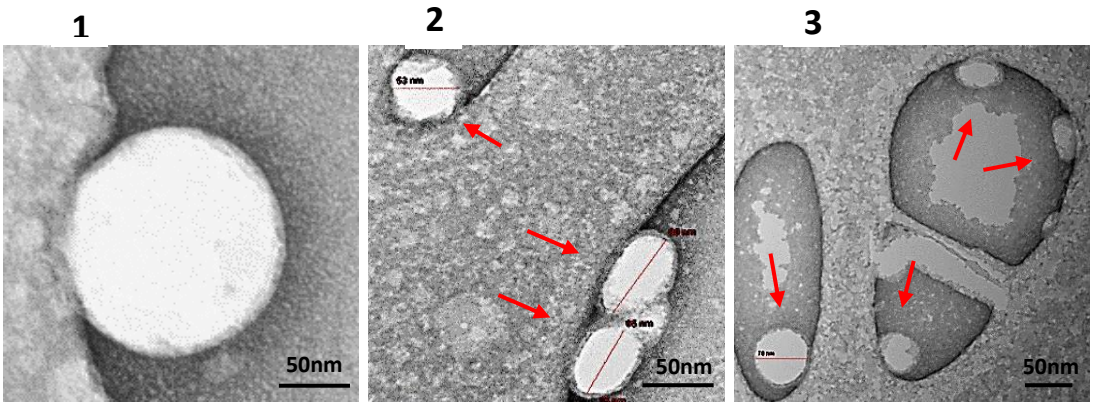

8.1.1.2.2 DLS

Batch 1

		Size (d.nm):	% Intensity:	St Dev (d.nm):
Z-Average (d.nm): 78.02	Peak 1:	87.45	100.0	30.24
PdI: 0.103	Peak 2:	0.000	0.0	0.000
Intercept: 0.921	Peak 3:	0.000	0.0	0.000
Result quality : Good				

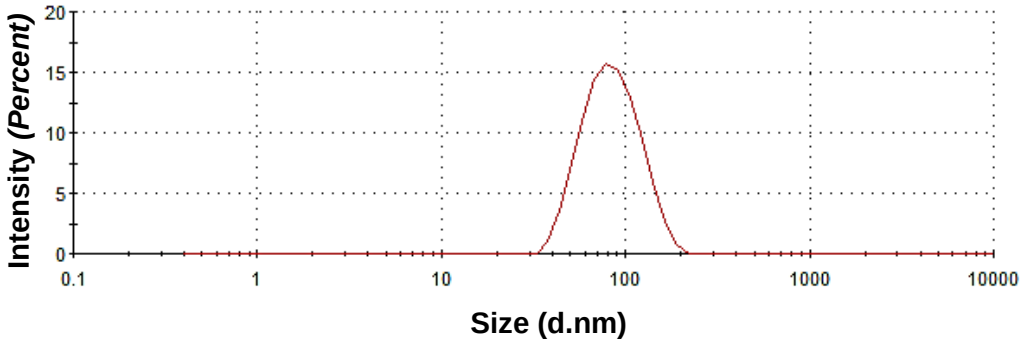

Batch 2

			Size (d.nm):	% Intensity:	St Dev (d.nm):
Z-Average (d.nm):	82.56	Peak 1:	90.13	100.0	26.49
PdI:	0.083	Peak 2:	0.000	0.0	0.000
Intercept:	0.952	Peak 3:	0.000	0.0	0.000

Result quality : Good

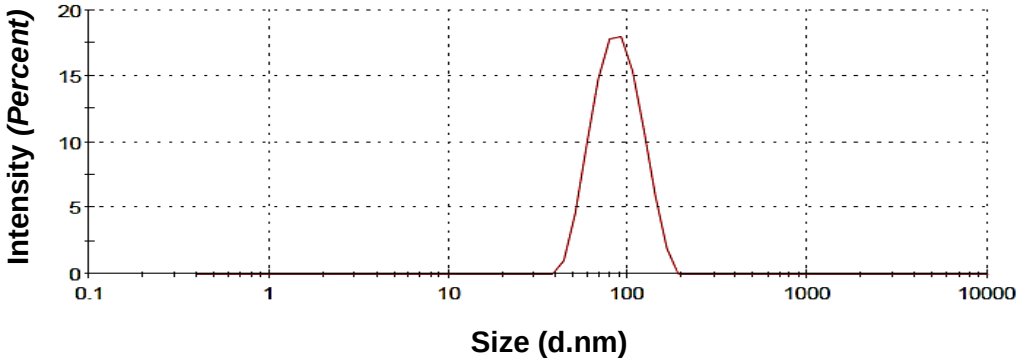

Batch 3

			Size (d.nm):	% Intensity:	St Dev (d.nm):
Z-Average (d.nm):	97.45	Peak 1:	106.8	98.4	39.91
PdI:	0.208	Peak 2:	5188	1.6	480.9
Intercept:	0.656	Peak 3:	0.000	0.0	0.000

Result quality : Good

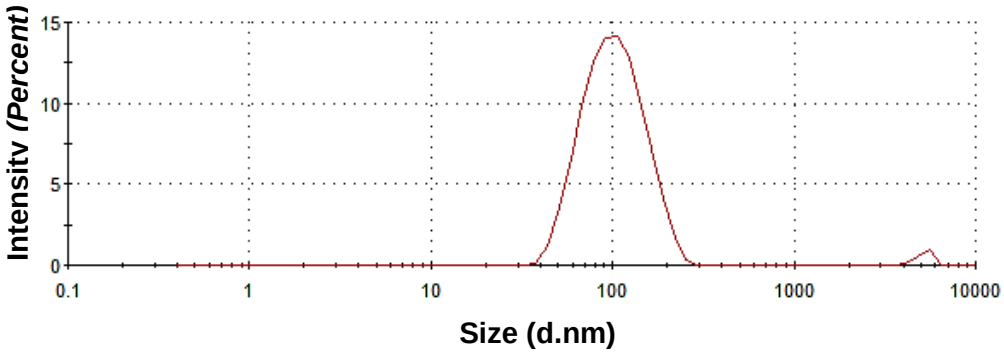

8.1.1.2.3 Zeta potential: Representative Surface charge of PLGA NP/MPs 2%/5% PLGA

Batch 1

			Mean (mV)	Area (%)	St Dev (mV)
Zeta Potential (mV):	-40.3	Peak 1:	-40.3	100.0	30.24
Zeta Deviation (mV):	7.56	Peak 2:	0.00	0.0	0.000
Conductivity (mS/cm):	0.112	Peak 3:	0.00	0.0	0.000

Result quality : Good

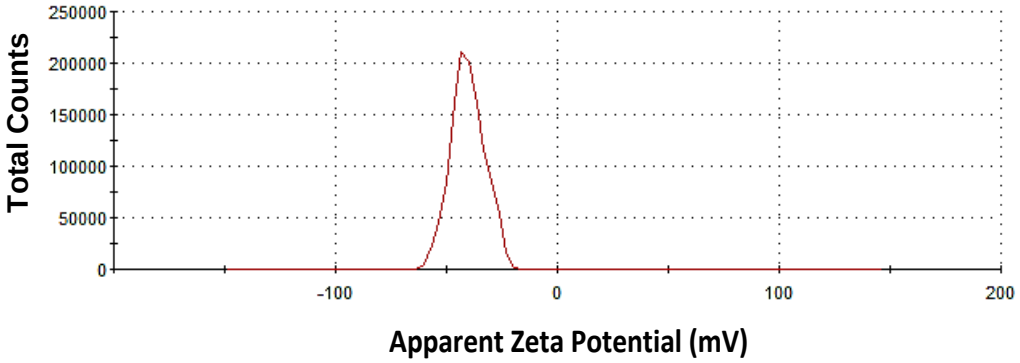

Batch 2

			Mean (mV)	Area (%)	St Dev (mV)
Zeta Potential (mV):	-40.2	Peak 1:	-40.7	99.6	8.13
Zeta Deviation (mV):	10.2	Peak 2:	51.4	0.4	0.00
Conductivity (mS/cm):	0.00241	Peak 3:	0.00	0.0	0.00

Result quality : Good

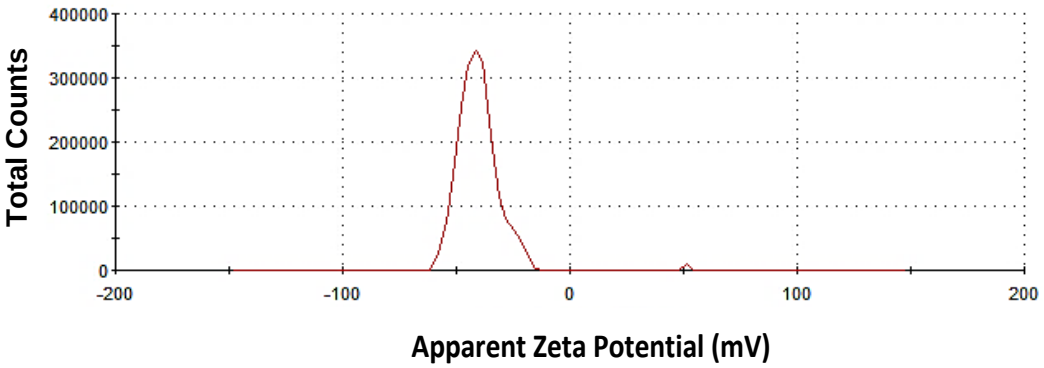

Batch 3

			Mean (mV)	Area (%)	St Dev (mV)
Zeta Potential (mV):	-42.1	Peak 1:	-42.1	100.0	5.45
Zeta Deviation (mV):	5.45	Peak 2:	0.00	0.0	0.00
Conductivity (mS/cm):	0.0195	Peak 3:	0.00	0.0	0.00
Result quality	Good				

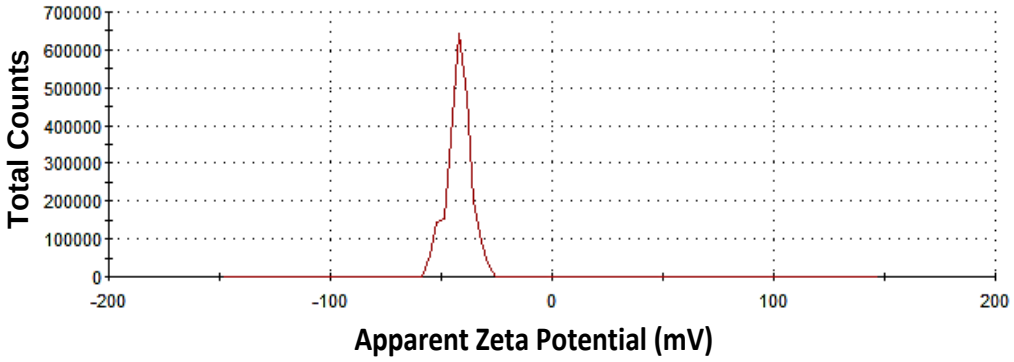

8.1.2 PLGA MPs prepared by double emulsion

8.1.2.1 PLGA MPs: 1.3 % PLGA, Surfactant: 1 % PVA

8.1.2.1.1 TEM

Batches

1 **2** **3**

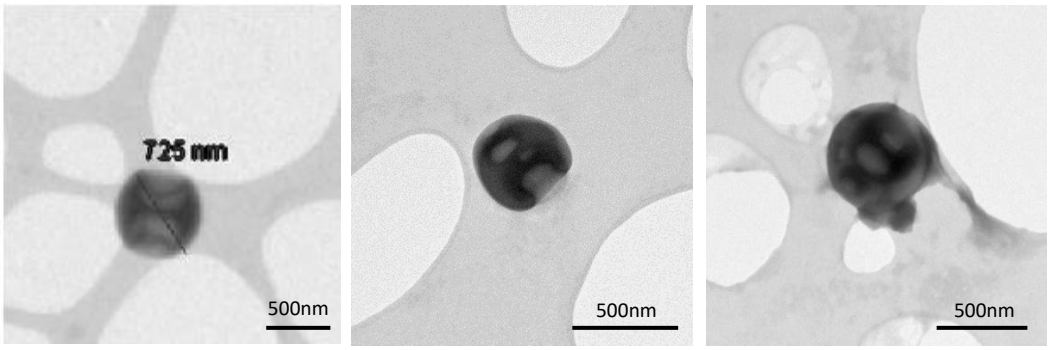

8.1.2.1.2 DLS

Batch 1

			Size (d.nm):	% Intensity:	St Dev (d.nm):
Z-Average (d.nm):	2027	Peak 1:	351.6	100.0	20.66
PdI:	1.000	Peak 2:	0.000	0.0	0.000
Intercept:	1.04	Peak 3:	0.000	0.0	0.000

Result quality Refer to quality report

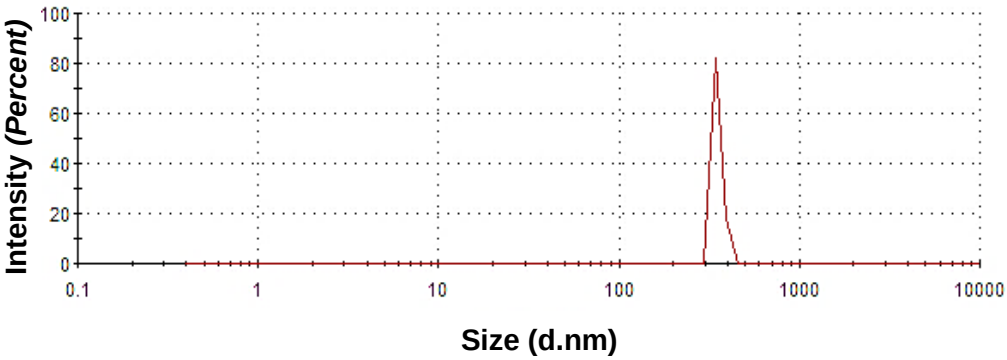

Batch 2

			Size (d.nm):	% Intensity:	St Dev (d.nm):
Z-Average (d.nm):	2597	Peak 1:	220.2	100.0	0.000
PdI:	1.000	Peak 2:	0.000	0.0	0.000
Intercept:	1.17	Peak 3:	0.000	0.0	0.000

Result quality : Refer to quality report

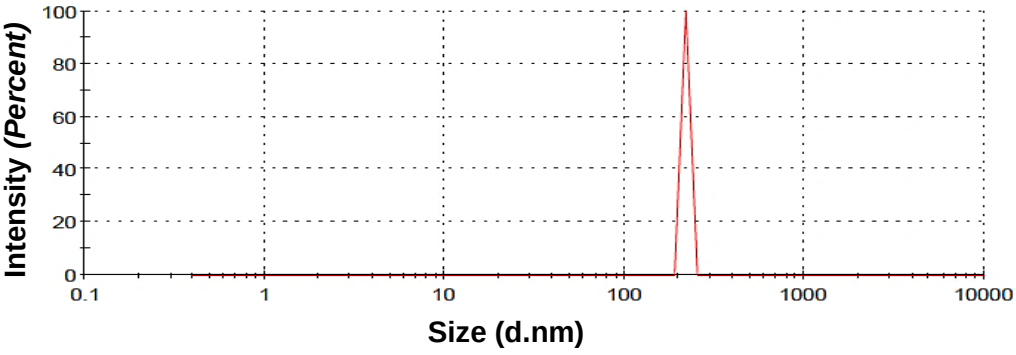

Batch 3

			Size (d.nm):	% Intensity:	St Dev (d.nm):
Z-Average (d.nm):	3798	Peak 1:	60.45	100.0	3.575
PdI:	1.000	Peak 2:	0.000	0.0	0.000
Intercept:	1.10	Peak 3:	0.000	0.0	0.000

Result quality : Refer to quality report

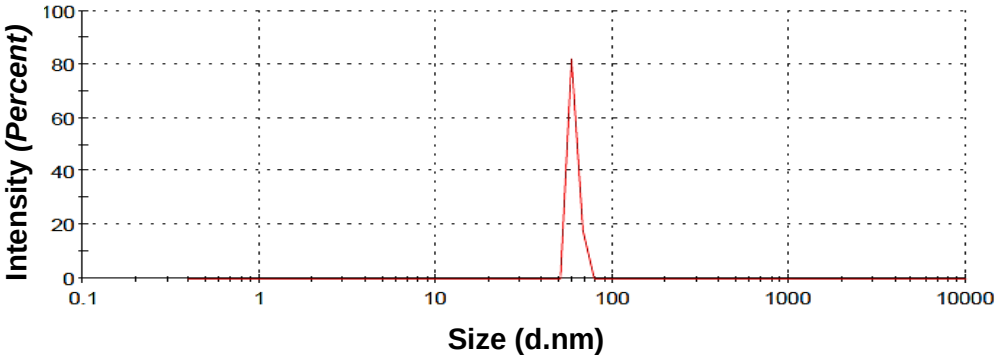

8.1.2.2 PLGA MPs: 0.5 % PLGA, Surfactant: 1 % PVA

8.1.2.2.1 TEM

Batches

1 **2**

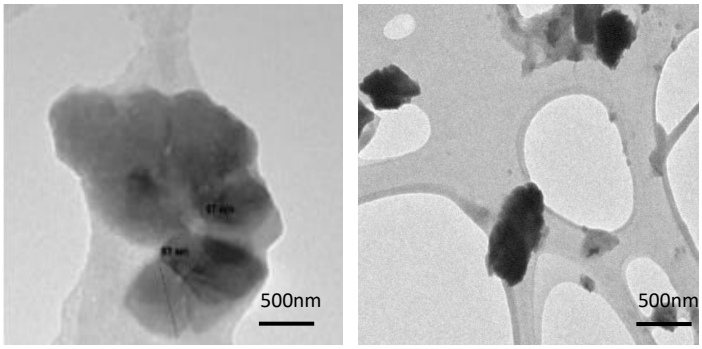

8.1.2.2.2 DLS

Batch 1

			Size (d.nm):	% Intensity:	St Dev (d.nm):
Z-Average (d.nm):	987.7	Peak 1:	1050	100.0	156.4
PdI:	0.101	Peak 2:	0.000	0.0	0.000
Intercept:	0.934	Peak 3:	0.000	0.0	0.000

Result quality : Refer to quality report

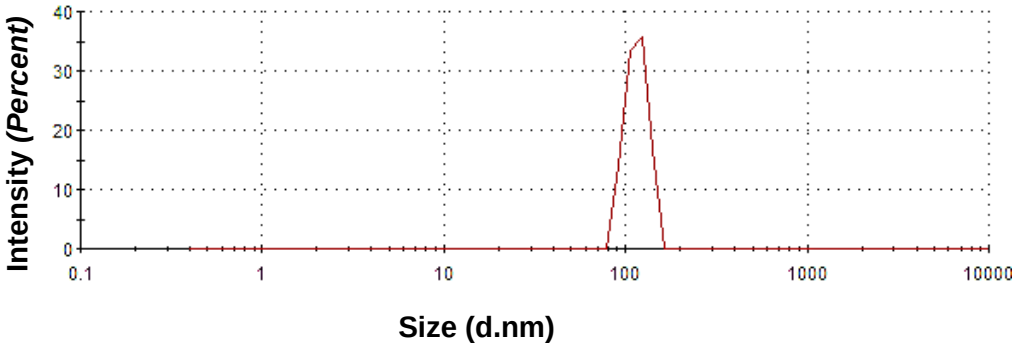

Batch 2

			Size (d.nm):	% Intensity:	St Dev (d.nm):
Z-Average (d.nm):	657.3	Peak 1:	347.3	100.0	53.93
PdI:	0.543	Peak 2:	0.000	0.0	0.000
Intercept:	0.970	Peak 3:	0.000	0.0	0.000

Result quality : Refer to quality report

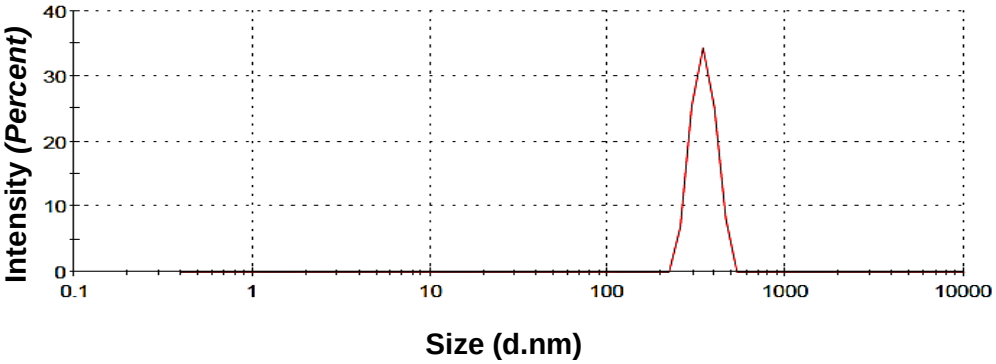

Batch 3

			Size (d.nm):	% Intensity:	St Dev (d.nm):
Z-Average (d.nm):	958.5	Peak 1:	1043	100.0	152.5
PdI:	0.185	Peak 2:	0.000	0.0	0.000
Intercept:	0.942	Peak 3:	0.000	0.0	0.000

Result quality : Refer to quality report

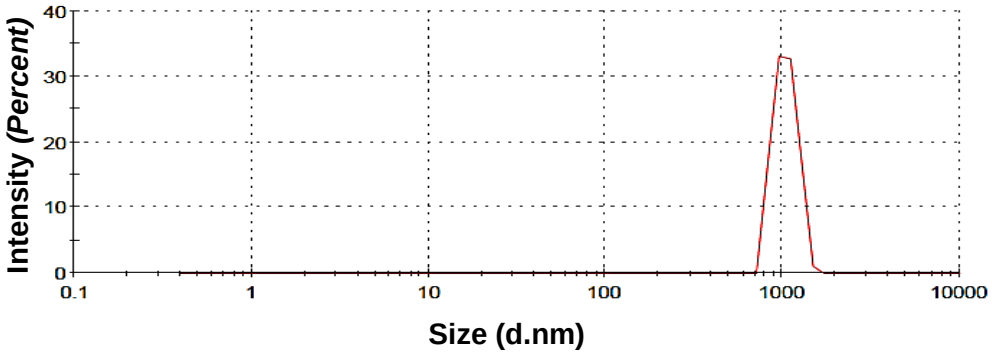

8.1.2.2.3 Zeta potential: Representative Surface charge for PLGA MPs 1.3 % PLGA, 1 % PVA and 0.5 % PLGA, 1 % PVA

Batch 1

			Mean (mV)	Area (%)	St Dev (mV)
Zeta Potential (mV):	-38.6	Peak 1:	-38.6	100.0	5.06
Zeta Deviation (mV):	5.06	Peak 2:	0.00	0.0	0.00
Conductivity (mS/cm):	0.00256	Peak 3:	0.00	0.0	0.00

Result quality : Good

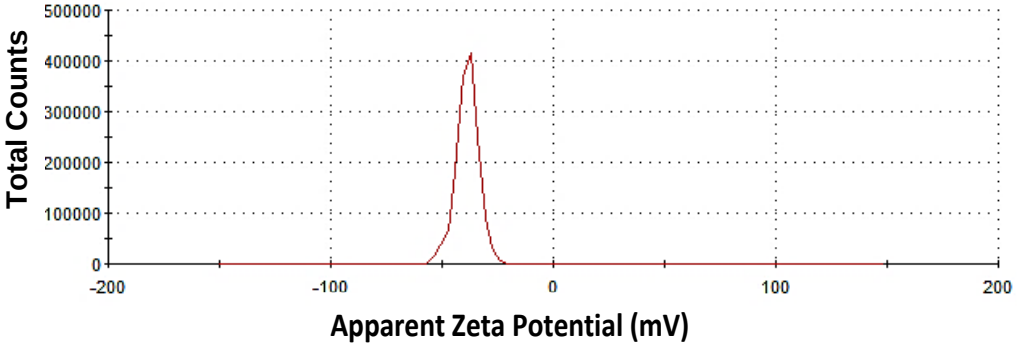

Batch 2

			Mean (mV)	Area (%)	St Dev (mV)
Zeta Potential (mV):	-40.6	Peak 1:	-41.9	95.4	5.34
Zeta Deviation (mV):	8.15	Peak 2:	-7.72	3.1	2.35
Conductivity (mS/cm):	0.00167	Peak 3:	-24.0	1.4	2.53

Result quality : Good

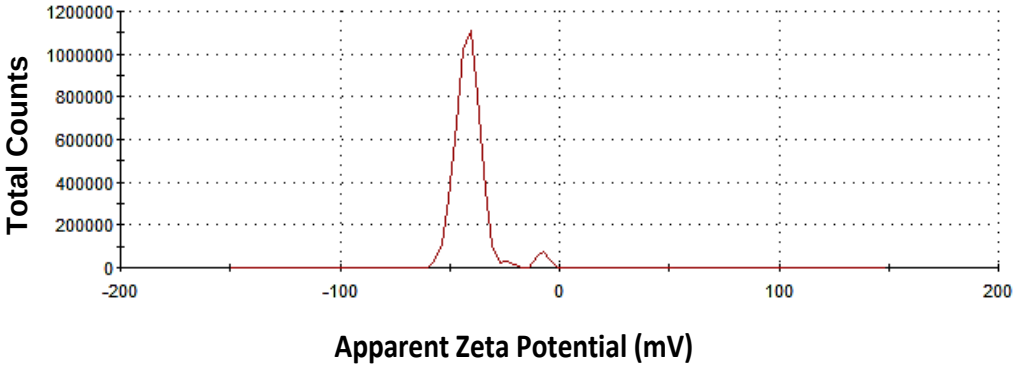

Batch 3

			Mean (mV)	Area (%)	St Dev (mV)
Zeta Potential (mV):	-42.3	Peak 1:	-42.3	100.0	5.88
Zeta Deviation (mV):	5.88	Peak 2:	0.00	0.0	0.00
Conductivity (mS/cm):	0.00429	Peak 3:	0.00	0.0	0.00

Result quality : Good

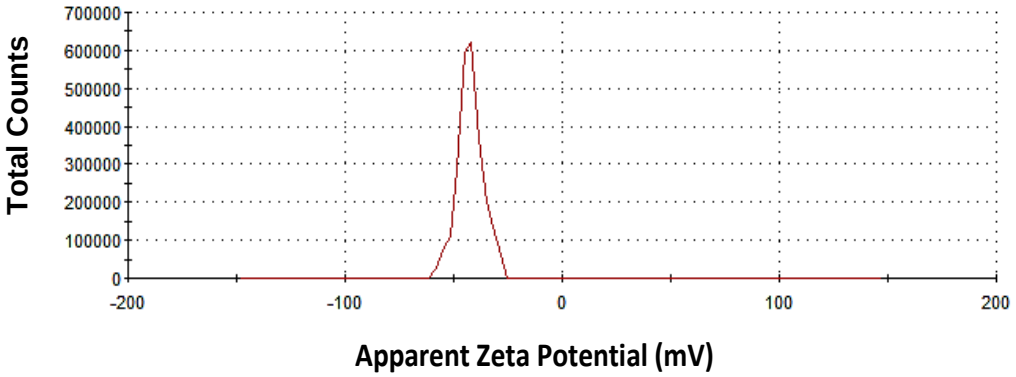

8.1.2.3 PLGA MPs: 1.3 % PLGA, Surfactant: 3 % PVA

8.1.2.3.1 TEM

Batches

1 **2** **3**

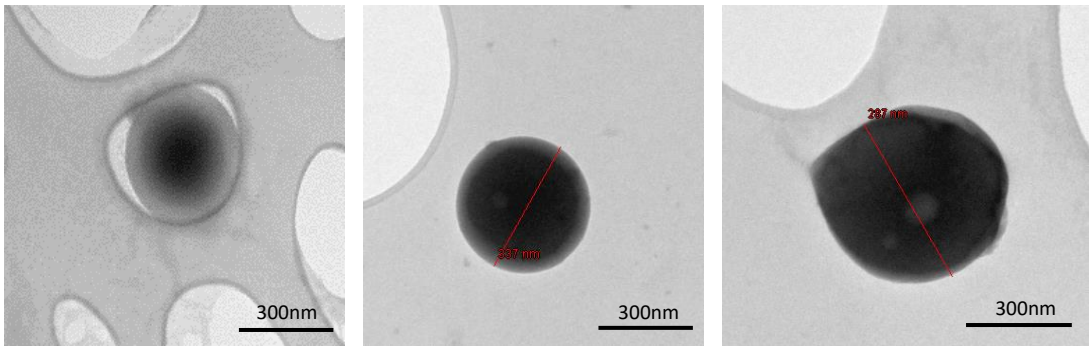

8.1.2.3.2 DLS

Batch 1

			Size (d.nm):	% Number:	St Dev (d.nm):
Z-Average (d.nm):	366.9	Peak 1:	354.2	100.0	96.70
PdI:	0.168	Peak 2:	0.000	0.0	0.000
Intercept:	0.964	Peak 3:	0.000	0.0	0.000
Result quality :	Good				

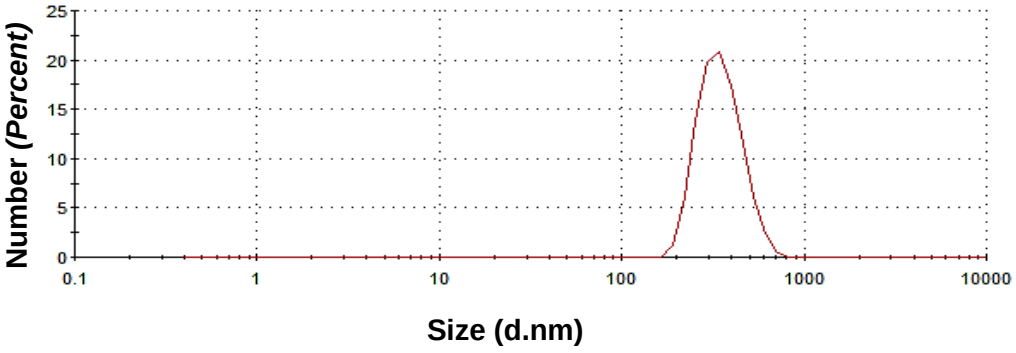

Batch 2

		Size (d.nm):	% Number:	St Dev (d.nm):
Z-Average (d.nm): 352.3	Peak 1:	348.3	100.0	87.32
PdI: 0.158	Peak 2:	0.000	0.0	0.000
Intercept: 0.943	Peak 3:	0.000	0.0	0.000

Result quality : Good

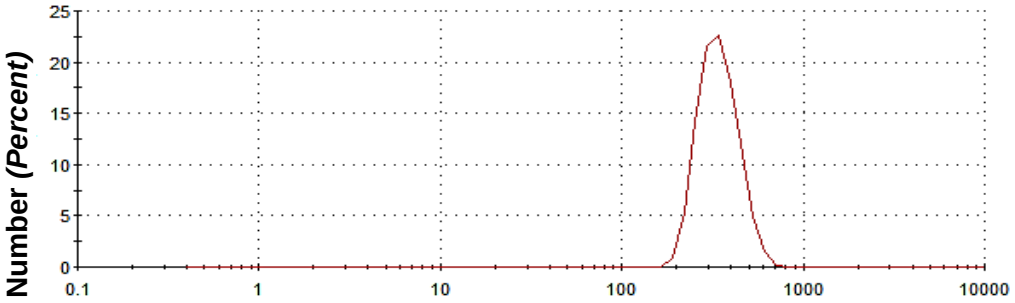

Size (d.nm)

Batch 3

		Size (d.nm):	% Number:	St Dev (d.nm):
Z-Average (d.nm): 335.7	Peak 1:	344.9	100.0	77.01
PdI: 0.157	Peak 2:	0.000	0.0	0.000
Intercept: 0.935	Peak 3:	0.000	0.0	0.000

Result quality : Good

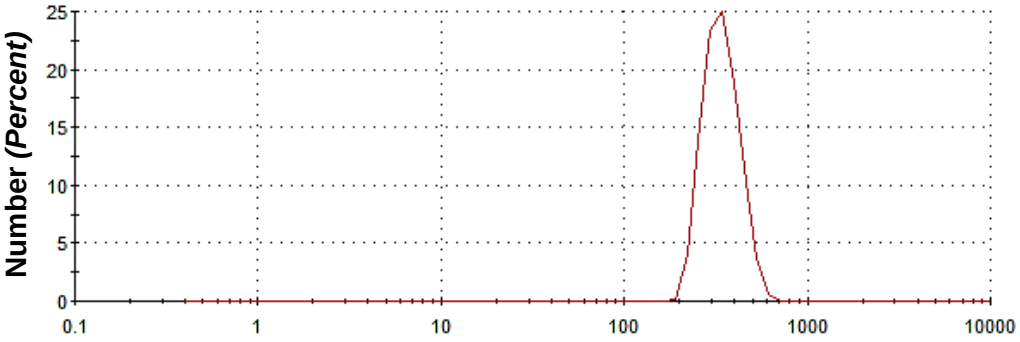

Size (d.nm)

8.1.2.3.3 Zeta potential: Comparision between blank and pDNA encapsulated PLGA MPs

8.1.2.3.3.1 **Blank PLGA MPs**

Batch 1

		Mean (mV)	Area (%)	St Dev (mV)
Zeta Potential (mV): -21.4	Peak 1:	-21.4	100.0	4.62
Zeta Deviation (mV): 4.62	Peak 2:	0.00	0.0	0.00
Conductivity (mS/cm): 0.00399	Peak 3:	0.00	0.0	0.00

Result quality : Good

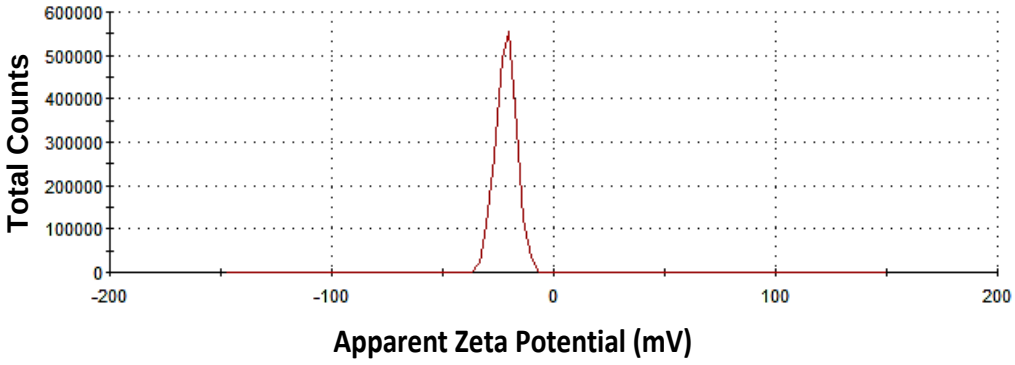

Batch 2

		Mean (mV)	Area (%)	St Dev (mV)
Zeta Potential (mV): -22.8	Peak 1:	-22.8	100.0	4.05
Zeta Deviation (mV): 4.05	Peak 2:	0.00	0.0	0.00
Conductivity (mS/cm): 0.00399	Peak 3:	0.00	0.0	0.00

Result quality : Good

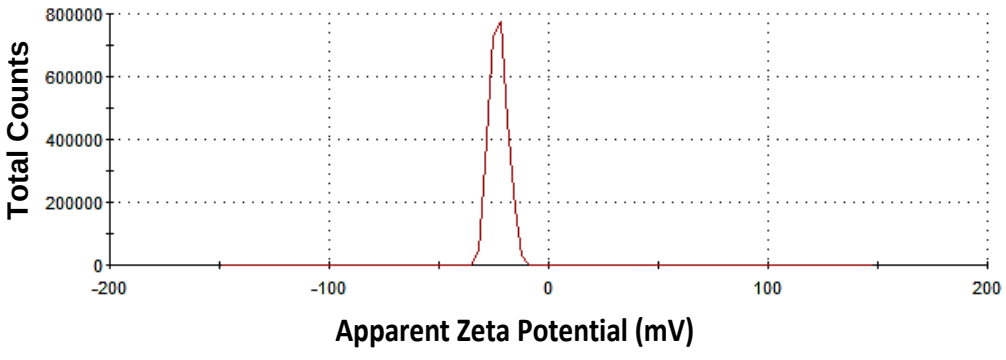

Batch 3

		Mean (mV)	Area (%)	St Dev (mV)
Zeta Potential (mV): -20.9	Peak 1:	-20.9	100.0	3.35
Zeta Deviation (mV): 3.35	Peak 2:	0.00	0.0	0.00
Conductivity (mS/cm): 0.00325	Peak 3:	0.00	0.0	0.00

Result quality : Good

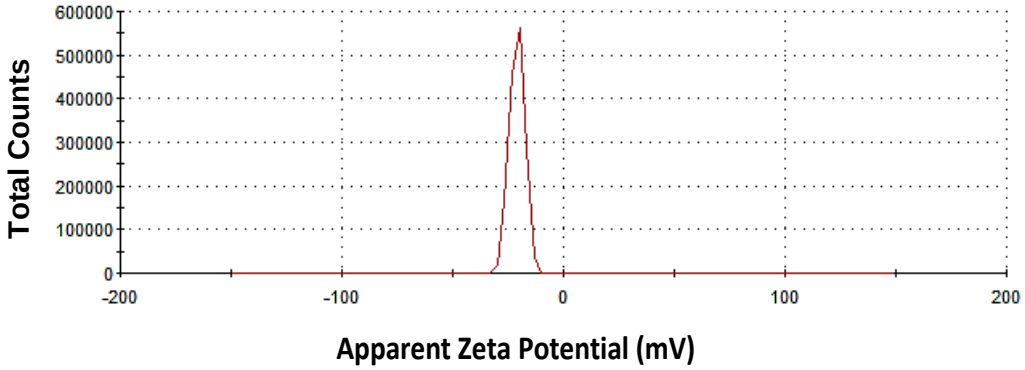

8.1.2.3.3.2 **pDNA encapsulad PLGA MPs**

Batch 1

		Mean (mV)	Area (%)	St Dev (mV)
Zeta Potential (mV): -22.0	Peak 1:	-22.0	100.0	3.65
Zeta Deviation (mV): 3.65	Peak 2:	0.00	0.0	0.00
Conductivity (mS/cm): 0.00263	Peak 3:	0.00	0.0	0.00

Result quality : Good

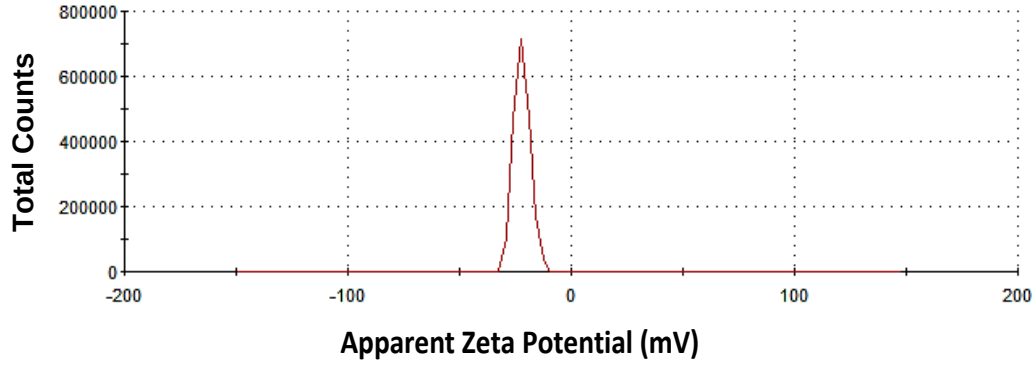

Batch 2

		Mean (mV)	Area (%)	St Dev (mV)
Zeta Potential (mV): -24.6	Peak 1:	-24.6	100.0	3.62
Zeta Deviation (mV): 3.62	Peak 2:	0.00	0.0	0.00
Conductivity (mS/cm): 0.00227	Peak 3:	0.00	0.0	0.00

Result quality : Good

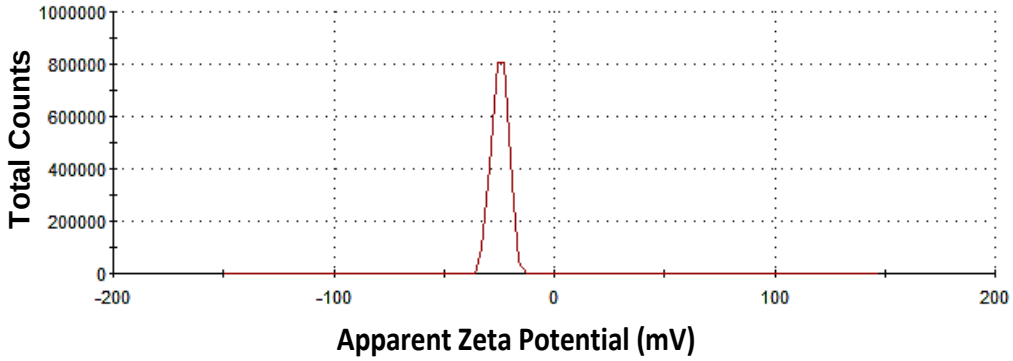

Batch 3

		Mean (mV)	Area (%)	St Dev (mV)
Zeta Potential (mV): -23.3	Peak 1:	-23.3	100.0	3.87
Zeta Deviation (mV): 3.87	Peak 2:	0.00	0.0	0.00
Conductivity (mS/cm): 0.00204	Peak 3:	0.00	0.0	0.00

Result quality : Good

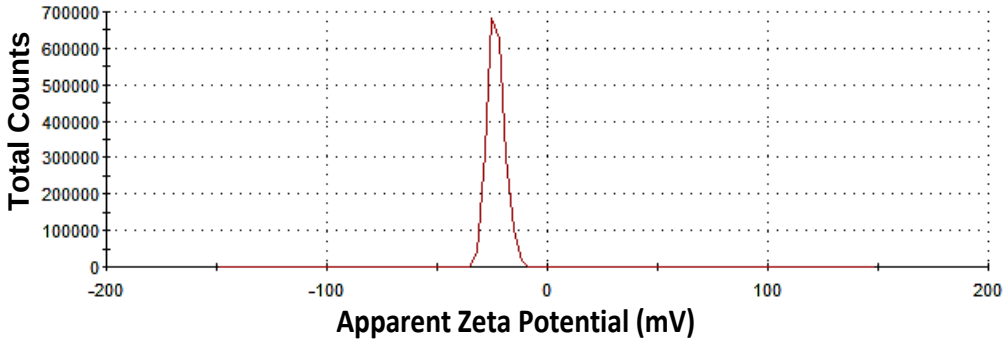

8.1.3 pDNA NP/MPs: Condensation with alcohol

8.1.3.1 TEM

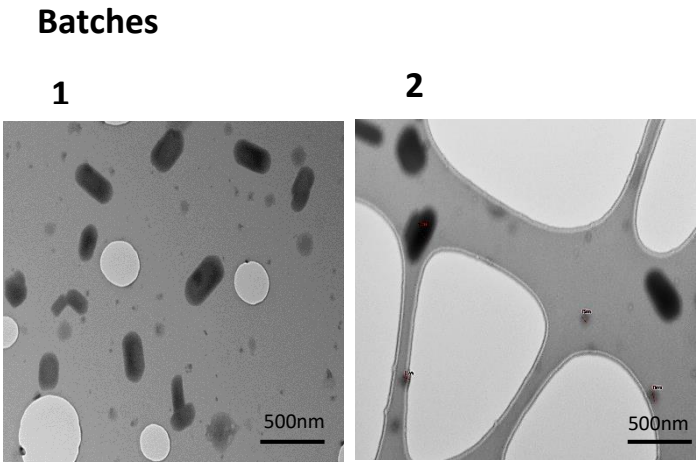

8.1.3.2 DLS

Batch 1

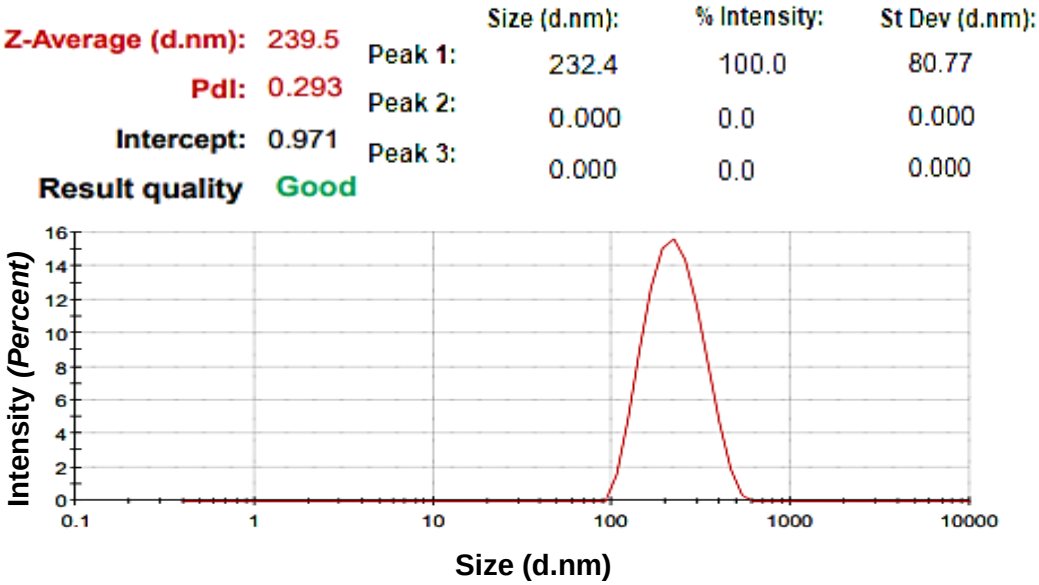

Batch 2

			Size (d.nm):	% Intensity:	St Dev (d.nm):
Z-Average (d.nm):	348.4	Peak 1:	438.3	68.5	104.9
PdI:	0.466	Peak 2:	108.6	31.5	22.16
Intercept:	0.944	Peak 3:	0.000	0.0	0.000

Result quality : Refer to quality report

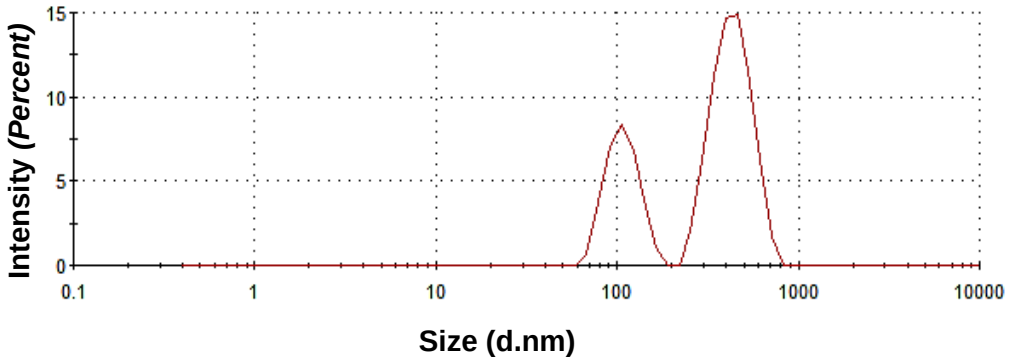

Batch 3

			Size (d.nm):	% Intensity:	St Dev (d.nm):
Z-Average (d.nm):	248.7	Peak 1:	521.3	76.8	219.1
PdI:	0.577	Peak 2:	95.46	14.7	29.47
Intercept:	0.891	Peak 3:	16.84	6.0	3.937

Result quality : Refer to quality report

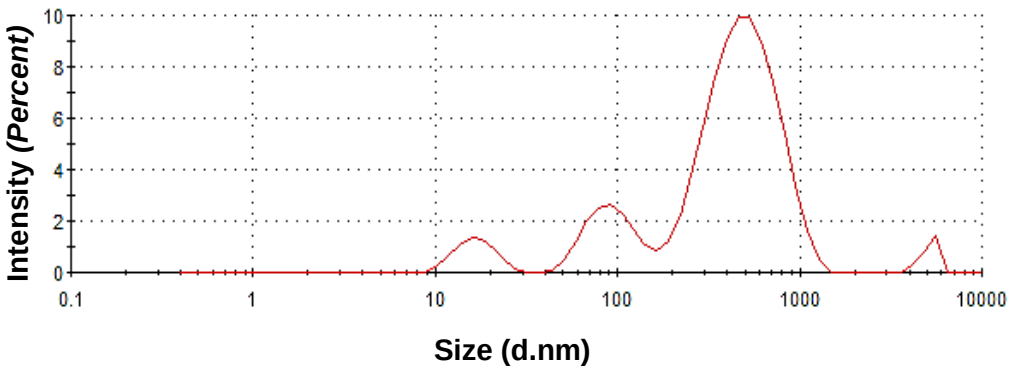

8.1.4 High Mw PLL

8.1.4.1 Charge ratio 1

8.1.4.1.1 DLS

Batch 1

			Size (d.nm):	% Intensity:	St Dev (d.nm):
Z-Average (d.nm):	95.53	Peak 1:	95.26	98.6	50.32
PdI:	0.299	Peak 2:	15.94	1.4	2.506
Intercept:	0.946	Peak 3:	0.000	0.0	0.000

Result quality : Refer to quality report

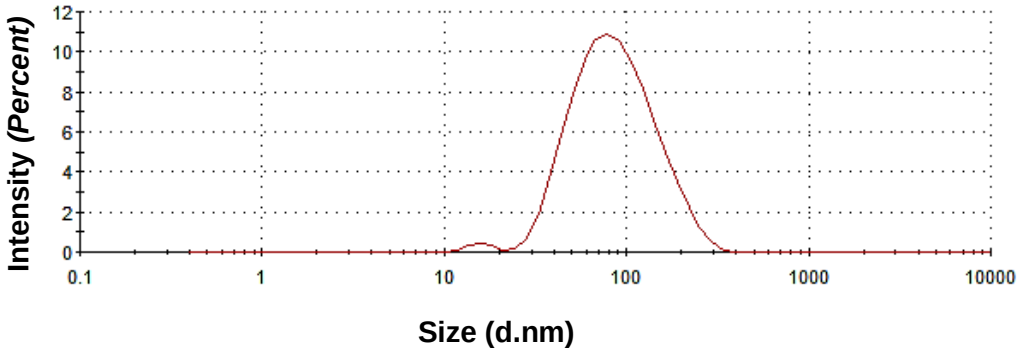

Batch 2

			Size (d.nm):	% Intensity:	St Dev (d.nm):
Z-Average (d.nm):	87.88	Peak 1:	103.9	81.6	71.41
PdI:	0.397	Peak 2:	684.4	16.4	346.9
Intercept:	0.937	Peak 3:	4312	2.1	990.0

Result quality : Good

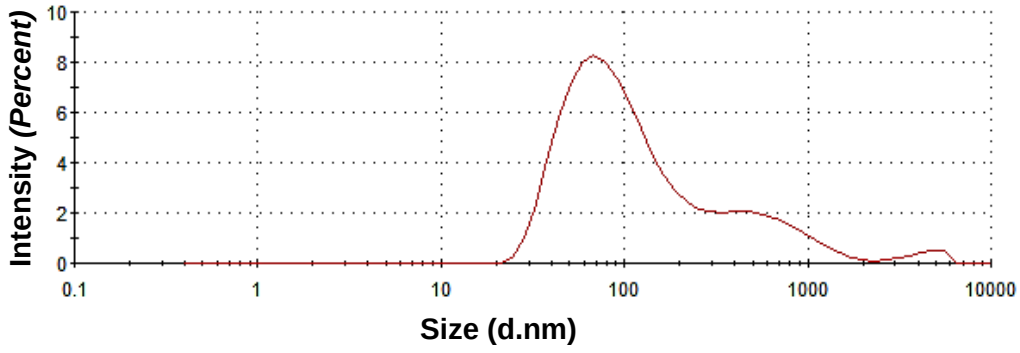

Batch 3

			Size (d.nm):	% Intensity:	St Dev (d.nm):
Z-Average (d.nm):	133.5	Peak 1:	156.4	92.4	90.41
PdI:	0.340	Peak 2:	4366	7.6	937.7
Intercept:	0.951	Peak 3:	0.000	0.0	0.000

Result quality : Good

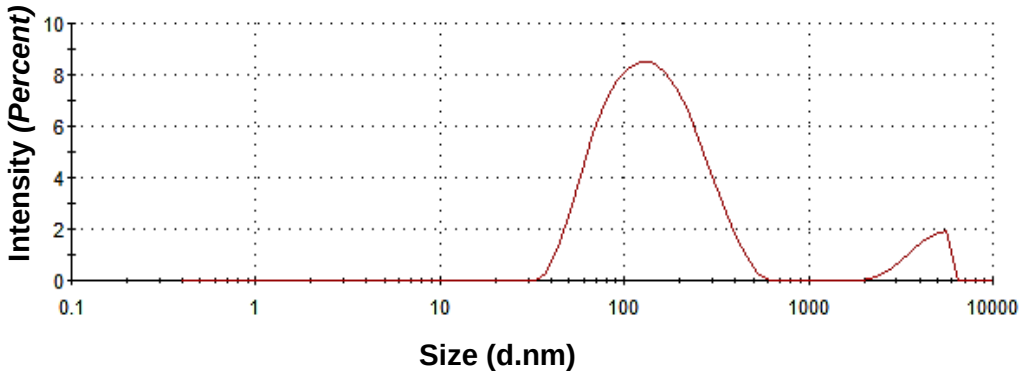

8.1.4.2 Charge ratio 3

8.1.4.2.1 DLS

Batch 1

			Size (d.nm):	% Intensity:	St Dev (d.nm):
Z-Average (d.nm):	105.0	Peak 1:	55.40	52.8	20.07
PdI:	0.384	Peak 2:	209.8	47.2	67.95
Intercept:	0.923	Peak 3:	0.000	0.0	0.000

Result quality : Refer to quality report

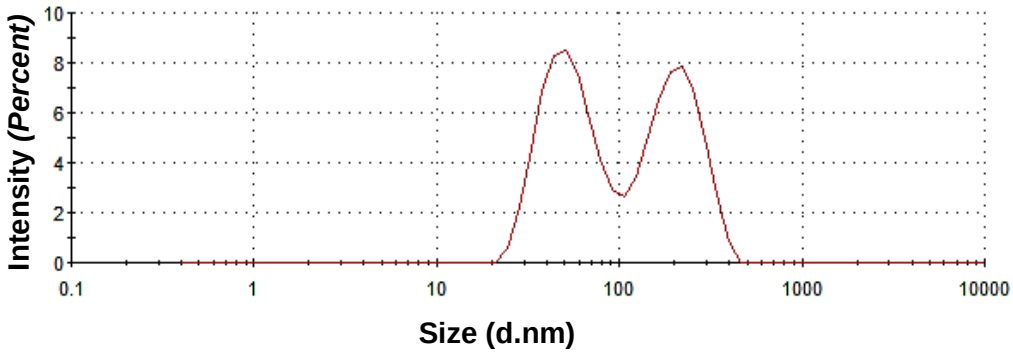

Batch 2

			Size (d.nm):	% Intensity:	St Dev (d.nm):
Z-Average (d.nm):	88.41	Peak 1:	87.16	78.6	39.09
PdI:	0.501	Peak 2:	918.5	16.0	385.4
Intercept:	0.934	Peak 3:	4520	5.5	919.9
Result quality :	Good				

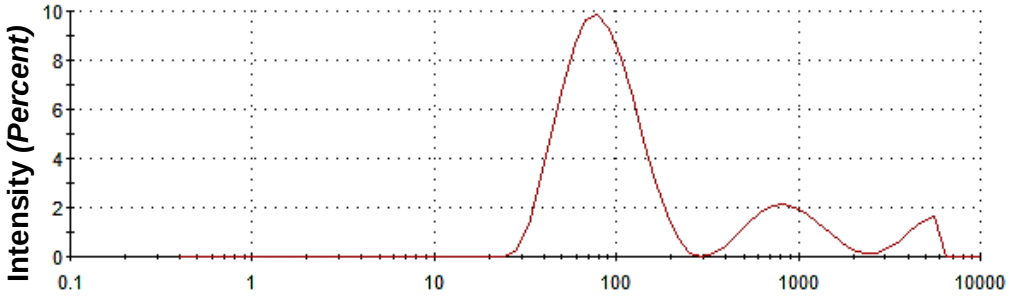

Size (d.nm)

Batch 3

			Size (d.nm):	% Intensity:	St Dev (d.nm):
Z-Average (d.nm):	78.68	Peak 1:	80.54	79.9	41.80
PdI:	0.370	Peak 2:	420.4	17.1	171.9
Intercept:	0.939	Peak 3:	4687	3.1	792.6
Result quality :	Good				

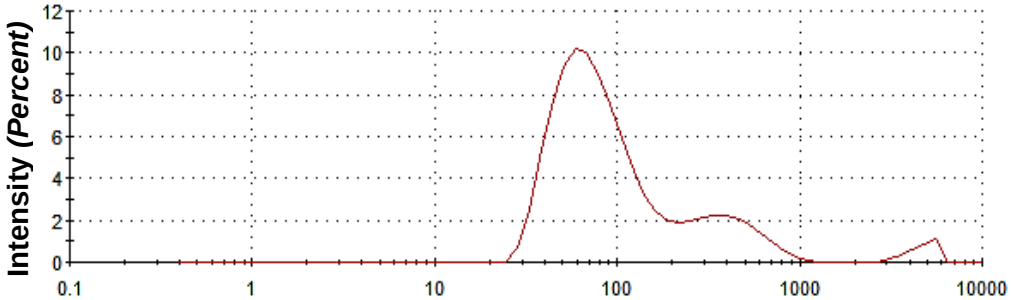

Size (d.nm)

8.1.4.3 Charge ratio 6

8.1.4.3.1 DLS

Batch 1

			Size (d.nm):	% Intensity:	St Dev (d.nm):
Z-Average (d.nm):	103.2	Peak 1:	66.36	70.4	25.81
PdI:	0.288	Peak 2:	280.7	29.6	94.06
Intercept:	0.919	Peak 3:	0.000	0.0	0.000

Result quality : Refer to quality report

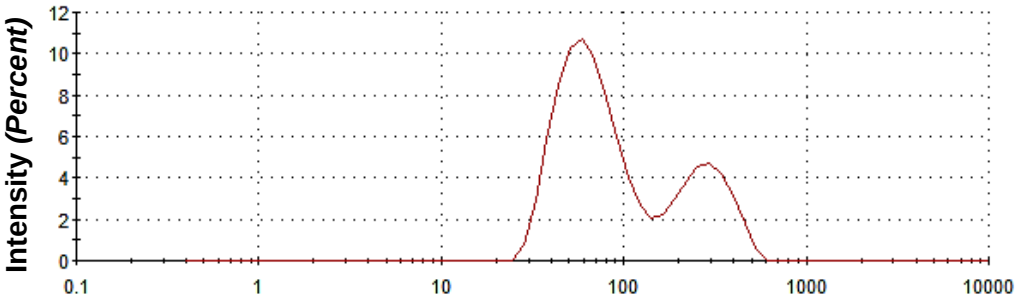

Size (d.nm)

Batch 2

			Size (d.nm):	% Intensity:	St Dev (d.nm):
Z-Average (d.nm):	104.0	Peak 1:	80.18	59.5	37.37
PdI:	0.476	Peak 2:	511.8	39.1	247.5
Intercept:	0.913	Peak 3:	4993	1.4	613.5

Result quality : Good

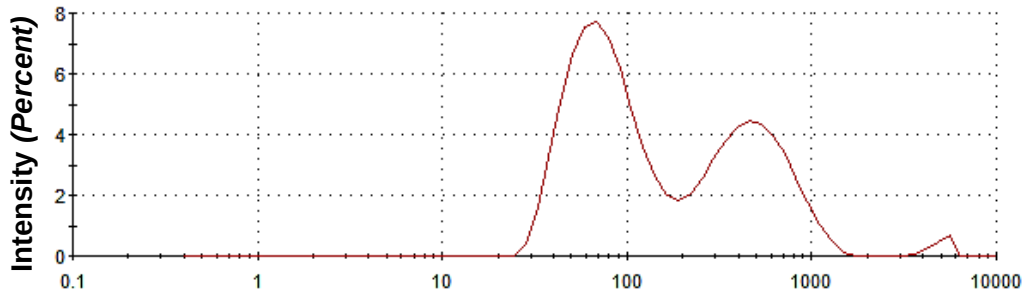

Size (d.nm)

Batch 3

			Size (d.nm):	% Intensity:	St Dev (d.nm):
Z-Average (d.nm):	119.0	Peak 1:	123.5	84.6	52.52
PdI:	0.344	Peak 2:	2345	15.4	1175
Intercept:	0.962	Peak 3:	0.000	0.0	0.000
Result quality :	Good				

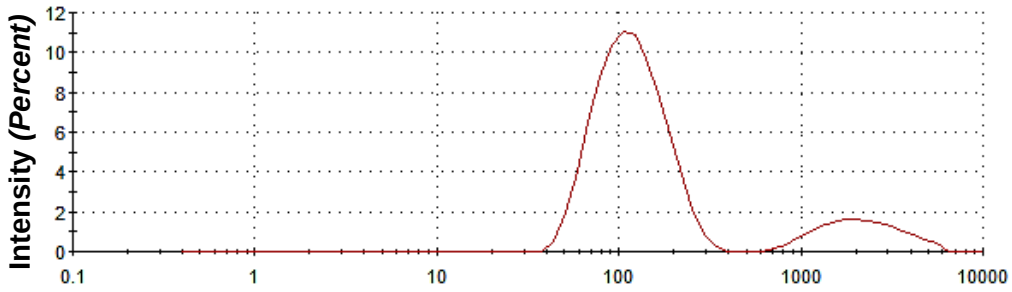

8.1.4.4 Charge ratio 9

8.1.4.4.1 DLS

Batch 1

			Size (d.nm):	% Intensity:	St Dev (d.nm):
Z-Average (d.nm):	195.2	Peak 1:	253.7	95.3	162.2
PdI:	0.399	Peak 2:	4965	4.7	630.4
Intercept:	0.947	Peak 3:	0.000	0.0	0.000
Result quality :	Good				

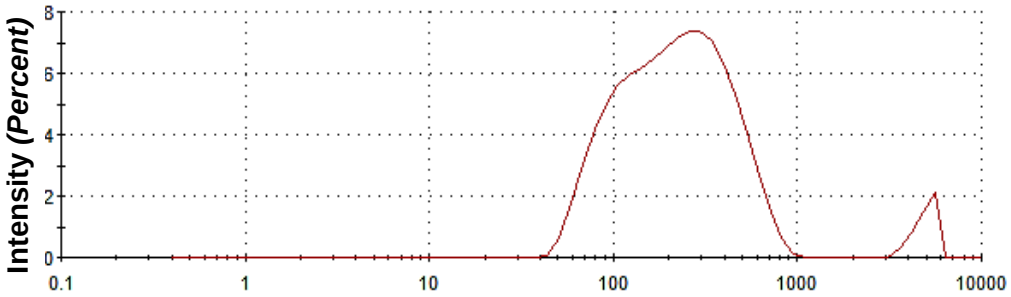

Batch 2

		Size (d.nm):	% Intensity:	St Dev (d.nm):
Z-Average (d.nm): 102.5	Peak 1:	108.4	100.0	25.47
PdI: 0.191	Peak 2:	0.000	0.0	0.000
Intercept: 0.933	Peak 3:	0.000	0.0	0.000

Result quality : Good

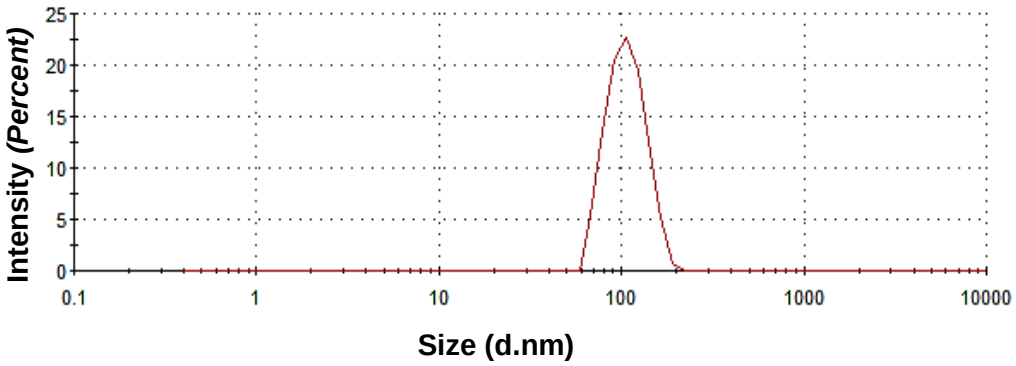

Batch 3

		Size (d.nm):	% Intensity:	St Dev (d.nm):
Z-Average (d.nm): 111.1	Peak 1:	150.7	96.0	104.6
PdI: 0.336	Peak 2:	4336	4.0	969.5
Intercept: 0.931	Peak 3:	0.000	0.0	0.000

Result quality : Good

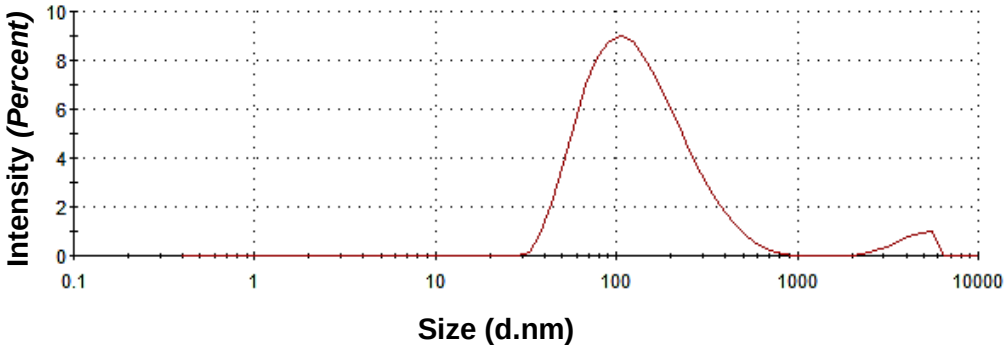

8.1.4.5 Charge ratio 12

8.1.4.5.1 DLS

Batch 1

			Size (d.nm):	% Intensity:	St Dev (d.nm):
Z-Average (d.nm):	284.1	Peak 1:	222.1	58.2	107.1
PdI:	0.698	Peak 2:	876.1	35.0	355.0
Intercept:	0.956	Peak 3:	4995	6.7	614.5

Result quality : Good

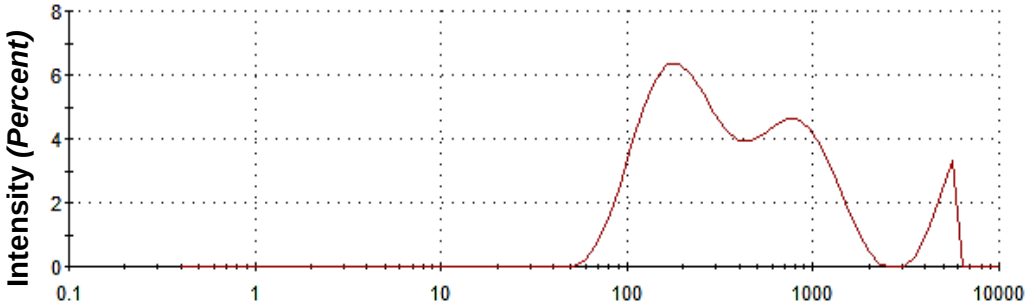

Size (d.nm)

Batch 2

			Size (d.nm):	% Intensity:	St Dev (d.nm):
Z-Average (d.nm):	393.4	Peak 1:	374.6	65.8	112.0
PdI:	0.509	Peak 2:	4116	25.4	999.1
Intercept:	0.966	Peak 3:	68.14	8.8	12.56

Result quality : Refer to quality report

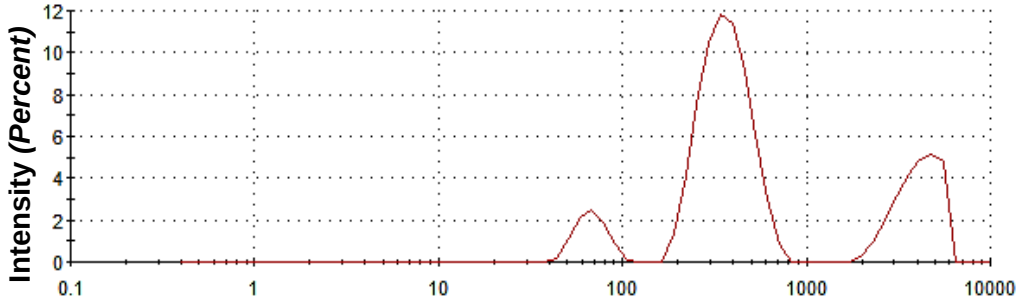

Size (d.nm)

Batch 3

		Size (d.nm):	% Intensity:	St Dev (d.nm):
Z-Average (d.nm): 285.1	Peak 1:	152.5	48.5	54.57
PdI: 0.626	Peak 2:	671.2	47.4	243.4
Intercept: 0.953	Peak 3:	5367	4.1	330.0
Result quality : Good				

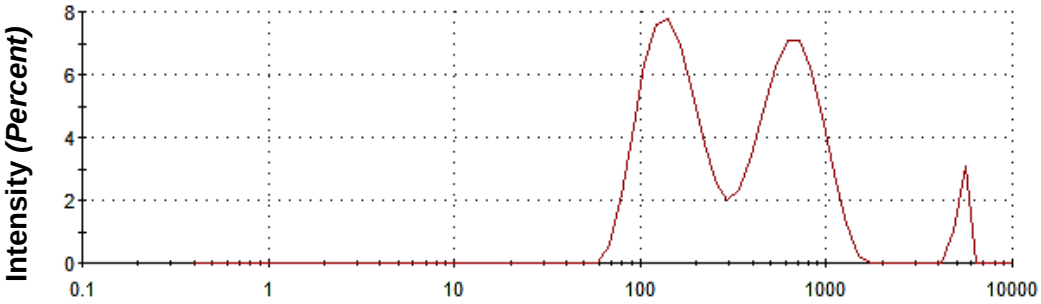

Size (d.nm)

8.1.5 Low Mw PLL

8.1.5.1 Charge ratio 1

8.1.5.1.1 DLS

Batch 1

		Size (d.nm):	% Intensity:	St Dev (d.nm):
Z-Average (d.nm): 1606	Peak 1:	1389	100.0	323.3
PdI: 0.247	Peak 2:	0.000	0.0	0.000
Intercept: 0.944	Peak 3:	0.000	0.0	0.000
Result quality : Refer to quality report				

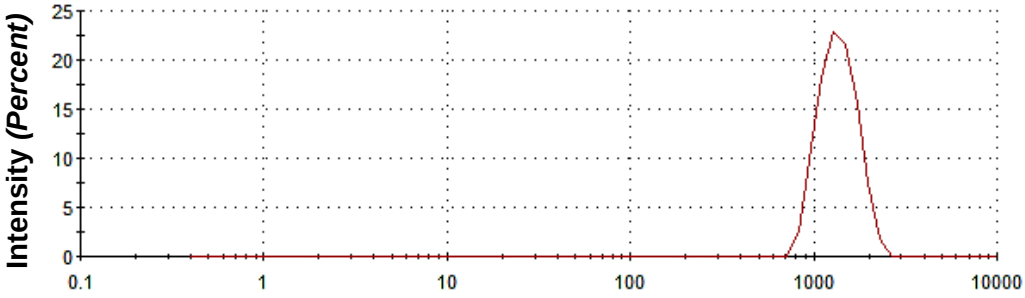

Size (d.nm)

Batch 2

			Size (d.nm):	% Intensity:	St Dev (d.nm):
Z-Average (d.nm):	1667	Peak 1:	1302	94.6	349.3
PdI:	0.332	Peak 2:	5392	5.4	314.8
Intercept:	0.943	Peak 3:	0.000	0.0	0.000

Result quality : Refer to quality report

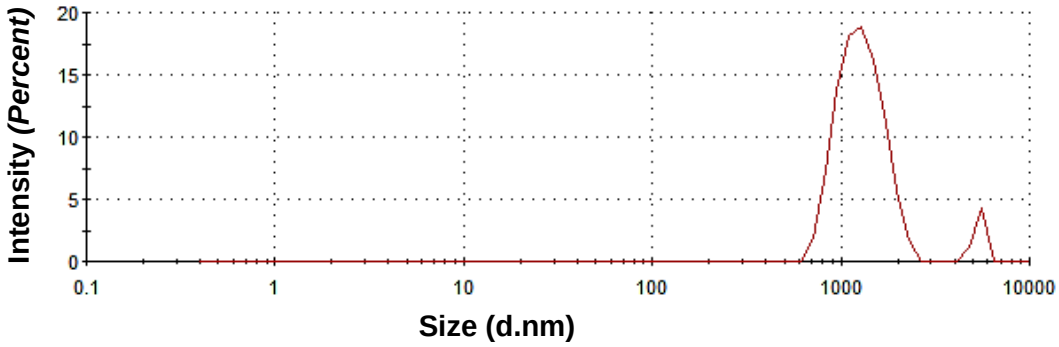

Batch 3

			Size (d.nm):	% Intensity:	St Dev (d.nm):
Z-Average (d.nm):	1622	Peak 1:	1430	94.0	437.7
PdI:	0.253	Peak 2:	5243	6.0	448.2
Intercept:	0.934	Peak 3:	0.000	0.0	0.000

Result quality : Good

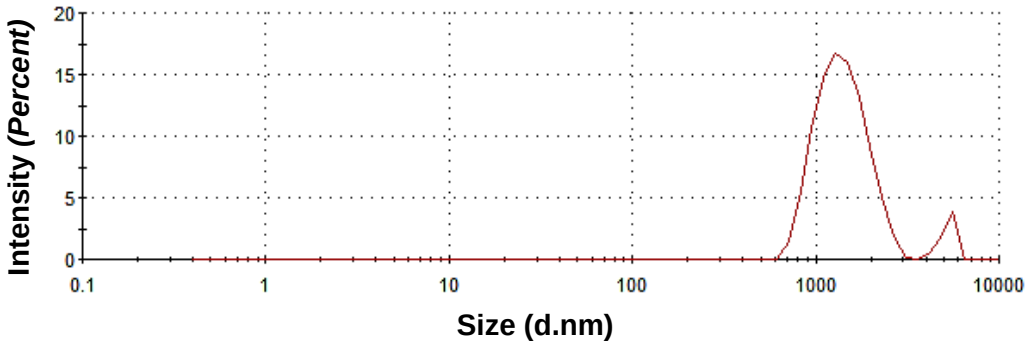

8.1.5.2 Charge ratio 3

8.1.5.2.1 DLS

Batch 1

		Size (d.nm):	% Number:	St Dev (d.nm):
Z-Average (d.nm): 124.5	Peak 1:	83.61	100.0	27.18
PdI: 0.121	Peak 2:	0.000	0.0	0.000
Intercept: 0.952	Peak 3:	0.000	0.0	0.000

Result quality : Good

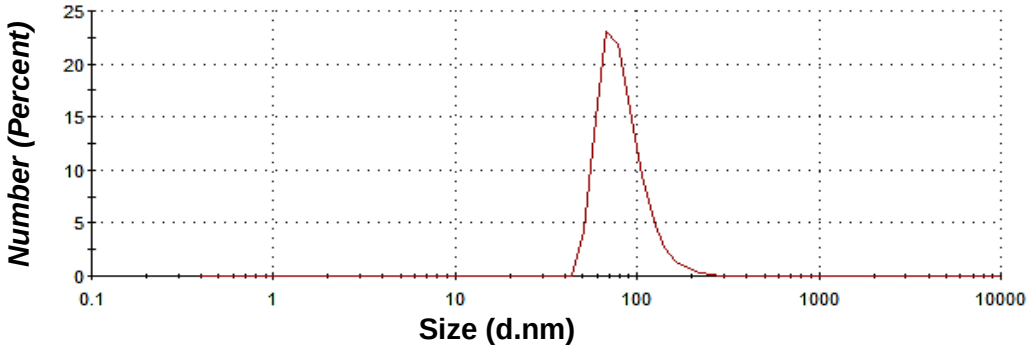

Batch 2

		Size (d.nm):	% Number:	St Dev (d.nm):
Z-Average (d.nm): 126.0	Peak 1:	84.42	100.0	27.90
PdI: 0.117	Peak 2:	0.000	0.0	0.000
Intercept: 0.953	Peak 3:	0.000	0.0	0.000

Result quality : Good

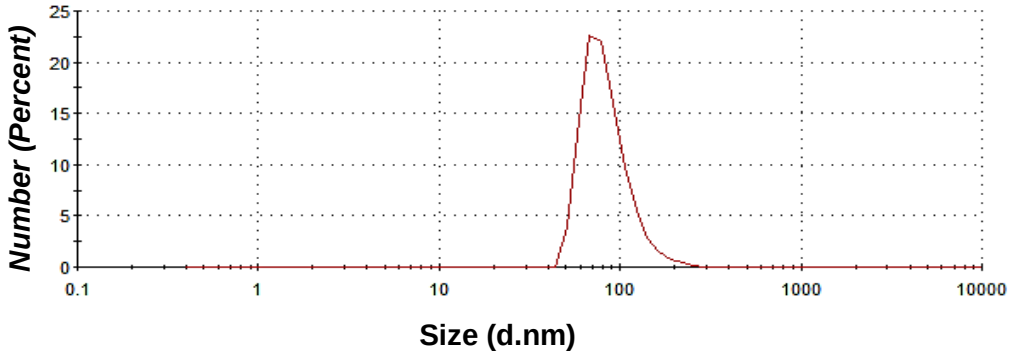

Batch 3

		Size (d.nm):	% Number:	St Dev (d.nm):
Z-Average (d.nm): 102.8	Peak 1:	65.60	100.0	20.29
PdI: 0.136	Peak 2:	0.000	0.0	0.000
Intercept: 0.953	Peak 3:	0.000	0.0	0.000

Result quality : Good

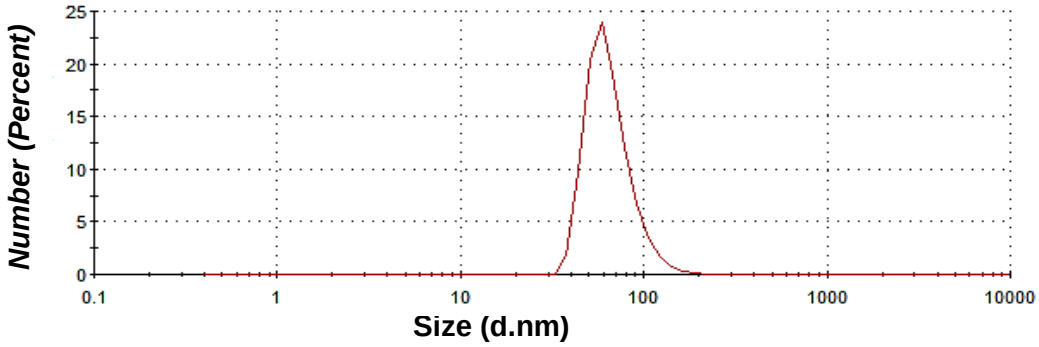

8.1.5.3 Chrge ratio 6

8.1.5.3.1 DLS

Batch 1

		Size (d.nm):	% Number:	St Dev (d.nm):
Z-Average (d.nm): 108.9	Peak 1:	62.91	100.0	21.12
PdI: 0.159	Peak 2:	0.000	0.0	0.000
Intercept: 0.930	Peak 3:	0.000	0.0	0.000

Result quality : Good

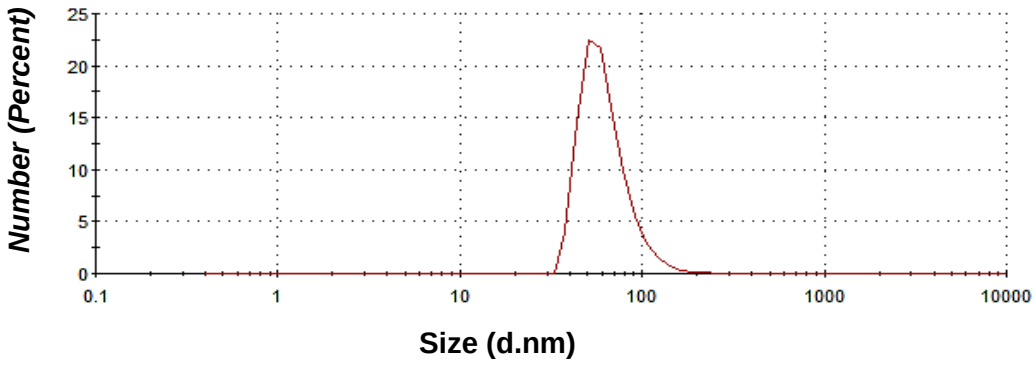

Batch 2

			Size (d.nm):	% Number:	St Dev (d.nm):
Z-Average (d.nm):	91.40	Peak 1:	73.40	100.0	17.27
PdI:	0.034	Peak 2:	0.000	0.0	0.000
Intercept:	0.958	Peak 3:	0.000	0.0	0.000

Result quality : Good

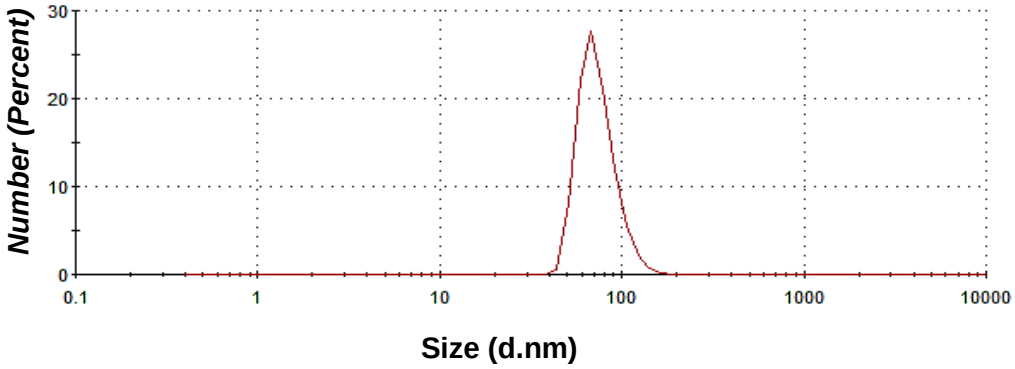

Batch 3

			Size (d.nm):	% Number:	St Dev (d.nm):
Z-Average (d.nm):	81.49	Peak 1:	66.89	100.0	15.31
PdI:	0.061	Peak 2:	0.000	0.0	0.000
Intercept:	0.933	Peak 3:	0.000	0.0	0.000

Result quality : Good

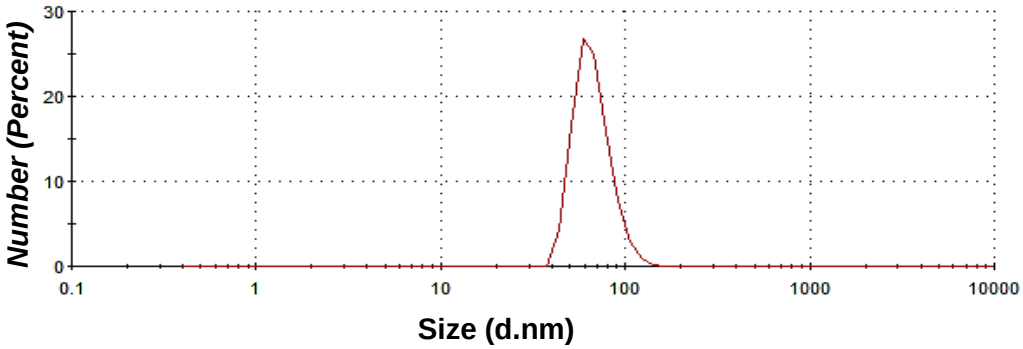

8.1.5.4 Charge ratio 9

8.1.5.4.1 DLS

Batch 1

			Size (d.nm):	% Number:	St Dev (d.nm):
Z-Average (d.nm):	134.0	Peak 1:	59.56	100.0	24.58
PdI:	0.217	Peak 2:	0.000	0.0	0.000
Intercept:	0.946	Peak 3:	0.000	0.0	0.000

Result quality : Good

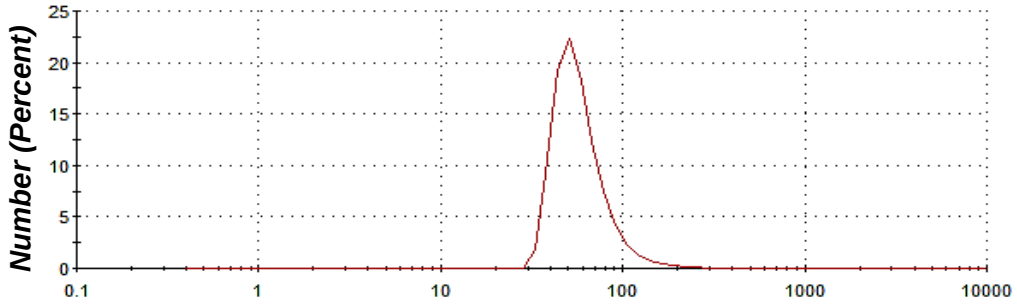

Batch 2

			Size (d.nm):	% Number:	St Dev (d.nm):
Z-Average (d.nm):	81.49	Peak 1:	66.89	100.0	15.31
PdI:	0.061	Peak 2:	0.000	0.0	0.000
Intercept:	0.933	Peak 3:	0.000	0.0	0.000

Result quality : Good

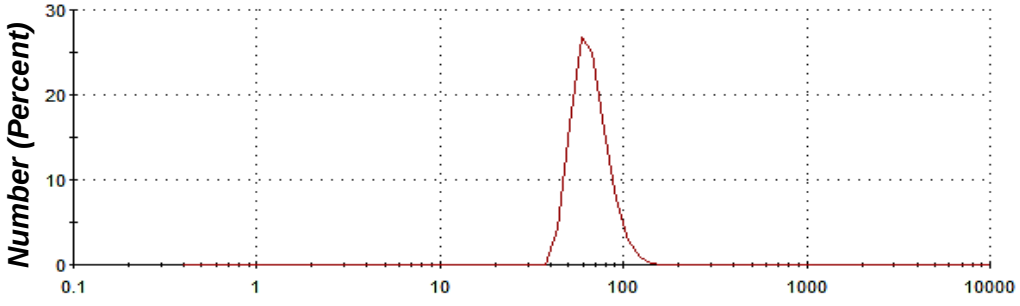

Batch 3

		Size (d.nm):	% Number:	St Dev (d.nm):
Z-Average (d.nm): 78.23	Peak 1:	66.20	100.0	14.17
PdI: 0.029	Peak 2:	0.000	0.0	0.000
Intercept: 0.935	Peak 3:	0.000	0.0	0.000

Result quality : Good

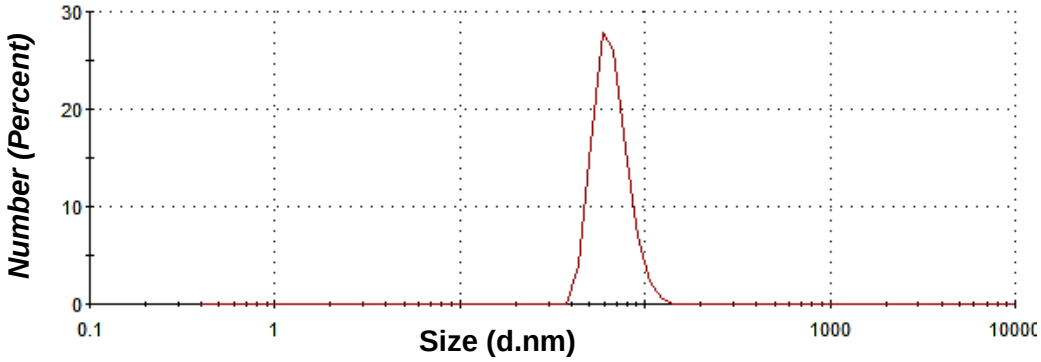

8.1.5.5 Charge ratio 12 (pDNA-PLL NPs)

8.1.5.5.1 TEM

Batches

1 **2** **3**

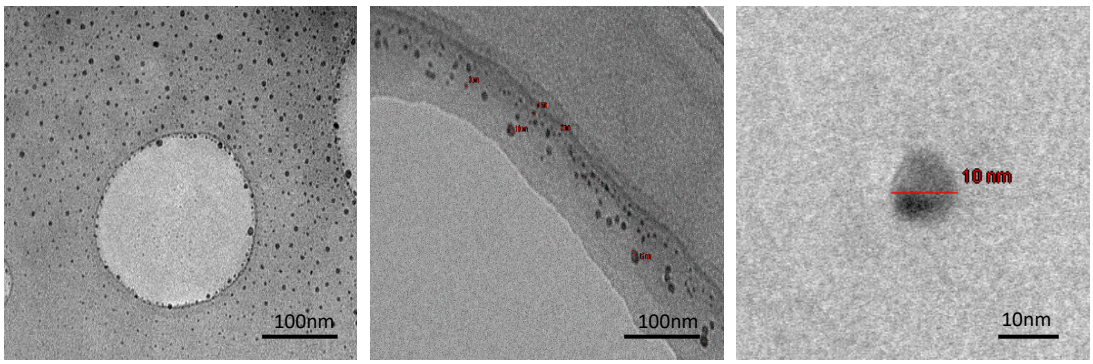

8.1.5.5.2 DLS

Batch 1

			Size (d.nm):	% Number:	St Dev (d.nm):
Z-Average (d.nm):	63.54	Peak 1:	44.66	100.0	11.88
PdI:	0.086	Peak 2:	0.000	0.0	0.000
Intercept:	0.926	Peak 3:	0.000	0.0	0.000

Result quality : Good

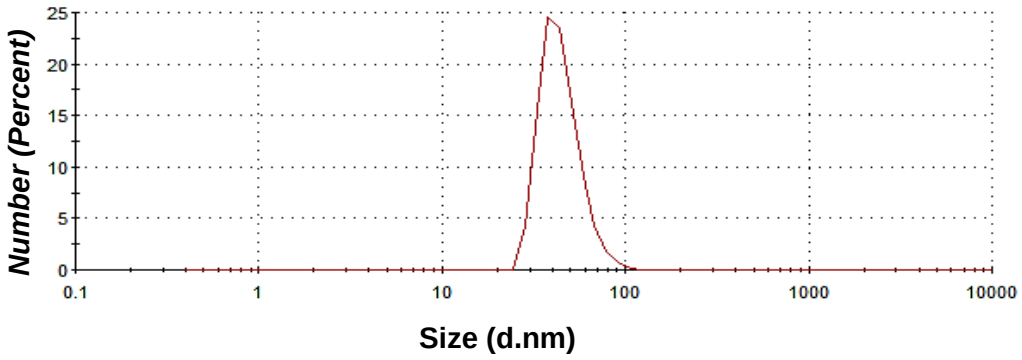

Batch 2

			Size (d.nm):	% Number:	St Dev (d.nm):
Z-Average (d.nm):	74.74	Peak 1:	45.86	100.0	13.58
PdI:	0.125	Peak 2:	0.000	0.0	0.000
Intercept:	0.943	Peak 3:	0.000	0.0	0.000

Result quality : Good

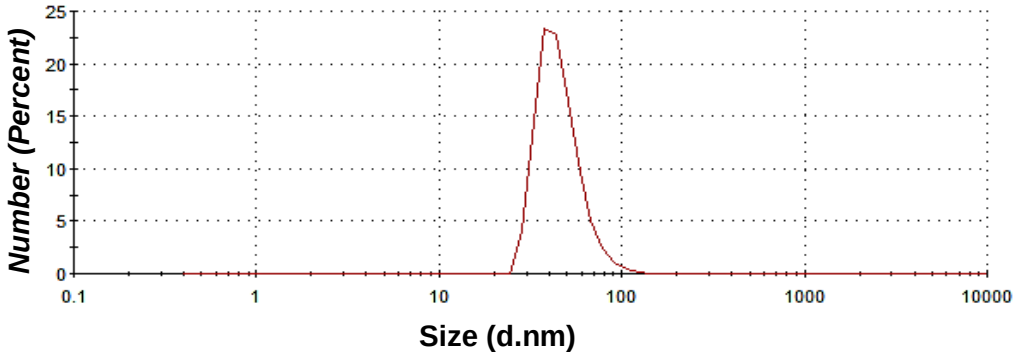

Batch 3

		Size (d.nm):	% Number:	St Dev (d.nm):
Z-Average (d.nm): 71.59	Peak 1:	50.42	100.0	13.36
PdI: 0.102	Peak 2:	0.000	0.0	0.000
Intercept: 0.952	Peak 3:	0.000	0.0	0.000

Result quality : Good

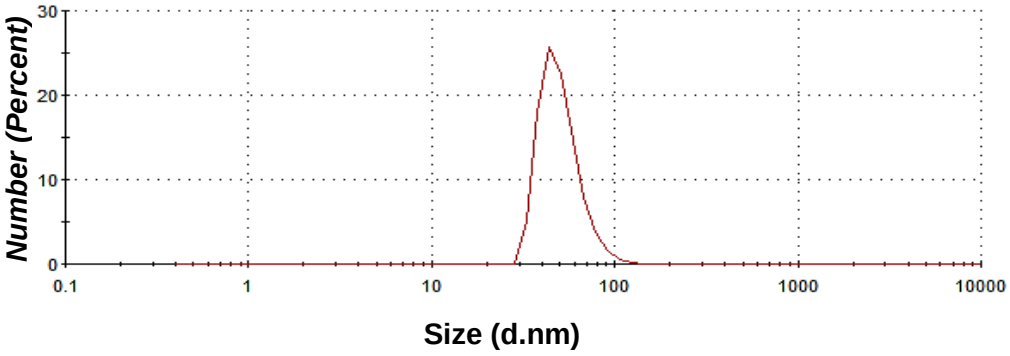

8.1.5.5.3 Zeta potential

Batch 1

		Mean (mV)	Area (%)	St Dev (mV)
Zeta Potential (mV): 25.0	Peak 1:	25.0	100.0	4.34
Zeta Deviation (mV): 4.34	Peak 2:	0.00	0.0	0.00
Conductivity (mS/cm): 0.0857	Peak 3:	0.00	0.0	0.00

Result quality : Good

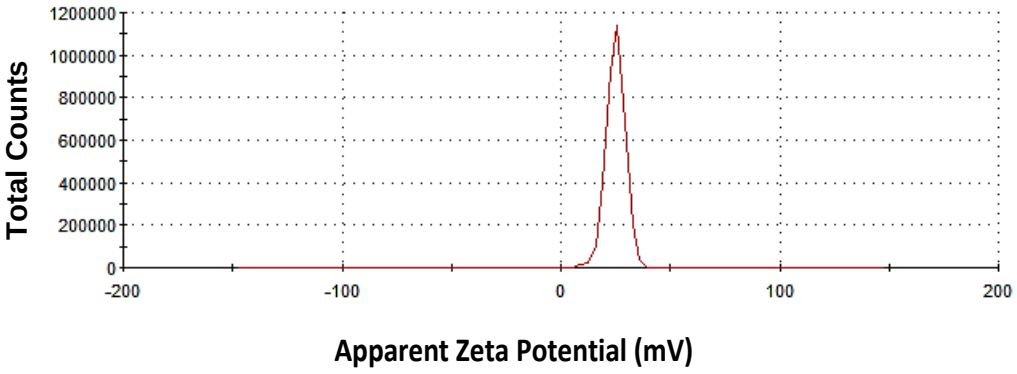

Batch 2

	Mean (mV)	Area (%)	St Dev (mV)
Zeta Potential (mV): 23.0			
Zeta Deviation (mV): 4.62			
Conductivity (mS/cm): 0.0715			
Result quality : Good			
Peak 1:	23.0	100.0	4.62
Peak 2:	0.00	0.0	0.00
Peak 3:	0.00	0.0	0.00

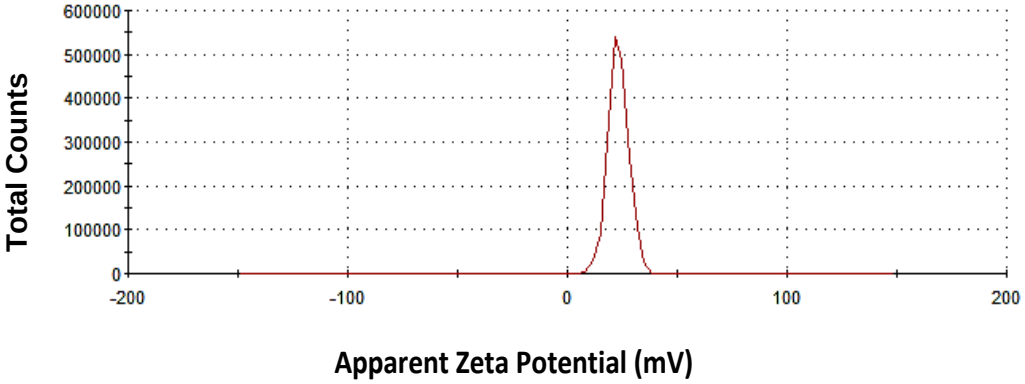

Batch 3

	Mean (mV)	Area (%)	St Dev (mV)
Zeta Potential (mV): 25.6			
Zeta Deviation (mV): 3.29			
Conductivity (mS/cm): 0.0782			
Result quality : Good			
Peak 1:	25.6	100.0	3.29
Peak 2:	0.00	0.0	0.00
Peak 3:	0.00	0.0	0.00

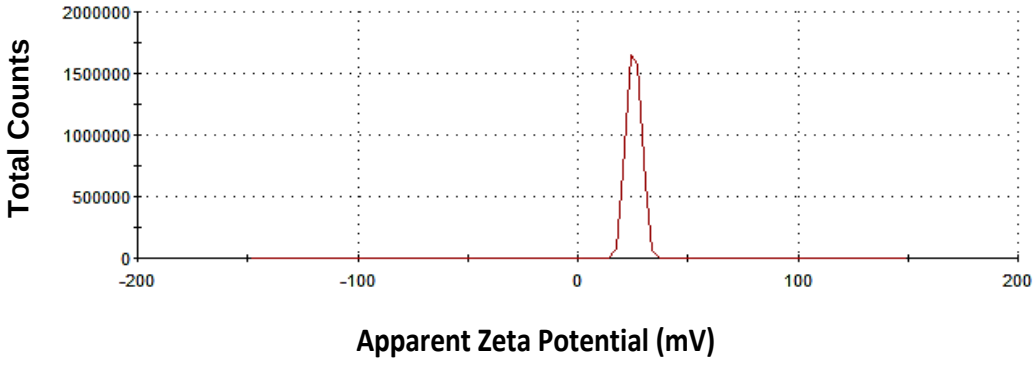

8.1.6 pBMP2-FLR NPs

8.1.6.1 TEM

Batches

1 **2**

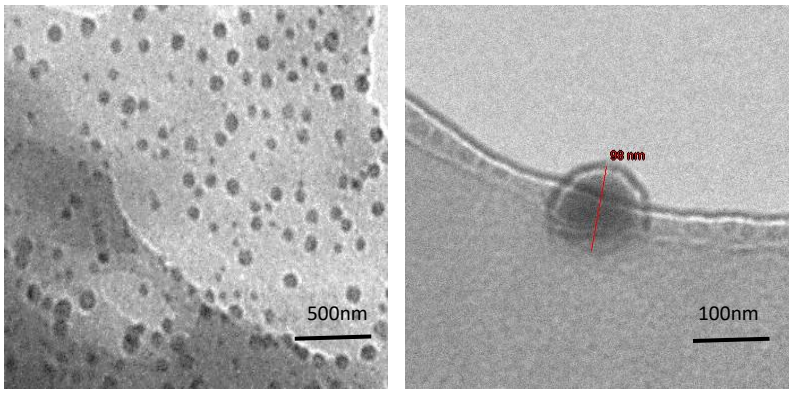

8.1.6.2 DLS

Batch 1

			Size (d.nm):	% Intensity:	St Dev (d.nm):
Z-Average (d.nm):	80.25	Peak 1:	96.73	96.7	50.87
PdI:	0.261	Peak 2:	4677	3.3	794.7
Intercept:	0.937	Peak 3:	0.000	0.0	0.000
Result quality :	Good				

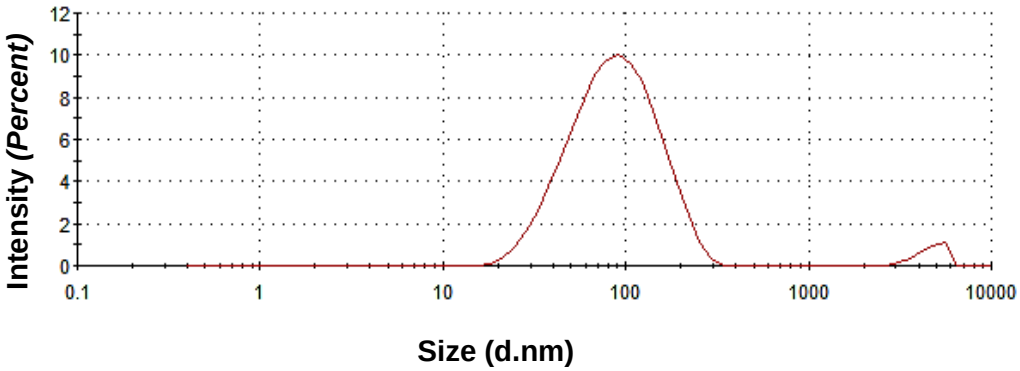

Batch 2

		Size (d.nm):	% Intensity:	St Dev (d.nm):
Z-Average (d.nm): 77.42	Peak 1:	89.77	96.6	42.45
PdI: 0.276	Peak 2:	4811	3.4	719.3
Intercept: 0.945	Peak 3:	0.000	0.0	0.000

Result quality : Good

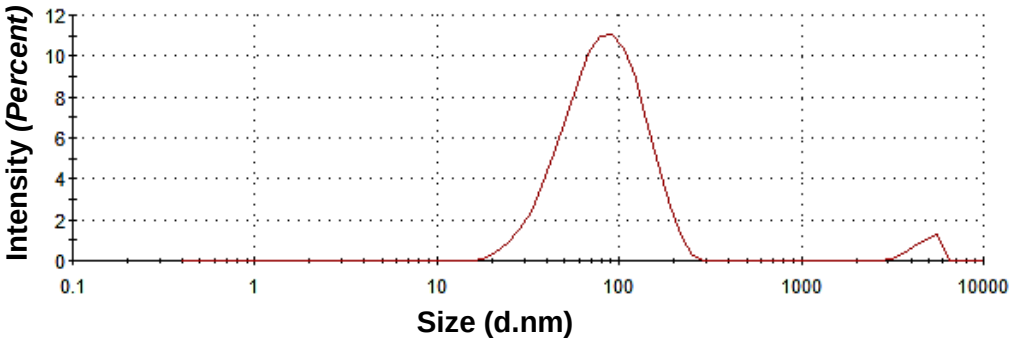

Batch 3

		Size (d.nm):	% Intensity:	St Dev (d.nm):
Z-Average (d.nm): 77.04	Peak 1:	100.6	96.9	67.44
PdI: 0.258	Peak 2:	4263	3.1	985.2
Intercept: 0.933	Peak 3:	0.000	0.0	0.000

Result quality : Good

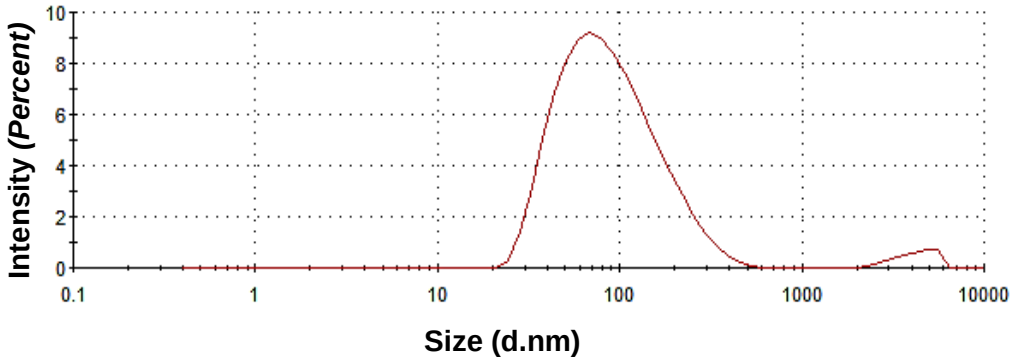

8.1.6.3 Zeta potential

Batch 1

		Mean (mV)	Area (%)	St Dev (mV)
Zeta Potential (mV): 37.4	Peak 1:	33.3	85.1	3.30
Zeta Deviation (mV): 11.0	Peak 2:	62.7	14.5	2.41
Conductivity (mS/cm): 0.0306	Peak 3:	10.9	0.4	1.66

Result quality : Good

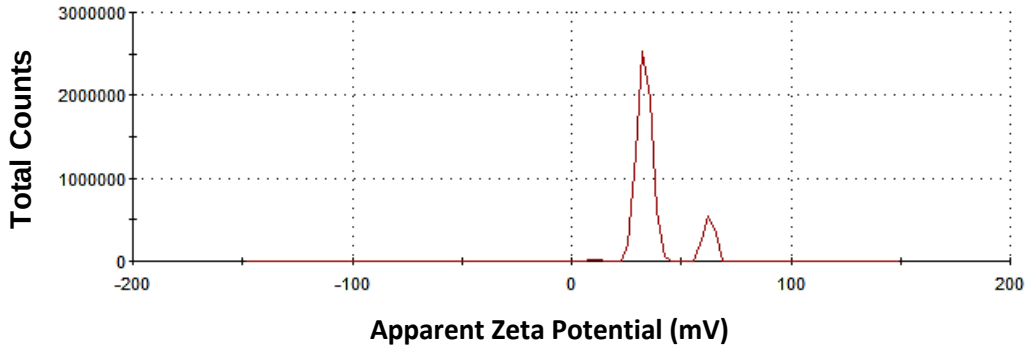

Batch 2

		Mean (mV)	Area (%)	St Dev (mV)
Zeta Potential (mV): 36.1	Peak 1:	36.1	100.0	2.66
Zeta Deviation (mV): 2.66	Peak 2:	0.00	0.0	0.00
Conductivity (mS/cm): 0.0262	Peak 3:	0.00	0.0	0.00

Result quality : Good

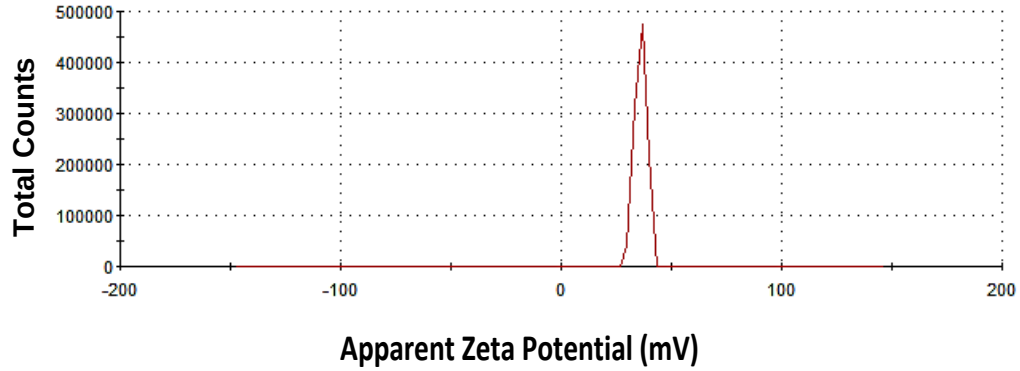

Batch 3

		Mean (mV)	Area (%)	St Dev (mV)
Zeta Potential (mV): 34.3	Peak 1:	34.3	100.0	3.28
Zeta Deviation (mV): 3.28	Peak 2:	0.00	0.0	0.00
Conductivity (mS/cm): 0.0261	Peak 3:	0.00	0.0	0.00

Result quality : Good

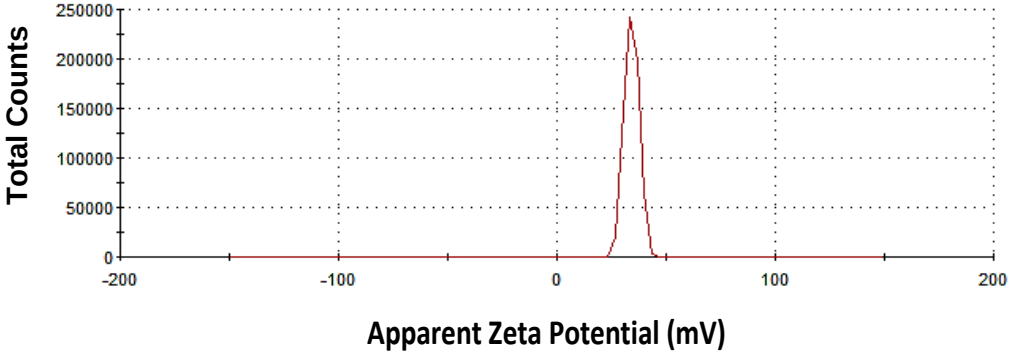

8.2 Appendix 2: Calculation of charge ratio of PLL to pDNA

Low Mw PLL: Average Mw = 5000 Da, Mass= 5 µg,

positive charge in PLL chain= $\frac{5000}{\text{Mw of Lysine}}$

$$\text{Mole} = \frac{\text{Mass}}{\text{Mw}} = \frac{0.000005\ \text{g}}{5000\ \text{g/mol}} = 1 \times 10^{-9}\ \text{mole}$$

No. of molecules = Mole x Avo.No.

$= 10^{-9} \times 6.022 \times 10^{23}$

$= 6.022 \times 10^{14}$

No. of positive charges = positive charge in a single PLL chain x No. of molecules

$= (5000/146) \times 6.022 \times 10^{14}$

$= 204.7 \times 10^{14}$

High Mw PLL: Average Mw = 50000 Da, Mass= 5 µg, positive charge in PLL chain= $\frac{50000}{\text{Mw of Lysine}}$

$$\text{Mole} = \frac{0.000005\ \text{g}}{50000\ \text{g/mol}} = 1 \times 10^{-10}\ \text{mole}$$

No. of molecules = $10^{-10} \times 6.022 \times 10^{23}$

$= 0.6022 \times 10^{14}$

No. of positive charges = $(50000/146) \times 0.6022 \times 10^{14}$

$= 204.7 \times 10^{14}$

pDNA: Average Mw = Mw of 1 base pair (bp) x No. of bp

$= 660 \times 5764$

$= 3804240$ Da

Mass= 1 µg, negative charge in every bp=2

$$\text{Mole} = \frac{0.000001\ g}{3804240} = 2.6 \times 10^{-13}\ \text{mole}$$

No. of molecules = $2.6 \times 10^{-13} \times 6.022 \times 10^{23}$

$= 1.56 \times 10^{11}$

No. of negative charges = $1.56 \times 10^{11} \times 5764 \times 2$

$= 17.2 \times 10^{14}$

$$\text{Low Mw PLL (+/-)} = \frac{204.7 \times 10^{14}}{17.2 \times 10^{14}} = 11.9 \sim 12$$

$$\text{High Mw PLL (+/-)} = \frac{204.7 \times 10^{14}}{17.2 \times 10^{14}} = 11.9 \sim 12$$